Targeting of B-cell malignancy using novel parallel chimeric antigen receptor (pCAR) engineered T-cells

Halim, Leena

Awarding institution:
King's College London

Targeting of B-cell malignancy using novel parallel chimeric antigen receptor (pCAR) engineered T-cells.

Leena Halim

(1112384)

Submitted to King's College London for the degree

Doctor of Philosophy in Cancer Studies

December 2020

Abstract

Second generation chimeric antigen receptors (CARs) containing a CD28 or 4-1BB costimulatory endodomain have shown remarkable efficacy against hematological malignancies. However, treatment failure and recurrence of disease after CAR T-cell therapy are considerable obstacles to overcome. Here, parallel (p)CARs in which a second-generation (CD28+CD3ζ) CAR is co-expressed with a 4-1BB containing chimeric co-stimulatory receptor (CCR), were engineered. The hypothesis underlying pCAR design is that optimal dual-costimulation requires positioning of endodomains *in trans* and proximal to the membrane which will, in turn, improve CAR T-cell efficacy. To investigate this premise, pCARs in which targeting moieties engage CD19, CD20 and CD22 were designed. In order to dual target CD19, the avidity of FMC63 scFv was altered using single-site mutagenesis thus creating a panel of second-generation CARs with a spectrum of binding avidities. These novel CARs demonstrated that an optimal window of avidity, lower than that of FMC63, improves T-cell responses *in vitro* and *in vivo*. Furthermore, using *in vitro* pre-clinical models, we demonstrated that CD19 pCARs showed greater cytotoxic responses, sustained cytokine release, increased proliferation and reduced expression of exhaustion markers upon repeated antigen exposure. *In vivo* CD19 pCAR T-cells showed significantly enhanced disease control and extended survival in a NALM-6 xenograft model, when compared to second-generation CAR T-cells. However, pCARs dual-targeting CD20 and CD19 or CD22 and CD19 did not show improved functionality *in vitro* or *in vivo,* respectively. The data shown here warrant further investigation and development of future pCARs to uncover the mechanisms behind their functionality.

Table of Contents

List of Figures

List of Tables

Abbreviations

293T	Cell line derived from HEK293 cells that have been stably transfected with the SV40 T antigen
AAV	Adeno-associated virus
AICD	Activation induced cell death
ALL	Acute lymphoblastic leukaemia
APC	Antigen presenting cell
B-ALL	B-lymphoblastic leukaemia
BLI	Bioluminescent imaging
CAR	Chimeric antigen receptor
CCR	Chimeric co-stimulatory receptor
CD	Cluster of differentiation
cDNA	Complementary DNA
CDR	Complementary determining region
CMV	Cytomegalovirus
CR	Complete response
CRS	Cytokine release syndrome
CTL	Cytotoxic T lymphocytes
CTLA-4	Cytotoxic T-Lymphocyte Associated Protein 4
DFS	Disease-free survival
D10	Dulbecco's Modified Eagle Medium + 10% FBS
DMSO	Dimethyl Sulfoxide
DNA	Deoxyribonucleic acid
dsDNA	Double stranded DNA
E. coli	Escherichia coli
E:T	Effector cell to target cell ratio
ELISA	Enzyme linked immunosorbent assay
env	Envelope
FACS	Fluorescence activated cell sorting
FBS	Foetal Bovine Serum
Fc	Fragment crystallisable region

ffLuc	Firefly luciferase
FDA	Food and Drug Administration
GALV	Gibbon-Ape Leukaemia Virus
GvHD	Graft versus host disease
HEK	Human Embryonic Kidney
HLA	Human leukocyte antigen
HS	Human serum
IFN	Interferon
Ig	Immunoglobulin
IL	Interleukin
ITAM	Immunoreceptor tyrosine-based activation motif
i.v.	intravenous
k_a	Association rate/On rate
K_D	Dissociation equilibrium constant
k_d	Dissociation rate/Off rate
LAG3	Lymphocyte activated gene-3
LB	Luria Broth
LTR	Long terminal repeat
mAb	Monoclonal Antibody
MFI	Mean fluorescence intensity
MHC	Major histocompatibility complex
mRNA	Messenger RNA
MTT	3-[4,5-dimethylthiazol-2-yl]- 2,5-diphenyltetrazolium bromide; thiazolyl blue
NHL	Non-Hodgkin lymphoma
NY-ESO	New York Oesophageal antigen-1
OR	Objective response
ORR	Overall response rate
PBMC	Peripheral blood mononuclear cells
PBS	Phosphate buffered saline
pCAR	Parallel Chimeric Antigen Receptor

PCR	Polymerase Chain Reaction
PD-1	Programmed death receptor-1
PI3K	Phosphatidylinositol 3'kinase
pMHC	Peptide-MHC complex
PSMA	Prostate-specific membrane antigen
r/r	Relapsed/refractory
RN	RetroNectin
RNA	Ribonucleic acid
RPM	Revolutions per minute
R10	Roswell Park Memorial Institute + 10% FBS
R5	Roswell Park Memorial Institute + 5% Human serum
scFv	Single chain variable fragment
SOC	Super optimal broth with catabolite repression
SPR	Surface plasmon resonance
STAT	Signal transducer and activation of transcription
T2A	Thosea asigna
TAA	Tumour associated antigen
TCR	T-cell receptor
TIL	Tumour Infiltrating Lymphocytes
TIM-3	T cell Ig and mucin domain containing protein-3
TNF	Tumour Necrosis Factor
TNFRSF	TNF receptor super family
TRAF	TNF-receptor-associated factor
Treg	Regulatory T-cell
UT	Untransduced
V_H	Variable heavy
V_L	Variable light

Acknowledgements

There are many people I am grateful to for their encouragement and support throughout this PhD, without whom this would not have been possible.

Firstly, I would like to extend a huge thank you to my supervisor Dr John Maher for his continued guidance and supervision. Your positivity, patience and commitment has made my PhD experience one I will cherish. It has been a privilege to work in the CAR Mechanics group so thank you for taking me on board those years ago! Additionally, I would like to thank my second supervisor, Dr Richard Dillon for his kind support throughout.

To everyone, past and present, in the CAR Mechanics, Leucid and Immunoengineering groups; it has been a pleasure to work with you all throughout the years. I feel very privileged having been surrounded by such supportive and kind colleagues that I can also call friends. A special mention to Marc, Antonella, Daniel and Erin for all the help, laughs, advice and countless coffees.

To my wonderful friends in London, thank you for reminding there is a whole world outside out work and for the many memories we made together. Life would have been a lot more stressful and a lot more boring without you all.

Lastly, I am forever grateful to my family who are my joy and inspiration. My parents' unwavering support and generosity made this all possible. Everything I have achieved is because of them.

Chapter 1: Introduction

1.1 B-cell Malignancy

The focus of this PhD project is the development of a novel cellular immunotherapy approach that is targeted against B-cell malignancies. Traditionally, B-cell malignancy has been subdivided into leukaemias, which primarily affect blood and bone marrow, and lymphomas, which infiltrate lymphoid tissues and other organs. B-cell leukaemias in turn occur in acute (e.g., rapidly progressive) and chronic (more indolent) forms. Many sub-types of B-cell lymphoma have also been described and present a spectrum of varying disease aggressiveness. Given this heterogeneity, the classification of B-cell malignancy is becoming increasingly complex and has undergone many iterations over the years. Recently, the World Health Organization (WHO) has provided an updated scheme which categorises B-cell malignancies into two broad classes of disease: (1) precursor B-cell neoplasms, which include B lymphoblastic leukemia/lymphoma with or without recurrent genetic abnormalities, and (2) mature B-cell neoplasms (Table 1.1)[1,2]. However, from the perspective of cellular immunotherapy of B-cell malignancy, two major disease groups warrant further consideration, namely B-cell acute lymphoblastic leukaemia (ALL) and B-cell lymphomas.

Table 1.1: Classification of most prevalent B-cell malignancies

Mature B-cell neoplasms	Precursor B-cell neoplasm
Chronic lymphocytic leukaemia (CLL) / Small lymphocytic lymphoma	Precursor B-lymphoblastic lymphoma
Mantle cell lymphoma (MCL)	Precursor B-lymphoblastic leukaemia
In situ follicular neoplasm (ISFN)	
Diffuse large B-cell lymphoma (DLBCL)	
Burkitt's lymphoma	
Marginal zone lymphoma (MZ)	
Hairy cell leukaemia	
Mucosa-associated lymphoid tissue (MALT) lymphoma	
B-lymphoblastic lymphoma	
Mediastinal large B-cell lymphoma	
Low-count / high-count monoclonal B-cell lymphocytosis	
Large B-cell lymphoma with IRF4 rearrangement	

1.1.1 Acute Lymphoblastic Leukaemia (ALL)

Acute lymphoblastic leukaemia (ALL) is a cancer of the lymphoid cells that is categorised into B-lymphoblastic and T-lymphoblastic leukaemia and, can be further subclassified according to the nature of genetic abnormalities that are be present. With regards to this thesis, I will focus on B-lymphoblastic leukaemia (B-ALL).

B-cell ALL is an aggressive disease that is most prevalent in children and young adults, with a peak incidence of age 2-5 years. In children under 15 years of age, B-ALL accounts for 25% of all malignancies while 19% of cancers that affect young adults aged 15-19 years fall within this category[3,4]. The pathogenesis of ALL is multi-factorial, including

genetic susceptibility, exogenous and endogenous influences[5]. Predisposing factors include exposure to ionizing radiation, pesticides, or viruses such as Epstein-Barr Virus [6–8]. However, the majority of B-ALL cases arise de novo in otherwise healthy individuals. In childhood ALL, long-term survival currently is approaching 90%. Despite this improvement in survival in paediatric and also in young-adult patients, prognosis of adult ALL has remained poor with only 30-40% of adult patients achieving long-term remission[9]. Predictors of prognosis are dependent on numerous factors including age, cytogenetic aberrations, leukocyte count and tolerance to therapy[10,11].

1.1.1.1 Pathophysiology of ALL

Acute lymphoblastic leukaemia arises because of the abnormal proliferation and differentiation of a clonal population of lymphoid cells. Next generation sequencing and microarray analysis of large ALL cohorts have provided considerable understanding and insight into the genetic basis of this disease. Genome-wide associate studies (GWAS) to understand the genetic susceptibility of B-ALL have identified single-nucleotide polymorphisms (SNPs) at eight loci influencing ALL risk including, 7p12.2 *(IKZF1)*, 9p21.3 *(CDKN2A)* and 10p12.2 *(PIP4K2A)*[12]. A meta-analysis of three independent GWAS data sets shed further light on the inherited predisposition to childhood ALL and described two additional risk loci at 2q22.3 and 8p24.21[12]. Furthermore, researchers found that certain SNPs display subtype-specific effects on high-hyperdiploid ALL and Ph-like ALL. Studies in the paediatric and young adult population have identified syndromes that predispose to ALL, such as Down syndrome, Fanconi anaemia and Bloom syndrome. Collectively however, these account for only a minority of cases[13–15]. Genetic aberrations are a hallmark of B-ALL and abnormalities frequently occur in genes encoding transcriptional regulators of lymphoid

development. For example, in 60% of all B-ALL patients the genes *PAX5, EBF1* and *IKZF,* which encode transcription factors associated with B-cell differentiation and development, are mutated[16,17]. Moreover, structural chromosomal alterations occur in most cases[16,17]. Such characteristic translocations include t(12;21) [ETV6-RUNX1] t(1;19) [TCF3-PBX1], t(9;22) [BCR-ABL1] and rearrangement of MLL[18]. Other commonly transformed pathways in ALL involve tumour suppression and cell-cycle regulation pathways; however, the precise genes involved varies among subtypes[19]. Classification of ALL began in 1987; the French American British (FAB) criteria divided ALL into 3 subtypes based on morphology (L1, L2 and L3)[20]. Later revised in 1997, the World Health Organisation (WHO) proposed a classification to account for morphology and cytogenetic profile of leukaemic blasts and identified three types of ALL: B-lymphoblastic, T-lymphoblastic and Burkitt-cell leukaemia[21]. In 2008, B-lymphoblastic leukaemia was divided into two subtypes: B-ALL with recurrent genetic abnormalities and B-ALL not otherwise specified. B-ALL with recurrent genetic abnormalities is further demarcated based on specific chromosomal rearrangements. Additionally, Burkitt-cell leukaemia was removed as a subtype as it was no longer seen as a separate entity from Burkitt lymphoma[22]. Finally, in 2016 two new provisional entries were added to redefine hypodiploid as either low hypodiploid or hypodiploid with TP53 mutations[23].

The best example to illustrate the clinical impact of a defined genetic abnormality in B-ALL is the Philadelphia chromosome. This reciprocal translocation between the long (q) arms of chromosome 9 and 22 (t(9;22)(q34;q11) leads to the formation of the BCR-ABL1 fusion gene, encoding for a protein with constitutive tyrosine kinase activity. Approximately 25% of adults and 3% of children with ALL have Ph-positive ALL, a subgroup in whom prognosis is correspondingly poorer. Recently, it has become apparent that a significant subset of B-ALL have a “Philadelphia-like” gene expression signature in the absence of this

translocation[24]. Genetic abnormalities are often predictive of prognosis and outcome because of subsequent poor response to chemotherapy.

The accumulation of malignant, poorly differentiated lymphoid cells within the bone marrow results in many of the clinical manifestations of ALL. Signs of bone marrow failure such as anaemia, thrombocytopenia and leukopenia alongside non-specific symptoms are typical at patient presentation. Other common symptoms include weight loss, fatigue, propensity to bruising or bleeding and infection. Diagnosis is supported by the presence of 20% or more lymphoblasts in the bone marrow or peripheral blood[25]. Diagnosis and risk stratification are confirmed by flow cytometry, evaluation of morphology, immunophenotyping and cytogenetic testing.

1.1.1.2 Current standard treatments for ALL

Standard lines of treatment of ALL utilise risk-based therapy to avoid over- or under-treatment of patients. Typical treatment regimens comprise three phases; namely remission-induction, consolidation and continuation[10]. The goal of remission-induction therapy is to achieve complete remission of disease and aims to restore normal haematopoiesis. To eradicate the leukaemic cell burden chemotherapy agents are used over the course of 4-6 weeks. Children with standard-risk ALL typically receive chemotherapy drugs such as L-asparaginase and vincristine in combination with a corticosteroid. In the case of high-risk children, an anthracycline such as daunorubicin may also be included. Other drugs that may be given early are methotrexate and/or 6-mercaptopurine[26,27]. To eliminate residual leukaemic cells after remission-induction, consolidation or intensification therapy is administered. This generally employs similar agents to those used for induction therapy[11]. Ongoing continuation therapy typically occurs for 2 years and comprises daily

mercaptopurine alongside weekly methotrexate[5]. Patients also receive intrathecal chemotherapy since the central nervous system is a common sanctuary site of ALL. Haematopoietic stem cell transplantation (HSCT) is considered after induction therapy for patients with high risk ALL and/or persistent disease[28]. Following induction therapy, the majority of patients enter remission. However, 10-15% of young patients relapse after chemotherapy treatment and 3% will present with primary refractory disease. As a result, ALL remains the leading cause of cancer-related deaths in children and young adults[29]. Furthermore, acute toxic side-effects from chemotherapy can lead to severe short- and long- term co-morbidities such as infertility and secondary malignancies. This underscores the need to further improve ALL patient outcomes in which CAR T-cell therapy has emerged as a new strategy.

1.1.2 Non-Hodgkin Lymphoma (NHL)

Non-Hodgkin lymphoma (NHL) is a heterogenous disease encompassing B-cell and T-cell subtypes. Non-Hodgkin lymphoma accounts for 4% of all new cancer cases within the UK and is the most common B-cell malignancy worldwide[30]. In 2018, an estimated 510,000 new cases of NHL were diagnosed worldwide, and an estimated 248,724 patients died as a result of the disease[31]. Diffuse large B-cell lymphoma (DLBCL) is the most common form of B-cell NHL and accounts for approximately 40% of all B-cell NHL worldwide[32]. Other subtypes of NHL include follicular lymphoma (FL), marginal-zone lymphoma (MZ) and mantle-cell lymphoma (MCL) however, these are less common and account for fewer cases.

1.1.2.1 Pathophysiology of DLBCL

Non-Hodgkin lymphomas arise from the expansion and progressive accumulation of a mature single clone of lymphocytes[33]. In 2016, the WHO revised classification of mature B-

cell lymphoid neoplasms to include low-count monoclonal B-cell lymphocytosis (MBL) and high-count MBL, which is a precursor to chronic lymphocytic leukaemia (CLL)[2]. Additionally, follicular lymphoma (FL) was renamed as in situ follicular neoplasm (ISFN) and large B-cell lymphoma with IRF4 rearrangement is now considered a distinct new entity. Diffuse large B-cell lymphoma is an aggressive B-cell NHL that is highly heterogeneous in nature and is characterised by a diffuse outgrowth of large and mature B lymphoid cells at different stages of differentiation[1]. Two main subtypes of DLBCL have been described based on cell or origin[2]. The first of these is the germinal centre B-cell subtype. Cells are commonly CD10 and BCL6 positive (akin to natural germinal centre B-cells) with highly mutated immunoglobulin genes due to ongoing somatic hypermutation. A second activated B-cell subtype has also been described in which these features are not evident. Molecular events involved in the pathogenesis of DLBCL have increasingly been elucidated and have been found to have prognostic impact. The RAG complex is one of the protein complexes involved in V(D)J recombination that is required for the diversification and development of the B-cell receptor (BCR). Genetic alterations can be generated by the RAG complex, such as through introduction of breakpoints in the locus encoding heavy Ig (IGH) chains, resulting in gene fusions such *as IGH-BCL2*[34]. During somatic hypermutation and class-switch recombination, activation-induced cytidine deaminase (AID) can target transcriptionally active genes including *BCL6* and *MYC*, thus generating breaks. In *IGH-BCL2* translocations, most breaks involve the switch region of *IGH*, suggesting that these translocations are generated during AID-mediated class-switch recombination[35]. Hypermutation mediated by off-target actions of AID provides a source of oncogenic mutations in DLBCL and has been reported in over half of patients with DLBCL[36,37]. These AID-induced mutations can occur in *BCL2, IGLL5, PIM1*

and *SGK1,* and are predominantly single-nucleotide substitutions targeting the hotspot RGYW/WRCY motif, where G:C is a mutable position; R=A/G, Y=C/T, and W=A/T.[38,39].

Overexpression of BCL-6 in DLBCL is common and results in the dysregulation of both cell cycle and DNA damage repair pathways[40]. The BCL2 gene also plays a central role in the molecular pathogenesis of DLBCL. When normally expressed, BCL2 encodes an anti-apoptotic protein. However, constitutive activation in DLBCL allows B-cells to avoid germinal centre apoptosis thereby enabling lymphomagenesis[34]. Many cellular functions are modulated by MYC such as metabolism, DNA replication and cell proliferation; hence MYC dysregulation contributes to lymphomagenesis. MYC translocations can occur in 4-14% of DLBCL, resulting in constitutive MYC expression and poorer survival rates[41]. High grade B-cell lymphomas with MYC rearrangement are commonly referred to a single hit lymphomas. In the presence of a concurrent translocation of BCL2 and/ or BCL6, disease is referred to as double-hit or triple-hit lymphomas respectively. These represent patient groups in whom prognosis is significantly poorer and more intensive treatment advocated.

1.1.2.2 Current standard treatments for B-cell NHL

The most common treatment modality used in patients with B-cell NHL is an anthracycline based immune-chemotherapy regimen known as R-CHOP (comprising Rituximab, Cyclophosphamide, doxorubicin (Hydroxydaunorubicin), vincristine (Oncovin) and Prednisone). Rituximab is a monoclonal antibody that targets the B-lymphocyte differentiation antigen, CD20, and its addition to the traditional CHOP regimen has improved patient outcomes across several B-cell NHL subtypes[42,43]. Nonetheless, many patients relapse or have primary refractory lymphoma. In this setting, the standard second line approach is salvage chemotherapy followed by autologous or allogenic HSCT. Patients

with primary refractory DLBCL or who become refractory to second-line therapy have especially poor outcomes. In addition, patients who cannot proceed to HSCT, either due to failure of salvage therapy, inadequate stem cell collection or unsuitability for this intensive treatment approach have a median overall survival of 3.3 months[44]. Patients who relapse after an initial response to auto-HSCT also have dismal median? survival of 10 months[45]. As indicated, the prognosis for patients with relapsed/refractory NHL is particularly poor and new treatment approaches are needed to address this gap.

1.2 Cancer immunotherapy

Cancer immunotherapy sets out to utilise the fundamental defence mechanisms of the immune system to target cancer. In recent decades, there has been immense progress in our understanding of the immune system and its interplay with cancer. An array of immunotherapy approaches are now available, most notably monoclonal antibodies directed against tumour or immune targets and emerging cell and gene therapy approaches. Tumour vaccines have also been trialled extensively, although impact in the therapeutic setting has been modest. Collectively, these therapies aim to assist or reinvigorate the immune system to eradicate cancer; either by slowing the growth of cancer cells, preventing cancer cells from metastasising and supporting the immune system to enable the destruction of malignant cells[46].

Conceptually, the manipulation of the immune system in a targeted manner enables immunotherapy to treat a broad range of cancers in a precise manner, including tumours that have spread. Immunotherapy aims to only destroy malignant cells, leaving healthy cells unaffected unlike traditional treatments such as surgery, chemotherapy or radiotherapy.

However, immunotherapy can promote significant toxicity as a result of excessive immune activation and therefore requires further optimisation. Moreover, despite remarkable progress in recent years, it remains true that only a minority of patients benefit from modern cancer immunotherapies, emphasising the need for further progress in this area.

1.2.1 Cancer immunoediting

To understand the mechanisms behind cancer immune evasion and to design effective immunotherapies, it is crucial to understand how cancer interacts with the immune system. Cancer immunoediting describes the dual role by which the immune system can suppress and/or promote cancer growth. Research has shown that immune and inflammatory processes can induce cellular transformation, influence the immunogenicity of tumours and control tumour growth. The interplay between these roles is determined by their temporal manifestation, the different arms of the immune system involved, the transformational process of the tumour and the tumour-associated antigens that are expressed. The tumour immune-editing process consists of three phases; elimination, equilibrium and escape[47,48]. In the elimination phase, surveillance by cells from both the innate and adaptive immune system detect and eradicate malignant cells that have arisen because of failed tumour suppressor mechanisms. If all tumour cells have been eradicated, the elimination phase is complete. However, if partial elimination of tumour cells occurs then the surviving tumour cells and host immune system enter into dynamic equilibrium. Whilst in the equilibrium phase, tumour cells may remain dormant or continue to evolve, accumulating further mutations or modifying gene expression providing them with increased resistance to immune attack. As this period continues, the immune system exerts selective pressure by destroying susceptible malignant cells, thus controlling tumour progression. However, the

sculpting forces of the immune system select tumour cell variants that are able to resist, avoid or suppress the anti-tumour response, leading to the escape phase. In the escape phase, tumour cell variants selected during equilibrium are able to grow by avoiding the immunosurveillance network. Mechanisms that tumour cells employ to "escape' immune recognition include down-regulation of human leukocyte antigen (HLA) class I antigens, loss of death receptor ligands Fas and TRAIL, down-regulation of tumour antigens and lack of expression of costimulatory molecules[49–51]. Moreover, tumour cells can express molecules that increase their resistance to immune surveillance such as STAT3, Bcl-2 (enhanced resistance to apoptosis) and PD-L1 (immune checkpoint ligand). Moreover, the tumour microenvironment facilitates tumour growth through the expression of immunosuppressive cytokines (e.g. interleukin (IL)-10 and transforming growth factor (TGF)-β) that subdue effector T-cell responses[52]. As the immune system is no longer able to contain cancer cell growth, tumour progression occurs, and disease becomes clinically detectable.

1.2.2 Evolution of cancer immunotherapy

The field of cancer immunotherapy has existed since the late 19th century when William B. Coley triggered an anti-tumour immune responses in cancer patients by local injection of bacterial toxins[53]. Coley's idea, ahead of its time, underlies the basis of immunotherapy whereby targeted cytotoxicity by the immune system can cause tumour cell killing. Recognition of the fact that T-cells play a major role in anti-tumour responses led to the clinical use of IL-2 to treat metastatic renal cell carcinoma and metastatic melanoma[54,55]. However, IL-2 therapy is non-targeted and non-specific and resulted in significant levels of toxicity with relatively low response rates. Nevertheless, it demonstrated further proof of

concept in support of the principle of cancer immunotherapy and underlined the need for new immunotherapeutic approaches.

The development of monoclonal antibody technology revolutionised cancer immunotherapy. In 1997, the US Food and Drug Administration (FDA) granted approved the use of rituximab as a treatment for B-cell lymphomas[56,57]. Rituximab is a genetically engineered monoclonal antibody directed against CD20 which triggers cell death by antibody-dependent cell-mediated cytotoxicity (ADCC), complement activation and directed induction of apoptosis. A further major breakthrough in cancer immunotherapy happened with the introduction of monoclonal antibodies targeted towards immune checkpoint receptors. Checkpoint receptors such as PD-1 and CTLA-4 are found on the cell surface of T-cells and, upon binding to their corresponding ligands, they signal to promote T-cell tolerance or the cessation of inflammatory response. In the context of the tumour microenvironment, the expression of co-inhibitory ligands alongside chronic exposure to tumour associated antigens can lead to suppression of T-cell responses[58]. As such, the blockade of such immune checkpoint ligands can unleash a T-cell mediated anti-tumour response[59,60]. The use of checkpoint blockade antibodies for the treatment of cancer has been approved for a variety of diseases including melanoma, head and neck squamous cell carcinoma, non-small cell lung cancer and Hodgkin lymphoma[61–64]. Data from multiple clinical trials has shown that ipilimumab, an anti-CTLA-4 antibody, increased long-term survival in 20% of melanoma patients for at least 3 years after treatment, with the longest reported survival reaching 10 years[65,66]. The checkpoint receptor PD-1 is expressed on activated $CD4^+$ and $CD8^+$ T-cells and negatively regulates T-cell activity upon binding to its ligands, PD-L1 and PD-L2. The PD1-specific monoclonal antibodies designated pembrolizumab and nivolumab successfully block these inhibitory pathways and have

achieved remarkable results in the treatment of different malignancies[67,68]. Clinical trials have also investigated the effect of combining different immunotherapies such as the simultaneous use of anti-CTLA-4 and anti-PD1 antibodies. The combined effect of CTLA-4 and PD-1 blockade was more effective than either agent alone and resulted in a further increased overall survival in melanoma patients[69,70].

1.3 Adoptive T-cell therapy

Adoptive T-cell therapy is an immunotherapeutic strategy that involves the *ex vivo* expansion of tumour-reactive T-cells followed by their adoptive transfer into patients to combat cancer. Different modalities of adoptive cell therapy have been investigated involving the use of tumour-infiltrating lymphocytes (TILs), antigen-specific autologous T-cell clones and genetically engineered human lymphocytes. Immunotherapy using TIL cells was pioneered by Steven Rosenberg at the National Institute of Health (NIH) who demonstrated that autologous TILs infused after lymphodepleting chemotherapy could induce regression of metastases *in vivo*[71]. In the first human study, the researchers showed that a single infusion of TILs could cause disease regression in up to 60% of patients with metastatic melanoma[72,73]. However, generation of TILs is time consuming (approximately 5-6 weeks) and labour intensive[74,75]. Moreover, TIL adoptive cell therapy is not applicable to many other tumour types because of low tumour immunogenicity and minimal TIL infiltration[76].

With improvements in gene transfer technology, genetically encoded receptors could be introduced to re-direct T-cells against tumours thereby broadening the applicability of adoptive cell therapy. With this approach, polyclonal T-cells with specificity for a tumour associated antigen (TAA) are rapidly generated. Two classes of receptors are

commonly used for this purpose, namely antigen specific αβ T-cell receptors (TCR) or chimeric antigen receptors (CAR). An early report of gamma retroviral vector TCR gene transfer described the treatment of a patient with melanoma by targeting MART-1 with a TAA specific TCR[77]. Since then, T-cells have been successfully re-targeted using TCRs directed against several antigens such as p53[78,79], glycoprotein-100 (gp100)[80], Wilm's tumour antigen-1 (WT-1)[81], carcinoembryonic antigen (CEA)[82,83] and others. The testis TAA NY-ESO-1 has been a particularly promising target as it is present in multiple cancer types and is highly immunogenic. In early-phase clinical trials NY-ESO-1 TCR engineered T-cells were used to treat multiple myeloma and synovial sarcoma, reporting response rates of 80% and 50% respectively[84,85]. A major restriction of TCR therapy is that a limited number of patients with the appropriate HLA alleles can receive treatment, owing to the need to match the TCR to the patient's HLA haplotype. To date, the vast majority of TCRs in clinical trial are restricted by HLA-A*0201, which is found in approximately 45% of Caucasians. Further modifications of TCR gene transfer have been made with the introduction of a disulphide bond linking the constant domains of α and β chains, leading to a reduced risk of mispairing with endogenous TCR subunits, a process which has resulted in lethal autoimmunity in mice[86]. The most effective method to avoid mispairing and subsequent toxicity involves knockdown of the endogenous TCR. Technology that enables this includes the Zinc finger nucleases[87], TALENs (Transcription activator-like effector nuclease), CRISPR and short-hairpin RNA (shRNA)[88].

1.4 Chimeric antigen receptors (CARs)

The introduction of chimeric antigen receptors (CARs) as a genetic engineering approach of T-cells has achieved remarkable results. Chimeric immune receptors were first developed in Japan in 1987 and were composed of monoclonal antibody variable regions coupled to the constant region of the T-cell receptor (TCR) α and β chains[89]. To achieve target specificity Eshhar et al. modified the chimeric immune receptor design to include a single chain antibody variable fragment (scFv) specific for a tumour associated antigen[90]. An scFv consists of an immunoglobulin light chain variable region (V_L) and the heavy chain variable region (V_H), typically derived from a monoclonal antibody, linked by a peptide linker sequence. The scFv was fused to a transmembrane domain, followed by the signal transducing elements FcR1γ or CD3ζ derived from the TCR/CD3 complex. Eshhar coined the term T-body to describe this fusion molecule and this is now generally referred to as a first generation CAR. These chimeric receptors combine the specificity of monoclonal antibodies with the cytolytic capacity of T-cells. Importantly, they recognise their target in an Major Histocompatibility Complex (MHC) independent manner[90,91].

1.4.1 Genetic modification of T-cells

Successful gene expression and modification of T-cells requires robust methods of gene delivery to efficiently express transgenes. In general, to achieve sustained CAR expression in proliferating T-cells, an integrating viral vector system is used. Viruses are obligate intracellular parasites that are able to exploit host cells to facilitate their replication[92]. In gene therapy, virus-based vectors harness the viral infection pathway whilst excluding viral genes required for replication and toxicity.

To ensure no virion replication post infection of cells, replication-defective vectors are used in which the coding regions for the four genes *gag, pro, pol* and *env,* which are crucial for the completion of the retroviral life cycle, are deleted and replaced with the DNA sequence intended for transfer. The genome of the retrovirus contains two RNA copies, these encode for the four genes *gag, pro, pol* and *env.* The *gag* sequence encodes for the three main structural proteins: matrix, capsid and nucleocapsid proteins. The *pro* sequence, encodes for proteases responsible for cleaving gag and gag-pro-pol during particle assembly, budding and maturation. The pol sequence encodes the reverse transcriptase and integrase enzymes; the former catalyses the reverse transcription of viral RNA to DNA during the infection process. The integrase enzyme is responsible for integrating the pro-viral DNA into the host cell genome. The env encodes both the surface and transmembrane subunits of the envelope glycoprotein

The retroviral life cycle is summarised in Figure 1.1. Infection of the host cell by retroviruses is initiated when the glycoproteins of the viral envelope attach to their receptors expressed on the surface on the host cell. Upon recognition, the viral envelope fuses with the host cell membrane and the viral RNA is released into the cytoplasm. Reverse transcriptase converts the viral RNA into double-stranded DNA which is then transferred to the host cell nucleus. The viral DNA gains access to the nucleus during mitosis after the dissolution of the nuclear membrane, at this time the double-stranded DNA is integrated into the host cell genome to form the provirus. This process occurs in an almost random manner throughout the host cell genome. The integrated provirus is then transcribed by RNA polymerase II to yield mRNA that encodes for viral proteins. The mRNA is exported from the nucleus and translated by the host-cell machinery, the translated proteins are further processed by the viral protease and are encapsulated into viral particles. These

newly formed viral particles exit the infected cell by budding to produce a mature infectious virion.

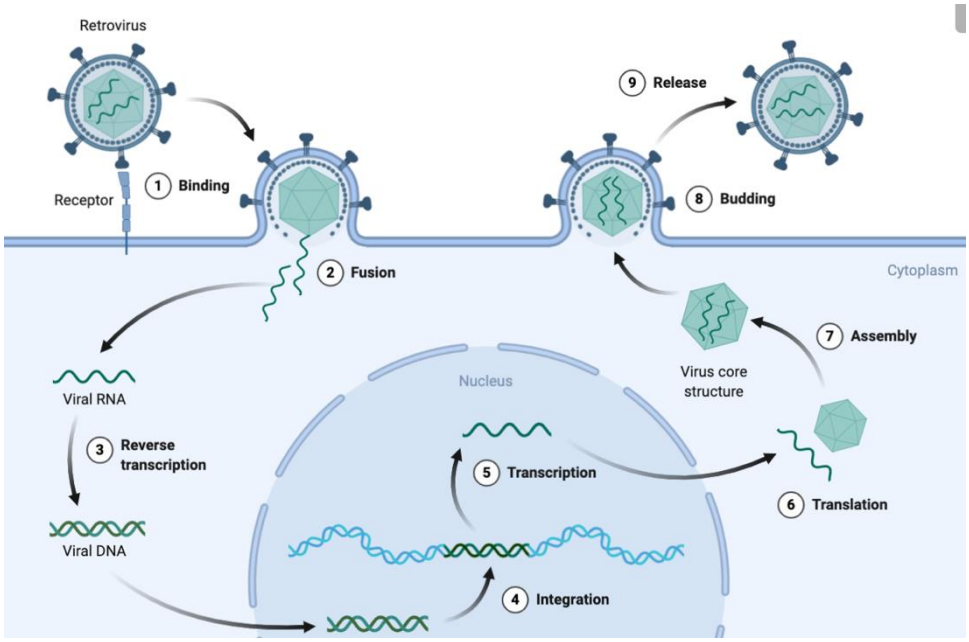

Figure 1.1 Life cycle of retrovirus. Infection of the host cell by the retrovirus begins when the viral envelope proteins bind to their receptors expressed on the cell membrane of the host cell (1). The viral and cell membranes are fused and the capsid including the viral RNA is released into the cytoplasm (2). Viral RNA is reverse transcribed to DNA and is transported to the nucleus upon mitosis (3). Viral cDNA is integrated to the host cell DNA, thus forming the provirus (4). Provirus is transcribed to mRNA by the host cell's transcription machinery (5). The mRNA is translated, leading to the production of viral proteins (6). The viral proteins are further processed by viral protease and subsequently are encapsulated together with new viral RNA in order to form new viral particles. The newly formed viral particles exit the host cell through budding (8) and they undergo maturation in order to initiate the infection of a host cell (9) (Figure created with Biorender.com).

Retroviruses are often used in CAR T-cell therapy to achieve stable expression of the CAR receptor. However, the ability of the retrovirus to replicate is undesirable and potentially dangerous. For this reason, replication defective retroviral vectors are used in which the *gag, pol, pro* and *env* genes are replaced by the DNA sequence of interest. Since these proteins are necessary for viral infection, dedicated packaging cells that provide the missing proteins *in trans* are used to produce the retroviral vector for delivery and integration into T-cells. The retroviral vector contains a cassette for transgene expression typically driven by the 5' LTR promoter. Further optimisation was achieved via the

development of U3-deleted self-inactivating (SIN) vectors, the use of cellular promoters rather than viral promoter elements and deletion of coding regions of the viral genome. This was an important improvement due to reports of severe adverse events related to oncogenesis in stem cells after retroviral insertion[93,94]. Various classes of virus vectors have been used to stably integrate CAR encoding DNA into the T-cell genome such as retrovirus, lentivirus and adeno-associated virus (AAV). Lentivirus and retrovirus are the most commonly used vectors in the generation of CAR T-cells. A key advantage for lentiviral vectors is the fact that T-cell activation or proliferation is not essential for genomic integration however, lentiviral transduction of quiescent T-cells is relatively inefficient. In addition, lentiviral vectors produce a higher viral titre and contain a larger insert capacity compared to retroviral vectors. To date, both retroviruses and lentiviruses have been used in CAR T-cell clinical trials and no cases of insertional mutagenesis has been reported for either[95].

Other non-viral methods that are employed to induce CAR expression include Clustered Regularly Interspaced Short Palindromic Repeats (CRISPR)/Cas9 using electroporation or lipid based transfection for genome editing[96]. CRISPR/Cas9 technology derives from bacteria and equips these organisms with adaptive immunity against viruses by using CRISPR RNAs to silence invading nucleic acids through the introduction of double-stranded breaks in target DNA[97]. Exemplifying this use of CRISPR/Cas9 system, Eyquem et al., targeted a CD19 CAR encoding gene sequence to the TCR α constant (TRAC) locus thereby placing the CAR expression under the control of endogenous regulatory elements[96]. As a result, the CAR was uniformly expressed in T-cells, but also CAR T-cell potency was enhanced and tonic signalling averted. Another incorporation of CRISPR/Cas9 in CAR T-cell therapy has been described whereby PD-1 deficient anti-CD19 CAR T-cells were generated

to diminish T-cell exhaustion[98]. The PD-1 disruption augmented CAR T-cell function *in vitro* and caused enhanced tumour clearance *in vivo.*

Thus far, only autologous CAR T-cell therapies have been approved for clinical use. However, manufacture of autologous CAR T-cell products is not always feasible, for example in heavily pre-treated or lymphopenic patients[99]. Furthermore, autologous manufacturing processes remain time-consuming, expensive and require access to complex facilities. Given these considerations, there has been considerable interest in the development of universal "off the shelf" CAR T-cells from healthy nonmatched donors. Using the genome-editing technology TALEN (Transcription activator-like effector nuclease), investigators have disrupted the constant region of the T-cell receptor α (TRAC) in donor T-cells in order to minimise risk of graft-versus-host disease (GVHD)[100]. A second TALEN pair was used to target the CD52 gene, the target antigen of the depleting monoclonal antibody, alemtuzumab. By this means, alemtuzumab could be used to achieve selective depletion of recipient T-cells, thus promoting survival of donor CAR T-cells. In 2015, two infants with relapsed/refractory B-ALL were successfully treated with universal anti-CD19 CAR T-cells, UCART19, that had been engineered in this manner. Both patients achieved molecular remission within 28 days and went on to receive allo-HSCT. Phase 1 clinical trials for UCART19 are now underway in paediatric (PALL; NCT02808442) and adult (CALM; NCT02746952) relapsed/refractory B-ALL patients. A recent update in 2018 stated that 21 patients had received UCART19 and that overall complete remission (CR) rate was 67%[101]. In 17 patients in whom the lymphodepletion regimen included alemtuzumab, the CR rate was 82%. Among the 4 patients who did not receive alemtuzumab, minimal CAR T-cell expansion was observed. None of these patients achieved clinical response, suggesting that $CD52^+$ cell depletion is important for allogenic CAR T-cell survival. These innovative gene-editing

developments suggest that off-the-shelf allogenic CAR T-cell therapy will be more widely accessible in the future.

1.4.2 CAR design

The prototype first generation configuration designed by Eshhar et al. provides a TCR-like "signal 1" alone[102]. Since then, several CAR iterations have been developed in the laboratory and trialled in the clinic. Most of these CARs comprise four elements, the structural details of which are discussed below (Fig. 1.2). Initial experiments with first-generation CARs, showed that CAR T-cells mediated cytotoxic responses against target cancer cells. However, in pre-clinical studies and in clinical trials, first generation CAR T-cells only achieved limited anti-tumour efficacy, accompanied by lack of T-cell persistence and expansion[102,103]. Pioneered by Finney et al.[104], second-generation CARs have proven to be transformative in the clinic and promote enhanced interleukin- 2 (IL-2) secretion and T-cell proliferation. Third generation CAR constructs combine two or more costimulatory domains such as CD28, 4-1BB, OX40 or ICOS. However, there is limited clinical data to support the superiority of third-generation CAR T-cells and true enablement of this technology remains open to question[105].

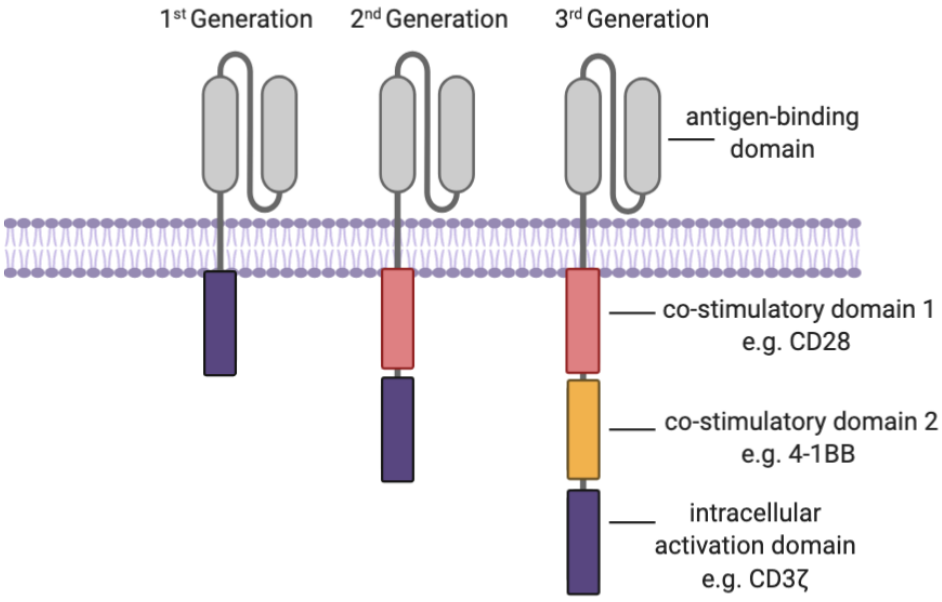

Figure 1.2 Evolution of chimeric antigen receptor (CAR) design over generations. First generation CARs consist of an antigen binding domain, usually an scFv, fused to a CD3ζ activation domain. Second generation CARs contain an additional intracellular costimulatory domain, usually CD28 or 4-1BB (CD137). Third generation CARs combine two or more costimulatory domains (Figure created with Biorender.com).

1.4.2.1 Antigen binding domain

Target selection is fundamental in the design of CARs to achieve optimal safety and efficacy. Nonetheless, challenges remain in ensuring specificity to the tumour[106]. The extracellular antigen-specific domain of a CAR is responsible for target recognition and binding. The antigen recognition domain most commonly integrated into a CAR is an scFv, as described previously. The V_H and V_L regions that comprise the scFv contain three hypervariable regions known as the complementarity determining regions (CDRs). The CDRs determine specificity and binding to the target antigen and are flanked by framework regions, which are more highly conserved. ScFvs are typically derived from murine, humanized or fully human antibodies or may be synthesized and screened via phage display libraries. The use of scFvs derived from murine antibodies increases risk of immunogenicity, favouring the rejection of CAR T-cells *in vivo* thereby limiting CAR T-cell persistence. Moreover, an IgE-based immune response has occurred in one case, leading to life-threatening anaphylaxis[107,108]. Humanizing murine scFvs or deriving scFvs from human antibodies may address this problem although inhibitory anti-idiotype antibodies may still develop[109].

1.4.2.2 Spacer and transmembrane domain

Selection of the hinge and transmembrane region can influence activity of the CAR and flexibility of the spacer can be important to allow binding to the target of interest[110]. The spacer connects the antigen binding domain to the transmembrane domain; many CARs

utilize immunoglobulin-G (IgG-) hinges or derivatives of CD28 or CD8α extracellular domains. Formation of the synapse between CAR and target is dependent on scFv epitope accessibility, location and spacer length, which has been investigated intensively. Several groups have observed that CAR T-cells are more potently activated when both the CAR binding moiety and target epitope reside close to the cell membrane[111–113]. The close proximity of CAR T-cell and target cell is important to exclude phosphatases with large extracellular domains such as CD45 and CD148 during synapse formation, which may otherwise attenuate signalling as negative regulators[114]. Furthermore, multiple studies have shown that CARs containing a short spacer induce stronger T-cell activation compared with longer spacer CAR T-cells[115,116]. In some cases, the use of longer spacers is essential because the target epitope is inaccessible and steric hinderance prevents the CAR from binding. For example, Wilkie et al[117]. demonstrated that targeting mucin-1 (MUC1) requires a CAR with a flexible and elongated spacer to overcome steric hinderance.

In anti-CD19 CAR T-cell therapy trials both CD8α and CD28 spacers have been used and demonstrated compelling anti-tumour efficacy but the impact of these spacers has not been extensively studied[118–120]. Comparison of anti-CD19 CARs incorporating either CD8α or CD28 based spacer and transmembrane region revealed CD8α-based CAR T-cells produced lower levels of cytokines, and underwent lower levels of activation induced cell death (AICD) compared to CD28-based CAR T-cells[110]. To explain the mechanism underlying these differences in CAR function, the crystal structures of CD8α and CD28 were compared[110]. In CD28-CARs the residues that comprise the hinge domain of the CD28 homodimer span the dimerization interface. Conversely, in CD8α-CARs the hinge region is less likely to be located at the dimerization interface. Moreover, the extracellular stalk of CD8α is heavily glycosylated and negatively charged further reducing the likelihood of self-association. As

such, the greater propensity of CD28 to dimerize may explain the difference in CAR activation and the ability of truncated CD28 molecules to contribute to T-cell activation[121].

1.4.2.3 Costimulatory domain

Second-generation CARs can differ in their choice of costimulatory domain, which affects the efficacy, phenotype and metabolic properties of the resulting CAR T-cells[122]. In CARs the most frequently used costimulatory domains derive from the CD28 family (CD28 and ICOS) or the TNFR family (4-1BB, CD27, OX40). In their endogenous contexts CD28 family and TNFR family molecules function with notable differences, these distinctions are translated in CAR T-cells comprising of the different costimulatory domains. Second-generation CARs used in the clinic that utilize either a CD28 or 4-1BB costimulatory module and both have shown impressive outcomes[123–125]. Preclinical evaluations of CD28 costimulation suggest it is fundamental for early activation of naïve T-cells and promotes the rapid development of T-cell effector functions. After initiation of signal 1, T-cells require co-stimulation (signal 2) to achieve optimal activation and prevent anergy[126]. Endogenous T-cell co-stimulation is usually provided by CD28 once it encounters its ligands B7.1 and B7.2. This ligation results in phosphorylation of membrane proximal YMNM motif by Src family tyrosine kinases, enabling PI3K to bind and activate AKT, which leads to initiation of signalling cascades including the mTOR[127,128], GRB2-SOS[129] and glycogen synthase kinase 3 pathways[130]. CD28 contains the proline rich motifs PRRP and PYAP which bind Lck and ITK and other SH3-containing proteins such as GRB2 and filamin A[129,131]. Furthermore, the YMNM and PYAP motifs are essential for immunological synapse formation[132].

In comparison, 4-1BB is up-regulated on T-cells 24 hours after activation to stimulate proliferation, effector function and to inhibit apoptosis[133,134]. 4-1BB contains binding sites

for TRAF1-3, and these adaptor molecules can modulate the activation of the canonical and noncanonical nuclear factor κβ (NF-κβ) pathway as well as mitogen-activated protein kinases (MAPKs)[135,136]. Signalling downstream of these TRAF family members up-regulates the transcription of pro-survival proteins such as BCL-2 and BCL-XL as well as proinflammatory cytokines such as IL-2 and IFN-γ[137]. However, in TNFR-containing CAR T-cells pathway activation occurs immediately upon CAR ligation, which potentially leads to differing biochemical function compared to non-transduced T-cells. Studies have demonstrated that activation of 4-1BB containing CARs leads to higher levels of BCL-2 and BCL-XL when compared to CD28 CARs, in keeping with the notion that TRAFs prompt transcription of anti-apoptotic proteins[137–139]. In contrast, 4-1BB CAR T-cells do not typically produce as much IFN-γ or IL-2 as CD28 CAR T-cells upon stimulation. In another study, a phosphoproteomic approach investigated phosphorylation differences between CD28 and 4-1BB CAR T-cells. Interestingly, it was revealed that CD28 CARs showed faster and higher intensities of phosphorylation, indicating higher signal strengths compared to 4-1BB CARs[140]. However, divergent phosphorylation pathways were not detected, suggesting differences in signalling kinetics and intensity explain the function disparities of CD28 and 4-1BB CAR T-cells.

Other costimulatory domains such as OX40 and ICOS have also been utilized in various CAR T-cell studies. ICOS signalling domains have been shown to promote Th17 polarisation[141]. Anti-GD2 third-generation CARs constructed with CD28 and OX40 co-stimulatory domains showed improved proliferation and expansion compared to second generation CARs using only the CD28 co-stimulatory domains[142]. Another CAR design utilizes truncated IL2Rβ along with a STAT3-binding motif with a CD28 and CD3ζ domain to activate downstream JAK-STAT cytokine signalling pathways[143]. Research by Pule et al[142] showed

that CD28-CD3ζ, OX40-CD3ζ and CD28-OX40-CD3ζ anti-GD2 CARs had comparable killing regardless of the costimulatory endodomain. However, the consequences of differential intracellular signalling mediated by CD28, 4-1BB and OX40 became apparent when comparing cytokine release and long-term expansion whereby OX40-CD3ζ CAR T-cells produced less IL-2, IFN-γ and TNFα compared to CD28-CD3ζ CAR T-cells. Nonetheless, third-generation OX40-CD28-CD3ζ CARs secreted the highest amounts of pro-inflammatory cytokines and maintained their proliferative capacity, upon multiple encounters with tumour cells, when compared to CD28-CD3ζ and OX40-CD3ζ CAR T-cells[142]. Both OX40 and CD28 domains activate NFκB but via different mediators, Vav and P13K for CD28 and TRAF2 for OX40, and NFκB independent signals Akt and AP1 are additionally transmitted[137,144]. In an attempt to modulate CAR T-cell activity, researchers developed an inducible MyD88/CD40 system[145]. MyD88 is the canonical adaptor molecule for toll-like receptor (TLR) and IL-1 receptor family signalling, known to activate NFκB and PI3K/AKT pathways to enhance T-cell effector function[146,147]. Likewise, CD40, expressed on T-cells, is a costimulatory molecule which plays an intrinsic a role in differentiation, memory formation and rescue from exhaustion[148,149]. The MyD88/CD40 CAR showed superior T-cell proliferation, cytokine production and significantly improved survival *in vivo,* relative to anti-HER2 CD28-CD3ζ CAR T-cells[145].

1.5 CAR T-cell therapy for B-cell malignancies

CAR T-cell immunotherapy has dramatically transformed the treatment of refractory B-cell malignancies[150]. Therapeutic efficacy of CAR T-cell therapy has proven unprecedented in this disease setting with response rates of up to 90% in patients with relapsed/refractory B-

cell acute lymphoblastic leukaemia (B-ALL) and up to 60% in B-cell non-Hodgkin's lymphoma (NHL)[118]. Following breakthrough clinical results in pivotal multicentre trials, the US FDA has approved three anti-CD19 CAR T-cell products for the treatment of relapsed/refractory B-cell malignancies, namely Kymriah (Tisagenlecleucel or Tis-cel), Yescarta (Axicabtagene ciloleucel or axi-cel) and Tecartus (Brexucabtagene autoleucel). Two of these products (Kymriah and Yescarta) have been approved by the European Medicines Agency (EMA). All three of these products involve second generation CAR designs in which co-stimulation is provided by CD28 (Yescarta and Tecartus) or 4-1BB (Kymriah).

1.5.1 Targeting CD19 with CAR T-cells

CD19 is a 950-kDa transmembrane glycoprotein required for normal B-cell development in humans and is expressed on the cell surface from early pro-B development through to the onset of terminal plasma cell differentiation[151,152]. It forms part of the B-cell receptor complex and its expression is restricted to lymphocytes of the B-cell lineage. The expression of CD19 at high levels by the majority of B-cell malignancies including B-ALL, chronic lymphocytic leukaemia (CLL) and B-NHL renders it as an attractive therapeutic target. B-cells are required for antibody production; however clinical experience of primary immunodeficiency disorders in which B-cells are absent (e.g. X-linked agammaglobulinaemia) show that B-cell aplasia can be effectively managed using intravenous or subcutaneous immunoglobulin replacement therapy[151]. Consequently, induction of B-cell aplasia may be viewed as a clinically acceptable on-target-off-tumour toxicity in patients with refractory B-cell malignancies treated with CAR T-cell immunotherapy.

1.5.2 Anti-CD19 CAR T-cell therapy for the treatment of B-cell NHL

As described earlier, diffuse large B-cell lymphoma (DLBCL) represents the most common subtype of NHL and the prognosis for patients with relapsed/refractory DLBCL is poor. There is a clear need for new treatment approaches to address the gap in effective therapy for patients who are refractory to standard immunochemotherapy treatments. The development of CD19-targeted CAR T-cell immunotherapy is an attractive approach to treat NHL given its superior efficacy to alternative more traditional treatment schedules. Case reports and Phase I/II trials detailing successful anti-CD19 CAR T-cell therapy led on to pivotal multicentre Phase II trials[153–156]. The ZUMA-1 trial (NCT02348216) is a multicentre Phase II trial in which 101 patients with DLBCL, primary mediastinal B-cell lymphoma and transformed follicular lymphoma (tFL) were treated with Axicabtagene ciloleucel (axi-cel), which is a second generation CD28-containing CAR T-cell product[125,157]. Long-term follow up data revealed an overall response rate (ORR) of 83% with 58% of patients achieving CR after a median follow up of 27.1 months. CAR T-cell therapy associated toxicities remain an unresolved issue. In this trial, grade 3 or higher cytokine release syndrome (CRS) occurred in 11% of patients while grade 3 plus neurotoxicity occurred in 32% of patient and unfortunately two treatment related deaths due to CRS occurred. Nonetheless, the durable responses observed represent a major improvement in outcome in a patient population that was refractory to several lines of treatment, and who otherwise have a median survival of approximately 6 months[44,45]. Based upon these results, the US FDA and EMA approved axi-cel in 2017 and 2018 respectively, for the treatment of relapsed/refractory DLBCL after two preceding lines of therapy.

Tisagenlecleucel is another anti-CD19 CAR T-cell therapy that is approved for the treatment of relapsed/refractory large B-cell lymphoma in the US and EU. Originally

developed by Dario Campana[158], it is also a second-generation CAR however, it employs 4-1BB as the costimulatory domain and is delivered by lentiviral transduction[159,160]. In multicentre Phase II trial for the treatment of relapsed/refractory DLBCL, 111 adult patients received an infusion. Of 93 evaluable patients, ORR was 52% with 40% of patients attaining CR and at 12 months the overall survival was 49%. Fortunately, no treatment related deaths occurred and grade 3 CRS and neurotoxicity occurred in 22% and 12% of patients respectively.

In total, four anti-CD19 CAR T-cell therapies have been approved for the treatment of relapsed/refractory B-cell NHL. However, comparisons of efficacy, toxicity and durability across these trials is difficult because of variations in patient populations, differences in prior treatment and conditioning regimens, including the use of bridging chemotherapy. Cross-trial comparisons are further complicated due to differences in CAR design, toxicity grading and cell manufacturing protocols. A summary of Phase II trials of CD19-specific CAR T-cell therapy targeting B-NHL is provided in Table 1.2

Table 1.2: Phase II clinical trials in B-NHL

Trial	JULIET / Novartis	ZUMA-1 / Kite	Transcend / Juno	ZUMA-2 / Tecartus
CAR-T	Tisagenlecleucel *Kymriah*	Axicabtagene ciloleucel *Yescarta*	Liscoabtagene maraleucel	Brexucabtagene autoleucel
Co-stimulatory domain	4-1BB	CD28	4-1BB: defined 1:1 CD4:CD8 ratio	CD28
Patients	111	108	268	68
Disease	DLBCL, tFL	DLBCL, tFL, PMBL	Aggressive B-NHL	r/r MCL
ORR	52%; 33% at 6-months	82%; 38% at 27.1-months	73%	85%
CR	40%; 29% at 6-months	58%; 37% at 27.1-months	53%	59%
CRS grade ≥ 3	22%	11%	2%	15%
Neurotoxicity grade ≥ 3	12%	32%	10%	31%

1.5.3 Anti-CD19 CAR T-cell therapy for the treatment of B-ALL

In a global Phase II pivotal clinical trial, 75 paediatric and young adult patients with relapsed/refractory ALL were treated with tisagenlecleucel[124]. At 12 months post CAR T-cell infusion, the rate of event-free survival was 50% and overall survival was 76%. Toxicity such as CRS occurred in the majority of patients whilst neurotoxicity occurred in 40%. However, many patients (28%) succumbed to relapse, most of which involved CD19-negative disease. Notably, tisagenlecleucel CAR T-cells were detectable for as long as 20 months after the initial treatment indicating long-term persistence. These data led to the FDA and EMA

approval of tisagenlecleucel as a treatment for B-ALL in children and young adults, under the trade name, Kymriah.

In parallel, researchers at Memorial Sloan Kettering Cancer Centre (MSKCC) published results involving 53 adult patients with relapsed/refractory ALL, reporting long-term outcome and safety (NCT01044069)[161]. In this study, 67% of patients achieved minimal residual disease (MRD) negative CR and median overall survival was 12.9 months at a follow up of 29 months. Here, disease remission was significantly associated with higher peak CAR T-cell expansion and severe toxicity was associated with high disease burden. A summary of Phase II trials of CAR T-cell therapy targeting B-ALL is provided in Table 1.3.

Table 1.3: Phase II trials in B-ALL

Author/ Trial	Centre	CAR	Patient	MRD-neg CR	CRS grade ≥ 3	Neurotoxicity grade ≥ 3
Maude/ ELIANA	Novartis/Multi centre	4-1BB	75 paediatric & young adult	81%	46%	13%
Park	MSKCC	CD28	53 adult	67%	26%	42%
Lee	NCI	CD28	21 paediatric & young adult	67%	16%	0%
Turtle	FHCRC	4-1BB	30 adult	86%	28%	50%
Gardner	Seattle Children's	4-1BB	45 paediatric & young adult	93%	23%	23%

1.5.4 CAR T-cell associated toxicities

The most common toxicities to occur following CAR T-cell infusion are CRS, neurotoxicity and B-cell aplasia. Symptoms typically occur soon after the infusion. However, incidence of severe CRS and neurotoxicity is varied across different trials. Management of toxicities include the use of IL-6 receptor blocking antibodies such as tocilizumab either alone or in combination with corticosteroid. Nonetheless, toxicity attributable to CRS can be fatal in some cases[118].

1.5.4.1 Cytokine release syndrome

Cytokine release syndrome is the most common toxicity associated with CAR T-cell treatment and it is characterised by a systemic inflammatory response[162,163]. Patients suffering with CRS usually present with fever, hypotension, malaise, cardiac dysfunction and renal failure among other symptoms. Higher disease burden and increased CAR T-cell dose have been related to higher risk of CRS. Unsurprisingly, severity of CRS is also correlated with higher peak blood CAR T-cell expansion which is further promoted by the intensity of prior lymphodepletion. Pro-inflammatory cytokines that are markedly increased include sIL-2 receptor α and interferon (IFN)-γ and are related to T-cell expansion. Activated macrophages release IL-6, IL-10 and macrophage inflammatory protein (MIP)-1β. Circulating IL-6 levels are correlated with CRS severity and administration of IL-6 receptor antagonist, tocilizumab, is a commonly used approach for management of CRS.

1.5.4.2 Neurotoxicity

Neurological toxicities are another common complication of CAR T-cell infusion and can occur independent of CRS. The majority of symptoms are reversible and self-limiting, and

include confusion, tremors, seizures and expressive aphasia[164]. The exact cause of neurotoxicity remains unclear. However, endothelial activation and leakage of elevated cytokine levels across the blood-brain barrier to promote pericyte stress may be contributing factors[165]. In a murine model of CRS established by van der Stegen et al.[166], IL-1 and IL-6 produced by activated macrophages proved to be key contributors to CRS and neurotoxicity[167,168]. As such, interventions that block both IL-1 and IL-6 may protect patients from lethal toxicity. In a recent paper, using single-cell RNA sequencing Parker et al.,[169] report of brain mural cells expressing CD19 across brain regions. Mural cells maintain blood-barrier integrity therefore, on target neurotoxicity by CAR T-cells recognising CD19+ mural cells causes increased blood-brain barrier leakiness.

Potential solutions to mitigate toxicity associated with CD19 CAR T-cells involve further engineering CARs to reduce cytokine production. A variant anti-CD19 CAR has been described in which the intracellular and extracellular CD8α hinge/transmembrane domain was genetically altered[170]. This modification significantly reduced levels of inflammatory cytokines whilst maintaining cytotoxicity against $CD19^{+}$ tumour cells. In a phase I study of this CD19-BBz(86) CAR, 6/11 B-NHL patients achieved complete remission. Importantly, no neurotoxicity was observed in any patients and only grade 1 CRS was reported. Serum cytokine levels were also analysed and IL-6, IFN-γ, tumour necrosis factor (TNF)-α remained at basal level at different time points after treatment. Another approach to limit toxicity is to reduce CAR binding affinity. The “CAT’ CAR was recently described with a substantially lower affinity for CD19 compared to FMC63, due to an enhanced off rate of CD19 binding. This modification translated into enhanced anti-tumour activity *in vitro*[171]. In a clinical study, efficacy results were comparable to those reported in trials of tisagenlecleucel and

other published data[124,172]. Toxicity profile was favourable and no patients developed severe CRS or neurotoxicity despite heightened expansion and persistence of CAT CAR T-cells.

1.5.5 The challenge of relapse following CD19 CAR T-cell therapy

Remarkable response rates have been achieved with anti-CD19 CAR T-cell immunotherapy in patients with relapsed/refractory B-cell malignancies. However, many patients relapse and a substantial proportion of these involve CD19-negative disease. One measure under investigation to prevent tumour escape due to antigen loss is to target other or multiple B-lineage antigens.

1.5.5.1 Antigen loss or diminution as a mechanism of disease relapse

Following successful CAR T-cell-induced disease remission, a common mechanism of relapse is target antigen modulation. Previously, similar mechanisms of disease recurrence have been described following the administration of other targeted immunotherapeutic approaches, such as monoclonal antibody therapies[173]. Reports from multiple trials and institutions involving anti-CD19 CAR T-cell therapy have suggested that 7-25% of patients relapse with CD19-negative disease[174]. A recognised mechanism leading to loss of CD19 is alternative splicing to generate isoforms that removes the cognate epitope and/or reduces surface expression and disrupts CD19 trafficking to the cell surface[175–177]. However, researchers at Novartis suggest that alternative splicing occurs at extremely low frequencies and accounts for a minor fraction of CD19 negative relapses[178]. In the study, specimens collected from paediatric and young-adult B-ALL patients at screening and at CD19 negative relapse underwent RNA and/or DNA sequencing. The results showed that nearly all tumour cells in relapsed samples contained a *CD19* mutation that was predicted to lead to a

truncated protein lacking membrane anchorage, leading to loss of surface expression. These mutations were not present prior to CAR T-cell therapy or in CD19 positive relapsed patient samples, suggesting that CAR T-cell driven immune pressure drives post-therapy mutations in the *CD19* gene.

Lineage switching, by which the phenotype of B-ALL tumour cells change from lymphoid to CD19-negative myeloid cells has been reported as another mechanism of CD19 antigen escape after CAR T-cell therapy[179]. The evolved myeloid cell population no longer expressed CD19 and acquired the phenotypic characteristics of acute myeloid leukaemia (AML). This form of relapse was observed in two paediatric and one adult patient after CAR T-cell therapy[108,180,181]. In a murine model, Jacoby et al[182]. showed that this phenomenon was dependent on the E2a:PBX transgene which can drive the development of either lymphoid or myeloid neoplasms.

Diminution of CD19 expression is sufficient to enable tumour escape and resistance to CAR T-cell therapy. A mechanism that affects antigen-low tumours is CAR T-cell mediated trogocytosis whereby CD19 is transferred to T-cells in a reversible manner[183]. As a result, T-cells co-expressing the CAR and CD19 succumb to T-cell fratricide and an exhausted phenotype. An example of antigen down-modulation leading to leukaemic relapse was described by Fry et al[184]. In this study anti-CD22 CAR T-cells were used to treat B-ALL in patients who had failed prior therapy with CD19 CAR T-cell therapy. However, a decrease in cell surface expression and antigen density of CD22, without any detectable mutation, was sufficient to evade CAR T-cell killing.

A unique case report of a paediatric patient with B-ALL who relapsed with CD19-negative disease describes that the CD19 CAR was introduced into a single leukaemic B-cell blast clone during CAR T-cell manufacturing[185]. The tumour clone was expanded and infused

into the patient alongside the CAR T-cells; once expressed on the leukaemia cell surface, the CAR bound adjacent CD19 and effectively masked the CD19 epitope from CAR T-cells. Although this case report was a rare occurrence, it does raise questions with regards to CAR T-cell manufacturing and implementing more stringent methods to remove all tumour cells from the engineered product.

Given the propensity of antigen modulation as a method of leukaemic evasion of CAR T-cell therapy, multi-antigen targeting CAR constructs have been developed that can overcome variability in antigenic expression. Preclinical development of a bivalent CAR co-targeting CD19 and CD22 described similar release of IL-2 and IFN-γ *in vitro* compared to single antigen-targeted CARs[186]. Moreover, CD19/CD22 bivalent CAR T-cells eradicated NALM-6 B-ALL leukaemic xenografts and patient derived xenografts *in vivo,* including a CD19-negative patient derived xenograft. Schneider et al. developed a tandem-CAR co-targeting CD19 and CD20 in which the anti-CD19 and anti-CD20 scFvs were joined via a linker[187]. The tandem-CAR was equally effective as single antigen targeted CARs *in vitro* and *in vivo* but induced less antigenic loss of CD19 and CD20. In a Phase I study treating patients with B-ALL or DLBCL, a single CAR construct that incorporates both anti-CD19 and anti-CD22 scFvs into one bivalent receptor, with 4-1BB and CD3ζ intracellular signalling domains was investigated[188]. Six adult patients with were treated, leading to induction of CR in two patients (1 each with ALL and DLBCL) while in paediatric B-ALL patients, 4/4 achieved CR. Amrolia et al. also developed a bi-cistronic vector encoding dual CARs against CD19 and CD22 with OX40 and 4-1BB costimulatory domains respectively[189]. To enhance sensitivity, a pentavalent hinge was used in the CD22 CAR and the product, AUTO3, was trialled in phase I/II studies treating DLBCL and ALL. In a recent update of the DLBCL trial, in which patients were treated with AUTO3 followed by the anti-PD1 antibody pembrolizumab, researchers

reported a CR rate of 57% and no dose limiting toxicities[190]. The AMELIA trial is evaluating AUTO3 in paediatric and young-adult ALL patients. Ten heavily pre-treated ALL patients received CAR T-cells and 9/10 achieved CR. At 12- and 15-months post infusion two patients remain in complete molecular remission. A lack of CAR T-cell persistence has been suggested as the cause for relapse in other patients.

1.5.5.2 Improving CAR T-cell persistence

Another mechanism of disease resistance relates to lack of CAR T-cell persistence, an issue unlikely to be solved by targeting multiple antigens. The use of murine scFvs has been associated with anti-transgene immune responses against CAR T-cells, leading to poor T-cell expansion and persistence. To decrease immunogenicity and improve efficacy, CARs that have been targeted using humanized scFv regions have been developed and tested in the clinic[191,192].

The intrinsic fitness of CAR T-cells has been implicated as the most important factor shaping the clinical response in patients with advanced CLL, a disease in which response to anti-CD19 CAR T-cell therapy varies from 26-71%[119,193,194]. In patients responding to anti-CD19 CAR T-cell therapy there was an upregulation of a transcription signature related to early memory differentiation. These patients also had a more robust expansion potential both *ex vivo* and *in vivo.* Furthermore, in responding patients the IL-6/STAT3 pathway was upregulated in CAR T-cells while blockade of STAT3 signalling diminished T-cell proliferation. In comparison, CAR T-cells analysed from non-responding patients upregulated genes related to effector T-cell differentiation, exhaustion and glycolysis. The results from this study promote the idea that CAR T-cell fitness may be used as a biomarker to determine likelihood of successful therapeutic efficacy[193].

A promising strategy to prolong CAR T-cell persistence involves selecting less differentiated T-cell subsets that have a greater proliferative capacity such stem cell memory T-cells (T_{SCM}) and central memory T-cells (T_{CM})[122,195]. A preclinical study investigated whether T-cell expansion and function could be improved by culture of the cells in the presence of a phosphatidylinositol 3-kinase δ (PI3Kδ) inhibitor and vasoactive intestinal peptide (VIP) antagonist[196]. Researchers demonstrated that antagonism of PI3Kδ and VIP signalling pathways *ex vivo* resulted in the generation of less terminally differentiated T-cells at greater numbers and with enhanced cytotoxic activity. Furthermore, *in vivo* CAR T-cell persistence was improved after expansion with both inhibitors.

Differential costimulatory signalling can influence CAR T-cell persistence and function thereby affecting the durability of anti-tumour activity. As such, engineering strategies to fine tune signalling are being developed, including modifying the costimulatory domain of the CAR. In a recent study, Guedan et al. showed that a single amino acid substitution within the YMNM motif of CD28 reduced exhaustion and differentiation of CD28 CAR T-cells, thereby enabling longer persistence and durable anti-tumour control[197]. In another study, researchers mutated the YMNM and PRRP while retaining the PYAP motif within the CD28 endodomain which resulted in optimized signalling and reduced T-cell exhaustion, thus enabling longer persistence *in vivo*[198]. To combine the benefits of the rapid activation kinetics of CD28 costimulation and the better persistence associated with 4-1BB signalling, Zhao et al. co-expressed constitutive 4-1BBL in CD28-containing second generation CAR T-cells[199]. This configuration resulted in increased CAR T-cell persistence, elevated CD8:CD4 ratio and decreased expression of exhaustion markers. These 4-1BBL expressing CAR T-cells have since been trialled in patients with B-NHL and CLL and deemed safe with a CR rate of 57%[200].

1.6 Parallel CAR (pCAR) platform

To refine the precision, potency and safety of CAR T-cell therapy, considerable further optimisation of CAR technology is underway at many centres. The key advancement that prompted the clinical breakthrough of CAR T-cell therapy was the delivery of CD28 or TNFr costimulation by second generation CARs[201]. When compared to first-generation CARs that provide TCR-like signalling alone, second-generation CAR T-cells had markedly superior anti-tumour activity in man and have achieved striking success against refractory B-cell and plasma malignancies[159,194,201,202]. Given this, it was logical to investigate whether potency could be further amplified by insertion of an extra tandemly aligned co-stimulatory module, to create third-generation CARs[203]. Early studies supported the predicted superiority of third-generation CAR T-cells, with results reporting enhanced survival, proliferation, synapse formation, higher activation status and anti-tumour activity[203–208]. Nonetheless, other studies with third-generation CARs have been inconsistent, achieving only marginal superiority or, sometimes explicitly inferior performance compared to second-generation designs[117,209,210]. Clinical outcomes with third-generation CARs have also been underwhelming, with no responses induced by third-generation CAR T-cells in a recent study[211]. In comparison, similarly targeted first-generation CAR T-cells elicited complete tumour regression in 3 of 11 patients in an earlier clinical trial[212,213]. Thus, the effect of each additional signalling module is not additive and, in fact, can be detrimental.

A potential explanation for this contradiction relates to the position of signalling modules in these synthetic receptors. Physiologically, the TCR/CD3 complex and costimulatory receptors are aligned *in trans* and instruct T-cell activation in this manner. Moreover, the juxta-membrane placement of the CD28 costimulatory endodomain is vital for its function[201]. In comparison, in third-generation CARs, two of the three signalling

modules are located away from the plasma membrane. This may reduce access to membrane-associated signalling partners and may also suffer as a result of steric hindrance between co-stimulatory units, limiting access to downstream intermediates. For example, a study investigating the CAR interactome and signalosome found that second-generation CARs induced expression of a constitutively phosphorylated form of CD3ζ that resembled the endogenous species. This phenomenon was dependent on the size of the intracellular domains as the second-generation CARs were able to engage additional species of CD3ζ in a supramolecular signalling complex[214]. Accordingly, it was hypothesised that integration of dual (CD28 and 4-1BB) costimulation in a "parallel" CAR (pCAR) platform would lead to potentiation of anti-tumour activity as this architecture would provide a more natural platform to achieve synthetic integration of signalling[215] (Figure 1.3).

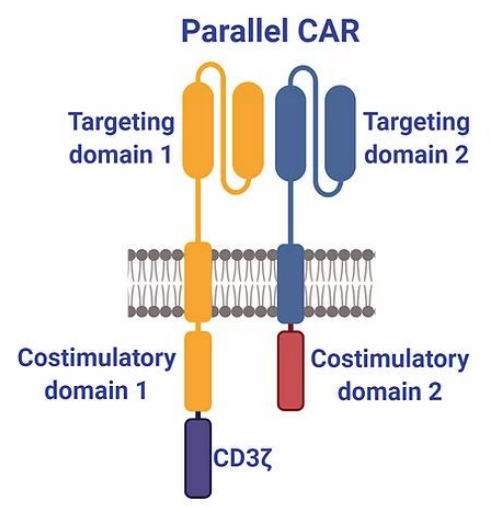

Figure 1.3 Parallel CAR (pCAR) structure. A second-generation CAR that contains a CD28 co-stimulatory domain is co-expressed with a CCR that contains a TNFr-type costimulatory domain, typically 4-1BB. As such, the two costimulatory domains are integrated in parallel across the cell membrane (Figure created with Biorender.com).

Split chimeric receptors have previously been designed to deliver TCR and CD28 costimulation and show that complementary signals can be delivered to enhance IL-2 production, proliferation and target-depended cytotoxicity. Nonetheless, this paradigm has

not been harnessed to provide dual costimulation. To address this, the pCAR platform was engineered and includes a second-generation CAR co-expressed *in trans* with a chimeric co-stimulation receptor (CCR) that provides complementary co-stimulatory signalling.

1.7 Aims & objectives

The overarching aim of this project was to investigate the potential utility of pCAR-engineered T-cells for the treatment of B-cell malignancies and to investigate pCAR T-cell function both *in vitro* and *in vivo.*

Specifically, my objectives were:

- To generate second-generation CARs in which the FMC63 scFv has been mutated to create a panel of CARs with a spectrum of affinities.
- To compare the avidity of these CARs for their target antigen, CD19.
- To generate anti-CD19 pCARs and study their cytotoxicity and re-stimulation potential *in vitro*, when co-cultivated with CD19-expressing target cells.
- To study the anti-tumour response of pCARs compared to second-generation controls in a clinically relevant xenograft NSG model.
- To generate dual-targeting pCARs that would recognise CD19 and another distinct B-cell lineage marker and compare their *in vitro* and *in vivo* efficacy.

Chapter 2: Materials and Methods

2.1 Engineering of CAR constructs

2.1.1 Generation of plasmids

All recombinant DNA constructs were expressed using the SFG retroviral vector. An example of all retroviral constructs is shown schematically in Figure 2.1. Successful cloning was confirmed by restriction pattern agarose gel analysis and sequencing identified no mutations within the coding sequences (Source Bioscience, UK).

Complementary DNAs encoding for the F-2, 1F5 and RFB4 scFvs were designed using published sequences and synthesized by Integrated DNA Technologies (IDT)[216–218]. The second-generation F-2 CAR was designed as follows; a CD8α leader was fused to the FMC63 scFv (arranged as V_H – V_L separated by a $[SerGly4]_3$ linker). For generation of R-2 and 1-2 CAR constructs, human colony stimulating factor-1 receptor (CSF-1R) leader sequence was fused to cDNA encoding either RFB4 or 1F5 scFvs, respectively (arranged as V_H – V_L separated by a Cooper linker[219]). The synthetic cDNAs were flanked with a 5' NcoI restriction sites (that coincided with the signal peptide start codon) and a 3' NotI restriction site. These fragments were subsequently cloned into the unique NcoI and Not1 restriction sites of SFG A20-28z[220] placing the CAR cDNA upstream of the fused myc epitope tag_CD28 hinge/transmembrane/ endodomain_CD3ζ endodomain. Ligation reactions are described in section 2.2.7. All leader-peptide fusions were predicted to undergo signal peptide cleavage at the correct junction (http://www.cbs.dtu.dk/services/SignalP/).

The CDR3 region of the V_H domain within the FMC63 scFv was identified using www.abyss.org. To generate variants with an altered ability to binding CD19, and alanine (A)

residue was substituted for the first or second glycine (G01, G02) or alternatively for the first, second, third, fourth or fifth tyrosine (Y01-Y05) within the CDR3 region of the V_H domain. The amino acid substitutions were introduced into the F-2 CAR via single site mutagenesis by Genscript (Piscataway, NJ, USA). Nomenclature and description of second-generation CARs is listed in Table 2.1.

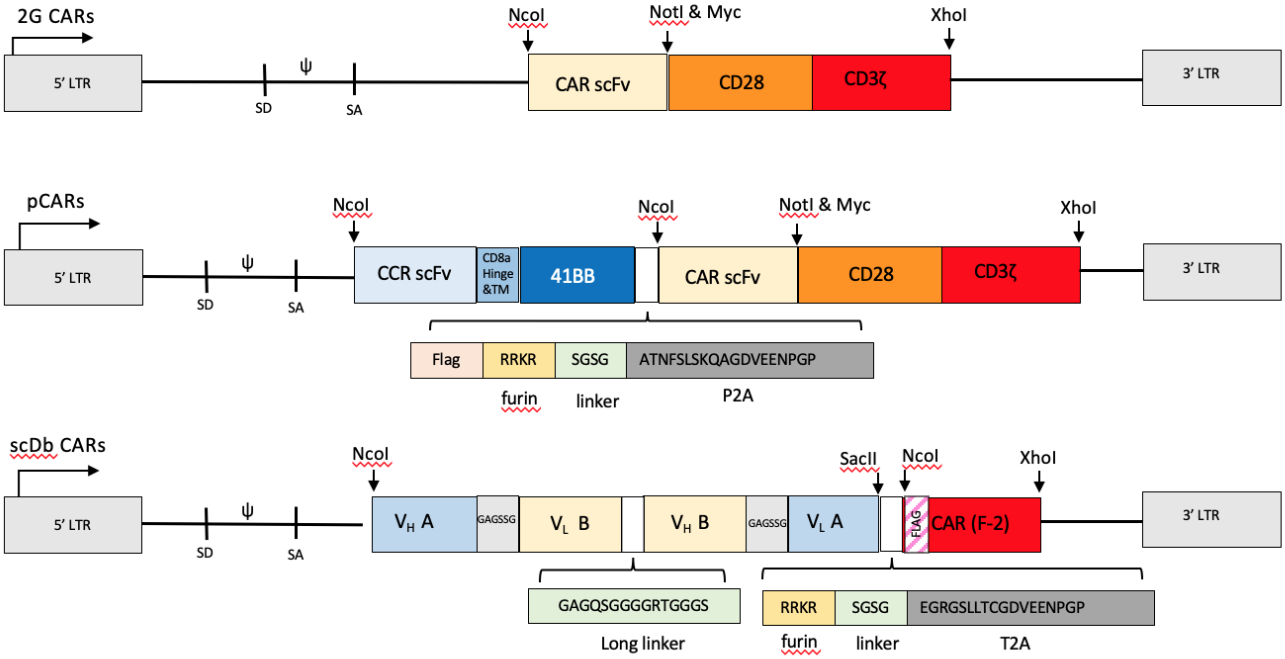

Figure 2.1 A schematic of the SFG retroviral vector encoding for CARs, pCARs and single-chain diabody (scDb) CARs. An example of each type of construct is shown with specific scFvs targeting CD19, CD20, CD22 or an anti-myc scFv (derived from 9E10 antibody) being inserted for CAR, CCR and scDb. All were cloned into the SFG retroviral vector containing 5' and 3' long terminal repeat (LTR) sequences and the psi (y) packaging signal. All CAR components contain a myc epitope tag recognised by the 9e10 antibody. All pCARs contain an intracellular flag epitope tag. scDb CAR constructs also contain a flag epitope tag upstream of the FMC63 scFv.

2.1.2 Generation of pCAR constructs

Codon optimised cDNAs encoding candidate pCARs were synthesised by Genscript (Piscataway, NJ, USA). To engineer FBB/Y01-Y05 or G01-G02 pCARs a CCR comprising of a linear fusion of the following elements; a CSF-1R leader peptide, FMC63 scFv binding domain (V_L-V_H order), CD8α spacer and transmembrane domain, a 4-1BB co-stimulatory

endodomain and FLAG epitope tag was synthesised ("FBB"). The CCR was flanked by NcoI and AflIII and cloned upstream of each of the CDR3 mutated CARs. The CCR and the CAR are linked by a furin cleavage site, $[SerGly4]_3$ linker and porcine teschovirus (P2A) ribosomal skip peptide. Codon wobbling has been used to minimise direct repeats within the scFv modules.

The 1BB/F pCAR was synthesised in a similar fashion. A CCR comprising a linear fusion of a CSF-1R leader peptide, 1F5 scFv binding domain (V_L-V_H order), CD8α spacer and transmembrane domain, a 4-1BB co-stimulatory endodomain and FLAG epitope tag was synthesised ("1BB"). The CCR was flanked by NcoI and AflIII and cloned upstream of each of the F-2 CAR. The CCR and the CAR are linked by a furin cleavage site, $[SerGly4]_3$ linker and T2A ribosomal skip peptide. Codon wobbling has been used to minimise direct repeats within the scFv modules. Alternative spacers have been used within both scFvs for the same motive.

To generate RBB/F pCAR a cDNA comprising a linear fusion of the following elements was synthesised by IDT; a CSF-1R leader peptide and RFB4 scFv binding domain (V_L-V_H order). The cDNA was flanked by AccI and SacII and inserted to replace the 1F5 scFv within the 1BB/F by restriction cloning. For RBB/G02 and RBB/Y05 pCARs, single site mutagenesis was used to substitute the 2nd glycine and 5th tyrosine with alanine, respectively.

Nomenclature and description of pCAR constructs is listed in Table 2.2.

2.1.3 Generation of single-chain diabody (scDb) CARs

For ease of detection, an extracellular flag tag was incorporated into F-2 after the CSF-1R leader peptide using PCR amplification and restriction cloning (see section 2.2). Briefly, primers listed in the appendix were used to PCR amplify FMC63 V_L - $[SerGly4]_3$ linker - FMC63 V_H -Myc from SFG F-2. The PCR amplified DNA was flanked with restriction sites MluI

and MfeI and inserted into SFG 3V5_T2A_FLAG_ICR62_MY (provided by Dr. Adam Ajina) to generate SFG 3V5_T2A_FLAG_F-2. To generate single-chain diabody CARs, a cDNAs comprising a linear fusion of the following elements was synthesised by IDT. For 9E10.R/F-2; a long CD8α leader peptide, 9E10 V_H, GAGSSG linker, RFB4 V_L -long linker- RFB4 V_H, GGGDAS linker, 9E10 V_L. The scDb and the CAR are linked by a furin cleavage site, $[SerGly4]_3$ linker and T2A ribosomal skip peptide. For R.9E10/F-2 the orientation of the scDb was reversed and RFB4 V_H was placed in the first position with the long linker between 9E10 V_L and 9E10 V_H. The cDNA was flanked by AgeI and SacII and inserted upstream of the T2A within SFG 3V5_T2A_FLAG_F-2.

Table 2.1 Second-generation CAR construct nomenclature and designation

	Name	Target	scFv	Costimulation	Signalling
Second-generation CAR	F-2	CD19	FMC63	CD28	CD3ζ
	Y01	CD19	mFMC63	CD28	CD3ζ
	Y02	CD19	mFMC63	CD28	CD3ζ
	Y03	CD19	mFMC63	CD28	CD3ζ
	Y04	CD19	mFMC63	CD28	CD3ζ
	Y05	CD19	mFMC63	CD28	CD3ζ
	G01	CD19	mFMC63	CD28	CD3ζ
	G02	CD19	mFMC63	CD28	CD3ζ
	1-2	CD20	1F5	CD28	CD3ζ
	R-2	CD22	RFB4	CD28	CD3ζ

Table 2.2 pCAR construct nomenclature and designation

	Name	CCR scFv	CAR Target	CCR scFv	CAR scFv	CCR costimulation	CAR costimulation	Signalling
pCAR	FBB/Y01	CD19	CD19	mFMC63	FMC63	41BB	CD28	CD3ζ
	FBB/Y02	CD19	CD19	mFMC63	FMC63	41BB	CD28	CD3ζ
	FBB/Y03	CD19	CD19	mFMC63	FMC63	41BB	CD28	CD3ζ
	FBB/Y04	CD19	CD19	mFMC63	FMC63	41BB	CD28	CD3ζ
	FBB/Y05	CD19	CD19	mFMC63	FMC63	41BB	CD28	CD3ζ
	FBB/G01	CD19	CD19	mFMC63	FMC63	41BB	CD28	CD3ζ
	FBB/G02	CD19	CD19	mFMC63	FMC63	41BB	CD28	CD3ζ
	1BB/F	CD20	CD19	mFMC63	FMC63	41BB	CD28	CD3ζ
	RBB/F	CD22	CD19	1F5	FMC63	41BB	CD28	CD3ζ
	RBB/G02	CD22	CD19	RFB4	FMC63	41BB	CD28	CD3ζ
	RBB/Y05	CD22	CD19	RFB4	FMC63	41BB	CD28	CD3ζ

2.2 Molecular Biology Techniques

2.2.1 Restriction enzyme digestion

DNA digestion and restriction patterns were used to accurately verify successful cloning and presence of inserts. Restriction endonucleases cut DNA at specific sites thus digesting plasmids using this method will produce DNA fragments of known lengths. An example of a double restriction enzyme digest is described below.

2.2.1.1 Protocol

1. A 20µl reaction mixture was used for each restriction digest reaction and all components were kept on ice throughout, prior to incubation.
2. 1µg DNA template
3. 2µl NEB Buffer
4. 10 units (U) Enzyme 1
5. 10U Enzyme 2
6. Xµl Nuclease free H_2O (to make up to 20µl)

7. Reaction mixtures were incubated at the appropriate temperature required for optimal activity (usually 37°C).
8. Once completed, each reaction was mixed with 6X DNA loading dye and separated by electrophoresis on an agarose gel of the appropriate percentage to achieve optimal separation of fragments (typically 1% agarose).

2.2.2 Polymerase chain reaction (PCR)

Polymerase chain reaction (PCR) provides the ability to amplify specific DNA sequences.

Table 2.3 PCR reactions. Reagents and quantities used in PCR reactions are listed.

Reagent	Quantity
DNA	100ng
Forward Primer	10µM
Reverse Primer	10µM
Q5 Reaction buffer	5µl
Q5 High Fidelity DNA polymerase	0.25µl
Nuclease-free water	Xµl (to 20µl)

Samples were subjected to a PCR program:

1. Initial denaturation at 98°C for 30 seconds
2. 30 cycles of denaturation, annealing and elongation.
    i. 98°C for 30 seconds
    ii. 50–72°C for 20 seconds (NEB Tm Calculator used to determine appropriate annealing temperature for primers)
    iii. 72°C for 20 seconds
    iv. Final elongation at 72°C for 10 minutes

3. The PCR product was run on an agarose gel to look for the presence of a single, discrete band.

2.2.3 Agarose gel electrophoresis

Agarose gel electrophoresis was used for separation of DNA fragments by size. The constant mass to charge ratio of DNA molecules allows separation of linearized DNA fragments according to fragment size. Migration rates are dependent on the pore size of the gel, which in turn is determined by the agarose concentration. The DNA fragments together with the 1kb DNA ladder (NEB, USA) were prepared accordingly by adding 1X gel loading dye (NEB, USA) and were loaded carefully into the wells. The gel was run at 100V for approximately 1 hour. The gel was visualised using a UV light device and the DNA fragments were isolated using a sterile razor blade and were placed at 4˚C until further processing. Excised bands were purified using a gel extraction kit (Qiagen) following manufacturers instructions.

2.2.4 Ligation reactions

Restriction digestion led to the generation of DNA fragments with compatible sticky ends thus allowing their ligation. The ligation was achieved by mixing the insert and vector of interest with QuickLigase (NEB, USA) for 5 minutes at room temperature (table 2.1). The ligated products were then validated by transforming *Escherichia (E.) coli* competent cells and by screening the DNA isolated from bacterial clones.

Table 2.4 Ligation reactions. Reagents and quantities used in ligation reactions are listed.

Reagent	Quantity
Nuclease-free water	Up to 20µl
NEB Quick Ligase buffer	10µl
Vector	50ng
Insert	37.5 ng
NEB Quick Ligase	1 µl

2.2.5 Transformation of *Escherichia (E.) coli*

To propagate and scale-up recombinant plasmid DNA used throughout the project, competent *E. coli* bacteria were used. Heat shock transformation of DH5α competent bacteria (C2987H, high efficiency, New England Biolabs) allows the introduction of circular DNA plasmid which confers resistance to a specific antibiotic thus allowing for selection with the antibiotic.

2.2.1.1 Protocol

1. A 25µl aliquot of competent DH5α competent *E. coli* (NEB, UK) was thawed.
2. 2µl of plasmid DNA was incubated with the *E. coli* for 30 minutes on ice.
3. Bacteria were then heat shocked for 90 seconds at 42°C and then placed on ice for 5 minutes.
4. 300µL SOC medium was added and samples were shaken at 220 rpm in an incubator shaker for at least 1 hour at 37°C.
5. Transformed bacteria were then spread onto antibiotic-containing agar plates cultured at 37°C for 12-16 hours and bacteria clones positive for the plasmid were identified.

2.2.6 Production of agar plates

To culture transformed bacteria for scaling up plasmid DNA, they were grown on agar plates. Ampicillin was used for growth selection as all plasmid vectors used in this study contain the ampicillin resistance gene.

2.2.5.1 Protocol

1. 500ml LB-agar (Fisher Scientific, Loughborough, UK) was melted in a microwave oven for 40 minutes at 40% power.
2. Molten agar was left to cool and 50mg ampicillin (Alfa Aesar, Massachusetts, United States) was added and mixed thoroughly by swirling.
3. The solution was poured into Petri dishes and left to cool and then solidify at room temperature.
4. Petri dishes were sealed with parafilm and stored at 4°C.

2.2.7 Isolation of plasmid DNA: Miniprep

Bacterial clones were selected for mini-culture and submerged in 4mL LB containing ampicillin. The bacterial culture was shaken at 37°C at 220rpm for 16 hours. After scaling up the bacterial culture the cells were pelleted. Preparation of DNA from minipreps was completed via the Miniprep kit (Qiagen). Analytic digestion with restriction enzymes and analysis of fragment size by agarose gel electrophoresis identified clones positive for the CAR construct. Sequencing (SourceBioscience) of positive clones was used to confirm successful cloning. A correct bacterial clone was then inoculated into 200mL LB with ampicillin and shaken at 37°C at 220rpm overnight. DNA was isolated from bacteria using the Maxiprep kit (Qiagen) following supplier's instructions.

2.2.8 Quantification of DNA concentration

The concentration of DNA eluted from Mini- and Maxiprep solutions was measured using a Nanodrop spectrophotometer (Nanodrop ND-100, Thermo Scientific Massachusetts USA). DNA concentration is directly calculate by the Nanodrop software and given as ng/µl using the Beer-Lambert equation: Absorbance = -log (intensity $_{sample}$ / intensity $_{blank}$)

2.3 Cell culture techniques

2.3.1 Media

D10: 500mL Dulbecco's Modified Eagle Medium (DMEM) + 4.5g/L glucose (Lonza, Basel)

50mL Foetal Bovine Serum (FBS)

L-glutamine (Sigma-Aldrich, UK).

I10: 500mL Iscove's Modified Dulbecco's Medium (IMDM) + 4.5g/L glucose (Lonza, Basel)

50mL Foetal Bovine Serum (FBS)

L-glutamine (Sigma-Aldrich, UK).

R5: 500mL Roswell Park Memorial Institute (RPMI) Media 1640 (Lonza, Basel)

25mL Human AB Serum (Sigma-Aldrich, UK)

L-glutamine (Sigma-Aldrich, UK)

2.3.2 Cell lines

All cells were incubated at 37°C, with 5% CO_2 with H_2O.

Table 2.5 Cell lines used throughout

Cell line	Description
Raji	Burkitt Lymphoma cell line
NALM-6	B cell precursor leukaemia
293T	Human retroviral packaging cell line derived from HEK293 cell line, expressing the gene encoding the SV40 large T antigen.
293Vec-GALV	HEK 293-based packaging cell line that produces retroviral vectors pseudotyped with the GALV envelope
LO68	Human malignant mesothelioma

2.4 Retroviral vector production

2.4.1 Transient transfection of 293T cells

Vectors were produced by transient transfection into 293T cells. 293T cells were chosen as the cell line for the production of retroviral particles due to its ease of transfection.

2.4.1 Protocol

1. 1.65 x 10^6 293T were seeded on a 100mm dish in 10mL of I10.
2. After 24 hours cells are 50-70% confluent and are ready for triple transfection.
3. Transfection mixture was prepared as follows:
    i. 470µl serum free IMDM
    ii. 30µl Gene Juice (Novagen, Merck)
4. The solution was incubated for 5 minutes at room temperature
5. 12.5µg total DNA was added to the transfection solution and incubated for 15 minutes at room temperature:
    i. 3.125µg env RD114

ii. 4.687µg gag-pol

iii. 4.687µg retroviral plasmid CAR construct

6. The mixture was added to the 293T cells dropwise and incubated at 37°C 5% CO_2.
7. Viral supernatant was harvested at 48 and 72 hours later and was snap frozen in 1.5ml aliquots and stored at -80°C.

2.4.2 Generation of retroviral packaging cell lines

To generated stable 293Vec-GALV retroviral packaging cells, retroviral supernatant produced by 293T cells (as described in 2.4.1) was used.

2.4.2 Protocol

1. $3x10^5$ 293Vec-GALV cells were seeded on to a 6-well cell culture plate in 1mL D10 media
2. After 24 hours, 293Vec-GALV cells had adhered.
3. 3mL of viral supernatant was rapidly thawed at 37°C and added to 293Vec-GALV cells.

2.5 PBMC isolation, expansion and retroviral transduction

2.5.1 PBMC isolation and activation

Peripheral blood mononuclear cells (PBMCs) were isolated from healthy donors by density gradient centrifugation. Recruitment of healthy volunteer donors for this study was approved by the National Health Service Research Ethics Committee (reference 09/H0804/92 and 18/WS/0047).

2.5.1.2 Protocol

1. Blood was drawn and immediately mixed with 1X citrate dextrose solution to prevent coagulation.
2. 25mL of fresh blood was slowly layered onto 15ml Ficoll-Paque.
3. Tubes were centrifuged at 800 x g for 35 minutes with acceleration and deceleration set to 0.
4. Mononuclear cells were aspirated using a Pasteur pipette into phosphate buffered saline (PBS) and centrifuged at 400 x g for 10 minutes.
5. The cell pellet was re-suspended and washed in PBS for 10 minutes at 400 x g.
6. Supernatant was aspirated and the cell pellet resuspended in 10ml R5 media and counted.
7. Isolated PBMCs were re-suspended in R5 at a density of 3 x 10^6 cells/mL and activated with 5µg/mL phytohemagglutinin (PHA).
8. Cells were fed with IL-2 (100U/mL) after 24 hours.

2.5.2 Production of RetroNectin coated plates.

RetroNectin (TakaRa, Japan) promotes co-localisation of retrovirus with target cells to enhance transduction efficiency[221]. RetroNectin is formed from a fragment from the extracellular matrix protein fibronectin that binds the target T-cell through a CS-1 domain and a cell-binding domain, which interacts with the VLA-4 and VLA-5 integrin receptors respectively. Attachment of the virus to the heparin-binding domain present in RetroNectin between the CS-1 and CBD causes co-localisation of the target cell and the virus, thus greatly improving gene transfer efficiency.

2.5.2.1 Protocol

1. 200µg of RetroNectin was resuspended in 18mL PBS

2. 1 or 3mL of the solution was transferred to non-tissue culture treated 24 or 6 well plates, respectively, using a Pasteur pipette.
3. RetroNectin plates were stored at 4°C prior to use.

2.5.3 Retroviral transduction of human T-cells

Retroviral mediated transduction of human T-cells caused stable CAR expression by integrating coding DNA into the host T-cell genome. Forty-eight hours after activation, T-cells were transduced in a 24- or 6-well plate. Activated T-cells were counted using trypan blue exclusion and 0.5 or 1 x 10^6 viable cells were added to each well. To each well, 1.5 or 3mL of retroviral supernatant was added and each well was supplemented with 100U/mL IL-2. Transduction efficiency of T-cells was determined by flow cytometry after 4-6 days in culture.

2.5.4 Retroviral transduction of tumour cells

To stably transduce tumour cells retroviral supernatant from 293T cells or 293Vec-GALV packaging cells was used. To generate LO69-CD19$^+$ cells, 0.3x10^5 parental LO68 cells were seeded on to a 6-well plate in 1mL. After 24 hours 3mL SFG CD19 retroviral supernatant, produced as in 2.4.1, was added to adhered cells. Transduction efficiency was determined by flow cytometry after 72 hours. To transduce NALM-6 cells with SFG ffLuc/RFP, 293Vec-GALV packaging cells were generated as described in 2.4.2. 1x10^6 NALM-6 were seeded on a RetroNectin plate and 3mL of viral supernatant from the packaging cell line was added. Transduction efficiency was determined by flow cytometry after 72 hours. To achieve >90% transduction efficiency, NALM-6 ffLuc/RFP$^+$ (NALM-6 LT) were facs sorted.

2.6 *In vitro* functional assays

For direct comparison of different CAR constructs, normalization for transduction efficiency was accomplished by the addition of untransduced T-cells from the same donor.

2.6.1 Cytotoxicity assays

The in vitro cytotoxic activity of CAR T-cells was investigated by performing co-cultivation assays. In order to perform these experiments, CAR T-cells were expanded for 10 days post transduction. Tumour cell viability was determined using the following formula:
% cell viability = (absorbance/luminescence of co-culture reaction /absorbance or luminescence of untreated tumour cells alone) x 100%.

2.6.1.1 MTT assay

Tumour cells were incubated with T-cells at specified effector to target (E:T) ratios. In the case of adherent targets, residual tumour cell viability was quantified using an MTT assay at 48 and/or 72 hours. After removal of the supernatant and residual T-cells, MTT (Sigma, Poole, UK) was added at 500 µg/mL in D10 medium for 40 minutes at 37°C and 5% CO_2. Formazan crystals were resuspended in DMSO and absorbance was measured at 560 nm.

2.6.1.2 Luciferase assay

Firefly luciferase catalyses the conversion of a molecule of D-luciferin to an electronically 'excited' molecule of oxyluciferin when in the presence of magnesium, ATP and oxygen. As dead cells cannot catalyse this reaction, the number of viable tumour cells is proportional to the amount of luminescence detected. By this means, the magnitude of T-cell induced cytotoxicity could be quantified. Tumour cell viability was monitored by luciferase assays

and 48 and/or 72 hours. D-luciferin was added at 150 mg/mL immediately prior to luminescence reading. In each case, tumour cell viability was calculated as follows: (absorbance or luminescence of tumour cells cultured with T cells/absorbance or luminescence of untreated monolayer alone) x 100%.

2.6.2 Restimulation assays

Target cells (NALM-6, Raji and LO68) and T-cells were co-cultured in triplicates in a 24-well plate at a 1:1 E:T ratio without further addition of cytokines. Supernatant was harvested after 24h for cytokine analysis. At 72 hours tumour viability was assessed by MTT (LO68) or luciferase assay (NALM-6 and Raji). If T-cells achieved more than 80% tumour cell destruction they were restimulated on a fresh tumour monolayer, without correction of T-cell number. This process was repeated until T-cells failed to destroy >80% of tumour cell monolayers.

2.6.3 Cytokine production

Cytokine release by T-cells were determined by analysing supernatants after 24-hours of co-culture using a human IFN-γ or human IL-2 enzyme-linked immunosorbent assay (ELISA) as described by the manufacturers. Plates were read at 450nm and the concentration of each sample calculated with respect to the known concentrations of the standard curve.

2.6.4 Flow cytometry

Multicolour flow cytometry was used to detect protein expression at the cell surface and intracellularly. Flow cytometry acquisition was performed using a LSRFortessa Flow Cytometer and data analysis using FlowJo LLC (both BD, Biosciences, USA). Cell staining was

performed using reagents listed in the appendix, maintaining cells on ice during incubations unless stated otherwise. Intracellular staining was performed by fixation with 0.4% formaldehyde followed by permeabilization using PBS+0.5% BSA+0.1% saponin. Cells were subsequently stained for intracellular proteins for 30 min at 4°C. All gates were set using isotype control antibodies and where necessary, a viability stain was included. All FACS plots presenting CAR T cell phenotype data were pre-gated on gated CAR+ cells. For non-transduced T cells, whole T cell populations were used for analysis

2.6.4.1 General staining protocol

1. A pre-determined number of cells were removed (adherent cells were removed with trypsin or cell dissociation buffer) and washed in PBS.
2. Cells were re-suspended in 100µl PBS in a flow cytometry tube and incubated with specified concentrations of primary or directly conjugated antibody/isotope on ice for 30 minutes.
3. *N.B. Additional step for non-conjugated antibodies: Samples were washed in 2ml PBS, centrifuged and re-suspended in 100µl PBS*.
4. *N.B. Additional step for non-conjugated antibodies: Cells were then incubated with matched concentrations of secondary antibody for 30 minutes on ice in the dark.*
5. Samples were again washed with PBS, centrifuged and re-suspended in 300µl PBS prior to analysis. Sample FACS tubes were kept on ice and in the dark until analysis.
6. Results were compared to control using a matched staining protocol (or to cells stained with the secondary antibody alone where stated).

2.6.5 Fluorescence activated cell sorting (FACS)

Fluorescence activated cell sorting (FACS) of live cells separates a population of cells into sub-populations based on fluorescent labelling. FACS was performed using a BD FACSAria II cells sorter. Briefly, 20-40x10^6 /mL CAR^+ T-cells were stained with 9E10 hybridoma supernatant (10µl/ 2.5x10^5 cells) for 30 minutes on ice. Samples were washed with PBS+2% BSA, centrifuged and resuspended with 20µl goat anti-mouse PE antibody for 30 minutes on ice. Samples were again washed with PBS+2% BSA, centrifuged and re-suspended at 40x10^6cells/mL. Sorted cells were collected in R5 medium and allowed to rest for 24 hours prior to functional assays.

2.7 CD19 CAR binding studies – z-Movi

Microfluidic chips were first cleaned with water, air, bleach, sodium thiosulphate, 12 mol/L HCl, and 1 mol/L NaOH several times. After adding poly-l-lysine (Sigma P4707) for 15 minutes, the chip was flushed with air and dried on a heat block (45–55°C) for 1 hour, pulling in air every 10 to 20 minutes. Chips were rehydrated with PBS before proceeding to cell immobilization. Trypsinized and washed LO68-$CD19^+$ cells were resuspended and added to the poly-l-lysine–coated chip, then incubated for approximately 16 hours. The next day, flow sorted CAR-T cells were serially flowed in the chips and incubated with the target cells for 5 minutes (at 37°C) prior to initializing a 3-minute linear force ramp reaching 100pN. During the force ramp, the z-Movi device captures time series of images using a bright field microscope integrated into the platform. Detached cells were levitated towards the acoustic nodes, this allows tracking of the cells based on their XY positions. Changes in the Z-position results in a change in the diffraction pattern, which allows the distinction between cells that

have adhered to the substrate and cells suspended to the acoustic nodes. This information is used to correlate cell detachment events with a specific rupture force. Cell detachment was acquired using z-Movi Tracking_v1.6.0 software and post experiment image analysis was performed using Cell Tracking offline analysis_v2.1. Data are presented as median acoustic force (rForce) which is the relative force required to elicit cell detachment and calibrated to 10µM polystyrene beads**.**

2.8 *In vivo* anti-tumour activity

All in vivo experimentation adhered to U.K. Home Office guidelines, as specified in project licence number 70/7794 or P23115EBF and was approved by the King's College London animal welfare and ethical review body (AWERB).

2.8.1 Intravenous injection of leukaemic cells and T-cells in mice

Mice were heated for 15 minutes in a warming box to encourage vasodilatation of the tail veins. 5 x 10^5 NALM-6 cells transduced with SFG ffLuc/RFP were injected intravenously in a volume of 0.2mL. Five days post NALM-6 injection, mice received 0.5 x 10^5 CAR+ T cells in a single injection within a volume of 0.2ml, depending on experimental outline. CAR+ T cells were analysed by FACS for CAR expression one day prior to injection and were generally injected as bulk (transduced and untransduced) populations.

2.8.2 Bioluminescent imaging of mice

To assess engraftment and anti-tumour activity of CAR T-cells, tumour growth was evaluated by bioluminescence imaging (BLI) using an IVIS Spectrum Imaging platform (PerkinElmer) with Living Image software (PerkinElmer, Beaconsfield, UK). To monitor

tumour status, mice were injected i.p. with D-luciferin (150 mg/kg) and imaged under isoflurane anaesthesia after 20 min.

2.8.3 Monitoring of mice

In all experiments, mice were inspected and weighed daily in the first week after CAR T-cell injection. After, mice were closely monitored and weighed weekly. End point predetermined by length of experiment or if animals became ill (indicated by piloerection, hunched posture or loss of response to the environment). In addition, a loss in weight of $\geq$15% would result in the animal being culled.

2.8.4 Spleen and peripheral blood preparation

After sacrifice, single cell suspensions were made of spleen by maceration through a cell strainer. Blood was collected by cardiac puncture from euthanised mice into Eppendorf tubes containing citrate-dextrose (Sigma, Poole, UK) as anticoagulant. Red blood cells were lysed using 1X RBC Lysis Buffer (Biolegend, UK) according to manufacturer's instructions. Cells were pelleted by centrifugation at 300G for 5 minutes and then staining according to protocol 2.7.1.

2.9 Statistical analyses

All data are derived from biological replicates unless otherwise indicated. For analysis of multiple groups, statistical analysis was performed using one-way or two-way ANOVA test (depending on the number of independent variables) followed by Tukey's multiple comparisons test. Alternatively, a paired or unpaired two-tailed Student's *t* test, Wilcoxon matched-pairs signed rank test, Mann-Whitney test or Kruskal-Wallis test was performed

where appropriate. Survival data was analyzed using a Log rank (Mantel-Cox) test. All statistical analyses were performed in GraphPad Prism v8.4.2. Unless otherwise stated, data were expressed as mean ± SEM. Statistical analyses of *in vitro* assays were undertaken as indicated in figure legends.

Chapter 3: *In vitro* characterisation of VH CDR3 mutated FMC63 CAR T-cells

3.1 Introduction

3.1.1 The CD19-specific F-2 CAR

Chimeric Antigen Receptor (CAR) T-cell immunotherapy has radically altered the treatment of refractory B-cell malignancies (see section 1.5). To date, all clinical anti-CD19 CAR trials have used an scFv as the binding domain of the CAR. More specifically, studies performed at the National Institutes of Health (NIH) and University of Pennsylvania (UPenn) have used the FMC63 scFv, whereas investigators at the Memorial Sloan Kettering Cancer Center (MSKCC) used an scFv derived from the SJ25C1 hybridoma[99,153,222]. However, both tisagenlecleucel and axi-cel which have been approved by the US FDA and European Medicines Agency (EMA) utilize the mouse-derived FMC63 scFv, which has a binding affinity for CD19 of ~ 5nM[216]. The influence of affinity on the function of CD19-specific CAR T-cells has been explored relatively recently, highlighting the need to for optimisation of thia attribute (discussed further below). Here, site directed mutagenesis was used to introduce single point mutations in the variable heavy (V_H) chain of FMC63 in order to generate scFvs with a spectrum of binding strengths for CD19.

3.1.2 Impact of CAR affinity on T-cell function

The interaction between the TCR and peptide-MHC (pMHC) complex regulates T-cell activation. Important factors that influence the sensitivity of T-cells to become activated in this manner are antigen density and TCR affinity. The affinity of a TCR for its cognate pMHC is typically between 1 – 50μM.[223,224] This affinity threshold is crucial for maintaining self-

tolerance toward cells that display pMHC which bind TCRs with lower affinity. However, native TCR affinity for pMHC is generally considerably lower than reported for scFvs that are commonly used to direct target specificy of CARs. Increased CAR affinity may increase specificity for ligand and enable recognition of low density antigens. However, this may also promote the occurrence of severe adverse effects due to on-target, off-tumour toxicity[225,226]. Moreover, T-cells can sequentially lyse multiple target cells, a mechanism known as serial killing, which may be reduced with a high affinity CARs[227]. This likely results from an unnaturally slow off-rate causing prolonged target cell association that can be detrimental to T-cell function, owing to exhaustion and susceptibility to AICD[228,229]. Conversely, an exceedingly low affinity CAR may cause suboptimal CAR T-cell activation as sufficient antigen recognition does not occur[115]. For these reasons, fine tuning of scFv affinity is an important factor to achieve optimal CAR T-cell function.

Multiple studies have shown that lowering affinity of scFv/ target interaction can lead to improved CAR T-cell function[230–232]. For instance, Park et al compared μM affinity CAR T-cells targeted against intracellular adhesion molecule (ICAM)-1 to nM affinity counterparts and showed improved cytokine production, T-cell expansion, anti-tumour efficacy and safety of lower affinity CAR T-cells[233]. Similarly, CD38-specific CAR T-cells in which scFv affinity had been reduced by ~1000-fold produced similar cytokine levels and exhibited improved proliferation and in vivo efficacy, when compared to CAR T-cells in which specificity was conferred by native scFv[230]. More recently, a substantially lower affinity anti-CD19 CAR dubbed “CAT” was developed which achieved enhanced in vitro anti-tumour activity compared with FMC63 CAR T-cells[171]. In a clinical study, paediatric patients with relapsed/refractory B-ALL were treated with CAT CAR T-cells and achieved comparable response rates to those reported in other published trials[124,172]. More impressively, CAT CAR

T-cells were detectable at up to 24 months post-infusion and showed heightened expansion in vivo in the absence of severe adverse events. These studies suggest that existing FMC63-based CAR T-cell affinities exceed the threshold required for optimal function. As such, it may be prudent to generate CARs with varied affinities for the same target and determine the lowest affinity at which CAR T-cells perform best.

3.1.3 Functional avidity and T-cell efficacy

The relationship between affinity and avidity is another aspect to consider when designing CARs. Avidity describes the overall binding strength of multiple receptor-ligand interactions including co-receptors and co-stimulatory molecules[234]. Therefore, assessing the functional avidity may more accurately describe functional outcomes of CAR T-cell and antigen interactions. Measurement and investigation of CAR T-cell avidity has been limited to date. In a study comparing engineered T-cells expressing low affinity αβ-TCR chains vs. high affinity TCR-like antibody-based CARs, researchers found that high avidity of TCR-like antibody-based CARs had a detrimental effect on T-cell function[235]. The higher avidity CAR T-cells were less sensitive to the target peptide at lower concentrations and secreted significantly reduced levels of IFN-γ. In addition, cytolytic activity of higher avidity CAR T-cells was less efficient toward tumour cells and did not maintain specificity.

So far, surface plasmon resonance (SPR) has been the predominant method used to assess antibody-antigen affinity. However, SPR requires production of recombinant soluble scFv-Fc and does not reflect the multiple CAR T-cell-target interactions involving various co-stimulatory molecules, adhesion molecules and co-receptors. Highlighting this disparity, a study showed affinity as a poor predictor of T-cell activation and high affinity was not deterministic for productive signalling[236]. To understand the avidity interactions between

different CAR T-cells and CD19, z-Movi™ (Lumicks) technology was used. z-Movi™ is a high throughput single-cell resolution, lab-on-a-chip technology that enables measurements of avidity of binding interaction between cells[237].

3.1.4 Aims

- To mutate the FMC63 scFv and create CARs with a spectrum of binding strengths for CD19.
- To investigate the avidity of the mutated derivative CAR T-cells using z-Movi™ technology.
- To investigate CAR T-cell functionality using *in vitro* assays to assess target cell killing and cytokine production.

3.2 Results

3.2.1 Generating novel CD19 CARs with differing affinities compared to FMC63

Recent clinical data indicates that the affinity of the widely used anti-CD19 FMC63 scFv is excessive for optimal CAR function[120]. To create CARs with varying affinity to CD19, I undertook alanine scanning mutagenesis of complementarity determining region (CDR)3 of the FMC63 variable heavy (V_H) chain and created a panel of seven scFv (Fig. 3.1a). To construct second-generation CARs, FMC63 (F-2) or each individual mutated scFv was incorporated into a 28ζ framework (Fig. 3.1b). All constructs contain an extracellular 10-amino acid myc epitope tag which was included to enable CAR detection by flow cytometry. Table 2.1 describes the nomenclature and components of second-generation CARs.

a

	FMC63 V_H CDR3
F-2	HYYYGGSYAMDY
Y01	- A - - - - - - - - -
Y02	- - A - - - - - - - -
Y03	- - - A - - - - - - -
G01	- - - - A - - - - - -
G02	- - - - - A - - - - -
Y04	- - - - - - - A - - - -
Y05	- - - - - - - - - - A

b

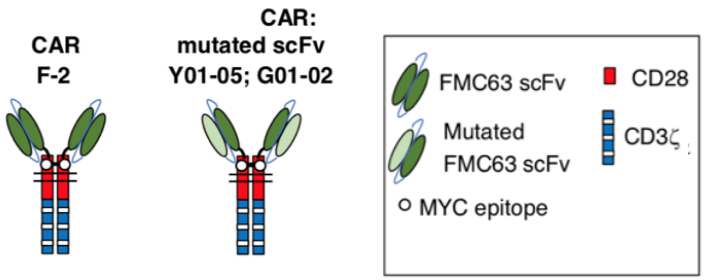

Figure 3.1 Schematic overview of second-generation CARs generated with mutated FMC63-derived scFvs. a, The indicated Y->A or G->A mutations were introduced into the V_H CDR3 region of FMC63 scFv. The resultant CARs were named as indicated in panel a. F-2 refers to the unmodified scFv sequence. b, Unmodified and mutated FMC63 scFv were used to target CD19 as a second-generation 28ζ CAR. All CARs contained a myc epitope tag to facilitate their detection by flow cytometry.

3.2.2 Expression of CARs by retrovirus transduced primary human T-cells

Peripheral blood mononuclear cells (PBMCs) isolated from healthy donors were transduced 48h post T-cell activation with SFG retroviral vectors encoding for the CD19-specific CARs shown in Fig. 3.1, as described in material and methods (section 2.5.3). After 5 days, cells were incubated with the 9e10 antibody, which binds to the myc epitope in the CAR extracellular domain, and then analysed by flow cytometry. Figure 3.2 shows that high levels of CAR expression were detected on the cell surface in all cases.

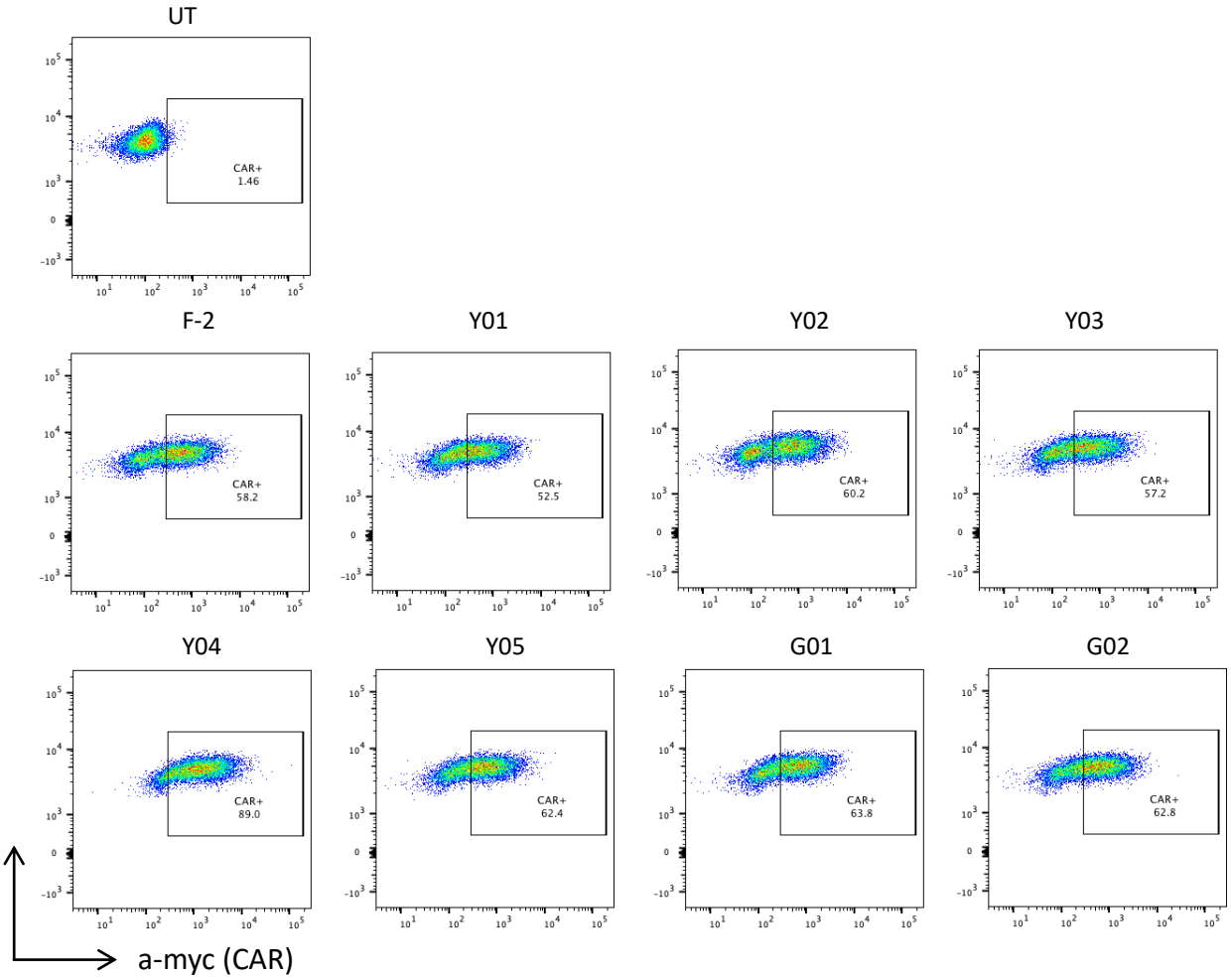

Figure 3.2 Expression of CDR3 mutated and control F-2 CAR in T-cells. Primary human T-cells were transduced with the indicated CAR-encoding retroviral vectors and assessed by flow cytometry on day 5 post-transduction. The presence of the CARs was detected by flow cytometry after incubation with 9e10 (anti-Myc) antibody followed by goat anti-mouse PE. The level of CAR expression in all cases was compared to untransduced (UT) T-cells probed with the same antibody combinations. Data shown are representative flow cytometry plots. Comparable results were obtained with 7 independent donors.

3.2.3 Binding of recombinant human CD19-Fc to wild type and mutated scFv-containing CAR T-cells

To determine if chimeric receptors containing a mutated FMC63 scFv could still recognise CD19, binding studies were performed with recombinant human CD19-Fc fusion protein. CAR expression was first detected using the myc epitope tag to confirm successful T-cell transduction (see supplementary Fig. 7.1). As expected, F-2 CAR T-cells bound CD19-Fc at both tested concentrations (Fig. 3.3 and Fig. 3.4). CAR T-cells Y01, Y04 and Y05 were also capable of binding CD19-Fc and the percentage bound increased with an increase in Fc-protein concentration (Fig. 3.4). However, CAR T-cells Y02, Y03, G01 and G02 showed minimal binding to CD19-Fc at both concentrations.

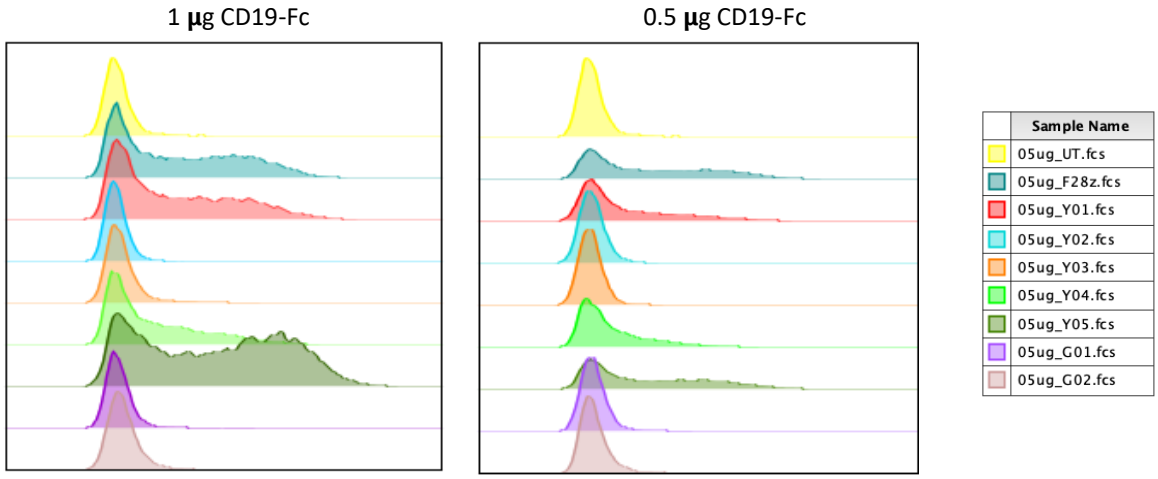

Figure 3.3 Ability of CAR T-cells to bind CD19-Fc recombinant protein. Primary human T-cells were transduced with the indicated CD19-specific CARs and were stained with 0.50 µg or 1.0 µg CD19-Fc protein. Binding of Fc fusion protein was detected with Alexa-Fluor conjugated anti-human IgG. Data shown are representative flow cytometry plots. Similar results were obtained with 2 independent donors.

Surface expression analysis showed that CARs Y02, Y03, G01 and G02 did retain the ability to bind CD19-Fc, however this was markedly reduced compared to F-2 (Fig. 3.4b).

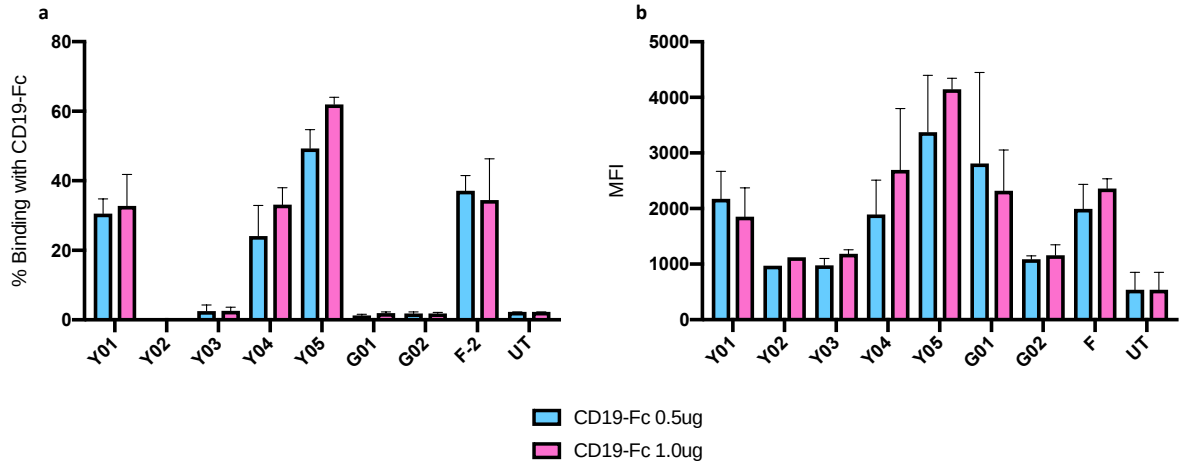

Figure 3.4 Binding and expression of CD19-Fc in CDR3 mutated CARs. a) Pooled data from 2 donors showing percentage of CAR binding CD19-Fc. b) Mean fluorescence intensity (MFI) of bound CD19-Fc from 2 independent donors (mean ± SEM from 2 independent donors). UT – untransduced T-cells.

3.2.4 Determining avidity for CD19 of CDR3 mutated CARs

Avidity describes the overall binding strength between cellular receptors and their corresponding ligands and determines how strongly a cell interacts with its target. To evaluate the binding avidity of F-2 and mutated derivatives for CD19, the high throughput cell interaction platform, z-Movi™ (Lumicks), was used. The z-Movi™ platform utilises acoustic waves to apply controllable forces to T-cells. The principle behind z-Movi™ is that the CAR T-cells will flow over the immobilized tumour cells and bind their target. Increasing acoustic force is applied and low avidity cells, that require less force to be separated from their target, will detach and move toward the nodal plane. A schematic of the workflow is shown in Fig. 3.5

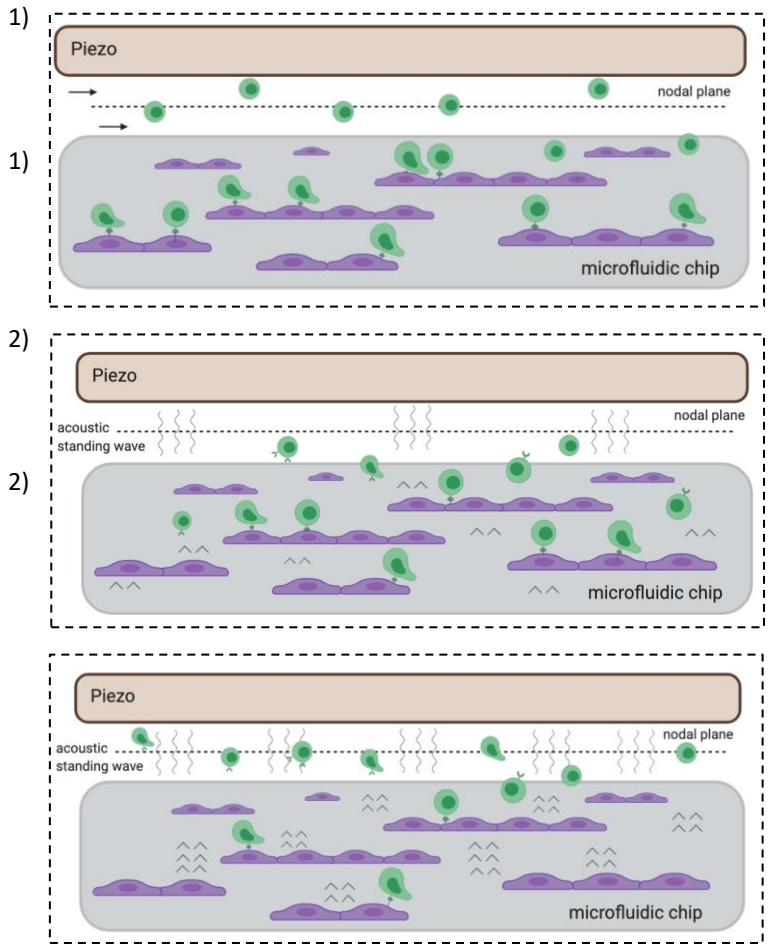

Figure 3.5 z-Movi™ avidity analyser principle and workflow. 1) Target cancer cells are immobilized on the surface of the microfluidic chip. CAR T-cells are flowed over the chip and allowed to sediment and attach onto target cells. 2) A voltage is applied which drives the piezo element to generate an acoustic wave that forces CAR T-cells to move vertically to the nodal plane. 3) Increasing levels of acoustic force are applied to separate T-cells on the basis of the strength of their adhesive interaction with the target cells. Low avidity cells require less force to be separated from the target and will detach before high avidity cells.

To measure avidity using z-Movi™ it was desirable to establish an adherent cell line with strong expression of CD19 and which could be immobilized on the chip. The human mesothelioma malignant cell line LO68 naturally lacks expression of B-cell markers and is not susceptible to killing by CD19-targeted CAR T-cells. Hence, LO68 cells were genetically engineered to express high levels of CD19 via retroviral transduction (LO68-CD19^{+}) (Fig. 3.6).

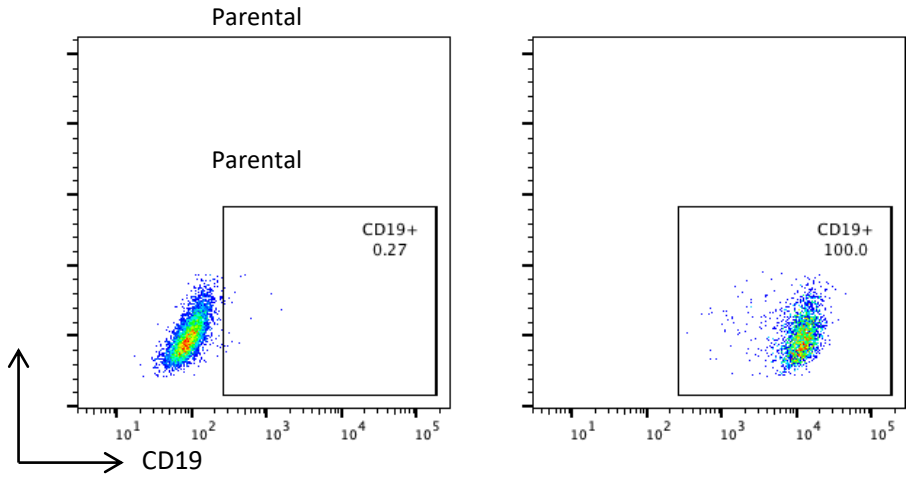

Figure 3.6 Retrovirus transduced LO68 cells engineered to express CD19. The mesothelioma line LO68 was transduced with an SFG retroviral vector that encodes for human CD19. Antigen expression was detected by flow cytometry after incubation with a directly conjugated anti-CD19 antibody.

Prior to avidity measurements, CAR T-cells were flow sorted to >90% purity (supplementary Fig. 7.2). Fig. 3.7a shows the CDR3 mutated CAR T-cells presented a spectrum of binding avidities for CD19. Specifically, Y03 and G01 exhibited significantly reduced binding avidity that was comparable to untransduced T-cells. Moreover, Y04 and F-2 CAR T-cells had the most similar avidity for CD19 whereas Y05 and G02 CAR T-cells displayed intermediate avidity. The percentage of CAR T-cells bound to LO68-CD19^{+} after the application of a minimal relative force (rForce) was also significantly different between T-cells engineered to express the CDR3 V_H mutated CARs (Fig. 3.7b).

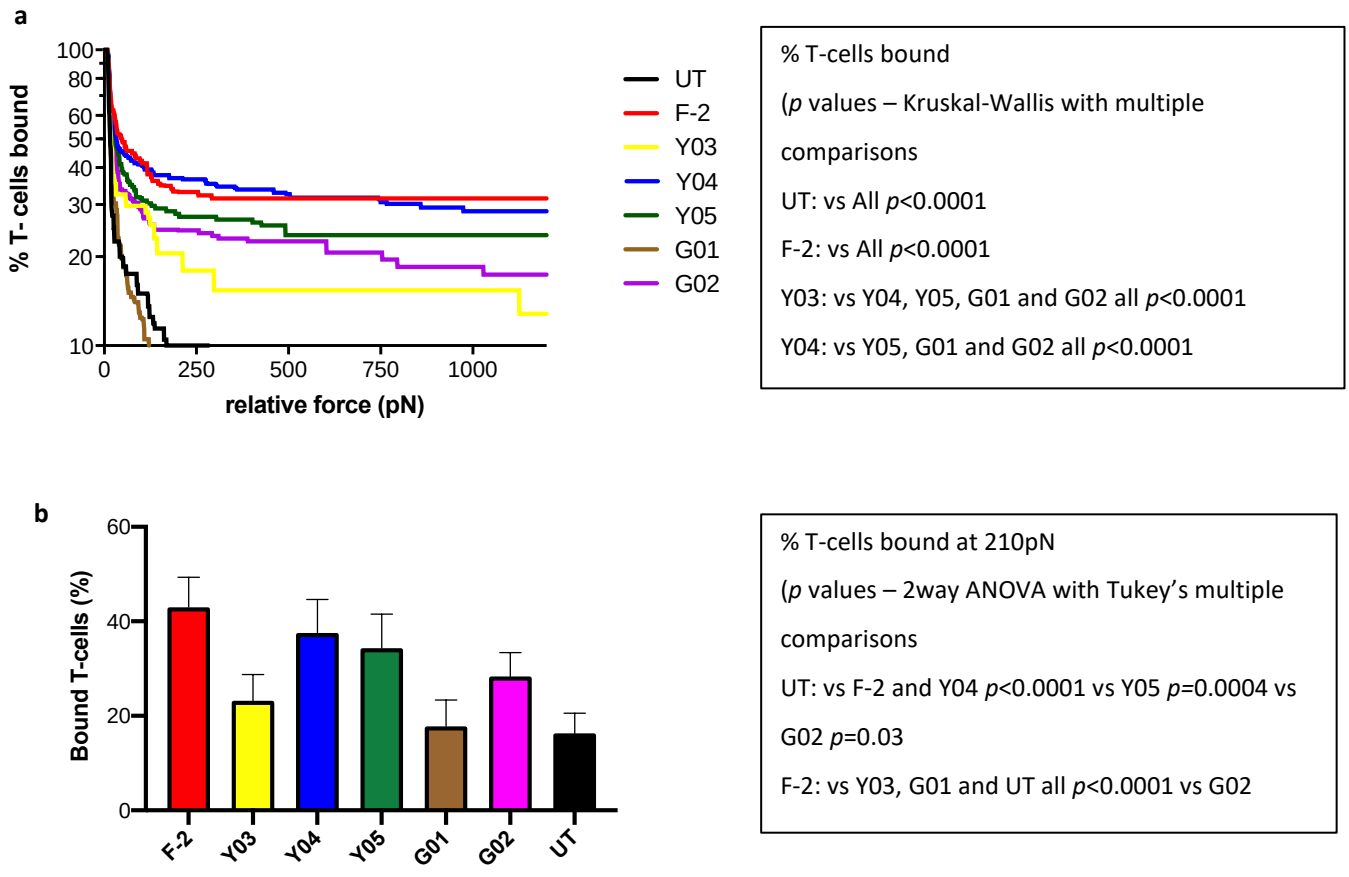

Figure 3.7 Analysis of CAR T-cell avidity for CD19-expressing LO68 tumour cells. a) T-cells were transduced to express F-2 CAR or derivatives with a mutated CDR3 VH region and flow sorted to >90% purity. CAR T-cells were incubated on a monolayer of LO68-CD19+ cells in a z-Movi microfluidic chip. Increasing acoustic force (rForce) was applied and the percentage T-cells bound to the monolayer was determined. Since data were not normally distributed, they are presented as median rForce which is the relative force required to elicit cell detachment and calibrated to 10µM polystyrene beads. b) Bar plot shows the overall mean percentage of bound T-cells after applying minimal rForce (210pN) to detach a mean of 90% UT T-cells. Mean ± SEM. (11 technical replicates from 3 independent donors**).**

The avidity score represents the ratio of the mean rForce per cell required to detach CAR T-cells from the LO68-CD19^{+} tumour monolayer, compared to untransduced (UT) T-cells. As expected, Y03 and G01 CAR T-cells with a lower avidity score also had increased detachment from the tumour monolayer (Fig. 3.8a). Again Y04, Y05 and G02 CAR T-cells showed an intermediary avidity score. The rForce require to detach individual CAR T-cells from the LO68-CD19^{+} monolayer is shown in Fig. 3.8b. When compared to F-2 CAR T-cells, Y03, Y05 and G01 CAR T-cells required significantly less rForce to disengage from their target. Moreover, G01 was significantly different to G02 and Y04 CAR T-cells.

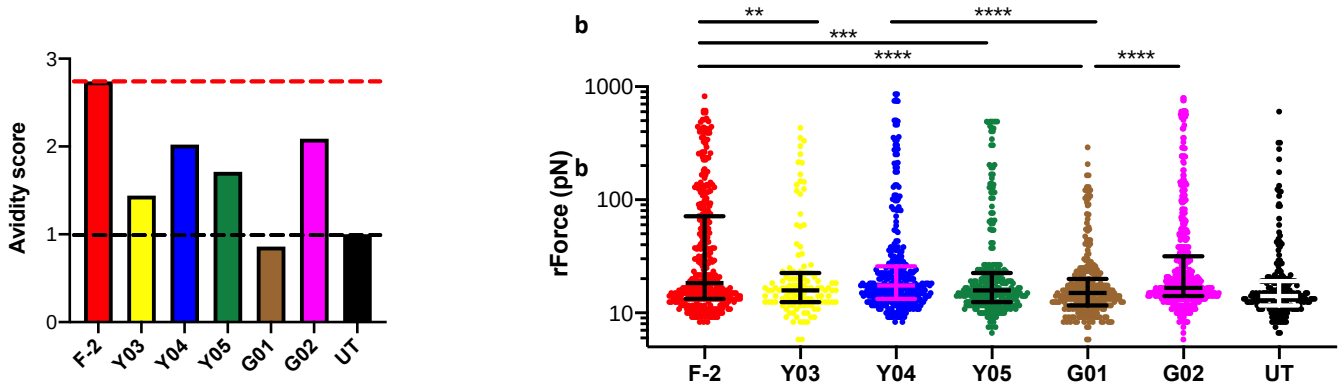

Figure 3.8 Representative z-Movi analysis of CAR T-cell avidity from a healthy donor. a) Bar plot represents avidity score i.e. the ratio of the mean rForce per cell required to detach T-cells from the LO68-CD19+ monolayer compared to UT T-cells (black dotted line represents UT avidity score; red dotted line represents F-2 avidity score). b) Dot plot represents the rForce per cell required to detach from tumour monolayer; where each dot represents a single cell. Bars indicate the median + interquartile range. Kruskal-Wallis test with Dunnett's multiple comparisons test. **** p=<0.0001; *** p=0.0007; ** p=0.005. For clarity, a single representative run for one healthy donor is plotted in which each dot represents a single cell. Collectively, these dots generate the avidity curve shown in Fig. 3.7a, meaning that all avidity curves are built with >1000 single cell observations per donor.

3.2.5 Cytotoxicity of CAR T-cells

To determine if CAR T-cells containing the CDR3 V_H mutated scFv derivatives of FMC63 had anti-tumour activity, CAR T-cells were co-cultured with the B-ALL and Burkitt lymphoma cell lines NALM-6 and Raji, respectively. The chosen cell lines both express high levels of CD19 (see Fig. 5.1).

To enable the quantification of tumour cell viability, firefly luciferase and the red fluorescent protein tdTomato were stably co-expressed in the Raji and NALM-6 cell lines. Both genes are contained in one open reading frame (separated by a ribosomal skip peptide) within the SFG retroviral vector, SFG LucTom. A 293Vec-GALV retroviral packaging cell line was generated (as described in 2.4.2) and 293Vec-GALV viral particles were then used to establish stable expression of SFG LucTom in Raji and NALM-6 cell lines (Fig. 3.9). Following transduction, Raji and NALM-6 cells were flow sorted to achieve >90% LucTom$^+$ (LT^+) expression in the population, and will be referred to as NALM-6 and Raji througout.

The tdTomato red fluorescent protein emits red fluorescence at a peak wavelength of 581nm. It was used as a fluorescent reporter for the identification of tumour cells within a co-culture with CAR$^+$ T-cells.

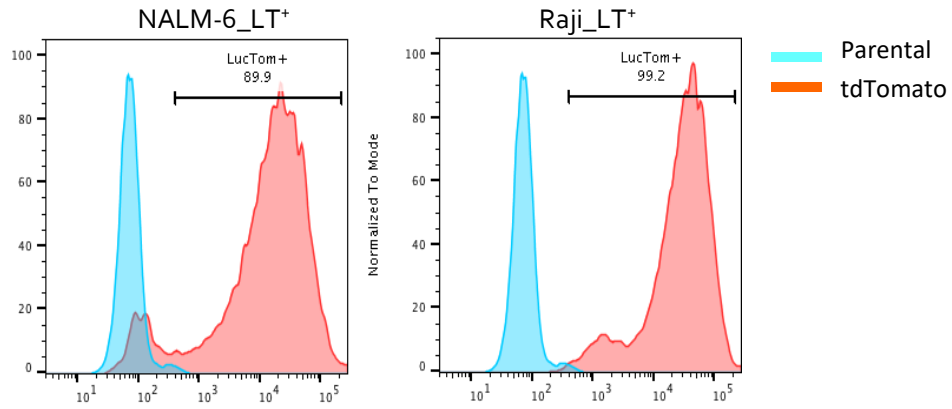

Figure 3.9 Stable expression of the SFG LucTom construct in leukaemia and lymphoma cell lines. Viral particles from a previously established 293Vec-GALV retroviral packaging cell line were used to transduce the above cell lines. Successful transduction was verified by flow cytometry (red histograms). Background fluorescence emission from unmodified (parental) cells is shown in blue.

Transduced T-cells were co-cultivated with tumour cells at an effector to target ratio of 1:1 and cytotoxicity was measure after 72h (Fig. 3.10). As expected, potent cytotoxic activity was seen when tumour cells were cultured with F-2 CAR T-cells. However, minimal cytotoxicity was observed by the Y02 CAR T-cells against both Raji and NALM-6 cells. All other CARs exhibited significant cytotoxicity against both cell lines. No significant killing was observed following the addition of untransduced (UT) T-cells, thus confirming that cytotoxicity was attributable to the anti-CD19 CAR T-cells. These data demonstrate that all V_H CDR3 mutated CARs, except Y02, could mediate anti-tumour killing against cell lines naturally expressing CD19. This observation suggests that minimal avidity for CD19 is required for CAR T-cell activation as both Y03 and G01 CAR T-cells presented marginal avidity in studies shown in Fig. 3.7 and Fig. 3.8.

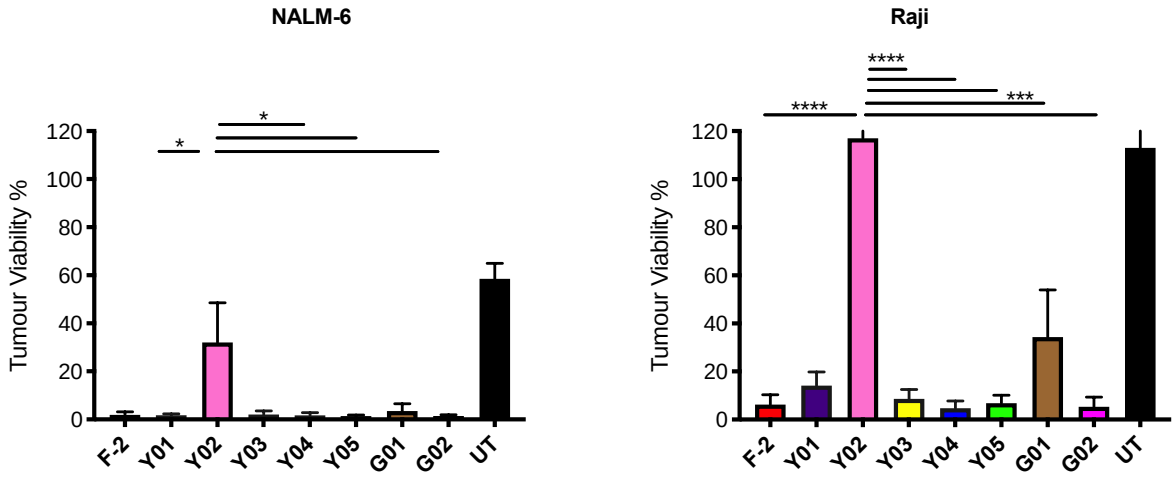

Figure 3.10 Cytotoxic activity of scFv mutated CARs against a, NALM-6 and b, Raji cell lines. 2x10^4 CAR T-cells were co-cultivated in duplicate with an equal number or Raji or NALM-6 cells. After 72h, viability of tumour cells was determined by luciferase assay. Data shown are mean ± SEM; 6 technical repeats from 3 independent donors. Statistical analysis was performed by One-way ANOVA followed by Tukey's multiple comparison test. **** p=<0.0001; *** p= ≤ 0.001; ** p= ≤ 0.01

3.2.6 Quantification of cytokine release by CAR T-cells

To assess activation of CAR T-cells in the above co-cultivation experiments, IFN-γ (Fig. 3.11) and IL-2 (Fig. 3.12) levels were quantified using ELISA. The analysis was performed on supernatants collected from co-cultures after 24h. In these experiments, neither Y02 or G01 CAR T-cells elicited IFN-γ release when co-cultured with NALM-6 or Raji cells, and Y03 CAR T-cells released minimal amounts when co-cultured with Raji cells. Substantial IFN-γ production was observed by F-2 and the other CDR3 mutated derivative CAR T-cells when co-cultured with both cell lines. Furthermore, G02 CAR T-cells produced higher amounts of IFN-γ compared to all other V_H mutated CARs in both NALM-6 and Raji co-cultures; however, this difference was not significant.

The ability of the CD19-targeted CAR T-cells to produce IL-2 in response to antigen stimulation was also assessed. All CAR T-cells produced IL-2 when co-cultivated with NALM-6 or Raji cells, however G01 CAR T-cells produced similar levels to UT T-cells, which served

as a negative control. In NALM-6 co-cultivations, Y05 CAR T-cells produced significantly more IL-2 compared to all other constructs, excluding Y04 and G02 CAR T-cells. Overall, CAR T-cells tended to produce increased IL-2 when co-cultured with Raji cells; however, there was no significant differences between constructs.

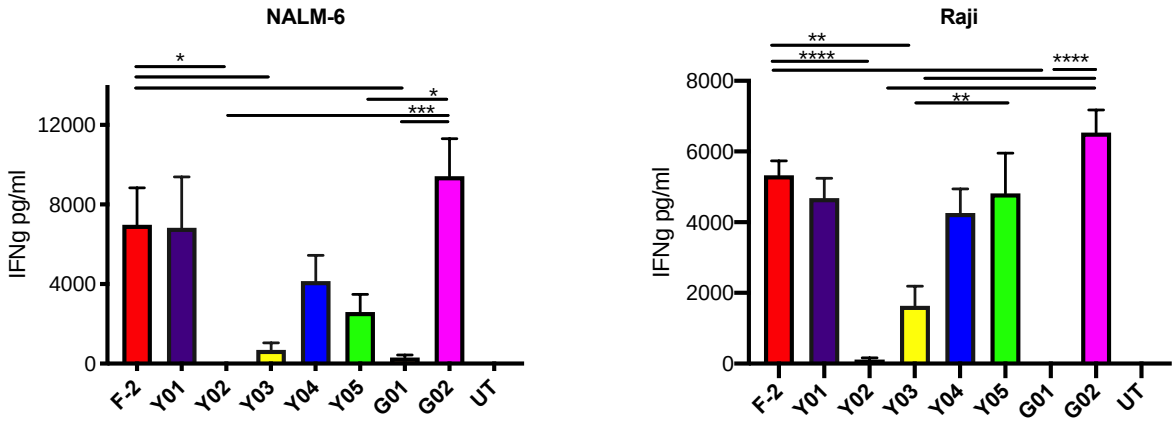

Figure 3.11 IFN-γ production by F-2 and V_H CDR3 mutated derivatives. Supernatants were collected 24h after co-cultivation experiments described in Fig. 3.10 and analysed for IFN-γ by ELISA. Data shown are mean ± SEM of 6 technical repeats from 3 independent donors. Statistical analysis was performed by One-way ANOVA followed by Tukey's multiple comparison test. **** p=<0.0001; *** p= ≤ 0.001; ** p= ≤ 0.01; * p= ≤ 0.05

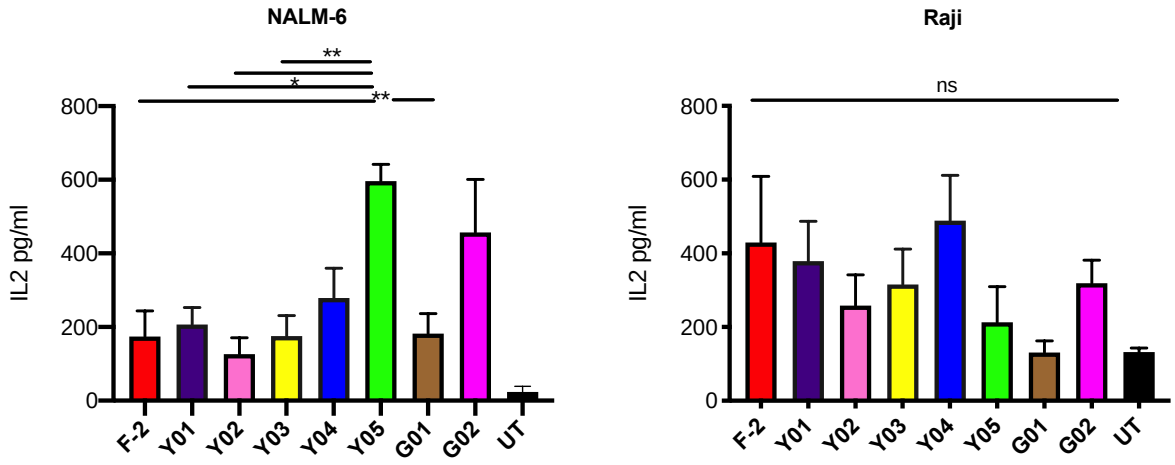

Figure 3.12 IL-2 production by F-2 and V_H CDR3 mutated derivatives. Supernatants were collected 24h after co-cultivation experiments described in Fig. 3.10 and analysed for IL-2 by ELISA. Data shown are mean ± SEM of 6 technical repeats from 3 independent donors. Statistical analysis was performed by One-way ANOVA followed by Tukey's multiple comparison test. ** p= ≤ 0.01; * p= ≤ 0.05; ns= non-significant.

3.2.7 CD19-specific anti-tumour activity of CDR3 mutated CAR T-cells

In order to investigate if the introduced V_H CDR3 mutations caused differences in CAR T-cell specificity for CD19, their ability to kill parental LO68 tumour cells that do not naturally express CD19 was assessed. Data from 3 independent replicate experiments is shown in Fig. 3.13. When co-cultured with LO68 cells that were engineered to express CD19 (LO68-CD19$^+$), cell lysis was induced by all CAR T-cells (Fig. 3.13). Lysis was also observed with untransduced (UT) T-cells, demonstrating a level of background killing by T-cells. Unexpectedly, co-culture of CAR T-cells with parental LO68 cells also resulted in killing, albeit less that observed with LO68-CD19$^+$ cells. However, this was equivalent across all CAR T-cells including F-2 suggesting this is not due to the V_H CDR3 mutations. A possible explanation is that the 72h incubation resulted in non-specific tumour cell death because of exhaustion of the culture medium.

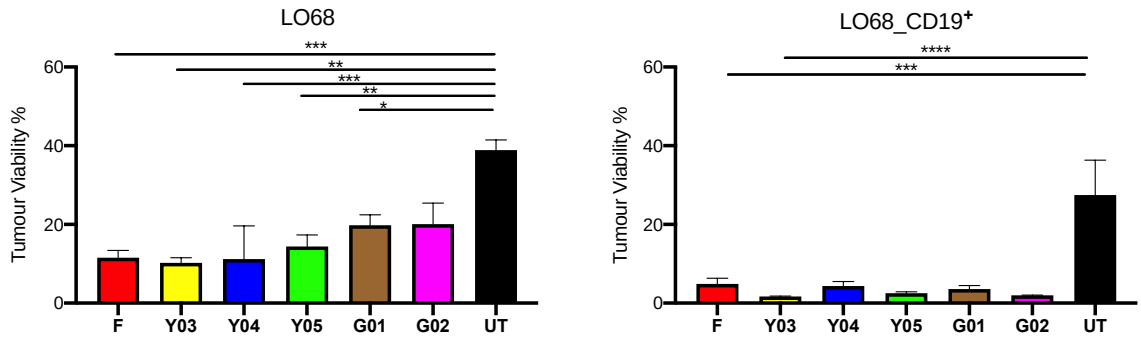

Figure 3.13 Antigen-specific cytotoxicity of CAR T-cells. 1 x 10^5 of the indicated CAR T-cells were co-cultivated in triplicate with an equal number of LO68 or LO68-CD19$^+$ cells. After 72 hours, viability of the tumour cells was determined by MTT assay. Statistical analysis was performed by One-way ANOVA followed by Tukey's multiple comparison test. **** p=<0.0001; *** p= ≤ 0.001; ** p= ≤ 0.01; * p= ≤ 0.05 Data shown are mean ± SEM of 6 technical repeats from 3 independent donors.

3.3 Discussion

Adaptive immune responses are initiated and perpetuated by αβ TCR engagement of peptides presented by MHC complexes. The recognition of pMHC by TCR results in phosphorylation of CD3 immunoreceptor tyrosine-based activation motifs (ITAMs), and initiates a downstream signalling cascade causing subsequent T-cell activation[238]. The affinity of the TCR for the pMHC complex is a pivotal factor influencing the sensitivity of activation. Whilst high affinity TCRs may increase specificity for pMHC and allow recognition of low density ligands, a threshold of affinity can be reached whereby TCR peptide sensitivity is reduced[228]. Unlike endogenous TCRs, CARs typically have a higher (typically nanomolar) affinity for antigen and recognise their target in an MHC independent manner[224]. However, the potency of TCR-pMHC and CAR-antigen interaction on the cell surface is determined by multiple factors including affinity, TCR/CAR clustering, co-receptor engagement and antigen expression density[239]. These combined effects are referred to as avidity, therefore measurement of avidity may correlate more accurately with functional outcomes. While some studies have addressed the impact of CAR binding affinity on functionality, few have explored the role of avidity[225,231,232,240].

To date, clinical trials have used different scFvs to target CD19 with CAR T-cell therapy. Nonetheless, the FMC63 scFv has been the most widely used. Here, a panel of seven CARs were generated by mutating the CDR3 region of the V_H of an FMC63 scFv with the aim to produce derivatives with varying binding strengths for CD19. Using z-Movi™ technology, the net avidity of these CAR T-cells was compared with that of F-2 CAR T-cells (FMC63-28ζ). T-cells that expressed Y03, Y04, Y05, G01 and G02 CARs all had significantly lower binding avidity to LO68-CD19$^+$ compared to F-2 CAR T-cells. The Y03 and G01 CAR T-

cells presented with the lowest avidity and required the smallest minimal rForce to break the interaction with $CD19^+$ tumour cells. When measured using the z-Movi™ platform, Y03 and G01 binding strength was comparable with UT T-cells and therefore the CAR T-cells are unlikely to be productively activated and function effectively. By contrast, the Y04, Y05 and G02 CAR T-cells showed intermediate avidity for CD19, leading me to hypothesize that they might behave differently to F-2. In a study of bi-specific T-cell engagers, Bortoletto et al[241] elegantly showed that mutated receptors with a lower affinity for CD3 had a rapid dissociation rate and effectively elicited T-cell activation and cytotoxicity. The improved cytotoxicity was hypothesized to be a result of enhanced serial killing that was more effective with lower affinity CD3 engagement. The experimental data presented here support the hypothesis of improved functionality in CAR T-cells with a lower avidity or affinity. Here, Y05 and G02 CAR T-cells with an intermediate avidity demonstrate an increased capacity to produce IL-2 when stimulated by NALM-6 leukaemic cells. Cytotoxic responses of the CAR T-cells, excluding Y02, were similar when co-cultured at a 1:1 effector: target ratio. Davenport et al. highlight that the rate of target cell killing via CAR and TCR is similar in the initial 20 hours of co-culture, particularly at high effector: target ratios[229]. Therefore, to uncover serial killing differences between CARs it is necessary to lower effector: target ratios which is demonstrated in the next chapter.

Notably, despite no detectable binding to CD19-Fc recombinant protein by CAR T-cells expressing a number of the mutant scFvs, the majority exhibited cytotoxicity when co-cultivated with NALM-6 and Raji cells. Moreover, G02 CAR T-cells produced substantial amounts of IL-2 and IFN-γ suggesting that the mutation of glycine to alanine in this position has a significant effect on binding strength. The data shown in this chapter provide a rationale for the design of pCARs in which the V_H CDR3 mutated CARs are paired with an

FMC63 scFv-containing CCR, with the hope to improve anti-tumour activity against B-cell malignancy.

Chapter 4: *In vitro* and *in vivo* characterisation of V_H CDR3 mutated anti-CD19 pCAR T-cells

4.1 Introduction

Pre-clinical development of CAR T-cells has progressively led to the development of newer generation CAR constructs with improved efficacy and functionality. Several innovative strategies have been deployed to enhance intrinsic CAR function[242], lower the threshold for activation[243], aid trafficking and intra-tumoural migration[244] and to enable the pharmacological elimination of CAR T-cells in the event of excessive toxicity[245].

In chapter 3, a panel of second-generation CARs were generated in which a single point mutation was introduced in the V_H CDR3 region of FMC63 scFv by site-directed mutagenesis. By this means, seven distinct CARs were generated which exhibited a spectrum of avidities for CD19 and varying functionality. In an effort to optimize performance, these mutant scFv-containing 28ζ CARs were co-expressed with a chimeric co-stimulatory receptor (CCR) in which an unmodified FMC63 scFv was coupled to CD137 (4-1BB). These constructs are known as parallel (p)CARs (see section 1.6) and effectively harness dual costimulatory signalling. The generic structure of a pCAR is illustrated in Fig 1.3 while pCARs used in this chapter are shown in Fig. 4.1.

The hypothesis underlying the development of the pCAR platform is that costimulatory endodomains aligned *in trans* rather than *in cis* will provide optimal signalling since signalling units are kept in proximity to the plasma membrane. Physiologically the TCR/CD3 complex and co-stimulatory receptors are aligned *in trans* and induce T-cell activation in this configuration. Additionally, the relative positions of the CD28 endodomain

in relation to the cell membrane is crucial for costimulatory function[201]. In the linear third-generation CAR format, one of the two costimulatory domains contained therein is placed away from the cell membrane, which may compromise its ability to engage with membrane-associated signalling partners. Another potential explanation for the relative underperformance of third-generation CARs is fact the close apposition of two costimulatory modules may cause steric hindrance, preventing efficient partnering with downstream signalling intermediates.

Optimal design of pCARs remains in its infancy. Nonetheless, one precedent has suggested that it may be preferable that the CAR component within a pCAR engages its target with lower affinity than applies to the CCR/ CCR target interaction[215]. When targeting colony-stimulating factor 1 receptor (CSF1R), pCARs were synthesised in which CSF-1 was the CAR targeting moiety and IL-34 was the CCR and *vice versa*. Both CSF-1 and IL-34 are the natural human ligands for CSF1R. However, IL-34 (K_d 1pM)[246] proved less effective that CSF-1 (K_d 34pM)[246] as a CAR targeting moiety when tested in the context of a pCAR, despite the fact that both CSF-1 and IL-34 engage an overlapping epitope in CSF1R. This raises the possibility that a lower affinity CAR is beneficial to pCAR T-cell function and that relative affinity of CAR and CCR for their target may modulate pCAR efficacy. In this chapter, I set out to test this further by generating a panel of CD19 pCARs in which CARs of varying binding strength were individually paired with an unmodified FMC63 scFv-targeted CCR.

4.1.1 Aims

- To design anti-CD19 pCARs in which the CAR targets CD19 with lower avidity than the CCR.
- To test efficacy of pCAR T-cells *in vitro*
- To test efficacy and safety of pCAR T-cells in a xenograft murine model of B-cell leukaemia

4.2 Results

4.2.1 Design and engineering of pCARs targeting CD19

Second-generation CARs with differing affinities for CD19 were synthesised as described in section 3.2.1. To engineer pCARs, mutated second-generation CARs were individually teamed with an FMC63 scFv-targeted 4-1BB CCR. The CCR comprises of an unmodified FMC63 scFv fused via a CD8α spacer and transmembrane domain to a CD137 (4-1BB) costimulatory endodomain. Equimolar expression of both CCR and CAR was ensured through inclusion of a furin cleavage site followed by a flexible serine-glycine linker and an intervening P2A) ribosomal skip 2A peptide. The CAR and CCR contain distinct epitope tags that allows co-expression to be demonstrated by flow cytometry. Figure 4.1 indicates the nomenclature and a structural overview of pCAR constructs used in this chapter and is also shown in Table 2.2.

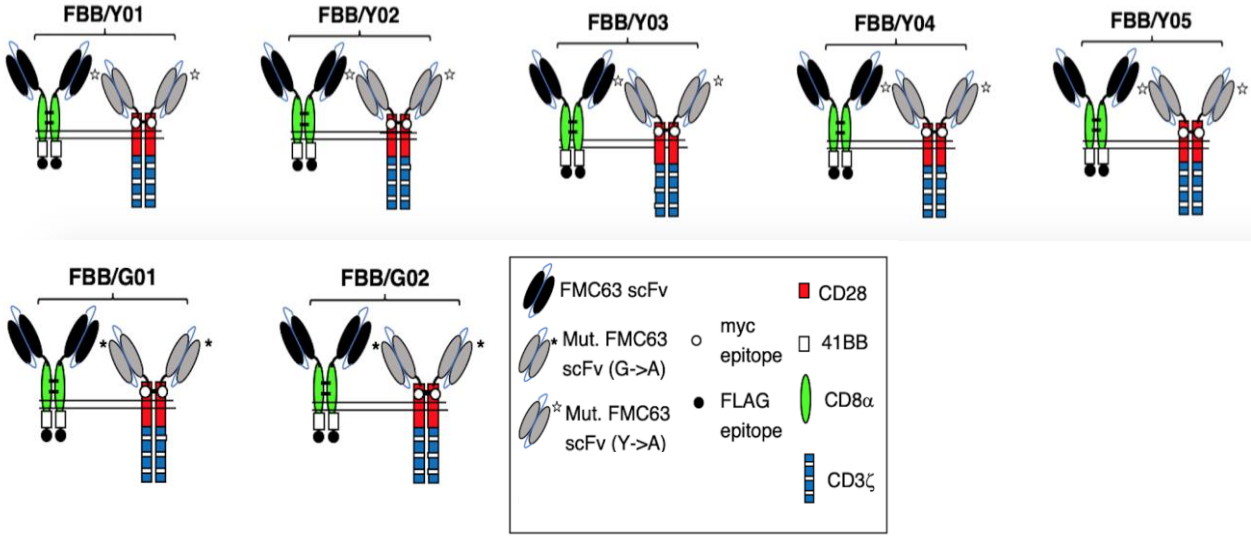

Figure 4.1 Schematic overview of CD19 targeted pCARs. The diagram shows the structural features of the CD19 targeted pCARs. The mutated scFvs described in 3.2.1 were used to target the 28ζ CAR component within the pCAR. An unmodified FMC63 scFv was used to direct specificity of the 4-1BB CCR. The resulting pCARs were dubbed FBB/Y01, FBB/Y02 and so on. Location of epitope tags in each receptor component is also indicated.

4.2.2 Detection of CAR and pCAR expression in human T-cells by flow cytometry.

Peripheral blood mononuclear cells (PBMCs) were isolated from healthy donors and were subjected to retroviral transduction 48 hours post activation in order to express the F-2 CAR or pCAR panel shown in Figure 4.1. T-cells were analysed for expression of encoded chimeric receptors using flow cytometry. CAR expression was detected using 9E10 antibody, which binds to an extracellular myc epitope tag located within the spacer region. CCR expression was detected in permeabilised cells using an anti-DYKDDDDK antibody, which binds a FLAG epitope tag located at the extreme C-terminus of the CCR. Transduction efficiency was found to be variable, dependent on donor, as assessed by myc expression. Representative FACS plots illustrating the detection methods used to determine transduction efficiency of chimeric receptors are displayed in Fig. 4.2.

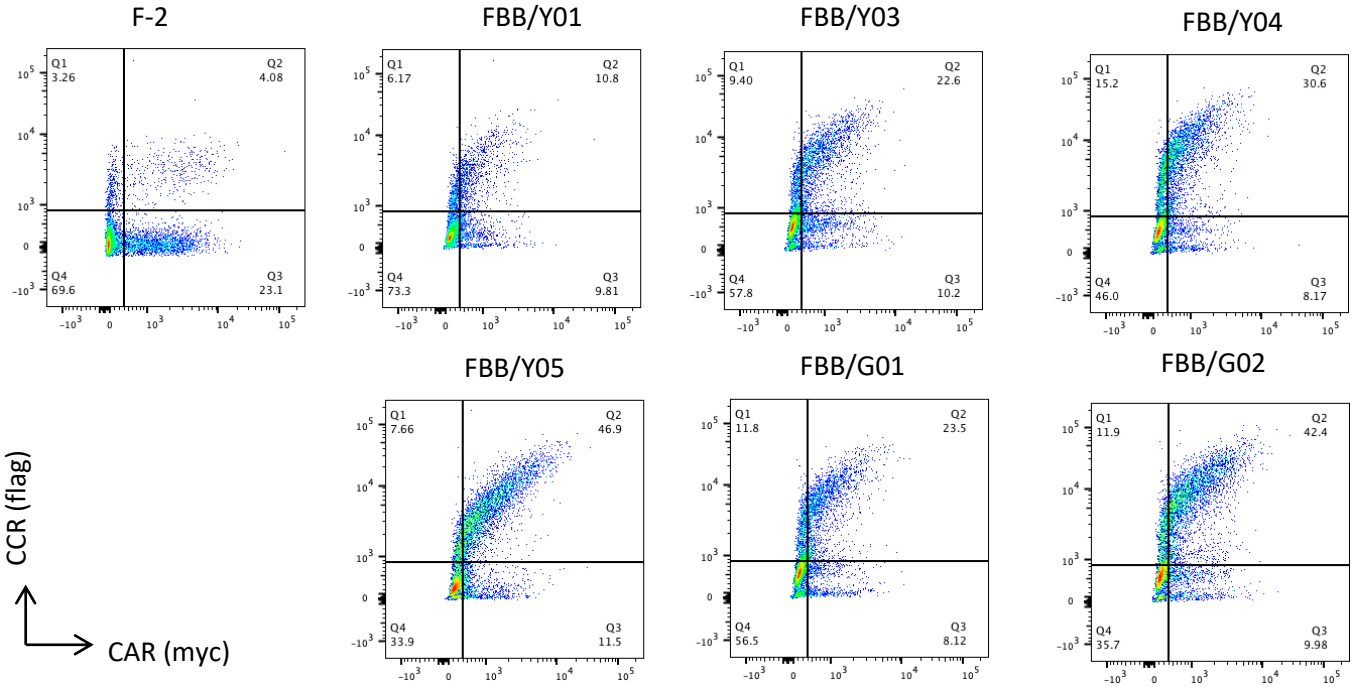

4.2.3 *In vitro* cytotoxic activity of V_H CDR3 mutated pCARs targeted against CD19

To characterise the *in vitro* anti-tumour activity of CD19-specific pCARs, cytotoxic activity against NALM-6 acute B-cell leukaemic cells was assessed, making comparison to V_H CDR3 mutated second-generation CARs and the unmodified F-2 CAR. As shown in previous research, long term cytotoxicity assays that are performed using low E:T ratios has revealed differences in the serial killing capabilities of CARs[229]. CAR and pCAR transduced T-cells were incubated with NALM-6 cells at decreasing E:T ratios for 72 hours, as illustrated in Fig. 4.3. At a 1:1 ratio, all CAR and pCAR transduced cells were able to effectively kill the majority of NALM-6 cells. Under conditions with lower E:T ratios, the residual live target cell percentage was lower after cocultivation with all pCARs excluding FBB/Y02 and FBB/Y03, when compared to F-2 CAR T-cells. These differences reached statistical significance when comparing F-2 vs. FBB/Y01, FBB/Y05, FBB/G01 and FBB/G02. Moreover, FBB/Y05 and FBB/G01 CAR T-cells significantly outperformed Y05 and G02 second-generation CARs. Notably, both FBB/G02 and G02 CAR T-cells had enhanced, albeit equivalent cytotoxic activity, when compared to F-2. These data provide evidence for superior killing of the majority of pCAR transduced cells compared to F-2 CAR T-cells.

Figure 4.2 Expression of CD19 targeted pCARs and control second-generation F-2 CAR in human T-cells. Transduction efficiency of PBMCs was evaluated three days after gene transfer. The presence of the CAR was detected by flow cytometry after incubation with 9E10 antibody followed by goat anti-mouse PE. The CCR was detected using an anti-FLAG PE antibody. The level of expression in all cases was compared to untransduced (UT) T-cells probed with the same antibody combinations. Comparable results were obtained from 7 independent donors.

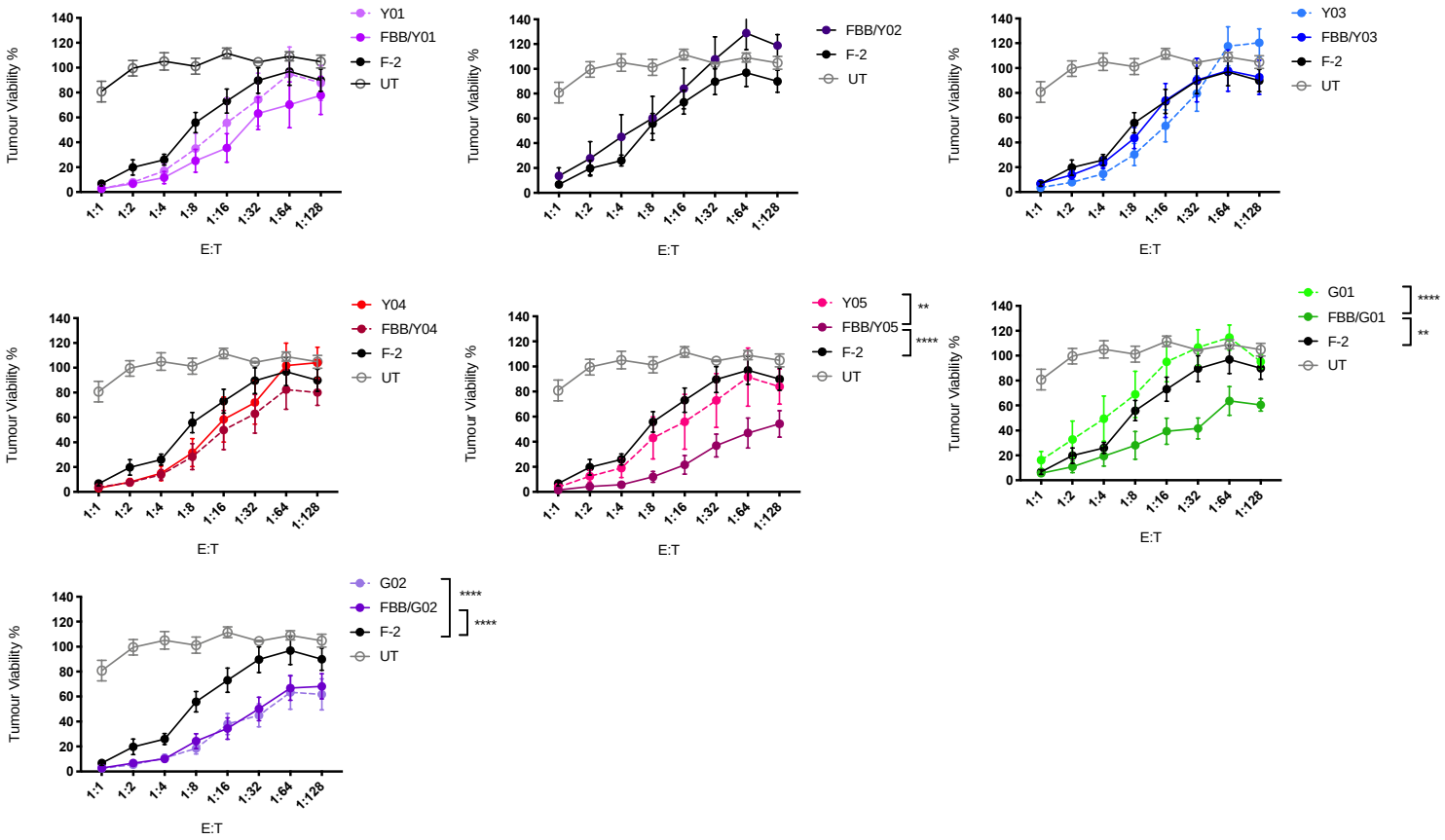

Figure 4.3 Cytotoxicity of CAR and pCAR T-cells in dose response killing assay when co-cultured with NALM-6 cells. CAR or pCAR T-cells were co-cultivated with NALM-6 leukaemia cells at the indicated E:T ratio. The Y02 mutant was discarded owing to lack of CD19 binding activity and CAR function. Target viability was quantified after 72h with a luciferase assay (Data shown is mean ± SEM of 7 replicates from 5 independent donors). Statistical analysis was performed with two-way ANOVA followed by Tukey post hoc test. **** p=<0.0001; *** p= ≤ 0.001; ** p= ≤ 0.01; * p= ≤ 0.05

4.2.4 Restimulation of anti-CD19 CAR and pCAR T-cells with LO68-CD19^{+} tumour cells

The activation and cytotoxic activity of CAR and pCAR T-cells was next investigated by performing co-cultivation experiments in which T-cells were repeatedly exposed to LO68-CD19^{+} tumour cell monolayers *in vitro*. This system was selected since many B-cell lines express co-stimulatory ligands, unlike LO68 mesothelioma cells. All engineered T-cell populations were initially co-cultured at a 1:1 E:T ratio and were restimulated on fresh LO68-CD19^{+} monolayers every 72 hours until tumour killing activity fell below 20%. After each restimulation all T-cells were placed on a fresh monolayer without correction of the T-

cell number to the starting effector to target ratio. As shown in Fig. 4.4, all pCAR CAR T-cells outperformed F-2 and V_H CDR3 mutated CAR T-cells by maintaining cytotoxic activity over more stimulation cycles. In particular, FBB/G02 and FBB/Y01 CAR T-cells sustained high levels of tumour cell killing for up to 29 stimulation cycles. Of note, Y04, Y05 and G02 CAR T-cells also restimulated for longer compared to F-2 CAR T-cells. These restimulation assays suggest that pCAR transduced T-cells have an improved capacity to engage in serial tumour cell killing compared to parental second-generation CARs.

Secretion of effector cytokines is an important indicator of the functionality of CAR T-cells. Twenty-four hours after each cycle of stimulation, supernatant was removed from the co-cultures and tested for IFN-γ and IL-2 content. As shown in Fig. 4.5, pCAR T-cells maintained the ability to produce IFN-γ through a greater number of restimulation cycles, compared to conventional second-generation CARs. In particular, FBB/Y01, FBB/Y04, FBB/Y05 and FBB/G01 continued to release IFN-γ for up to 15 stimulation cycles. Prolonged release of IL-2 may reflect enhanced activation and serial killing. Production of IL-2 by pCAR T-cells over many restimulation cycles is demonstrated in Fig. 4.6. All pCAR T-cells secreted higher amounts of IL-2 at initial stimulation cycles compared to F-2 and V_H CDR3 mutated CAR T-cells and continued to produce IL-2 for many cycles, although differences were not as pronounced. Furthermore, when compared to second-generation CAR T-cells, pCAR T-cells expanded to a greater number over the first three stimulation cycles (Fig. 4.7).

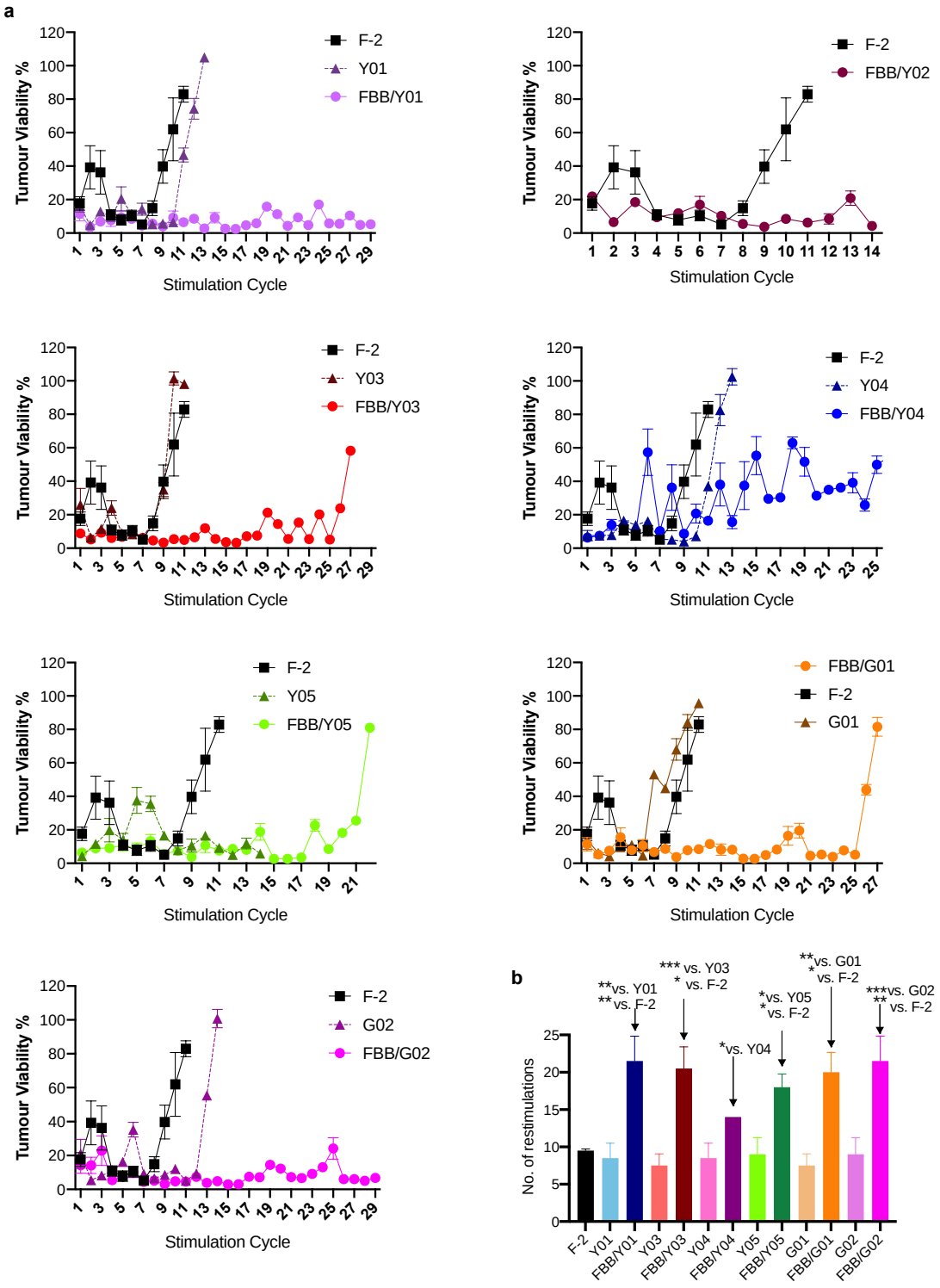

Figure 4.4 Restimulation of CD19 targeted CAR and pCAR T-cells on LO68-CD19$^+$ tumour cell monolayers. (a) T-cells were engineered to express the indicated CARs or pCARs. 1x10^5 of the indicated transduced CAR or pCAR T-cells were co-cultivated in triplicate with an equal number of LO68-CD19$^+$ tumour cells, engineered to express CD19. After 72h, T-cells were transferred to a fresh monolayer of CD19$^+$ LO68 cells and viability of the original tumour monolayer was determined by MTT assay. Plots indicate tumour viability at each stimulation cycle. Cultures were terminated when tumour cell viability was > 80%. (Data shown is mean ± SEM of 4-6 replicates from 2-3 independent donors). (b) Statistical analysis was performed using an unpaired Student's *t* test comparing the indicated CARs/ pCARs. *p<0.05; **p<0.01; ***p<0.001; ****p<0.0001

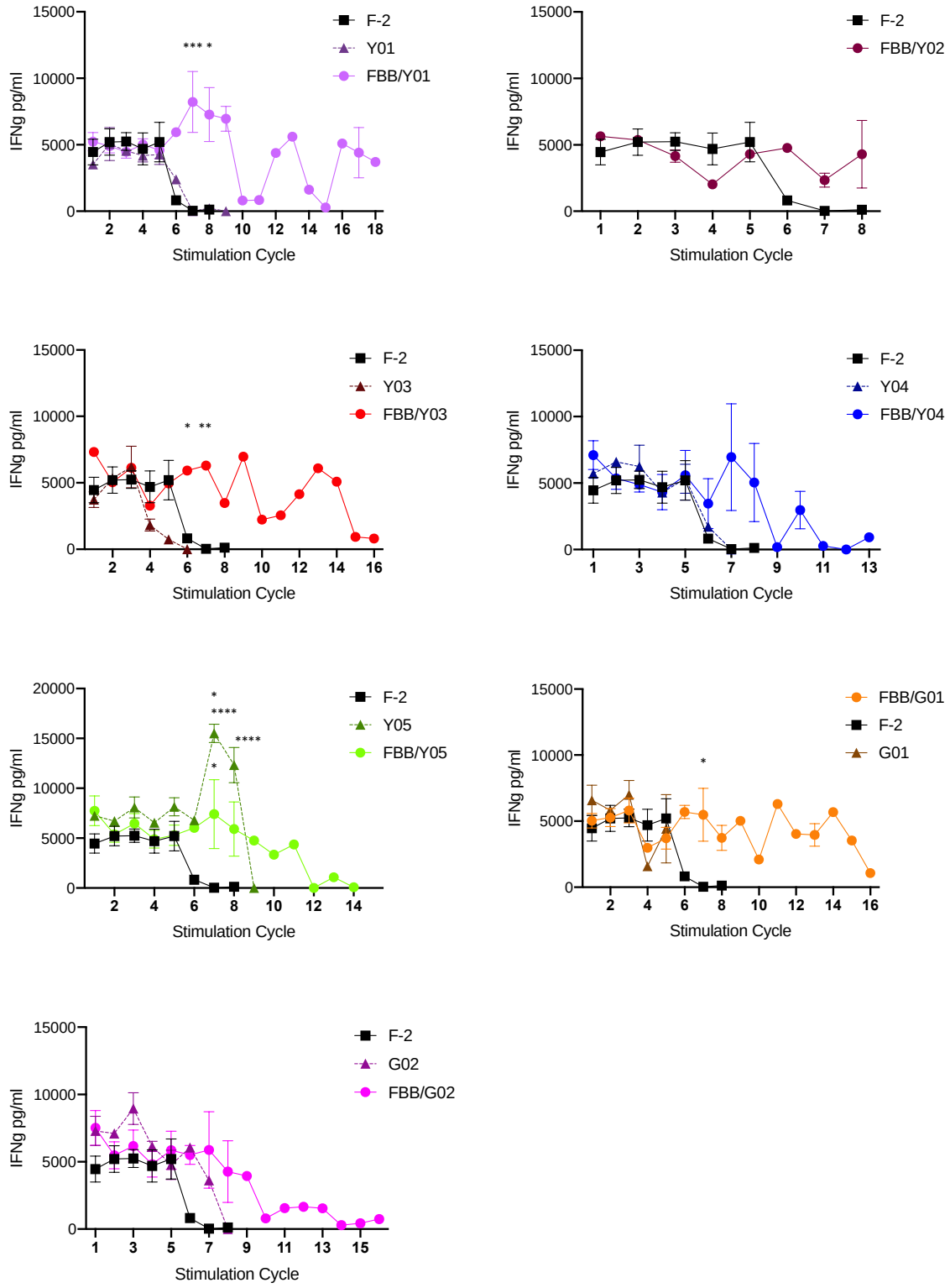

Figure 4.5 IFN-γ cytokine release by pCAR T-cells is maintained upon serial restimulation. CAR or pCAR T-cells were co-cultivated with LO68-CD19^{+} in experiments described in Fig, 4.4. Twenty-four hours after co-culture supernatant was removed and analysed for IFN-γ. (Data shown are mean ± SEM of 4-6 replicates from 2-3 independent donors). Statistical analysis vs.F-2 was performed using unpaired Student's *t* test followed by Holm-Sidak post hoc test. **** p=<0.0001; *** p= ≤ 0.001; ** p= ≤ 0.01; * p= ≤ 0.05

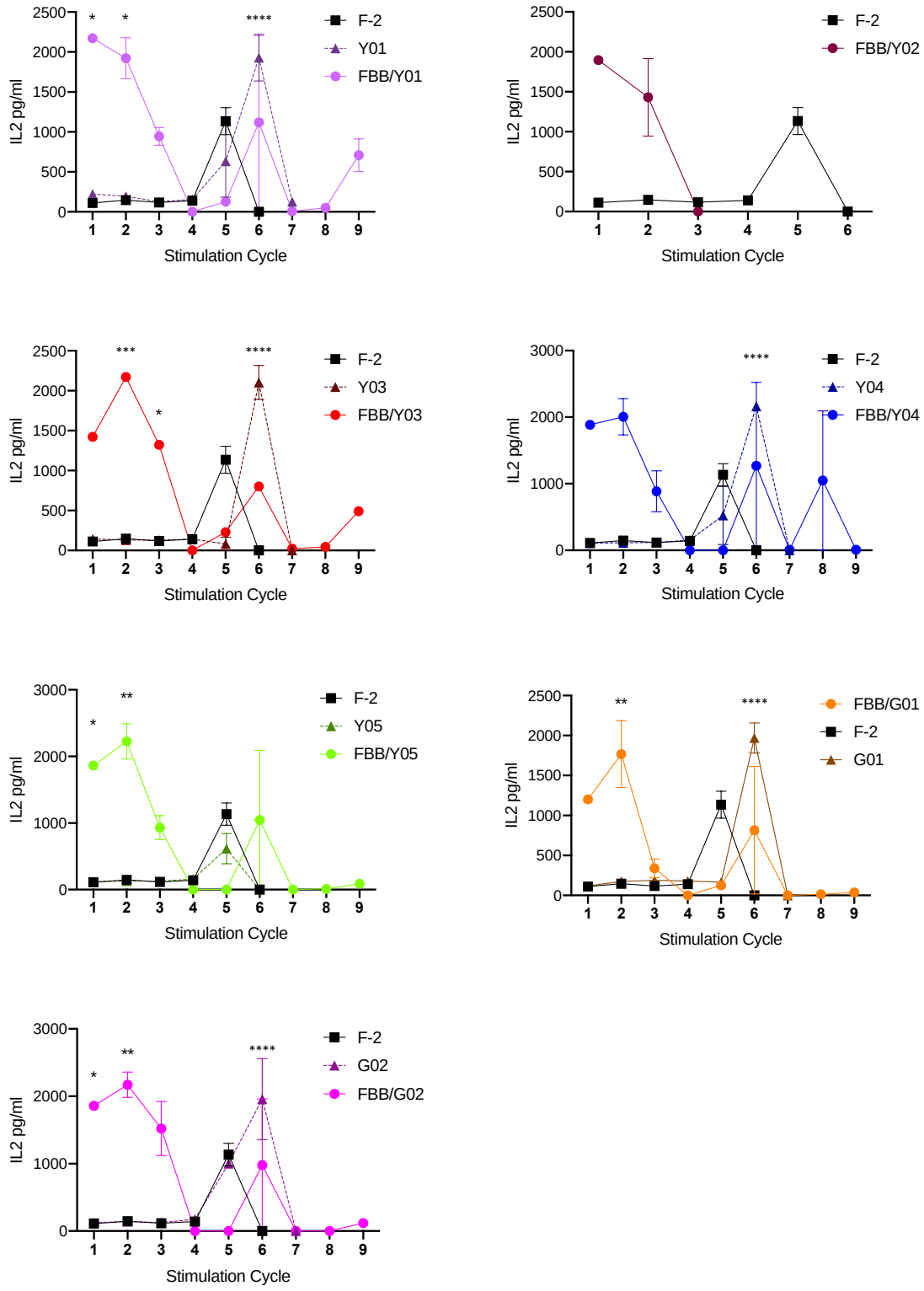

Figure 4.6 IL-2 cytokine release by pCAR T-cells is maintained upon serial restimulation. CAR or pCAR T-cells were co-cultivated with LO68-CD19^{+} in experiments described in Fig, 4.4. Twenty-four hours after co-culture supernatant was removed and analysed for IL-2. (Data shown are mean ± SEM of 4-6 replicates from 2-3 independent donors). Statistical analysis vs.F-2 was performed using unpaired Student's *t* test followed by Holm-Sidak post hoc test. **** p=<0.0001; *** p= ≤ 0.001; ** p= ≤ 0.01; * p= ≤ 0.05

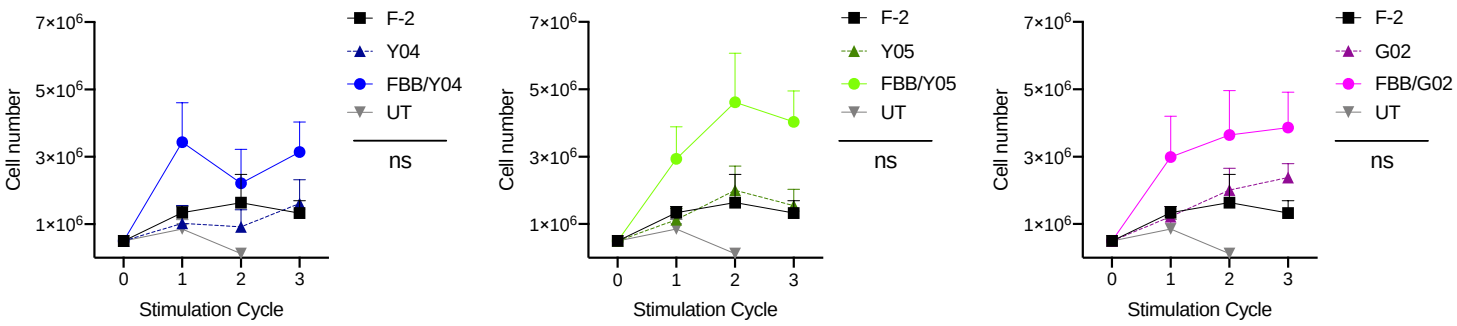

Figure 4.7 CAR and pCAR T-cell expansion upon restimulation with LO68-CD19 tumour cell monolayers. T-cells were engineered to express the indicated CARs or pCARs. $5x10^5$ of the indicated transduced CAR or pCAR T-cells were co-cultivated with $2.5x10^5$ LO68-CD19 tumour cells. After 72h, T-cells were harvested, counted and transferred to a new tumour monolayer. (Data shown are mean + SEM of 6-8 replicates from 3-4 independent donors).

4.2.5 Expression of activation/exhaustion markers following antigen encounter

Elevated and/or prolonged expression of multiple inhibitory receptors such as Programmed death 1 (PD1) and TIM-3 are typical features of exhausted T-cells[247]. To compare CAR and pCAR T-cell exhaustion, the expression of LAG3, PD1 and TIM3 on CAR vs pCAR transduced T-cells was assessed during expansion and after stimulation cycles 1 and 3. As shown in Fig. 4.8, expression of exhaustion markers was comparable across CAR and pCAR T-cells when in culture. Flow cytometry plots illustrating the gating strategy are shown in supplementary Fig.7.3. Upon stimulation with CD19-expressing LO68 cells, FBB/Y04, FBB/Y05 and FBB/G02 pCAR T-cells maintained lower co-expression of LAG3, PD1 and TIM3 compared to all second-generation CARs. Overall expression of PD1 was also significantly lower after restimulation 1 in pCAR T-cells when compared to F-2 and other second-generation CARs (Fig. 4.9). These data are consistent with reduced exhaustion of pCAR T-cells due to enhanced co-stimulation.

Finally, co-stimulation plays a key role in enabling T-cell differentiation and memory formation. In keeping with this, stimulated CAR and pCAR T cells demonstrated a

progressive enrichment of effector-memory cells however, there was no clear difference between constructs (Fig. 4.10).

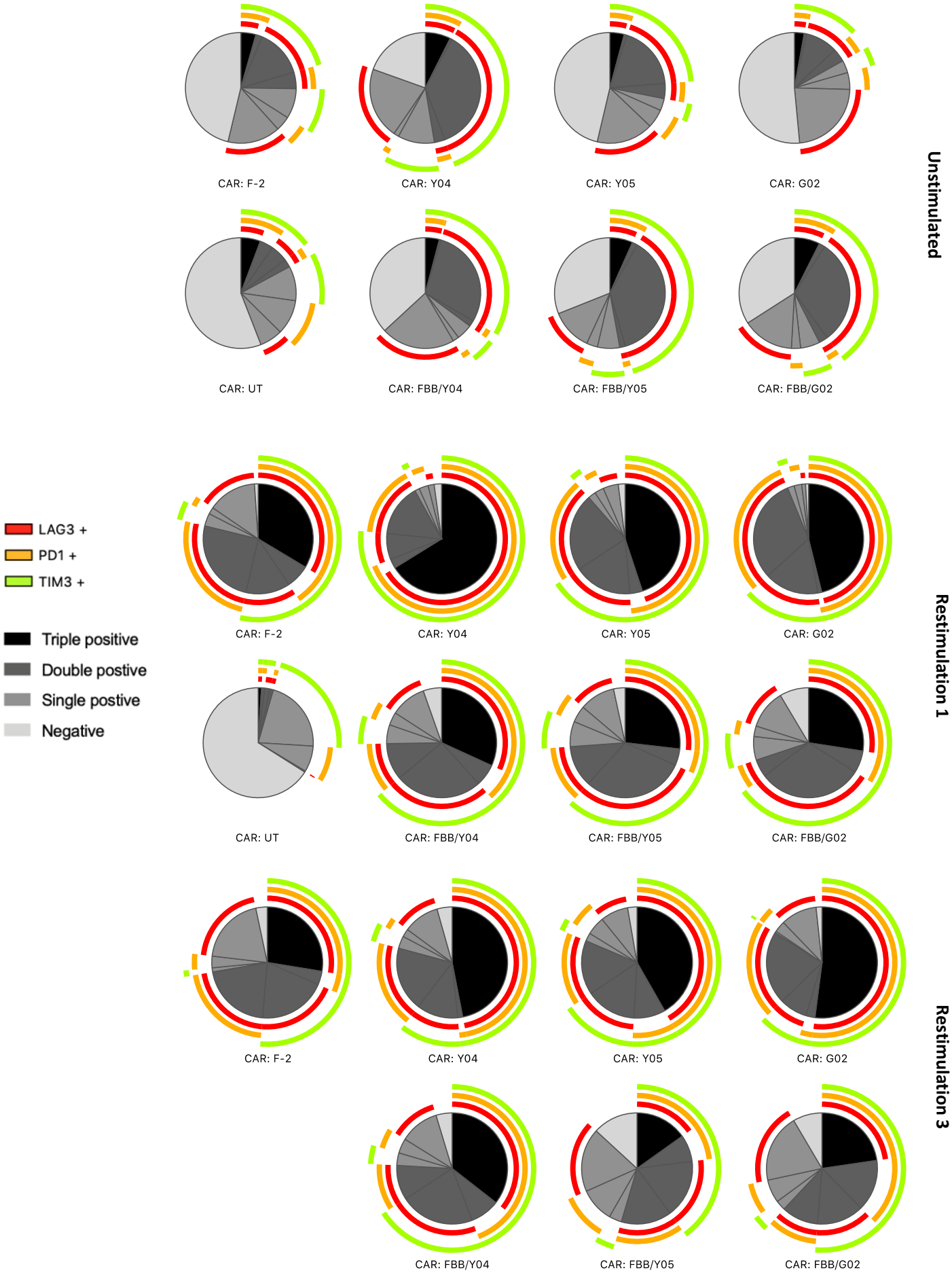

Figure 4.8 Expression of activation/exhaustion markers on CAR+ T-cells after restimulation with LO68-CD19^{+} tumour cell monolayers. T-cells were engineered to express the indicated CARs or pCARs. 5x10^{5} of the indicated transduced CAR or pCAR T-cells were co-cultivated with 2.5x10^{5} LO68-CD19 tumour cells. After 72h, T-cells were harvested and expression of LAG3, PD1 and TIM3 analysed by flow cytometry (Data shown are mean of 3 independent donors).

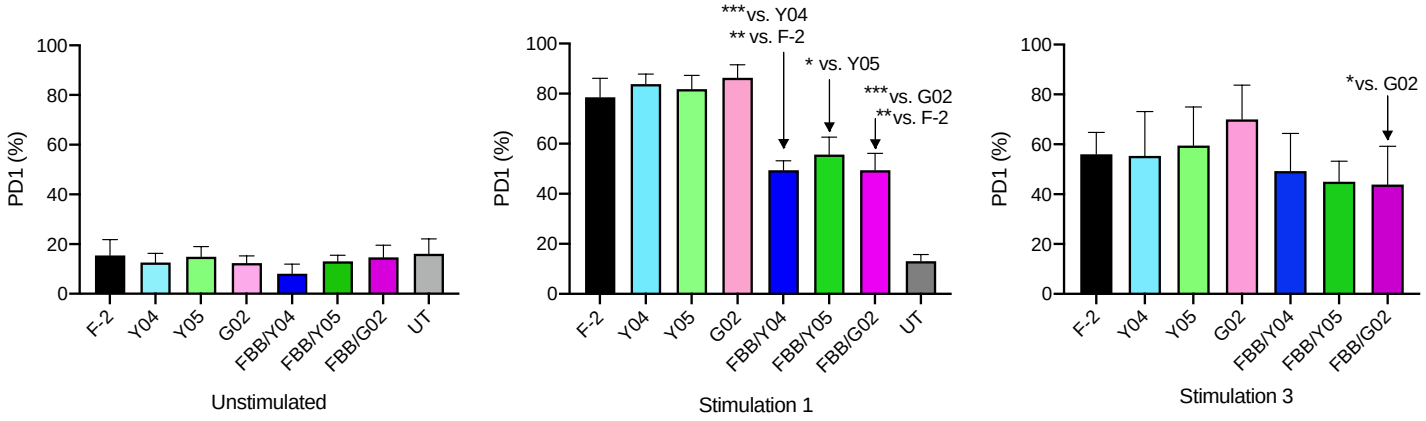

Figure 4.9 Expression of PD1 on CAR+ T-cells after restimulation with LO68-CD19^{+} tumour cell monolayers. T-cells were engineered to express the indicated CARs or pCARs. 5x10^{5} of the indicated transduced CAR or pCAR T-cells were co-cultivated with 2.5x10^{5} LO68-CD19 tumour cells. After 72h, T-cells were harvested and expression of PD1 analysed by flow (Data shown are mean ± SEM from 3 independent donors). Statistical analysis was performed using 2-way ANOVA analysis followed by Tukey's multiple comparisons test **** p=<0.0001; *** p= ≤ 0.001; ** p= ≤ 0.02; * p= ≤ 0.05.

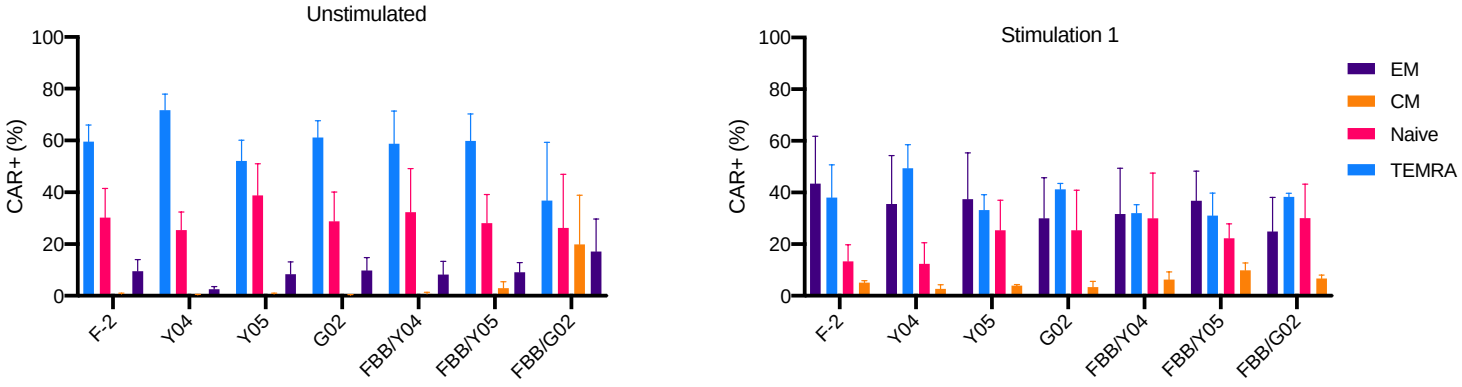

Figure 4.10 Investigated of CAR and pCAR T-cell differentiation after stimulation. Cells were engineered to express the indicated CARs or pCARs. 5x10^{5} of the indicated transduced CAR or pCAR T-cells were co-cultivated with 2.5x10^{5} LO68-CD19 tumour cells. After 72h, T-cells were harvested and expression of CD45RA and CCR7 analysed by flow cytometry. CM – central memory CD45RA-CCR7+; EM – effector memory CD45RA-CCR7-; TEMRA – terminal effector CD45RA+CCR7-; Naïve CD45RA+CCR7+. (Data shown are mean ± SEM from 2-3 independent donors).

4.2.6 Establishing a xenograft mouse model.

To study anti-tumour efficacy of CAR and pCAR T-cells in vivo, I set out to establish a mouse xenograft model of B-cell malignancy. Models derived using Raji and NALM-6 cells have previously been utilised to test the *in vivo* anti-tumour activity of experimental anti-CD19 therapies[159,248]. To establish this model, tumour cells were engineered to express firefly

luciferase (ffLuc) and the fluorescent protein tdTomato, thereby allowing non-invasive monitoring of leukaemia or lymphoma growth using bioluminescence imaging (BLI). Next, titration experiments were performed to evaluate the optimal tumour cell number required to establish a model in which disease progression occurred over a number of weeks. Raji and NALM-6 cells were inoculated i.v. at 3 doses of 0.5, 1.0 or 1.5 x 10^6. At day 5 following injection, disease engraftment was present in all cohorts in both NALM-6 and Raji groups (Fig. 4.11). The growth rate of all cohorts was similar, and all mice presented with progressive disease over time. The NALM-6 model was chosen for further *in vivo* experiments because Raji cells express greater levels of co-stimulatory receptors, such as CD80 and CD86, which could potentially deliver proliferative signals to CAR T-cells *in vivo*. For the NALM-6 model, the lowest dose of 0.5x 10^6 was chosen, on the basis of equivalent tumour growth kinetics and disease engraftment efficiency across all doses. Following injection of NALM-6 cells, bioluminescence imaging demonstrated that disease was primarily located in the bone marrow, specifically in the femur (Fig. 4.11c).

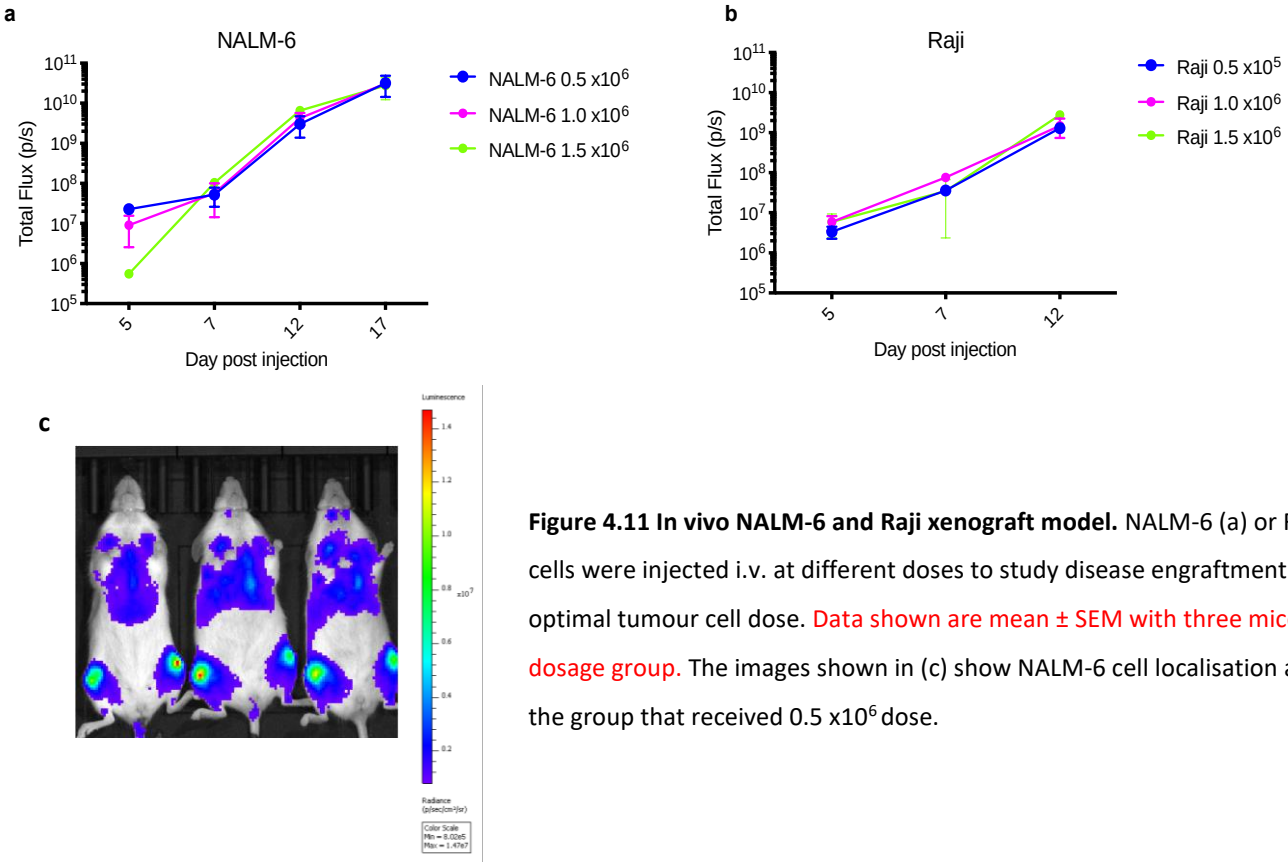

Figure 4.11 In vivo NALM-6 and Raji xenograft model. NALM-6 (a) or Raji (b) cells were injected i.v. at different doses to study disease engraftment and optimal tumour cell dose. Data shown are mean ± SEM with three mice per each dosage group. The images shown in (c) show NALM-6 cell localisation at day 5 in the group that received 0.5 x10^6 dose.

4.2.7 *In vivo* anti-tumour efficacy of pCAR T-cells against NALM-6 leukaemic xenograft

In order to compare CAR and pCAR T-cell anti-leukaemic activity, a modest CAR T-cell dose of 0.5 x10^6 cells was chosen. The assumption was that temporary disease control would occur, rather than complete leukaemia clearance. The experimental model is shown in Fig. 4.12. Mice were imaged on day 5 to evaluate tumour burden and animals were re-assorted prior to T-cell treatment so that tumour burden was evenly distributed across all groups. Based on *in vitro* results shown above, the pCARs chosen for *in vivo* testing were FBB/Y04, FBB/Y05, FBB/G01 and FBB/G02, alongside the V_H CDR3 mutated second-generation CAR counterparts and F-2. Pooled results of two independent experiments are shown in Fig. 4.13. CAR and pCAR T-cell transduction efficiency was determined 24 hours prior to intravenous infusion by flow cytometry and the transduction efficiency was normalised

across groups through the addition of untransduced T-cells. After CAR/ pCAR T-cell treatment, all animals were monitored by BLI weekly. Control mice that had received only PBS showed rapid disease progression and required sacrificing by day 17. F-2 CAR T-cells elicited transient delay in disease progression while Y04 and Y05 V_H CDR3 mutated derivatives achieved superior anti-leukaemic activity. All pCAR T-cells, excluding FBB/G01, were achieved further enhancement of disease control and were more effective at inhibiting tumour growth. At several timepoints post treatment, significant differences were seen in luminescence signal between groups (Fig. 4.13). Survival data are shown in Fig. 4.14 and highlight the significantly improved survival of all mice treated with pCAR T-cells. Moreover, Y05 and G02 CAR T-cells exhibited better disease control compared to wildtype F-2 CAR T-cells.

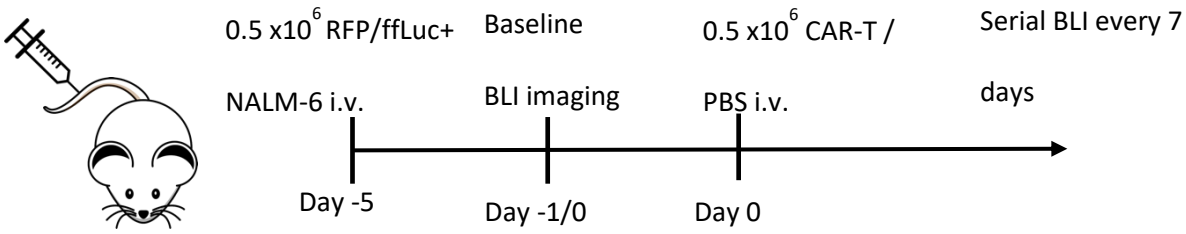

Figure 4.12 Experimental schematic of in vivo efficacy study in NALM-6 NSG xenograft mouse model. To assess the in vivo efficacy of anti-CD19 CAR and pCAR T-cells in an established xenograft model, mice were injected with 0.5 x10^6 RFP/ffLuc$^+$ NALM-6 cells. Disease engraftment was evaluated on day -1 or day 0 of T-cell treatment. Cohorts were randomised and tumour burden was distributed evenly across groups. T-cells were injected 5 days after tumour inoculation. BLI was carried out using the IVIS imaging system.

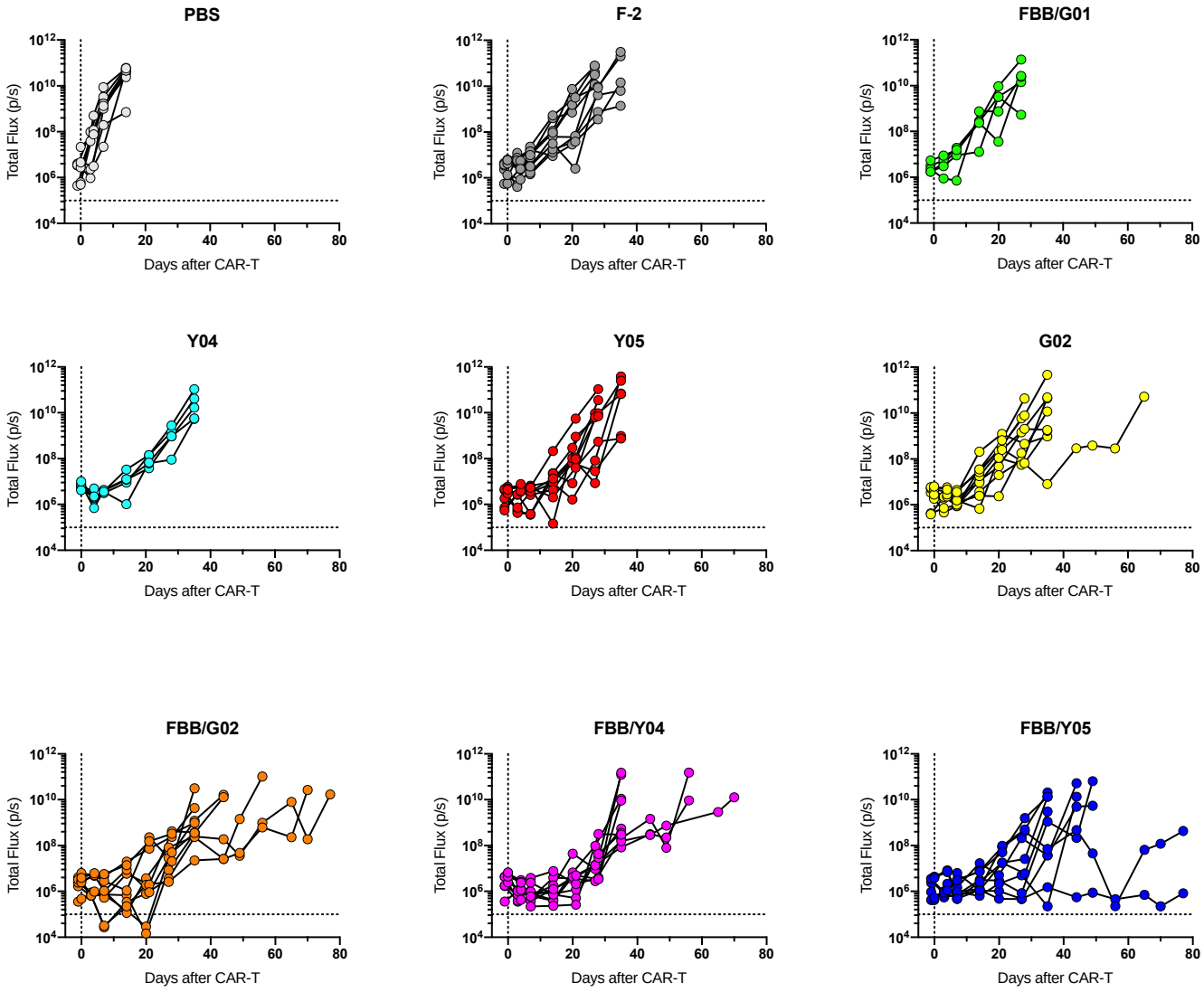

FBB/Y04 vs Y04 p<0.001 day 7	F-2 vs Y05 p=0.046 day 4
FBB/Y04 vs Y04 p=0.008 day 14	F-2 vs Y05 p=0.024 day 7
FBB/Y04 vs Y04 p=0.003 day 21	F-2 vs Y05 p=0.009 day 27
FBB/Y04 vs Y04 p=0.031 day 28	F-2 vs G02 p=0.005 day 7
FBB/Y05 vs Y05 p=0.022 day 35	F-2 vs G02 p=0.007 day 27
FBB/G02 vs G02 p=0.038 day 21	

Figure 4.13 pCAR T-cells show enhanced disease control in the NALM-6 xenograft model. NSG mice were injected i.v. with 0.5 x10^6 RFP/ffLuc$^+$ NALM-6 cells. Disease engraftment was assessed on day -1/0 using the IVIS imaging system. On day 5, 0.5 x10^6 of the indicated CAR or pCAR T-cells were administered i.v. Disease burden was monitored by BLI. Data are pooled from 2 independent experiments with 5-10 mice per group. Statistical analysis performed using unpaired Student t test, comparing the indicated two groups.

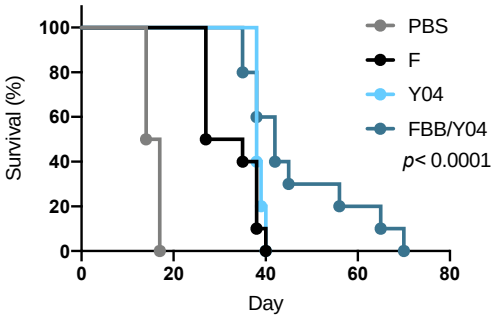

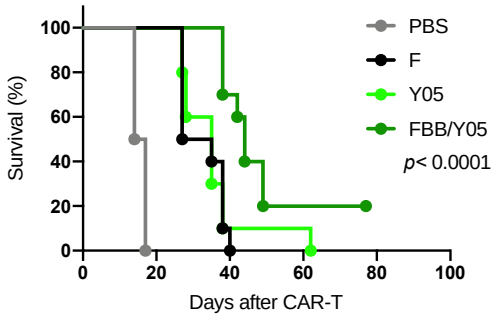

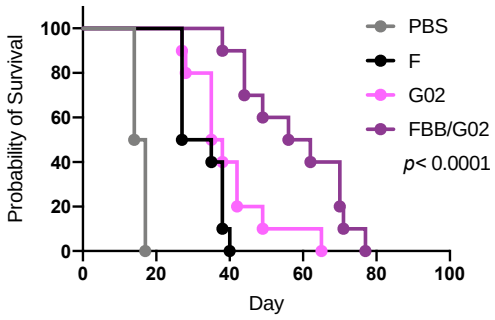

Figure 4.14 Mice treated with pCAR T-cells show better survival outcomes. Kaplan-Meier survival analysis of indicated treatment groups shows significant survival differences for mice treated with all pCAR T-cells. Data are pooled from 2 independent experiments with 10 mice per group. Statistical analysis was performed using the Log rank Mantel-Cox test.

4.3 Discussion

In this chapter, I present results related to the evaluation of the *in vitro* and *in vivo* anti-tumour activity of pCAR T-cells that engage CD19. A key aim of this project was to compare the novel pCAR platform to second-generation anti-CD19 CAR T-cells which have transformed the treatment of patients with relapsed/refractory B-cell malignancies. Here, comparison was made with an analogue of the FDA- and EMA-approved CD19-specific CAR known as axicabtagene ciloleucel (axi-cel). The F-2 CAR extracellular domain contains the FMC63 scFv, CD28 hinge and transmembrane domains, and intracellular signalling domains that consist of CD28 and CD3ζ for T-cell activation and costimulation, respectively[154,249]. Additionally, a myc epitope tag was incorporated to aid detection of T-cell transduction while an intracellular FLAG epitope tag was added to the 4-1BB endodomain to facilitate the detection of CCR expression in pCAR-transduced T-cells.

The in vitro characterisation of V_H CDR3 mutated pCARs showed that when co-cultured with NALM-6 leukaemic cells in dose response killing assays, almost all pCARs had higher cytotoxic responses at low effector: target ratios. Of note, the G02 second-generation CARs proved significantly superior to F-2 CAR T-cells. This suggests that under more challenging conditions of lower E:T ratio, pCAR and G02 CAR T-cells are more cytotoxic, perhaps through serial killing of multiple targets as previously reported[229]. When compared in restimulation assays, all pCAR T-cells maintained cytotoxic activity against LO68-CD19$^+$ cells over an increased number of cycles, highlighting their durability of effector function. Again, in restimulation assays several V_H CDR3 mutated second-generation CAR T-cells outperformed F-2, specifically Y01, Y04, Y05 and G02, suggesting FMC63 avidity can be optimised. CAR T-cells have improved functionality. When tested *in vitro*, pCAR T-cells had

an increased capacity over several stimulation cycles to produce IFN-γ, which is a key effector cytokine for T-cells[250]. Additionally, pCAR T-cells produced higher amounts of IL-2 in initial co-cultivations that gradually decreased over time. This may account for an enhanced proliferative capacity of pCAR T-cells[215], although this was not investigated in my study. Furthermore, the enhanced cytokine production by pCAR compared to second-generation CAR T-cells is consistent with the effects of dual co-stimulation via CD28 and 4-1BB, as described previously[199]. Upon repetitive stimulation assays to model tumour-induced exhaustion[251], FBB/Y04, FBB/Y05 and FBB/G02 pCARs exhibited enhanced proliferation and lower expression of exhaustion markers. In the context of persistent antigen exposure, T-cell functions such as cytokine production, proliferative capacity and cytotoxicity are typically lost first. These *in vitro* restimulation assays provide insight into the effect of repeated antigen stimulation on CAR T-cell exhaustion.

To investigate *in vivo* efficacy, CAR and pCAR transduced T-cells were adoptively transferred into mice bearing NALM-6 xenografts and anti-tumour activity examined by serial BLI. All pCAR and CAR T-cells mediated anti-tumour responses in this leukaemic disease model; however pCAR T-cells achieved enhanced disease control, leading to significantly improved survival. Mice receiving FBB/Y04 pCAR T-cells showed the greatest difference in disease burden compared to its second-generation control Y04, reaching significance at multiple time points. Nevertheless, FBB/G02-treated mice had the most dramatic decrease of disease burden following T-cell infusion, with BLI signal dropping below background level and reaching significance at day 21. Additionally, FBB/Y05- and FBB/G02- treated mice demonstrated the greatest improvement in survival, extending for 80 days or longer. Although T-cell imaging was not undertaken to analyse *in vivo* persistence

of CAR T-cells, the *in vitro* data suggest that pCAR T-cells produce higher amounts of IL-2 which may support their survival *in vivo* for longer. Together, these results illustrate that pCAR T-cells have a superior *in vivo* ability to control an established tumour burden, an outcome of the synergistic effects of 4-1BB and CD28 costimulation when aligned laterally.

Despite the demonstration of significant anti-leukaemic activity *in vivo* of CD19-specific pCAR T-cells, disease control was transient and most of the mice exhibited disease progression. A possible explanation for this observation is the downregulation or loss of CD19 by tumour cells under the selective pressure of pCAR T-cells as has been well documented in clinical research[123,124,252,253]. Post-mortem analysis of bone marrow demonstrated that loss of CD19 was detected in treatment groups compared to NALM-6 that remained in culture (data not shown). The mechanisms of CD19 loss or modulation include alternative splicing, whereby CD19 isoforms are generated that interrupt or mask the target epitope[175,176], disruption of trafficking of CD19 to the cell surface[177] and trogocytosis of the receptor by CAR T-cells[183].

Overall, the results shown in this chapter show that pCAR T-cells achieve superior anti-tumour activity and delayed disease progression *in vivo* when compared to mice treated with F-2 or V_H mutated CDR3 second-generation CAR T-cells. Mice showed no symptoms of xenograft GvHD such as weight loss, signifying that improved survival was a result of the low tumour burden. Nonetheless, to achieve complete tumour regression, increasing the CAR T-cell dose may be considered for future efficacy studies. Finally, further study is required to uncover the mechanistic differences between CAR and pCAR T-cells as caused by modifications in costimulation. Nanostring analysis performed after pCAR and

CAR encounter target antigen will show any differential gene expression as caused by the different signalling pathways initiated such as increased JAK-STAT signalling in pCAR T-cells.

Chapter 5: Investigating treating B-cell malignancies with dual targeting pCARs

5.1 Introduction

In recent years, CAR T-cell immunotherapy has shown substantial success against refractory B-cell malignancies[150] and has revolutionised the manner in which cellular therapies are developed. Considerable progress has been made in further engineering CAR T-cells to optimize performance and safety[254]. Nevertheless, several challenges have emerged from clinical research which will inevitably guide further preclinical development of CAR T-cell therapy. First, advancement of effective treatments for patients who relapse with CD19-negative disease is a frontline need and will require re-engineering of CAR T-cells to refine potency and precision. A number of approaches to address this issue have been presented below and undoubtably more strategies will continue to emerge.

5.1.1 Dual antigen targeting using CAR T-cells

The emergence of acquired resistance to CAR T-cell immunotherapy through antigen loss or lineage plasticity has been predicted using several preclinical models[182,255]. Furthermore, remarkable success has been achieved with anti-CD19 CAR T-cell therapy however, many patients relapse with CD19-negative disease[252]. One approach under investigation to prevent tumour escape is to target multiple B-lineage antigens using co-expressed CARs, whereby selective pressure against two antigens may reduce the likelihood of antigen loss variants[256]. Furthermore, dual or multi-antigen targeting by CARs may overcome interpatient variability in antigen expression[257,258]. Indeed, expression levels of CD19, CD20 and CD22 may be heterogeneous in tumour cells from patient to patient and further

immunophenotypic changes may occur with relapse[259,260]. Based on the approach used to target multiple antigens, Boolean logic has been applied to "gate" the activity of CAR T-cells. The "OR" gate describes CAR T-cells that are able to mount an anti-tumour response in the presence of either target antigen such as T-cells transduced with two independent CARs or a pooled mixture of different CAR T-cells. Conversely, "AND' gated CAR T-cells require expression of both antigens for activation thus are potentially capable of reducing off-target toxicity[261,262]. Finally, "NOT" logic-gated CAR T-cells aim to distinguish target cells from normal tissue and improve safety of CAR T-cells. For example, co-expressed inhibitory CARs contain an immune checkpoint-derived endodomain (e.g. PD-1 or CTLA-4) that transiently inhibits CAR T-cell activation when both cognate and inhibitory targets are expressed[263].

The scarcity of unique tumour associated antigens (TAA) means that the risk of on-target off-tumour toxicity remains a concern. To address this concern, AND gates have been described, capable of sophisticated pattern recognition such that a combination of antigens is required for activation. Sadelain et al. proposed a dual-signalling system that targeted prostate stem cell antigen (PSCA) using a first-generation CAR, providing signal 1, combined with a dual co-stimulatory CCR specific for prostate specific membrane antigen (PSMA), thus providing signal 2[264]. This system requires engagements of both targets for optimal activation and augments CAR T-cell reactivity against double positive tumours. In a similar approach, co-expression of a HER2- and MUC1- specific CAR that signal through CD3ζ and CD28 respectively enabled lysis of $HER2^+$ cells efficiently[265]. However, maximal proliferation and IL-2 release required the presence of both HER2 and MUC1.

Another approach to dual targeting involves coupling two distinct scFv domains using a linker into a single CAR construct, known as tandem CARs (TanCARs) utilising the "OR' gate[266]. As such, the TanCAR can bind to more than one target molecule in tandem. An

advantage to this system is that only one of the targets is required to activate T-cells' cytolytic activity against the tumour but synergistic enhancement of effector function may be achieved when more than one antigen is encountered. Pre-clinical investigation of a CD19-CD20 TanCAR highlighted that the dual construct could prevent the emergence of CD19-negative tumour cell variants *in vivo*[267]. Another example of a TanCAR was generated by Schneider et al, who made variants in which either CD19 or CD20-specific scFvs were expressed as the distal binding moiety on the CAR, and these were compared to traditional second-generation CARs[187]. Both TanCARs exhibited superior efficacy in a lymphoma xenograft model compared to a second-generation anti-CD19 CAR. In addition, CD19 and CD20 expression was better maintained on Raji lymphoma cells when co-incubated with TanCARs, but more significantly diminished by exposure to single targeted CAR T-cells. These pre-clinical findings led to a phase I study in patients with relapsed/refractory NHL and demonstrated CR or PR in 3/6 heavily pre-treated patients with no dose limiting toxicities[268]. Importantly, down-regulation of both targets was not identified among the patients who relapsed, suggesting that other mechanisms had resulted in treatment failure.

5.1.2 Aims of this chapter

- To design and engineer a dual-targeting pCAR construct that would recognise distinct B-cell lineage markers and exert cytotoxicity against leukaemia and lymphoma cell lines.
- To compare dual-targeting pCARs to second-generation CARs in terms of cytotoxicity, restimulation potential and *in vivo* anti-tumour efficacy.

5.2 Results

5.2.1 Expression of B-cell lineage markers on Acute Lymphoblastic Leukaemia (ALL) and Burkitt lymphoma cell lines

To determine the suitability of targeting two distinct antigens to treat B-cell malignancies, the expression of CD19, CD20 and CD22 was investigated on a panel of human leukaemia and lymphoma cell lines. Flow cytometry demonstrated that CD19 was highly expressed on the cell surface of Daudi, Raji and NALM-6 tumour cell lines (Fig. 5.1). The human ALL cell line NALM-6 has been previously reported to express low levels of CD20, however expression was found to be below the level of detection here. Both Burkitt lymphoma cell lines, Daudi and Raji, express high levels of CD20 and a range of CD22 expression was detectable on the cell surface of all these tumour cell lines.

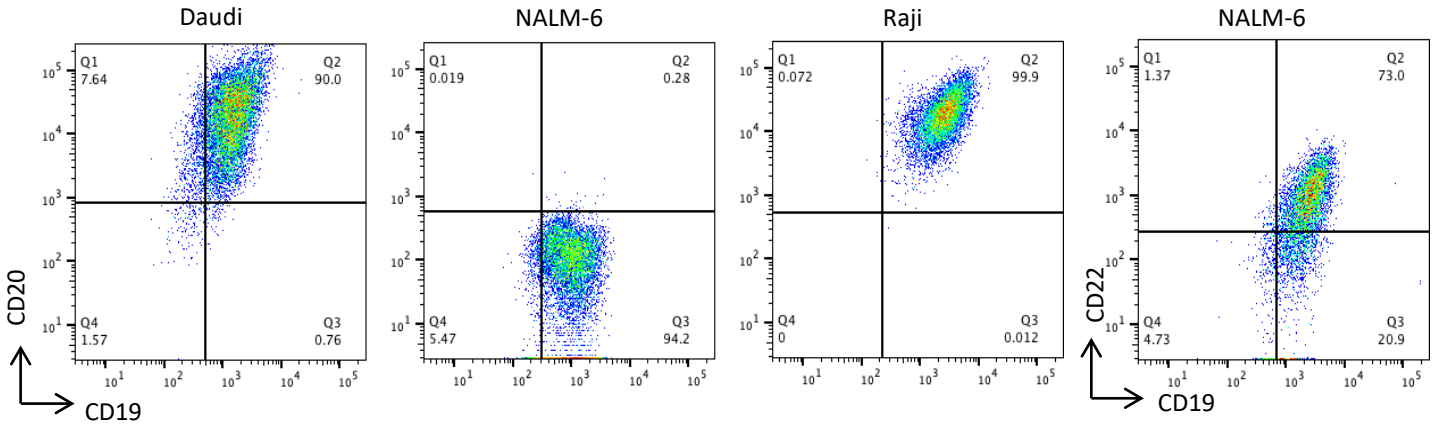

Figure 5.1 B-cell receptor expression on leukaemia and lymphoma cell lines. A panel of leukaemia and lymphoma cell lines was probed for the cell surface expression of CD19, CD20 and CD22 using monoclonal mouse anti-human CD19, CD20 and CD22 antibodies. Cells were also stained using a mouse IgG1k isotype to show the specificity of staining. Data are representative of three independent replicate studies, all of which yielded similar results.

5.2.2 Engineering of second-generation CAR and dual specificity pCARs targeted against CD19 and CD20

Two second generation CARs were engineered by molecular cloning, namely the CD19-specific SFG F-2 construct (FMC63-28ζ) and the CD20-specific SFG 1-2 construct (1F5-28ζ). In addition, a pCAR was engineered in which the SFG F-2 CAR was paired with a chimeric co-stimulatory receptor (CCR) comprising the 1F5 scFv fused via a CD8α spacer to 4-1BB. The 1F5 scFv is derived from a murine anti-human CD20 mAb, the avidity of the native bivalent antibody is 7.56 x 10^8 M^{-1} which was measured by scatchard analysis[218]. In the pCAR construct, equimolar expression of both CCR and CAR was ensured through inclusion of a furin cleavage site followed by a flexible serine-glycine linker and an intervening P2A ribosomal skip 2A peptide. All constructs contain an extracellular 10-amino acid myc epitope tag which was incorporated to enable CAR detection by flow cytometry. All CAR and pCAR constructs were expressed using the SFG retroviral vector[269]. Fig. 5.2 and Table 2.2 provides nomenclature and a structural overview of the CAR and pCAR constructs described.

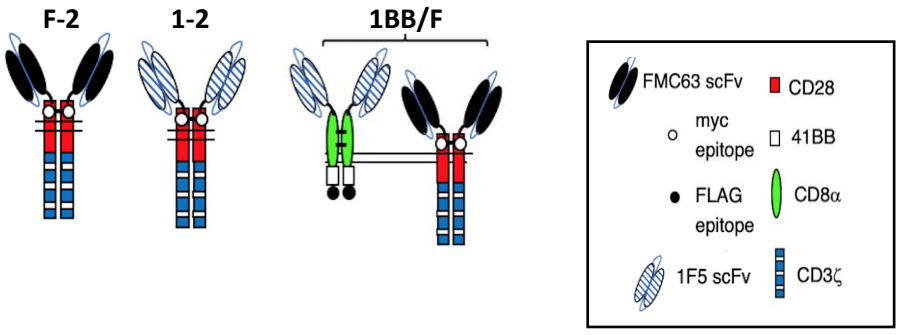

Figure 5.2 Schematic overview of CD19-CD20 dual targeted pCAR and control second generation CARs. The diagram shows the structural features of the 1BB/F pCAR and the second-generation controls F-2 and 1-2 targeting CD19 and CD20, respectively. In the CAR position, 1BB/F contains the CD19 targeting scFv FMC63 followed by a CD28 hinge transmembrane and endodomain and a CD3ζ signalling domain. In the CCR position, the CD20 targeting scFv 1F5 is followed by a CD8α hinge and transmembrane domain and 4-1BB endodomain.

5.2.3 Expression of CARs and pCARs by retrovirus transduced primary human T-cells

Prior to testing of anti-tumour activity, expression of CARs and pCARs was demonstrated in primary human T-cells. Peripheral blood mononuclear cells (PBMCs) were isolated from healthy donors and retrovirally transduced 48 hours post activation. Following retroviral-mediated gene transfer using 293VEC-GALV packaging cells, T-cells were tested for cell surface expression of encoded chimeric receptors using flow cytometry. As shown in Fig. 5.3, all three CARs could be detected at the cell surface.

To further confirm CAR and CCR expression and to confirm that chimeric receptors could recognise their target antigens, the ability of recombinant human CD19-Fc and CD20-Fc chimeric proteins to bind transduced T-cells was tested (Fig. 5.4). Binding to CD19- and CD20-Fc was observed by the dual-targeting 1BB/F pCAR while, as expected, the second-generation constructs F-2 and 1-2 bound CD19 and CD20, respectively.

Taken together, this data demonstrate that T-cells can be efficiently and stably transduced with 1BB/F, F-2 and 1-2 constructs.

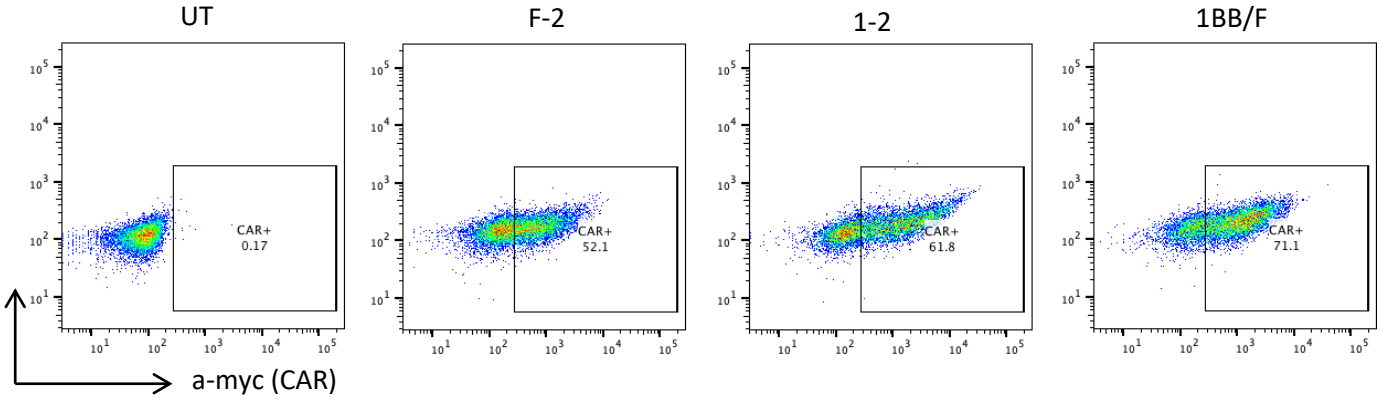

Figure 5.3 Expression of CD19-CD20 dual targeted pCAR and control second generation CARs in human T-cells. Primary human T-cells were transduced with the indicated pCAR/CAR-encoding retroviral vectors and were assessed by flow cytometry on day 3 post transduction. The presence of CD19-specific CARs (F-2 and 1BB/F) and the CD20-specific CAR (1-2) was detected by flow cytometry after incubation with myc specific 9e10 antibody followed by goat anti-mouse PE. The level of CAR expression in all cases was compared to untransduced (UT) T-cells probed with the same antibody combinations. Data is representative of 5 independent donors.

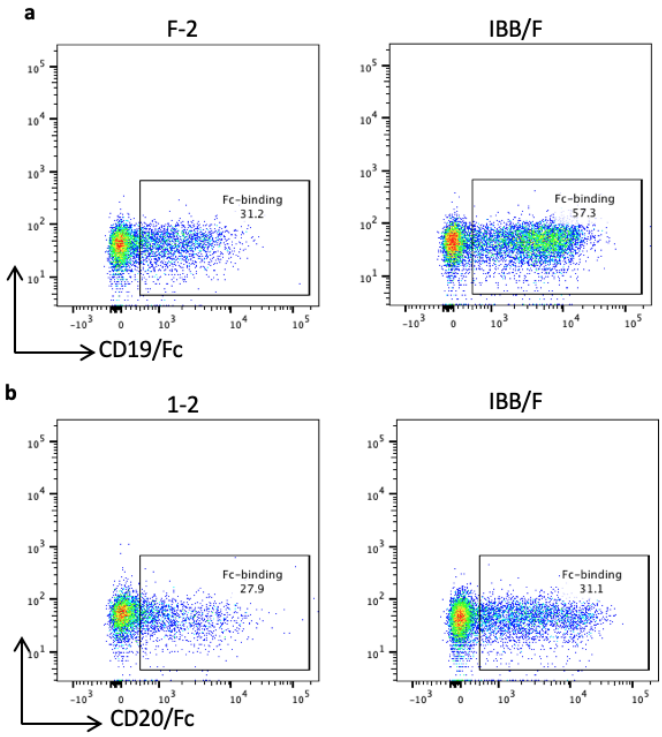

Figure 5.4 Detection of CAR and pCAR expression in human primary T-cells using Fc recombinant proteins. Primary human T-cells were transduced with the indicated CARs or pCAR and were stained with (a) CD19-Fc which is expected to bind the FMC63 scFv. Cells were also stained with (b) CD20-Fc to detect the 1F5 scFv in the 1-2 CAR and 1BB/F pCAR. Binding of the Fc fusion proteins was detected with Alexa-Fluor conjugated anti-human IgG. Boxes demarcate specific staining when compared to cells that were incubated with secondary reagent alone. Data is representative of 5 independent donors.

5.2.4 Investigation of anti-tumour activity of B-cell-targeted CAR and pCAR T-cells in serial restimulation assays with Raji and NALM-6 tumour cells

In order to investigate the ability of the dual CD19/CD20 targeted pCAR to promote T-cell proliferation and continued cytotoxicity upon multiple rounds of *in vitro* antigen exposure, co-culture experiments were performed with Raji and NALM-6 cell lines. T-cells were exposed to fresh cancer cell co-cultures twice weekly, in the absence of exogenous cytokines, and T-cell expansion was quantified using counting beads at the time of each restimulation cycle by flow cytometry. Pooled data from 4-5 independent replicate experiments are shown in Fig. 5.5 and shows the number of restimulation cycles undertaken by each CAR T-cell population. Cultures were terminated when tumour cell cytotoxicity fell below 20%. At the time of each re-stimulation cycle, the percentage of viable NALM-6 and

Raji cells was determined by luciferase assay (Fig. 5.5a-b). Supernatant was removed from these cultures after 24h and analysed for IL-2 and IFN-γ concentration by ELISA (Fig. 5.6). As shown in Fig. 5.5 and 5.6 the dual-targeting pCAR 1BB/F did not outperform either of the CD19- or CD20-specific second-generation CARs in terms of proliferative capacity, tumour cell cytotoxicity or cytokine production.

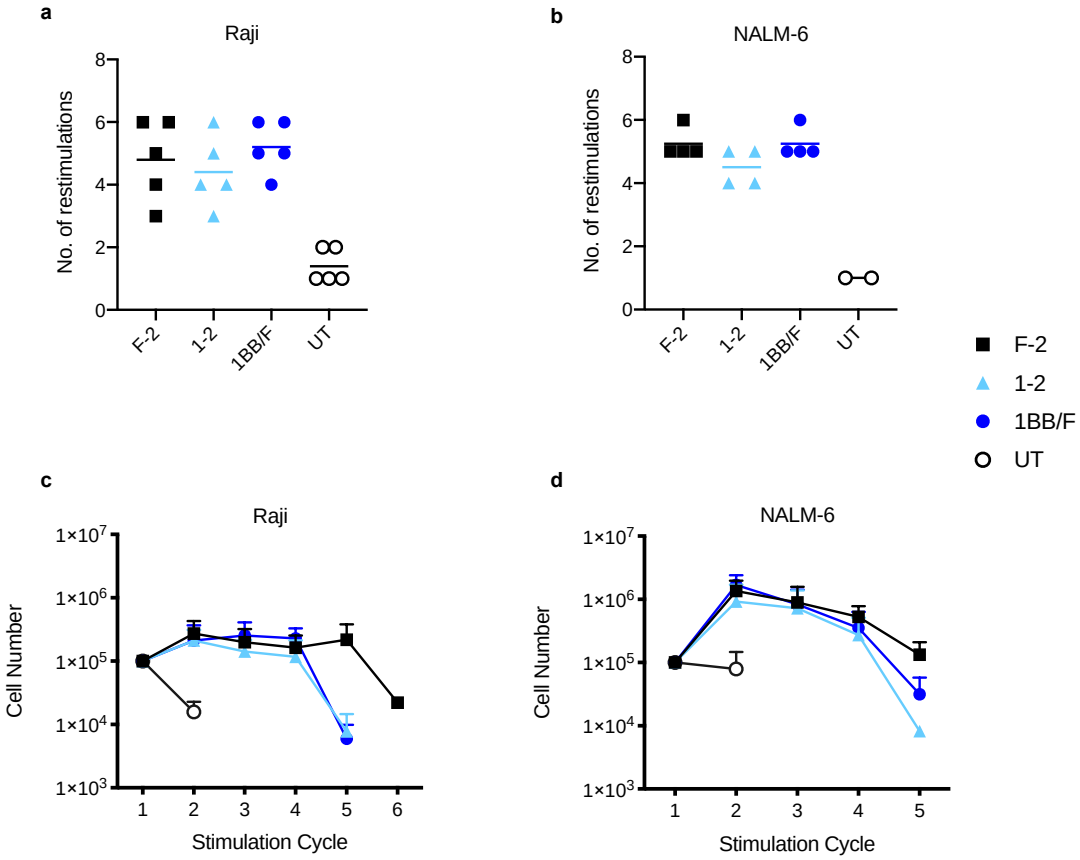

Figure 5.5 In vitro evaluation of 1BB/F pCARs. 1 x 10^5 of the indicated transduced CAR or pCAR T-cells were co-cultivated in triplicate with an equal number of Raji or NALM-6 tumour cells. After 72 hours, viability of the tumour cells was determined by luciferase assay and 1 x 10^5 fresh tumour cells were added to re-stimulate the T-cells. Cultures were terminated when T-cells exhibited less than 20% killing. Re-stimulation cultures shown in panels a-b were evaluated for Raji (a) and NALM-6 (b) viability at 72h (mean ± SEM). CAR T-cell numbers were enumerated for Raji (c) and NALM-6 (d) at the indicated cycles using counting beads. T-cells were identified as RFP negative events Data presented as mean ± SEM from 5 independent donors.

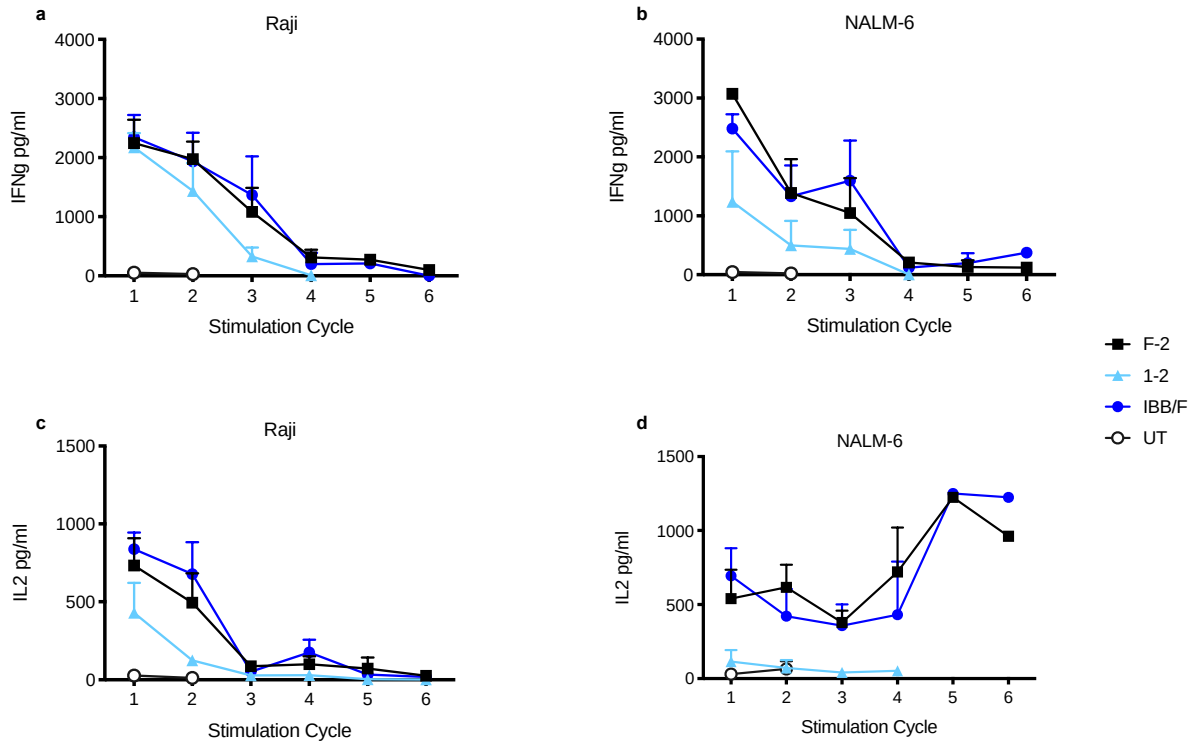

Figure 5.6 Cytokine release by CAR$^+$ T-cells is maintained upon serial re-stimulation. 1 x 10^5 of the indicated transduced CAR or pCAR T-cells were co-cultivated in triplicate with an equal number of Raji or NALM-6 tumour cells in the absence of exogenous cytokine support. One day after each cycle of stimulation, supernatant was removed from these cultures and tested for IFN-γ (a-b) or IL-2 (c-d) release by ELISA. Data presented as mean ± SEM from 5 independent donors.

5.2.5 Engineering of LO68-CD19$^+$CD20$^+$ cell lines

As shown previously, NALM-6 leukaemic cells express very low levels of CD20. Furthermore, Raji lymphoma cells express high levels of CD80 and CD86, which are known to provide co-stimulatory signalling by engaging CD28 on T-cells [270,271]. Consequently, to compare CAR and pCAR function, it was desirable to establish a model in which both antigens were expressed strongly while co-stimulatory ligands were absent. The human mesothelioma malignant cell line LO68 naturally lacks expression of B-cell markers and is not susceptible to killing by CD19-targeted CAR T-cells. As shown previously, LO68 cells were genetically engineered to

express high levels of human CD19 alone (Fig. 3.6). Here, LO68-CD19$^+$ were further engineered to express human CD20 and CD22 via retroviral transduction (Fig. 5.7).

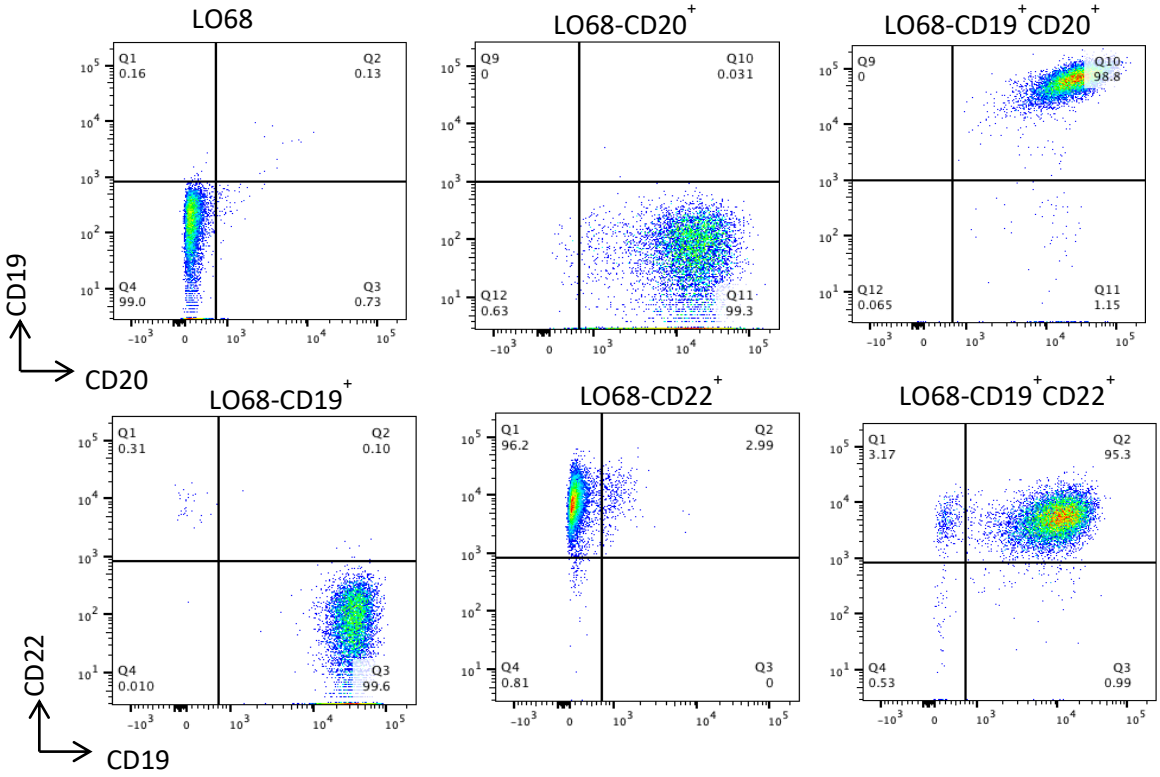

Figure 5.7 Retrovirally transduced LO68 cells engineered to express CD19, CD20 and CD22. The mesothelioma line LO68 was retrovirally transduced to express human CD19, CD20 and CD22. Antigen expression was detected by flow cytometry after incubation with the indicated directly conjugated antibodies. Data are representative of 3 independent replicate experiments.

5.2.6 Investigation of anti-tumour activity of B-cell-targeted CAR and pCAR T-cells in serial restimulation assays with LO68-CD19$^+$CD20$^+$ tumour cells

The activation and cytotoxic activity of CAR and pCAR T-cells was next investigated by performing co-cultivation experiments in which CAR T-cells were co-cultured with LO68 tumour cells engineered to express CD19 and/or CD20 at different effector to target ratios (Fig. 5.8). The anti-tumour activity of CAR T-cells in the presence of their target was compared to that achieved with untransduced T-cells (UT) and assessed by MTT assay after 72 hours. When tested in dose-response cytotoxicity assays, CAR and pCAR T-cells exhibited cytotoxic activity against LO68-CD19$^+$CD20$^+$ cells in a dose dependent manner. However,

equivalent performance of the 1BB/F pCAR and F-2 or 1-2 CAR T-cells was observed and tumour specific killing was no longer apparent an E:T ratio of 1:128. When tested against LO68-CD20^{+} tumour cells, 1BB/F pCAR T-cells were able to mediate approximately 30% killing in the absence of CAR activating CD19. Supernatant from the cocultivation with LO68-CD19^{+}CD20^{+} was harvested after 24h and analysed for IL-2 and IFN-γ cytokine release (Fig. 5.8b-c). At E:T 1:4, 1BB/F pCAR T-cells released significantly more IL-2 compared to F-2 and UT T-cells. All CAR and pCAR T-cells released significantly higher levels of IFN-γ compared to UT T-cells however, there was no significant difference between CAR and pCAR T-cells.

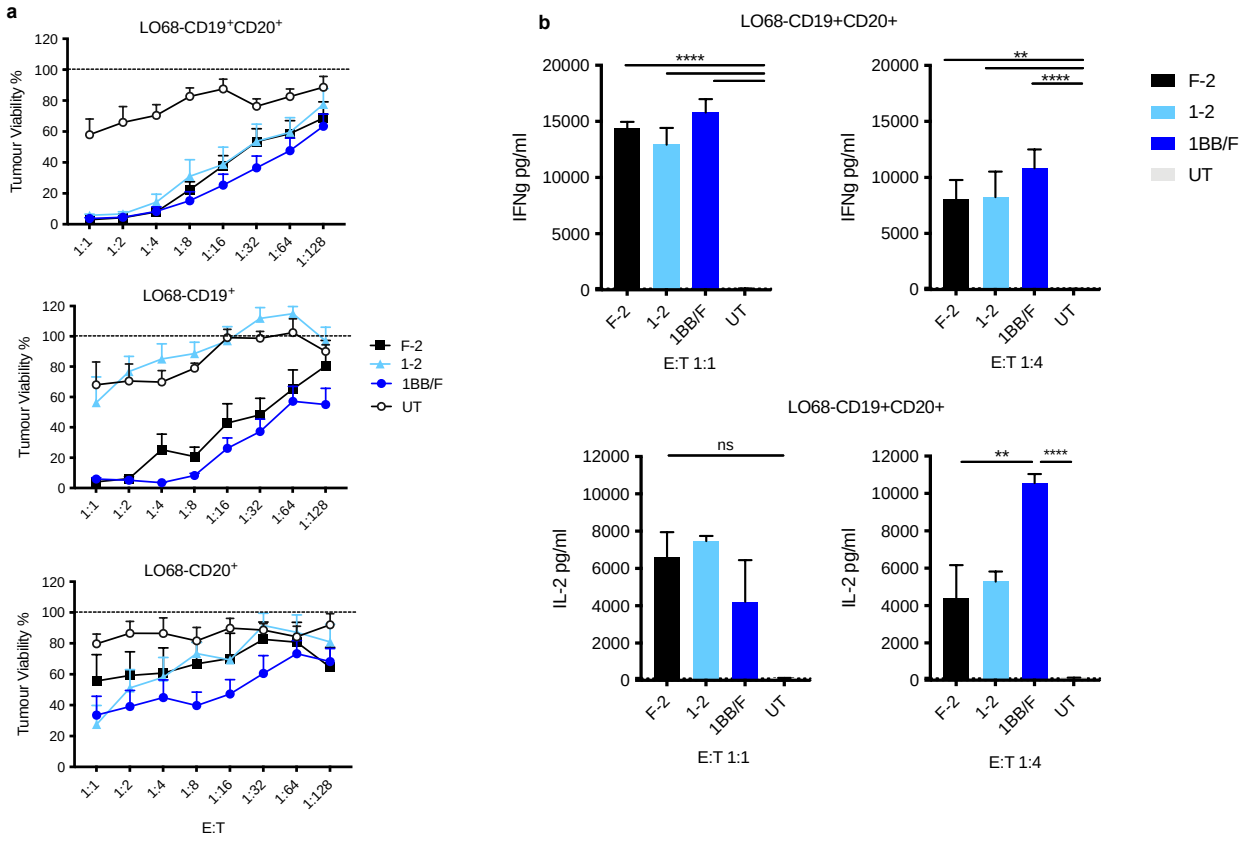

Figure 5.8 Cytotoxic activity and cytokine release of CAR and pCAR T-cells against LO68 tumour cells engineered to express CD19 and CD20. a) CAR or pCAR T-cells were co-cultivated with LO68 tumour cells engineered to express CD19 and/or CD20 at the indicated E:T ratio. Target viability was quantified after 72h by MTT assay (mean ± SEM, n=4). b-c) Supernatants were collected after 24h from co-cultivations established at a 1:1 and 1:4 effector to target ratio and were analysed for IFN-γ (b) and IL-2 (c). Data shown are mean ± SEM from 4 independent donors. Statistical analysis was performed with one-way ANOVA followed by Tukey post hoc test. **** p=<0.0001; *** p= ≤ 0.001; ** p= ≤ 0.01 n=3 independent replicates.

The restimulation potential of pCAR and CAR-engineered T-cells in the absence of CD80/CD86 co-stimulation was next investigated. All engineered T-cell populations were re-stimulated on LO68-CD19^{+}CD20^{+} monolayers every 72 hours until tumour killing activity fell below 20%. Notably, both second generation CAR and pCAR T-cells would undergo an increased number of re-stimulation cycles on LO68 cells, when compared to Raji and NALM-6 cells. 1BB/F and F-2 T-cells retained their cytotoxicity for an equivalent number of stimulation cycles and destroyed >80% of the tumour monolayer at each round of antigen exposure. Furthermore, re-activated F-2 and 1-2 CAR T-cells demonstrated more sustained IFN-γ release against LO68-CD19^{+}CD20^{+} tumour cells (Fig. 5.9). However, taken together, the data shows no significant difference between conventional second-generation CARs and the 1BB/F pCAR as there was no statistical difference between their functionality.

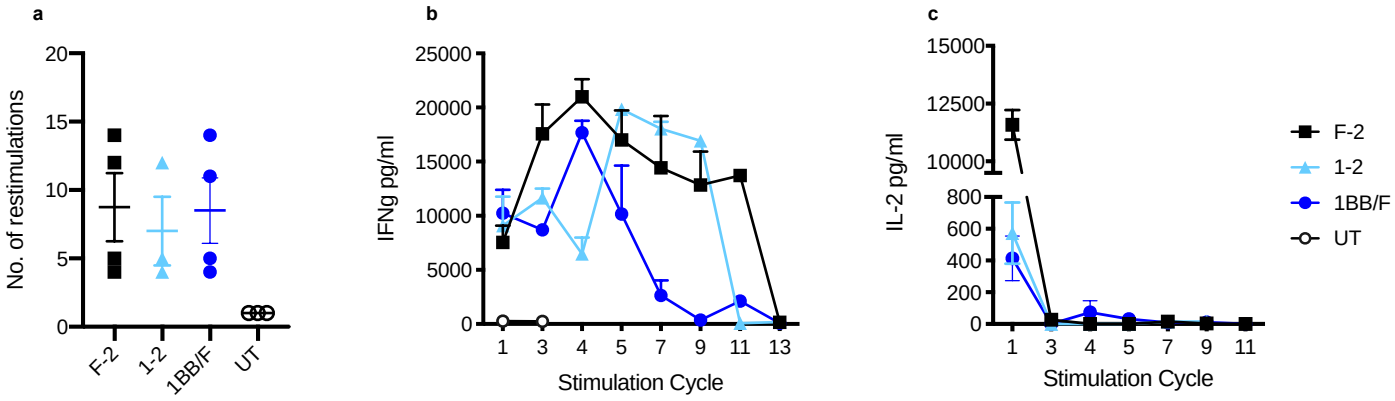

Figure 5.9 Re-stimulation of CD19- and CD20-specific CAR and pCAR T-cells on LO68-CD19^{+}CD20^{+} tumour cell monolayers. (a) T-cells were engineered to express the CARs F-2, 1-2 or the 1BB/F pCAR. 1x10^{5} transduced CAR or pCAR T-cells were co-cultivated in triplicate with an equal number of LO68-CD19^{+}CD20^{+} tumour cells. After 72hs, T-cells were transferred to a fresh monolayer of LO68-CD19^{+}CD20^{+} cells. Plots indicate number of re-stimulation cycles completed. Cultures were terminated when tumour cell viability was 80% or greater. **(c-d)** 24h after each cycle of stimulation, supernatant was removed from these cultures and tested for IFN-γ **(c)** and IL-2 **(d)** release by ELISA (Data presented as mean ± SEM from 4 independent donors).

5.2.7 Design and engineering of second-generation anti-CD22 CAR and dual targeting pCARs against CD19 and CD22

Given the lack of superior anti-tumour activity of the 1BB/F pCAR when tested using B-cell leukaemia and lymphoma cells, I next explored an alternative approach to target two different B-cell antigens. Given its widespread expression in B-cell malignancy, I selected CD22 as a target antigen alongside CD19. To engineer CARs and pCARs with specificity for CD22, the RFB4 scFv was used as the targeting moiety. The RFB4 scFv is derived from a murine anti-CD22 mAb with a K_d of 5.8 nM[272], which can mediate significant anti-tumour activity when incorporated into a CAR[273], but has not been testing clinically. Figure 5.10 illustrates the structure and nomenclature assigned to the newly engineered constructs R-2, RBB/F, RBB/G02 and RBB/Y05.

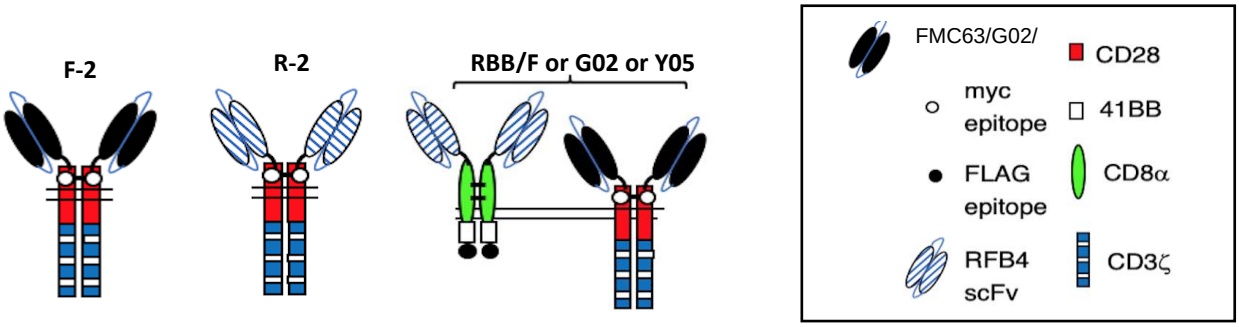

Figure 5.10 Schematic overview of CD19-CD22 dual targeted pCAR and control second generation CARs. The diagram shows the structural features of the RBB/F, RBB/G02 and RBB/Y05 pCARS and the second-generation controls F-2 and R-2, targeted against CD19 and CD22 respectively. In the CAR position, RBB/F, RBB/G02 and RBB/Y05 contain the CD19 targeting scFv FMC63, G02 or Y05 respectively followed by a CD28 hinge, transmembrane and endodomain and a CD3ζ signalling domain. In the CCR position, the CD22 targeting scFv RFB4 is followed by a CD8α hinge and transmembrane domain and 4-1BB endodomain.

5.2.8 Expression of RBB/F pCAR in primary human T-cells

Stable expression of CARs in primary human T-cells was achieved using transient virus produced from 293T cells using the triple transfection method (as described above), thus

avoiding the need to generate stable retroviral packaging cell lines. Successful T-cell transduction is illustrated in Fig. 5.11. Since the CAR and CCR contain distinct epitope tags, their equivalent co-expression was demonstrable by flow cytometry.

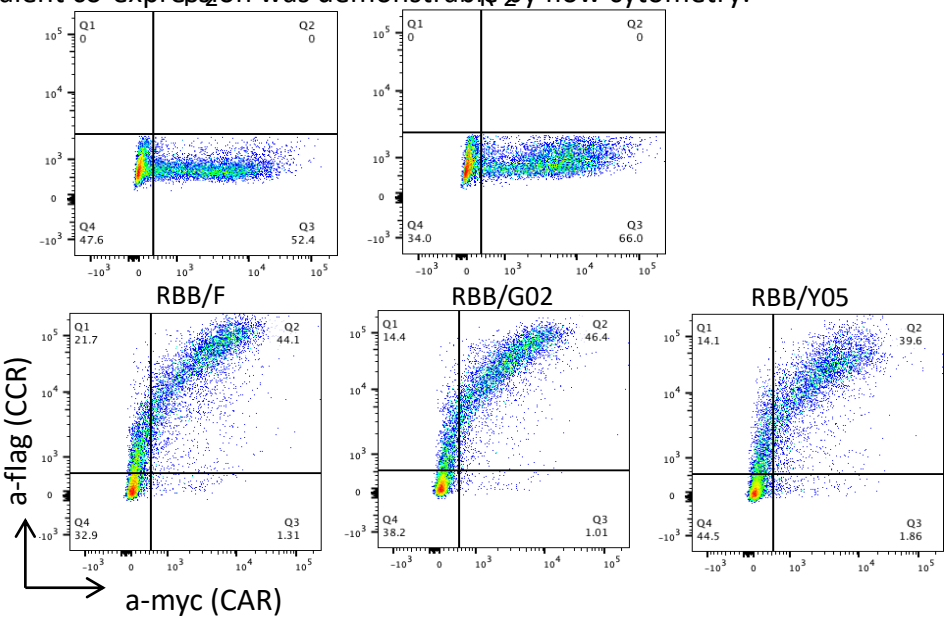

Figure 5.11 Expression of CD19-CD22 dual targeted pCAR and control second generation CARs in human T-cells. Human T-cells were engineered by retroviral transduction to express the indicated CAR or pCAR. T-cells were incubated with antibodies directed against both MYC (CAR) and FLAG (CCR) epitope tags and then analysed by flow cytometry. Data are representative of three independent donors.

5.2.8 *In vitro* evaluation of pCAR T-cells targeted against CD22 and CD19

T-cells were engineered to express CARs and pCAR constructs to compare cytotoxicity and cytokine release when co-cultured with firefly luciferase-expressing NALM-6 cells at varying effector to target (E:T) ratios. Surface expression of CD22 on NALM-6 leukaemic cells was approximately 80%. When tested in dose-response luciferase assays, potent cytotoxicity was observed after 72 hours by all CAR T-cells, compared to UT T-cells. Furthermore, all RBB/ pCARs outperformed both F-2 and R-2 second-generation CARs. In particular, RBB/G02 and RBB/Y05 significantly destroyed NALM-6 cells to a higher degree compared to F-2 and R-2 CAR T-cell. Of note, RBB/G02 pCAR T-cells performed significantly better than RBB/F

further highlighting that a lower avidity CAR improves function in this system (Fig. 5.12a). To quantify activation of CAR T-cells, IFN-γ and IL2 levels were measured in supernatants collected after 24 hours from co-cultures established at 1:1 and 1:4 E:T ratios. As expected, untransduced T-cells elicited minimal cytokine release while all signalling competent CAR T-cells produced IL2 and IFN-γ upon recognition of CD19 and/or CD22 (Fig. 5.12b-c). The CAR T-cells RBB/Y05 produced the greatest levels of IFN-γ whereas there was no statistical differences in IL-2 release.

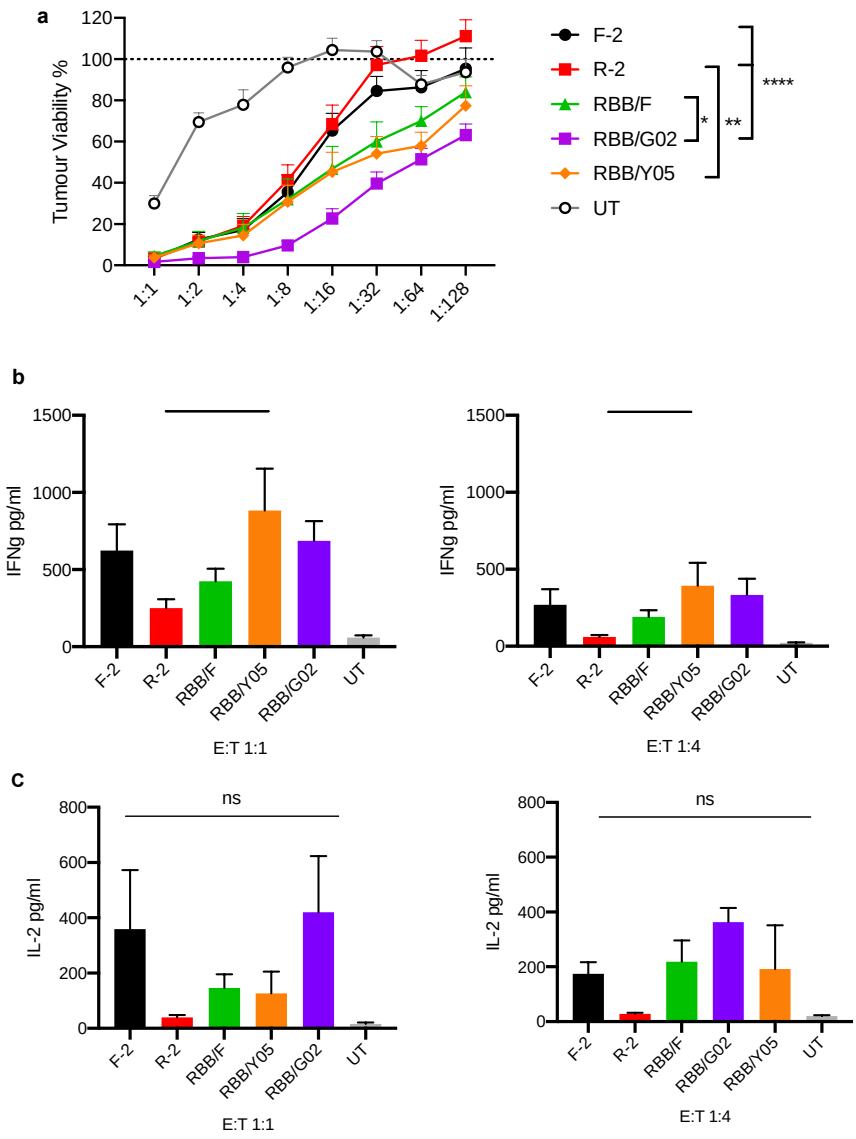

Figure 5.12 Cytotoxic activity and cytokine release by CAR and pCAR T-cells when co-cultured with NALM-6 cells. (a) CAR or pCAR T-cells were co-cultivated with NALM6 leukaemia cells at the indicated E:T ratio. Target viability was quantified after 72h (mean ± SEM, n= 4-8 independent replicates). (b) Supernatants were collected after 24h from the co-cultivation experiments at a 1:1 and 1:4 E:T ratio and were analysed for IFN-γ. Data shown are mean ± SEM from 4-8 independent donors. Statistical analysis was performed with one-way ANOVA followed by Tukey post hoc test. ** p= ≤ 0.01; *p=≤ 0.05.

5.2.9 Validation of anti-tumour potential of RBB/F pCAR$^+$ T-cells upon serial restimulation

In order to investigate the ability of RBB/F pCAR T-cells to repeatedly kill leukaemic cells, re-stimulation co-culture experiments were performed with NALM-6 cells. Engineered T-cells and NALM-6 cells were initially co-cultured at a 1:1 ratio and subjected to successive rounds of antigen stimulation in the absence of exogenous cytokine. As shown in Fig., 5.13, RBB/F T-cells repeatedly outperformed F-2 and R-2 T-cells by maintaining cytotoxicity for as many as 29 stimulation cycles. Furthermore, RBB/F T-cells maintained IFN-γ production over numerous restimulation cycles although differences were not significant.

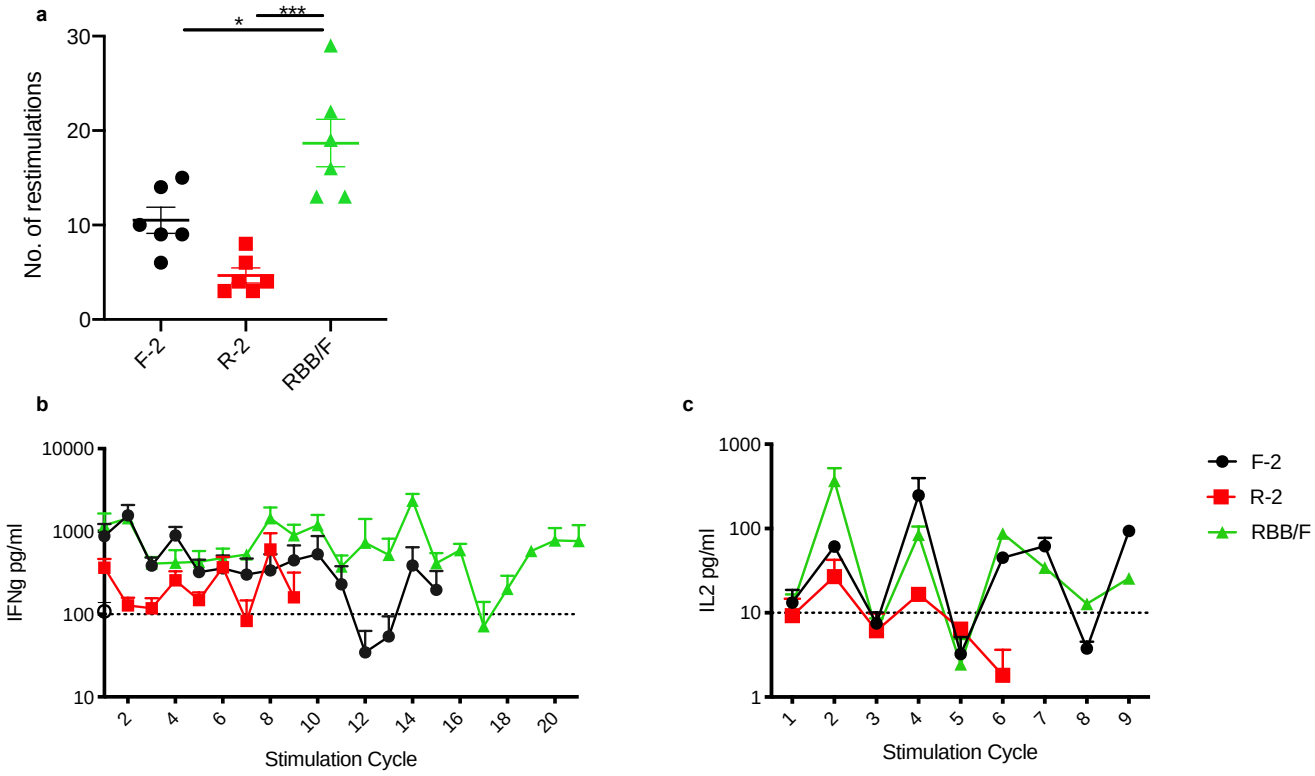

Figure 5.13 In vitro restimulation potential of RBB/F pCAR T-cells. 1 x 10^5 of the indicated CAR or pCAR T-cells were co-cultivated in triplicate with an equal number of NALM-6 cells. After 72 hours, viability of the tumour cells was determined by luciferase assay and 1 x 10^5 fresh tumour cells were added to re-stimulate the T-cells. Cultures were terminated when T-cells exhibited less than 20% tumour cell killing. **a)** Number of re-stimulation cycles in which ≥80% tumour cell destruction was seen. 24h after each cycle, supernatant was removed and tested for IFN-γ **(b)** and IL-2 **(c)** by ELISA. Data are presented as mean ± SEM from 4 independent donors. Statistical analysis was performed with 2-way ANOVA followed by Tukey post hoc test. *** p= ≤ 0.001; *p=≤ 0.05.

5.2.10 NALM-6 antigen escape after incubation with CAR T-cells

In light of recent reports of CD19-negative disease relapse occurring in patients after CAR T-cell therapy, an experiment to model leukaemia escape under CAR T-cell immune pressure was established. It was hypothesised that RBB/F T-cells would exert equal immune pressure on CD19 and CD22 and therefore cause moderate down-regulation compared to single specificity CARs. CAR T-cells were co-cultured with NALM-6 cells at a low E:T ratio of 1:10. After 48 hours the expression of CD19 on NALM-6 cell surface was analysed by flow cytometry. When NALM-6 cells were co-cultured with T-cells, CD19 was down-modulated from the cell surface (Fig. 5.14) and F-2 cells demonstrated a trend towards promoting greater CD19 loss. RBB/F T-cells induced less antigenic loss of CD19 compared to R-2 and F-2 suggesting a lesser ability to select for leukaemia escape.

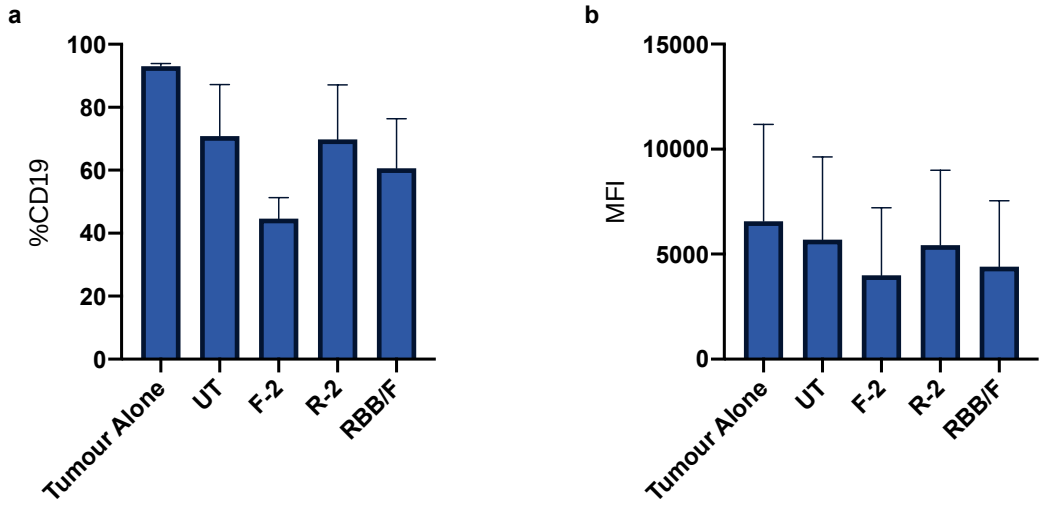

Figure 5.14 Determination of CD19 and CD22 down-modulation on NALM-6_LT cell surface. NALM-6 and CAR or pCAR T-cells were co-cultured at E:T ratio of 1:10. After 48h incubation, cultures were harvested, and viable NALM-6 cells examined for CD19 surface expression by flow cytometry. Graphs of CD19 surface expression (a) and MFI (b) in surviving NALM-6 cells after 48h of co-culture with CAR T cells, as determined by flow cytometry. (n=3 Bars represent means + SEM).

5.2.11 Anti-tumour activity of pCAR and CAR T-cells in the NALM-6 LT xenograft model

To compare the *in vivo* activity of CD19 targeting and dual CD19-CD22 pCARs, a study was performed using NSG mice with established NALM-6 leukaemic xenografts. NSG mice were intravenously injected with $5x10^5$ NALM-6 cells and leukaemia engraftment was evaluated on day 5 post leukaemic inoculation using bioluminescence imaging (BLI). Mice were then randomly assigned into groups with similar average leukaemia-derived bioluminescence. In parallel, PBMCs from a healthy donor were retrovirally transduced to express CARs or pCARs and then expanded for 12 days and assessed for transduction efficiency. On day 5 post NALM-6 inoculation, mice were treated with a modest CAR T-cell dose of $5x10^5$ cells in order to compare *in vivo* anti-tumour activity. Control mice that had received only PBS showed rapid disease progression. Overall, in this experiment all treated mice displayed only a transient delay in disease progression with disease relapse occurring 14 days post treatment in many mice. However, there was a trend towards pCAR treatment groups causing superior leukaemic reduction 14 days after T-cell transfer (Fig. 5.15).

To determine if the *in vitro* finding of sustained re-stimulation potential of pCAR T-cells correlated with increased persistence *in vivo*, the percentage of pCAR or CAR T-cells present after infusion was analysed. Fourteen days after T-cell infusion, three mice from each group were sacrificed and presence of CAR or pCAR T-cells was investigated by flow cytometry. Analysis of harvested spleens and peripheral blood revealed an increased percentage of pCAR T-cells. Recipients of RBB/Y05, RBB/G02 and FBB/Y05 pCAR T-cells showed significantly increased pCAR T-cells compared to F-2 treated mice (Fig. 5.16)

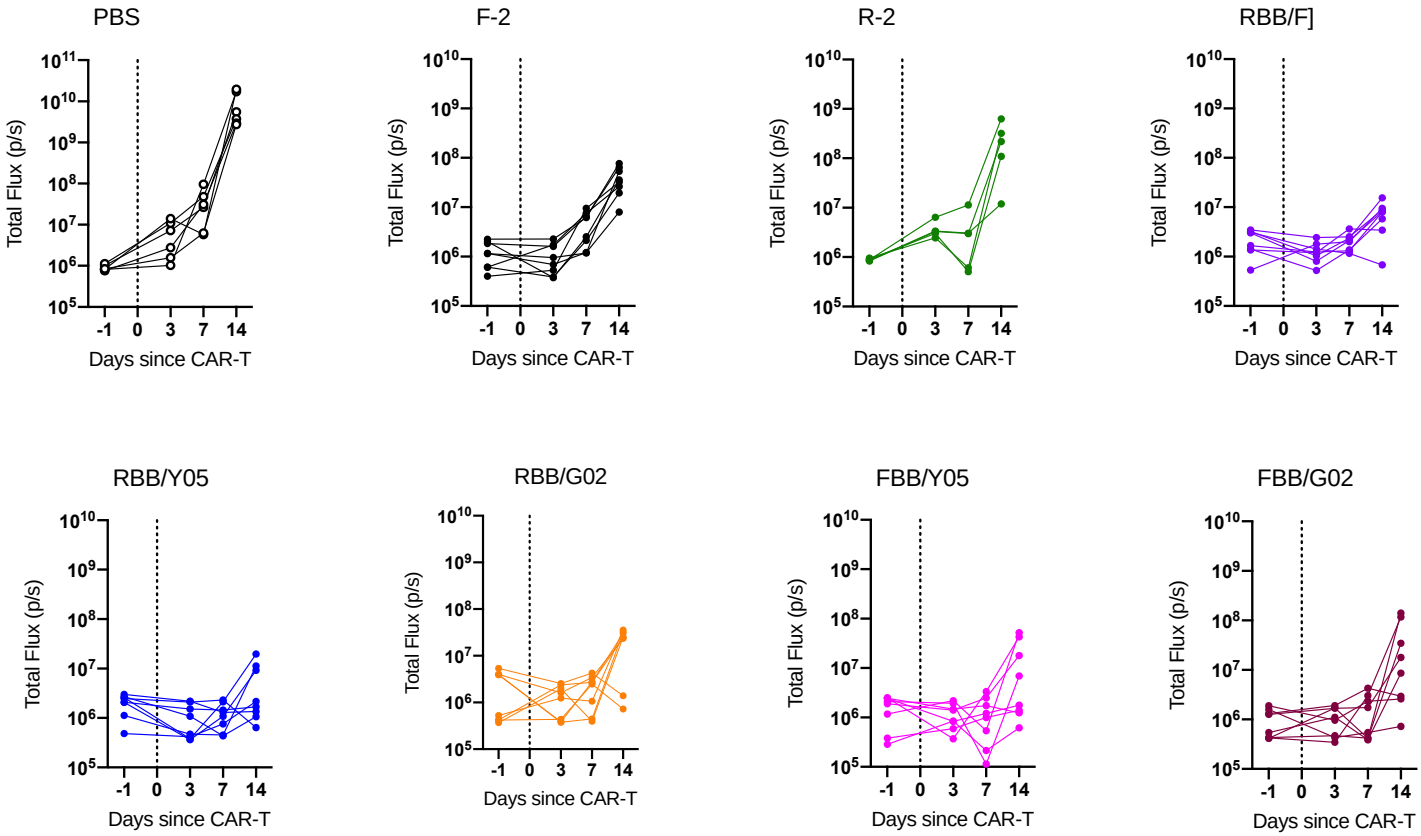

Figure 5.15 pCAR and CAR T-cells show transient disease control in the NALM-6 xenograft model. NSG mice were injected i.v. with 0.5 x10^6 RFP/ffLuc$^+$ NALM-6 cells. Disease engraftment was assessed on day -1/0 using the IVIS imaging system. On day 5, 0.5 x10^6 of the indicated CAR or pCAR T-cells were administered i.v. Disease burden was monitored by BLI.

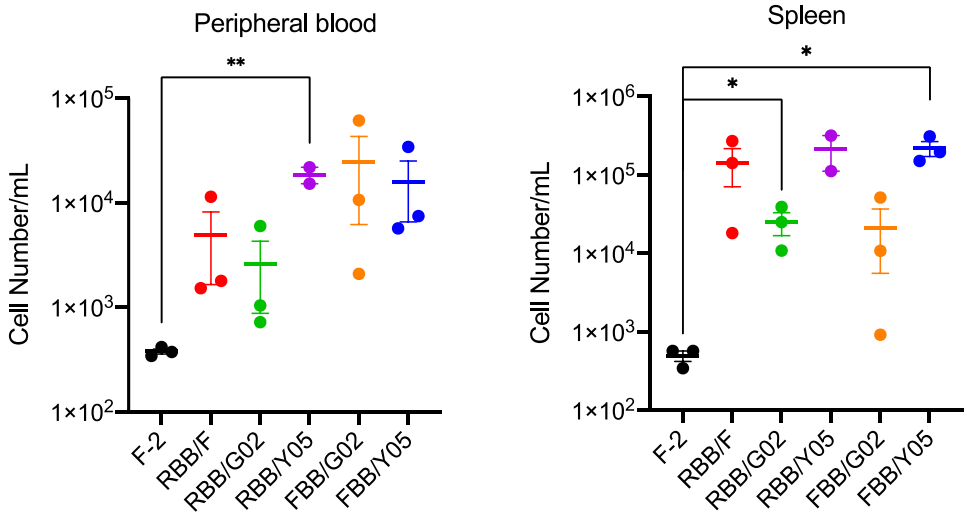

Figure 5.16 pCAR and CAR T-cells are detectable after 14 days in vivo. After termination of the experiment 14 days following infusion of CAR or pCAR T-cells, spleen and peripheral blood were investigated for presence of CAR T cells. Statistical analysis was performed with an unpaired Student's *t*-test. **p= ≤ 0.01; *p=≤ 0.05

5.2.12 Design and engineering of single-chain diabody CARs targeting CD19 and CD22

With the aim of combating CD19 antigen loss and, consequent disease relapse, diabody construct were designed in which single-chain fragments specific for CD22 and Myc are secreted by the F-2 second-generation CARs. Figure 5.10 illustrates the structure and nomenclature assigned to the newly engineered constructs. The premise behind these constructs is that the F-2 CAR T-cells will recognise CD19 and destroy tumour cells whilst the RFB4 scFv will recognise and bind CD22 and activate the F-2 CAR via the 9E10-Myc interaction. As such, if the CD19 antigen undergoes loss or downregulation the F-2 CAR can be redirected to the tumour cell as the single chain diabody will recognise CD22. Briefly, the 9E10.R/F-2 construct consists of the 9E10 V_H chain linked to the RFB4 V_L chain by a GAGSSG linker which is then joined via a long liner to the RFBG V_H – 9E10 V_H. Equimolar expression of both diabody and CAR was ensured through inclusion of a furin cleavage site followed by an intervening T2A ribosomal skip 2a peptide. The R.9E10/F-2 is designed in the reverse orientation, with the RFB4 scFv joined by a long linker flanked by the 9E10 scFv. Additionally, it was predicted that the CAR myc tag would be masked by binding of the 9E10 diabody therefore a FLAG tag was incorporated for ease of detection.

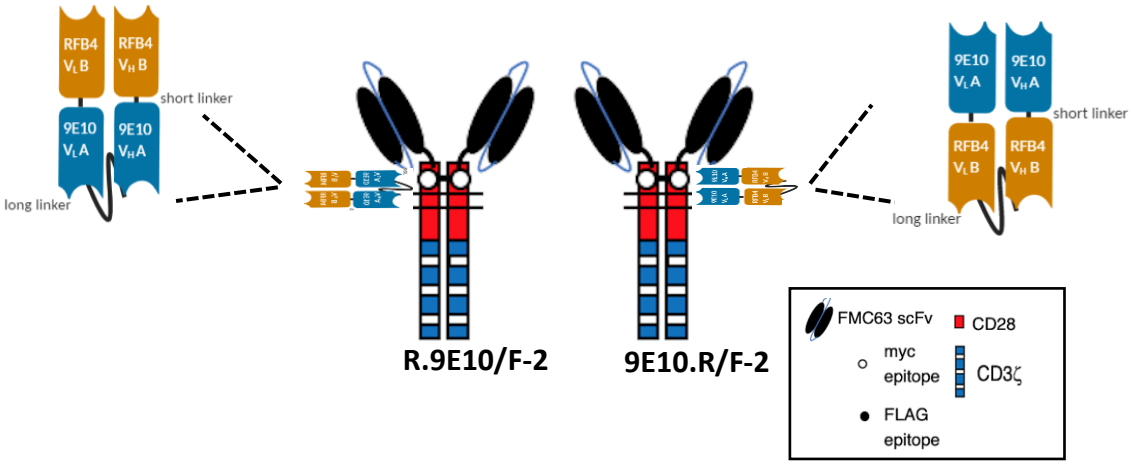

Figure 5.17 Schematic overview of CD19-CD22 single chain diabody CARs. The diagram shows the structural features of the R.9E10/F-2 and 9E10.R/F-2 constructs targeted against CD19 and CD22 respectively. The CAR contains the CD19 targeting scFv FMC63 followed by a CD28 hinge, transmembrane and endodomain and a CD3ζ signalling domain. The diabody position, the CD22 targeting scFv RFB4 is followed by a CD8α hinge and transmembrane domain and 4-1BB endodomain.

5.2.12 Expression of single-chain diabody CARs targeting CD19 and CD22

Stable expression of diabody CARs in primary human T-cells was achieved using transient virus produced from 293T cells using the triple transfection method (as described above), thus avoiding the need to generate stable retroviral packaging cell lines. Successful T-cell transduction is illustrated in Fig. 5.18. Since the CAR contains a distinct epitope tags and the diabody recognise CD22, co-expression was demonstrable by flow cytometry.

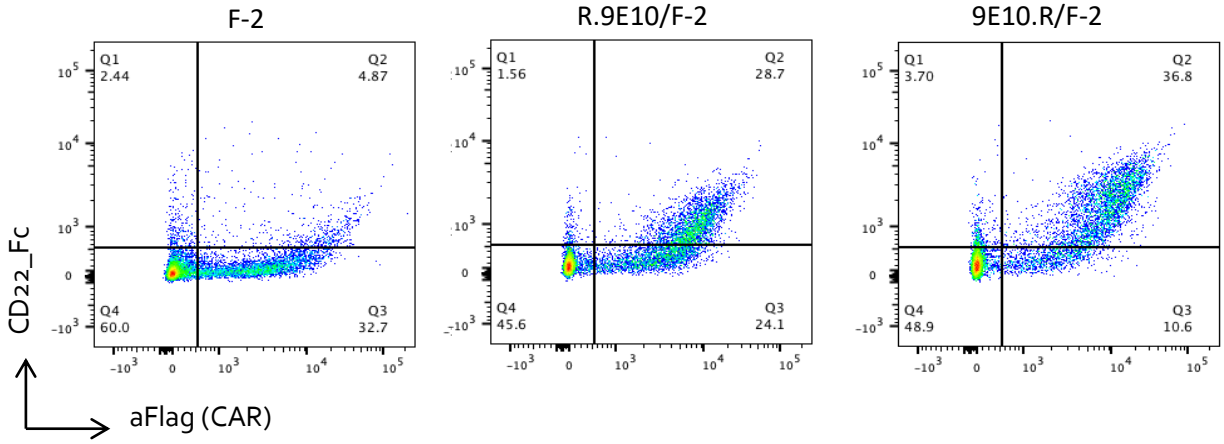

Figure 5.18 Expression of CD19-CD22 targeted diabody CARs in human T-cells. Human T-cells were engineered by retroviral transduction to express the indicated CARs. T-cells were incubated with antibody directed against FLAG (CAR) epitope tag and CD22-Fc to detect the RFB4 scFv. Binding of the Fc fusion protein was detected with Alexa-Fluor conjugated anti-human IgG Data are representative of three independent replicate experiments.

5.2.13 In vitro evaluation of diabody CAR T-cells targeted against CD22 and CD19

T-cells were engineered to express CARs and diabody constructs to compare cytotoxicity and cytokine release when co-cultured with firefly luciferase-expressing NALM-6 cells at varying effector to target (E:T) ratios. As shown in Fig.5.19a both diabody CARs had slightly greater cytotoxic activity compared to F-2 and R-2 CAR T-cells at several E:T ratios. To quantify activation of CAR T-cells, IFN-γ and IL-2 levels were measured in supernatants collected after 24 hours from co-cultures established at 1:1 and 1:4 E:T ratios. As expected,

untransduced T-cells elicited minimal cytokine release while F-2 CAR T-cells produced increased levels of IFN-γ compared to R-2 and both diabody CARs (Fig. 5.19b). Nevertheless, use of an antigen-negative target cell line is a required control to determine if non-specific activation through the scDb interaction alone is occurring.

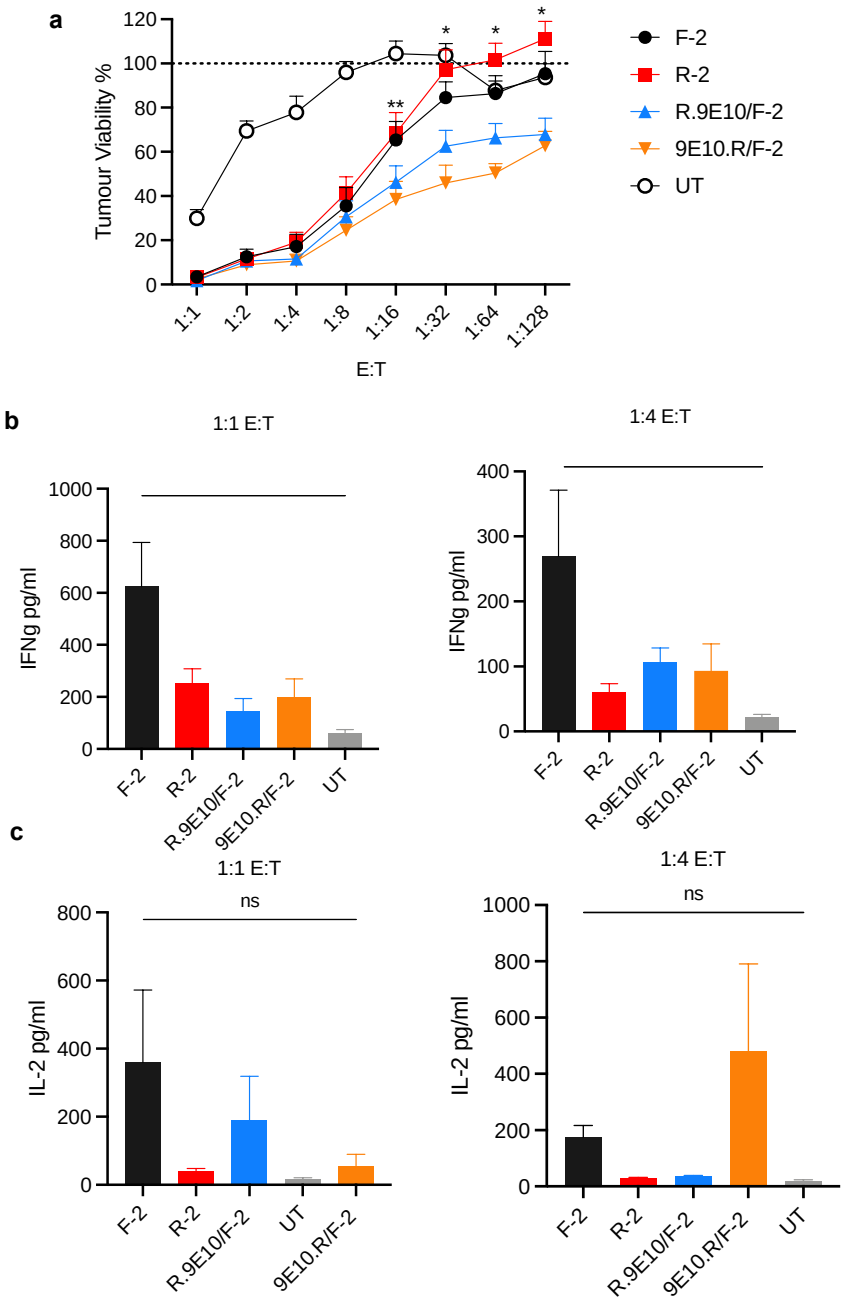

Figure 5.19 Cytotoxic activity and cytokine release by CAR and diabody CAR T-cells when co-cultured with NALM-6 cells. (a) CAR T-cells were co-cultivated with NALM-6 leukaemia cells at the indicated E:T ratio. Target viability was quantified after 72h (mean ± SEM, n= 7-8 independent replicates). Supernatants were collected after 24h from the co-cultivation experiments at a 1:1 and 1:4 E:T ratio and were analysed for IFN-γ **(b)** and IL-2 **(c)**. Data shown are mean ± SEM, n=7-8. Statistical analysis was performed with one-way ANOVA followed by Tukey post hoc test. ** p= ≤ 0.01; *p=≤ 0.05.

5.2.14 *In vitro* functionality of diabody CAR and pCAR T-cells against LO68-CD22$^+$ cells

It was important to determine if the diabody CARs were capable of recognising and destroying CD19 negative tumour cells. Furthermore, the capacity of RBB/ pCARs to kill tumour cells when only the CCR is engaged also required determination. As such, LO68 tumour cells retrovirally transduced to express only CD22 were used as the target cell in a cytotoxicity assay alongside LO68-CD19$^+$CD22$^+$ cells. In Fig. 5.20a, tumour viability of LO68-22$^+$ cells after 72h co-culture with CAR and pCAR T-cells is shown (left panel). As expected, R-2 CAR T-cells caused approximately 20% tumour cell destruction whereas F-2 and untransduced (UT) T-cells caused minimal monolayer damage. The diabody CARs and pCARs showed similar levels of cytotoxicity. When co-cultured with LO68-CD19$^+$CD22$^+$ (right panel) all CAR and pCAR T-cells showed increased cytotoxicity and effectively destroyed the monolayer. Supernatant from the cocultivations was harvested after 24h and analysed for IFN-γ cytokine release (Fig. 5.20b). In co-cultivations with LO68-CD22$^+$, R-2 CAR T-cells produced significantly higher levels of IFN-γ compared to all other constructs. Diabody CAR T-cells released similar amounts of IFN-γ when co-cultured with LO68-CD22$^+$ or LO68-CD19$^+$CD22$^+$, which was significantly less than all other CAR T-cells. In comparison, F-2 CAR T-cells released significantly higher IFN-γ when co-cultured with LO68-CD19$^+$CD22$^+$ cells.

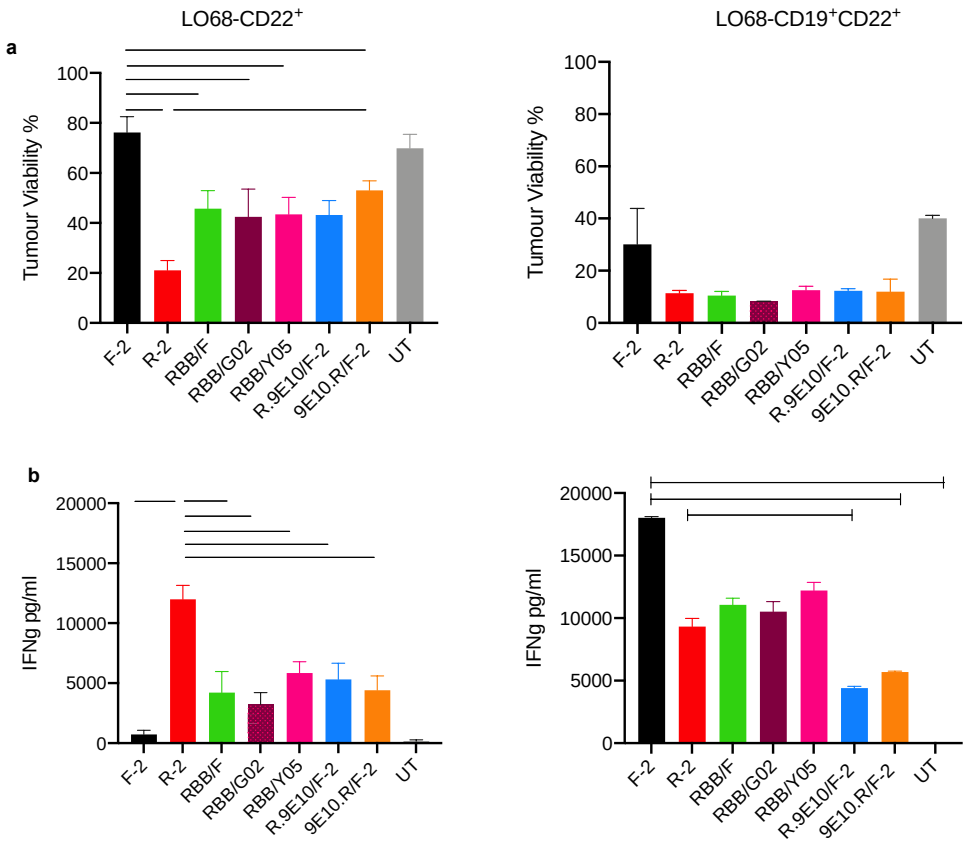

Figure 5.20 Cytotoxic activity and IFN-γ release of CAR, diabody and pCAR T-cells. (a) 1x10^5 CAR T-cells were co-cultivated in duplicate with an equal number or with LO68-CD22+ (left) or with LO68-CD19$^+$CD22$^+$ cells (right). After 72h, viability of tumour cells was determined by MTT. (b) Supernatants were collected after 24h from the co-cultivation experiments and analysed for IFN-γ. Data shown are mean ± SEM of n=2. Statistical analysis was performed by One-way ANOVA followed by Tukey's multiple comparison test. **** p=<0.0001; *** p= ≤ 0.001; ** p= ≤ 0.01; *p= ≤ 0.05

5.3 Discussion

In this chapter, I present results related to the evaluation of the *in vitro* and *in vivo* anti-tumour activity of pCAR T-cells that engage two distinct targets found on B-cell malignancies. A key aim of this project was to compare the novel pCAR platform to second-generation anti-CD19 CAR T-cells which are currently in the clinic and which have transformed the treatment of patients with relapsed/refractory B-cell malignancies. Here, comparison was made with the FDA and EMA approved CD19-specific CAR known as axicabtagene ciloleucel (axi-cel). The CAR extracellular domain contains the FMC63 scFv, CD28 hinge and transmembrane domains, and intracellular signalling domains that consist of CD28 and CD3ζ for T-cell activation and costimulation, respectively[154,249]. Additionally, a myc epitope tag was incorporated to aid detection of T-cell transduction while an intracellular FLAG epitope tag was added to the 4-1BB endodomain to facilitate the detection of CCRs in pCARs.

Despite the remarkable success of CAR T-cell therapy, relapse with CD19-negative disease occurs in a large fraction of patients[124,176,182,253]. Disease-associated heterogeneity of antigen expression coupled with immune pressure caused by single antigen targeting may increase susceptibility for immune escape via antigen loss [256,274]. Furthermore, antigen negative escape is not exclusive to CD19, as relapse due to CD22 loss or diminution of surface expression was also seen following immunotherapy with CD22-directed CAR T-cells[184]. As such, I hypothesized that simultaneous targeting of two antigens may reduce the likelihood of relapse due to single antigen loss. To investigate this, I set out to engineer pCARs that would target CD19 and CD20 (1BB/F) and CD19 and CD22 (RBB/F, RBB/Y05 and RBB/G02).

Prior to engineering the 1BB/F pCAR construct, second-generation CD19- and CD20-targeting CARs were designed and cloned using conventional techniques. Expression of transgene products was demonstrated by flow cytometry, indicating that all chimeric receptors both folded and trafficked correctly to the plasma membrane. Using CD19- and CD20-Fc fusion proteins, I demonstrated that both CD19 and CD20-specific scFvs bound their targets and stoichiometric co-expression of CAR and CCR was confirmed. However, slight variation in expression of CAR and CCR were observed which could be attributed to the different binding affinities of the reagents used for their detection.

In order to assess *in vitro* anti-tumour activity, second-generation CAR and pCAR T-cells were co-cultivated with two different cell lines expressing various levels of CD20. 1BB/F pCAR T-cells exhibited significant cytotoxicity activity against NALM-6 and Raji cell lines and maintained cytotoxicity for up to five restimulation cycles. Nevertheless, this activity did not prove superior when compared to F-2 CAR T-cells. In fact, there were no notable differences with regards to proliferation or cytotoxicity between the constructs. Destruction of Raji and NALM-6 cells was correlated with preceding CAR T-cell activation. The release of significant quantities of IFN-γ and IL-2 by CAR and pCAR T-cells but not by control untransduced T-cell populations demonstrates their ability to mediate target-dependent activation of primary human T-cells.

Analysis of cytokine release showed that F-2 and 1BB/F CAR T-cells released similar amounts of IFN-γ and IL-2. Notably, F-2 and 1BB/F CAR T-cells maintained production of IL-2 over six restimulation cycles when co-cultured with NALM-6 cells. It is important to note that CD20 was not detected on the cell surface of NALM-6 cells by flow cytometry. However, it is likely that CD20 was expressed by these cells at very low levels as 1-2 second generation CAR T-cells lysed NALM-6 tumour cells and released cytokines, indicating T-cell

activation. Nonetheless, the decreased IL-2 production by 1BB/F CAR T-cells when co-cultured with Raji compared to NALM-6 cells was surprising. Diminished IL-2 production has been implicated as one of the steps leading to T-cell exhaustion and may indicate a late-stage effector phenotype[275]. The high surface expression of CD20 on Raji cells was expected to improve the activation status of 1BB/F T-cells as a result of the CCR providing co-stimulation through 4-1BB upon target recognition. However, high expression of costimulatory molecules CD80 and CD86 on Raji cells[270] may cause activation-induced cell death (AICD) due to the prolonged potent stimulation[276]. In order to objectively compare 1BB/F pCAR with F-2 and 1-2 CAR T-cells, a tumour cell model in which CD19 and CD20 are highly expressed without the presence of additional costimulatory ligands was required. To establish such a model, LO68 tumour cells were retrovirally transduced to express high levels of human CD19 and CD20. Co-culture of LO68-CD19$^+$CD20$^+$ cells with CD19- or CD20-specific CAR T-cells resulted in complete target cell lysis at a 1:1 E:T ratio. At the lower effector to target ratios, similar cytotoxicity was observed by all CAR T-cells however, there was a trend towards greater anti-tumour activity by 1BB/F CAR T-cells across four donors. In restimulation assays, all CAR T-cells restimulated for many more cycles against LO68-CD19$^+$CD20$^+$ cells compared to Raji and NALM-6 cells. Cytokine release measured by ELISA revealed much higher quantities of IFN-γ and IL-2 produced by all CAR T-cells when co-cultured with LO68-CD19$^+$CD20$^+$ cells. These observations can be attributed to a number of factors. Expression of both CD19 and CD20 is significantly higher on LO68-CD19$^+$CD20$^+$ cells, when compared to NALM-6 or Raji cells. While this may favour CAR T-cell activation, it may not be physiologically representative. Another possible contributory factor is the methodology of the assay. As NALM-6 and Raji are suspension cell lines, at each stimulation cycle, fresh lymphoma or leukaemia cells are added to the co-culture which may already

contain surviving tumour cells. As such, the effector to target ratio may fluctuate in favour of the tumour cells. In comparison, LO68-CD19^{+}CD20^{+} is an adherent cell line thus allowing CAR T-cells present in the medium to be removed and added to a new monolayer. Moreover, PD-L1 expression is inducible on NALM-6 and Raji cells upon exposure to pro-inflammatory cytokines such as IFN-γ[277,278] and can mediate T-cell exhaustion, inhibiting the cytotoxic CAR T-cell response[279].

In light of the results showing no improvement in anti-tumour activity of the 1BB/F pCAR, CD22 was chosen as an alternative target, leading to the engineering of the RBB/F pCAR. Surface expression of the B-cell marker CD22 has been extensively studied in leukaemia and lymphoma patient samples and found to be widely expressed in both disease settings[260,280–283]. Additionally, rituximab (a chimeric anti-CD20 monoclonal antibody) is widely used in combination with chemotherapy for the treatment of NHL. Consequently, CD20-negative transformation has been reported as a mechanism of disease progression in many patients[284,285]. As such, there is convincing rationale for engineering a dual targeting pCAR against CD19 and CD22.

CD22 is a developmentally regulated antigen expressed on developing and mature human B-cells and B-cell malignancies that has been targeted via immunotherapy. Studies using the anti-CD22 scFv RFB4 as a CAR targeting moiety have shown anti-tumour activity against B-cell malignancies in pre-clinical research[112,273]. Comparison of RFB4-28ζ with HA22-28ζ CAR T-cells, an affinity matured derivative of RFB4, showed no appreciable differences in anti-tumour functionality thus supporting the concept of a "affinity ceiling"[112]. Importantly however, the possibility that affinity may affect function against low antigen expressing was not investigated.

In chapter 3 and 4, the superiority of lower avidity second-generation CARs Y05 and G02 was demonstrated using *in vitro* and *in vivo* tumour models. As such, it was hypothesised that using these binding moieties as the CAR component within the pCAR would further improve function. A somewhat unexpected result was the significant improvement of cytotoxicity of RBB/F, RBB/G02 and RBB/Y05 pCAR T-cells compared to F-2 and R-2 second generation CAR T-cells in dose-response assays against NALM-6 cells. Furthermore, RBB/G02 pCAR T-cells had significantly higher anti-leukaemic activity compared to R-2, F-2 and RBB/F CAR T-cells. Higher levels of IFN-γ were produced by RBB/Y05 CAR T-cells compared to all other constructs when co-cultured with NALM-6 targets. Repeated antigen restimulation revealed that the RBB/F CAR T-cells maintained cytotoxic potency and ability to release IFN-γ for several more rounds of antigen-stimulation than second-generation CAR T-cells. However, similar levels of IL-2 were produced by RBB/F and F-2 CAR T-cells. A possible explanation is that the cytokine is rapidly sequestered by the RBB/F CAR T-cells to stimulate expression of granzyme B, perforin and by promoting effective target cell killing[286–288].

Following the demonstration of superior leukaemia cell destruction of NALM-6 cells by RBB/F pCAR T-cells, I next investigated the ability of this pCAR to modulate target antigen expression on leukaemic cells. To allow for *in vitro* measurement of antigen loss, CAR T-cells and NALM-6 cells were co-cultured at an effector to target cell ratio of 1:10. When lower effector to target ratio was used, the surviving leukaemia cells could be harvested and analysed for surface expression of CD19 and CD22. Flow cytometry allowed gating for viable cells, exclusion of T-cells and quantification of MFI and antigen expression. After 48 hours incubation with F-2 CAR T-cells, down-modulation of CD19 was observed. The RBB/F CAR T-cells induced less antigen loss of CD19. However, CD22 down-modulation was also detected,

albeit less than was seen with R-2 CAR T-cells. This suggests that the dual targeting pCAR applies immune pressure that is more evenly distributed than single specificity CARs. However, with a low E:T ratio of 1:10 it is possible that the lower CD19 antigen is caused by trogocytosis mediated by the CAR. Hamieh et al investigated the mechanism of antigen-low leukaemia escape and showed reversible CD19 loss was mediated by CAR T-cell trogocytosis[183]. Whole protein CD19 extraction from leukaemia to CAR T-cells decreased target density and promoted antigen low tumour relapse. Additionally, CD19-trogocytic CAR T-cells became subject to fratricide by neighbouring CAR T-cells, accompanied by upregulation of exhaustion markers. In support of this hypothesis, direct contact between Raji cells and CAR T-cells was necessary to down-modulated surface expression of CD19, CD20 and CD22[187].

Taken together, the *in vitro* data warranted investigation of the *in vivo* anti-leukaemic activity of RBB/F CAR T-cells. CAR T-cells were adoptively transferred into NSG mice bearing NALM-6-xenografts and their therapeutic activity measured by bioluminescence imaging. All pCAR and CAR T-cells mediated anti-tumour responses in this leukaemic disease model; with RBB/Y05 and RBB/F pCAR T-cells having enhanced disease control 7 days after treatment. However, this was a transient response with the majority of mice showing rapid disease progression after day 14. As such, these data do not reflect the *in vitro* findings or the previous NALM-6 xenograft experiments presented in chapter 4 (Fig. 4.13 and Fig. 4.14). Prior to infusion, there were no significant differences in the expression of T-cell exhaustion markers or cytotoxic activity of CAR T-cells used in this experiment. Additionally, T-cell transduction efficiency for all CAR constructs used *in vivo* was comparable. Nevertheless, post-mortem analysis of pCAR and F-2 CAR treated groups showed a trend towards improved pCAR T-cell survival, in the periphery and spleen,

following adoptive transfer when compared to F-2 treated mice. This suggests that the lack of sustained response to CAR T-cell treatment was not due to poor persistence. Unfortunately, further analysis of expression of exhaustion markers or anti-tumour functionality *ex vivo* was not carried out. Nonetheless, limited conclusions can be drawn from the study as control CAR T-cells bearing avidity adjusted CD19 binders alone were not included. As such, it is difficult to tease apart the role of the avidity modulated CAR from the role of the co-stimulatory receptor. However, informative results can be gleaned when comparing RBB/F and F-2. Here, the pCAR T-cells showed improved persistence and tumour control compared to control F-2 CAR T-cells.

Finally, an obstacle of achieving more profound *in vivo* anti-tumour activity of CAR T-cells has been the aggressive nature of the NALM-6 leukaemia model, while at the same time the CAR T-cell dose infused was modest.

In an attempt to address the issue of CD19 negative disease relapse following anti-CD19 CAR T-cell therapy, single-chain diabody (scDb) producing F-2 CAR T-cells were designed and engineered. Here, the scDbs have two antigen-binding sites specific for CD22 and Myc and concurrent binding of the scDb to the T-cell and the tumour cell should trigger a cascade of events including T-cell activation, release of cytokines and secretion of perforin and granzyme B, leading to tumour cell apoptosis. In the R.9E10 and 9E10.R single-chain diabodies, the long linker connecting the first scFv chain to the second chain forces correct assembly whilst improving stability and flexibility. Unlike BiTEs, the scDb is synthesised and released by the CAR *in situ*. As such, this strategy will circumvent problems of short half-life and additional production costs. The results showed that both scDb CAR T-cells had superior cytotoxicity against NALM-6 tumour cells in dose response assays. However, these T-cells produced significantly less IFN-γ when compared to F-2 CAR T-cells. By using the genetically

engineered LO68-CD22^{+} tumour cells, the ability of scDb CAR T-cells to destroy CD19 negative tumour monolayer was elucidated. Compared to UT and F-2 CAR T-cells, scDb CAR T-cells were significantly more potent; however, they were not as cytotoxic as R-2 CAR T-cells. Release of IFN-γ by scDb CAR T-cells indicates that the scDb are capable of activating the F-2 CAR T-cell via the Myc tag. However, an irrelevant CAR producing the scDb is an absent control required in these experiments, this would exclude self-activation of the CAR through binding of the scDb in the absence of cognate interactions. Furthermore, half-life and concentration of released scDb needs to measured. Of note, RBB/ pCARs also mediated anti-tumour cytotoxicity and IFN-γ despite only receiving costimulatory signal via the CCR.

Chapter 6: General discussion

6.1 Overview

CAR T-cell therapy holds great promise for the therapy of cancer, but the optimal design of CARs has yet to be established. The overarching aim of this project was to develop a clinically relevant CAR system to more safely and effectively treat B-cell malignancies when compared to second-generation CARs. CAR T-cell therapies have transformed the treatment of patients with B-cell malignancies and are likely to become the new standard of care for refractory/relapsed patients. FDA and EMA approvals for tisagenlecleucel, axi-cel and brexucabtagene autoleucel were achieved as a result of rapid pre-clinical and clinical development of these products and it is anticipated that other B-cell specific CAR T-cell products will soon be approved. Nevertheless, many issues remain to be resolved including high cost, complexity of manufacture and clinical delivery, toxicity and relapse with both $CD19^{+}$ and $CD19^{-}$ disease. Given the remarkable pace at which CAR T-cell immunotherapy of B-cell malignancy has developed in the past decade, rapid development and implementation of novel solutions are to be expected.

Consequently, I set out to test a pCAR based approach that attempted to deliver improved dual co-stimulation leading to enhanced anti-tumour superiority. To initiate this project, a panel of seven CARs with a spectrum of avidities was generated. To create the CARs with varying affinity for CD19, alanine scanning mutagenesis of the CDR3 region of the FMC63 V_H chain was undertaken. Following incubation with a recombinant CD19-Fc fusion protein, I determined that four of seven scFvs failed to exhibit detectable binding to CD19 (Fig 3.3 and Fig 3.4). However, significant target-dependent cytotoxicity was induced by almost all of these newly engineered CAR T-cells, with the exception of the Y02 mutant, This

suggests that binding studies using the Fc fusion protein was insufficiently sensitive to detect low affinity interactions. Studies using the z-Movi™ platform revealed distinct avidities for the panel of CARs, which was reflected in their avidity score. The z-Movi platform is a unique technology that measures the avidity between immune cells and their targets. To further explore the kinetic profile of these scFvs, surface plasmon resonance (SPR) by Biacore would be necessary to determine on- and off-rates. It is important to appreciate nonetheless that this assay does not fully recapitulate the binding of a T-cell membrane bound CAR to CD19 on the target cell. This is because the Biacore assay only provides insight into the binding of soluble scFv-Fc to immobilised antigen (or vice versa), thus eliminating cell adhesion and binding of other ligand-receptor pairs which may affect functional avidity. Affinity of an scFv (as determined using Biacaore) is described by the thermodynamic parameter known as the K_D value, in turn defined by a simple equilibrium reaction. By contrast, functional avidity (as determined by z-Movi) describes the ability of a CAR T-cell to respond to the stimulation provided by tumour associated antigens and is influenced by the CAR T-cell affinity, CAR expression levels and the location of the recognised epitope on the antigen[289]. The comparisons shown in this project demonstrate that higher avidity scFvs do not necessarily yield CARs direct enhanced cytotoxicity or functionality. In fact, lowering the avidity resulted in significantly increased release of IL-2 by Y05 and G02 CAR T-cells when co-cultured with NALM-6 cells (Fig 3.12). However, further lowering the avidity, as illustrated by the Y03 and G01 CAR T-cells detrimentally affected cytokine release without dramatically impacting CAR T-cell cytotoxicity against target cells. This outcome is most likely the result of insufficient signal strength provided by the low avidity CAR to effectively achieve T-cell potency.

6.1.1 The impact of binding affinity on CAR T-cell function

TCR affinity influences the sensitivity and polyfunctionality of T-cells. In targeting of antigens for therapeutic purposes, it was previously assumed that a higher affinity of interaction, the greater the associated cellular response. This was based on the observations such as TCRs specific for pathogens have a higher affinity and K_D that are generally lower when compared to TCRs specific for TAAs[290]. The optimum kinetic properties required for best T-cell activation and signalling has been studied and modelled with a low antigen density, which is physiologically relevant as TAAs are typically present at fewer than 50 copies per cell[291]. Successful T-cell activation at low antigen density requires serial triggering. Consequently, it is possible that TCR-pMHC interactions that have exceedingly long off-rates could impair the serial engagement of TCRs because of the low density of cognate pMHC on the target cell surface. Conversely, in the setting of increased antigen density, this leads to simultaneous binding of sufficient pMHC complexes, thus bypassing the need for serial triggering. Nonetheless, a supraphysiological affinity threshold exists above which T-cell function is not improved and very high affinity TCRs are prone to cross-react with self-derived peptides[291]. Another study demonstrated there is a maximal T-cell response that can be achieved at lower affinities[292]. However, reducing TCR affinity below 1uM affects parameters of T-cell activation such as phosphorylation of CD3ζ, the activation of the MAP kinase pathway and the ability to recruit cytotoxic granules[293–295]. As such, there appears to be a defined window of affinity that facilitates productive TCR triggering and efficient TCR serial engagement.

In an early study by Turatti et al.[240] researchers show that the threshold for complete CAR T-cell activation is readily met when antigen and CAR levels are both high regardless of CAR affinity. The high numbers of simultaneous CAR antigen binding events induced optimal signalling potency and complete activation was quickly achieved. Conversely, when both

expression levels of the CAR and antigen are low, the function of the CAR is determined by its affinity. In this scenario, low affinity CARs with faster off-rates remain functional due to their ability to serially trigger. In a similar fashion, Lehner et al[296]. reported that CAR T-cells require at least 100-fold higher target antigen densities that natural TCRs. The higher affinity of the CAR for the antigen results in a longer half-life of interaction and an inability to support efficient serial triggering as a result. By analogy, TCRs designed to possess enhance affinity for pMHC have been described in which 100-fold higher pMHC densities were required to trigger T-cell responses, compared to wild-type TCR[228].

A recent clinical study described the treatment of relapsed/refractory paediatric B-cell acute lymphoblastic leukaemia patients with CAT CAR T-cells[120]. The CAT CAR has a >40-fold lower affinity for CD19 than FMC63 scFv-containing counterparts, largely owing to a much faster off-rate. In that study, researchers reported enhanced CAR T-cell expansion in patients compared to published data and persistence was demonstrated in 11 of 14 patients at last follow up. The preclinical data suggest the enhanced expansion and persistence of CAT CAR T-cells is partly mediated through the higher expression of Bcl-2 and IL-7R, preventing apoptosis and promoting proliferation. As such, CAR affinity is a relevant determinant of CAR T-cell activation and function. Here, lowering the avidity of the FMC63 scFv to create Y04, Y05 and G02 CAR T-cells, translated into enhanced efficacy when repeatedly stimulated with NALM-6 leukaemic cells (Fig 4.4). These findings were replicated *in vivo* with Y05 and G02 CAR T-cells, which showed superior anti-tumour activity compared to F-2 CAR T-cells (Fig 4.13).

In 2004 Chmielewski *et al.*[231] investigated the effect of receptor binding affinity on CAR effectiveness through the use of a library of affinity matured anti-ErbB2 scFvs with a broad range of affinities. These scFvs were specific for the same epitope and were inserted

into an identical CAR backbone. They elegantly showed that there is a threshold affinity beyond which no improvement in T-cell function is achieved, demarcated as “the affinity ceiling”. The plateau effect is likely explained by the concept that the avidity of the CAR needed for maximal T-cell activation is a function of the number and density of the expressed receptors as well as their affinity. At an affinity above $K_D < 1x10^{-8}$ M, release of IL-2 and IFN-γ and CAR mediated cytotoxicity of target cells did not increase.

In a study by Maus et al[297]. they sought to extend the applicability of antibody-based CARs to intracellular antigens by developing an scFv specific for HLA-A2/NY-ESO-1. The T1 scFv was determined to bind the HLA-A2/NY-ESO-1 complex in a similar fashion as the native TCR specific for the same MHC/peptide antigen and was assembled into a second-generation CD28-CD3ζ CAR framework. Despite the specificity of the high affinity T1 antibody, when the same antigen-binding region was used in the form of a CAR there was loss of specificity and only moderate lysis of targets. The researchers hypothesized that the high CAR T-cell avidity caused excessive CAR binding to HLA and therefore mutated residues to significantly lower affinity. Conversely, CARs specific for ROR1 with scFvs of varying affinities were investigated to determine the impact of affinity on CAR T-cell function[115]. In this study higher affinity and slower dissociation was associated with increased T-cell function as measured by cytokine production, proliferation and *in vivo* efficacy. Discrepancies between studies may be accounted for by the different targets chosen and methodological dissimilarities.

6.1.2 CD19 pCAR T-cells show improved *in vivo* anti-leukaemic efficacy

An obstacle impeding effective and long-lasting CAR based immunotherapy is poor *in vivo* longevity of the genetically modified T-cells and their sub-optimal effector function within

the tumour microenvironment. These limitations may be attributed at least in part to inefficient CAR^+ T-cell costimulation. Physiological costimulation of T-cells is a dynamic process that relies upon a large number of receptor types that display great diversity in their expression, structure and function. In an attempt to fine-tune CAR mediated T-cell costimulation, I hypothesized that provision of integrated dual CD28 and 4-1BB costimulation would lead to further meaningful potentiation of anti-tumour activity. To recapitulate the signals necessary for T-cell effector function and proliferation most CAR constructs combine the CD3ζ endodomain in a single chain with a costimulatory domain from CD28 or 4-1BB. CAR T-cell therapy using both CD28-CD3ζ and 4-1BB-CD3ζ have been effective for treating patients with B-cell malignancies; however, T-cells that express these CARs behave differently *in vivo.* In general, CD28-CD3ζ CAR T-cells undergo intense proliferation within 7 days of adoptive transfer and seldom persist for longer than 60 days after infusion. In comparison, 4-1BB-CD3ζ CAR T-cells can persist for several months to years and reach peak numbers between days 7-14 after adoptive transfer[108,119,124,259,298]. These clinical differences have partially been explained by studies comparing CD28-CD3ζ and 4-1BB-CD3ζ CAR T-cells *in vitro* and in animal models. Researchers have demonstrated that as a member of the TNFr family, 4-1BB-CD3ζ CAR T-cells predominantly use fatty acid oxidation, have a greater mitochondrial mass, a more memory T-cell phenotype and are able to better retain effector functions when chronically stimulated[299]. Contrastingly, CD28-CD3ζ CARs yield effector memory T-cells with a reliance on aerobic glycolysis.

Differences in phenotype and function of CD28-CD3ζ and 4-1BB-CD3ζ CAR T-cells are widely assumed to be caused by activation of divergent signalling pathways through the distinct costimulatory domains. Ligation of CD28 recruits phosphatidylinositol 3-kinase (PI3K), the adaptor Grb-2 and the protein tyrosine kinases Lck and Itk. The adaptor Grb-2

and PI3K are activated and bind the YMNM cytoplasmic motif in CD28, leading to downstream production of IL-2 and proliferation of T-cells[300,301]. Comparatively, upon binding its ligand 4-1BBL, 4-1BB recruits TNFr associated factor family members (TRAF1-3) to its cytosolic region, forming the 4-1BB signalosome and leading to downstream activation of NF-κB, MAPK and ERK[302]. The stimulation of 4-1BB and subsequent downstream signalling leads to the upregulation of anti-apoptotic proteins and release of IL-2 and IFN-γ. While 4-1BB costimulation promotes proliferation of both $CD4^+$ and $CD8^+$ T-cells, it preferentially supports $CD8^+$ T-cell expansion. To further understand how costimulatory signalling by CARs directs T-cell functionality and cell fate decisions, Salter *et al*[140]., studied the changes in the phosphoproteome of T-cells after CAR ligation and described the changes induced by CD28-CD3ζ and 4-1BB-CD3ζ CARs. Their data suggests both by CD28-CD3ζ and 4-1BB-CD3ζ CAR activation initiated nearly identical directional changes in protein phosphorylation. As such, focusing solely on the costimulatory domains within the synthetic receptor cannot predict the signalling cascade initiated. Instead, their data demonstrates that CD28-CD3ζ receptors signal with distinctly increased kinetics and intensity compared to 4-1BB-CD3ζ CARs which proceed more slowly with reduced intensity. This induced an effector T-cell transcriptional profile and more robust cytokine production in CD28-CD3ζ CARs but reduced *in vivo* anti-tumour activity. The reduced persistence of CD28-CD3ζ CAR T-cells is consistent with previous findings highlighting that intense TCR signalling and IL-2 production promote T-cell differentiation and exhaustion. A recent study by Philipson *et al.,*[303] showed that the 4-1BB costimulation domain incorporated into a CAR potently activates the noncanonical nuclear factor κB (ncNF-κB) signalling pathway in T-cells. Disruption of this pathway led to impaired T-cell survival and reduced expansion. The increased abundance of the pro-apoptotic protein Bim was associated with the reduced

expansion and survival of T-cells as it is regulated by ncNF-κB and ERK signalling. An implication from these studies is that CAR T-cells utilising both CD28 and 4-1BB may be superior as they would mimic a natural immune response, comprised of T-effector cells with intense kinetics and then an upregulation of memory associated genes within T-cells. Potential mechanisms to increase accumulation of CAR T-cells are being investigated, including using T-cell populations with a higher percentage of less differentiated T-cell subsets. Preclinical studies using CAR T-cells engineered from preselected naïve T-cell populations or manufactured in the presence of kinase inhibitors to generate CAR T-cells with a less differentiated phenotype have revealed superior engraftment and proliferation compared with traditional CAR T-cell products[196,304]. Another mechanism to increase accumulation of CAR T-cells is through modulation of chemokine signalling to enhance T-cell localisation to tumours. This engineering strategy is especially important to increase trafficking to solid tumours. Expression of the macrophage colony-stimulating factor 1 (CSF-1R) in CAR T-cells made these cells responsive to CSF-1, a monocyte recruiting chemokine that is enriched in many solid tumours, this enhanced the proliferative effect of CAR signalling without compromising cytotoxicity[305].

The underwhelming clinical impact of third generation CARs led to the reassessment of CAR structure and further fine tuning of costimulation. The juxta-membrane positioning of costimulatory signalling domains *in trans* has recently been established as a general principle for effective CAR function[215]. In an attempt to modify CAR mediated T-cell costimulation, a panel of seven pCARs targeting CD19 were designed and cloned. Two targeting moieties with distinct target affinities have been utilised to assess the impact of target dissociation on CAR activation. Classical second-generation CARs were used to compare efficacy to the novel pCARs. A tentative principle that has emerged in the design of

pCARs is the impact of relative affinity of CAR and CCR. Muliaditan *et al* [215]*.,* designed a pCAR to target colony-stimulating factor 1 receptor (CSF1R) using the natural ligands CSF1 and IL-34. They found that IL-34 (K_D 1pM) proved less effective than CSF-1 (K_D 34pM) as the CAR targeting moiety in the pCAR architecture[246]. This suggests that excessive affinity for target decreases tumour selectivity and is also detrimental to CAR T-cell function. Furthermore, incorporation of the high affinity CAR in the pCAR format will not rescue sub-optimal binding molecules.

A key starting point in the *in vitro* characterisation of the panel of pCARs was the demonstration that they could be stably expressed on the surface of primary human T-cells. This was confirmed by flow cytometry and, importantly, comparable co-expression of the CCR and CAR was demonstrated through staining of embedded flag and myc epitope tags within each receptor component (Fig 4.2) . Anti-leukaemic activity of pCAR T-cells was first evaluated using the leukaemic cell line NALM-6, which has been shown to express high levels of the target CD19. Successful genetic re-targeting of T-cells was confirmed by target cell destruction within 72h of co-culture. Moreover, pCAR T-cells showed a trend towards improved ability to kill leukaemic cells compared to second-generation CARs at low E:T ratios (Fig 4.3). This observation suggests that provision of pCAR derived co-stimulation *in trans*, by co-expression of CAR and CCR, elicits more robust and sustained anti-tumour activity *in vitro.* All CD19 targeting CAR and pCAR constructs showed high cytolytic capacity upon encountering the target for the first time. Successive rounds of antigen stimulation revealed that all pCAR T-cells repeatedly outperformed matched second-generation CAR T-cells (Fig 4.4). Enhanced function of pCAR T-cells was also indicated by enhanced proliferation and lowered expression of markers of exhaustion (Fig 4.7 and Fig 4.8). These findings were consistent using pCARs in which the CAR component encompassed a range of

affinities. Furthermore, superior secretion of IL-2 and IFN-γ upon consecutive rounds of antigen stimulation was observed by all pCAR T-cells compared to matched CAR counterparts, excluding the FBB/Y02 group (Fig 4.5 and Fig 4.6). The activation of the JAK-STAT signalling pathway through the cytokine-cytokine receptor interactions supports effector functions, T-cell proliferation, suppress terminal differentiation, and promote memory formation, which has been shown to result in superior anti-tumour activity by CAR T-cells[143]. Muliaditan et al, (unpublished data)[215]. showed that the restimulated pCAR T-cells also demonstrated greater resistance to AICD, an established limitation of third-generation CAR T-cells[306]. These results suggest that providing costimulation *in trans* results in favourable spatial and temporal differences in the recruitment, kinetics and regulation of costimulation, fine-tuning of costimulation through the CAR affinities is necessary to achieve optimal potency of the constructs.

A central aim of these studies was to characterise the therapeutic impact of CD19 pCAR T-cells on *in vivo* tumour growth in comparison to second-generation CARs, including F-2, which is in the clinic. The selection of pCARs chosen to test *in vivo* was based upon their relative performance *in vitro*. Broadly, these findings correlated with the use of an intermediate avidity CD19-specific scFv mutant (as determined by z-Movi™) to direct CAR specificity. In order to identify differences that may have not become clear in the *in vitro* studies, such as T-cell exhaustion resulting in reduced anti-leukaemic efficacy, tumour cells were allowed to fully engraft prior to infusion of a suboptimal CAR T-cell dose. All groups treated with CAR T-cells demonstrated delayed cancer progression indicating that the CAR grafted T-cells retained their anti-tumour activity *in vivo.* However, pCAR T-cells caused significant delay in tumour growth and improved long-term survival in the NALM-6 xenograft model (Fig 4.13). Enhanced tumour control by pCAR T-cells may have been

attributable to superior functional persistence *in vivo* following adoptive transfer. In support of this, a higher percentage of pCAR T-cells persisted compared to F-2 CAR T-cells (Fig 5.16). In future studies, imaging of CAR T-cells could provide valuable information on their *in vivo* longevity and bio-distribution, providing further insight into this question. Increased TCR-pMHC interactions *in vivo* have been shown to result in decreased proliferation, cytokine production and memory formation. As such, ligands with intermediate TCR-pMHC half-lives demonstrate optimal *in vivo* responses[307]. Furthermore, various groups have shown that $CD8^+$ T-cells expressing high affinity TCRs fail to infiltrate tumours, lose their cytotoxic effector properties and are rapidly eliminated from within the tumour and the periphery[308–310]. The results shown here, from two independent experiments, indicate that greater disease control was achieved by pCAR T-cells and lower affinity CAR T-cells *in vivo.*

Safety of CAR T-cell immunotherapy remains an important issue. CD19-targeted on-target toxicity is linked to CRS and neurotoxicity, which can be lethal in a subset of patients. The severity of CRS and neurotoxicity can be influenced by disease burden, lymphodepletion regimen and CAR T-cell dose. The most common toxicity associated with CAR T-cell therapy is CRS, it occurs at an incidence ranging from 35% to 93%[123,124,157,160,161,311]. Assessing the potential toxicities of targeted therapy is extremely difficult in the preclinical setting owing to the need for cross-reactivity with the murine analogue of the target. The *in vivo* study revealed that the CAR T-cell treatment was well tolerated, causing no more than temporary loss of body weight within some groups. No other side effects attributed to the treatment were observed despite clear anti-tumour activity. Nonetheless, as this was an immunocompromised model, the interaction between CAR T-cells and other components of the immune system could not be studied. The myeloid compartment plays a pivotal role in toxicities caused by CAR T-cells by producing IL-6 and

iNOS, thus contributing to the pathophysiology of CRS[168,312]. Whether pCAR T-cells will influence bystander immune cells is yet unclear.

6.1.3 Dual targeting CD19-CD22 pCAR T-cells show superior efficacy *in vitro*

A key factor to the clinical success of anti-CD19 CAR T-cell therapy is the high expression of the target on the surface of B-cells. Despite inducing B-cell aplasia, which is clinically manageable, CD19 is considered an attractive target based on its widespread expression on B-cell malignancies. However, multi-centre clinical trials have demonstrated that the relapse rate following CD19 targeted CAR T-cell therapy is approximately 30%[124]. Many of the reported cases of relapse result from antigen escape, allowing tumour cells to evade CAR T-cells. Multi-antigen targeting may provide a potential strategy to circumvent this risk. To explore if pCAR T-cells with specificity of multiple targets also out-performed second-generation CARs, constructs targeting CD19 and CD20 (1BB/F) or CD22 (RBB/F/Y05/G02) were designed. Comparison between F-2 and 1BB/F CAR T-cells showed no advantage of the pCAR in restimulation or dose response assays (Fig 5.8). However, the dual targeting pCAR system revealed a potentiating effect of the CCR independent of the signalling CAR. This is illustrated by the comparison of F-2 and 1BB/F and RBB/F on LO68-CD20$^+$ and LO68-CD22$^+$ tumour cells, respectively (Fig 5.8 and Fig 5.20). Despite the lack of CD19, pCAR T-cells achieved greater anti-tumour activity compared to F-2 counterparts. This increment in function likely reflects the T-cell activation threshold being lowered. Another potential advantage of dual-targeting pCARs is the “docking effect” of the CCR to favour closer T-cell and target interaction. The pCAR may enhance sensitivity to detect lower levels of CD19 since the CD22 CCR can help dock T-cells on the leukaemic cell surface, contributing to superior function and minimising low antigen tumour escape. A similar effect was illustrated

when comparing H-2, a MUC1-specific CAR with TTr/H, H2 combined with a panErbB-targeted truncated CCR, which lacks an endodomain (Muliaditan et al, unpublished data). Despite the signalling defective CCR, TTr/H pCAR T-cells achieved greater anti-tumour activity compared to H-2 counterparts. This phenomenon may also account for the reported functional rescue of a sub-optimal first-generation CAR by co-expressed dual CD28+BB CCR[264].

Activation of pCAR T-cells that is not strictly dependent on CAR target engagement poses a problem with regards to safety. B-cell aplasia following anti-CD19 CAR T-cell therapy for B-cell malignancies is a manageable toxicity. However, similar on-target off-tumour toxicity may be untenable when targeting systemic tumour antigens. Contrastingly, Muliaditan et al[215]., reproducibly presented activation of MUC1 specific pCAR T-cells remained contingent on CAR target engagement.

Despite the encouraging *in vitro* results, none of the RBB/ dual antigen-targeted pCAR panel induced a significant delay in tumour progression when compared to F-2 (Fig 5.15). One possible explanation for this disparity relates to the binding site of the CAR on the CD22 antigen. Haso et al[112]., altered the binding site of an anti-CD22 scFv (m971) to a more proximal epitope and found that this significantly enhanced CAR efficacy. Using an m971 scFv as the targeting moiety of the CCR in future experiments may improve function that is translated *in vivo.* Prior to infusion of CAR T-cells in this experiment, the CD4 to CD8 ratio was determined revealing that a majority of the T-cells were $CD8^+$ (>80%). This skewing towards $CD8^+$ CAR T-cells might be detrimental to *in vivo* function as synergistic activity of CD4 and CD8 T-cells has been observed in murine models[313,314]. Moreover, formulating CAR T-cells at a 1:1 CD4:CD8 ratio led to eradication of Raji lymphoma *in vivo* that was not

achievable with either subset alone. Researchers found that $CD8^+$ T-cells produced little IL-2 which was largely produced by $CD4^+$ T-cells. Furthermore, efficacy *in* vivo correlated with greater proliferation of $CD8^+$ CAR T-cells, suggesting the IL-2 produced $CD4^+$ T-cells helped sustain the CD8 response. In future, defining the composition of T-cells used *in vivo* may enhance anti-tumour activity.

6.1.3 Single-chain diabody CARs destroy CD19 negative tumour cells

An alternative approach to tackling the issue of CD19 negative relapse was tried through the design of single-chain diabody (scDb) CARs. Similar in theory to bi-specific T-cell engagers (BiTEs), the scDb binds to tumour antigen (CD22) and F-2 CAR T-cells simultaneously to mediate tumour cell killing even in the absence of CD19. In dose response cytotoxicity assays with NALM-6 tumour cells, both scDb CARs showed encouraging results, outperforming both F-2 and R-2 CAR T-cells (Fig. 5.19). Importantly, scDb CAR T-cells recognised and destroyed LO68-$CD22^+$ tumour cells albeit, not as efficiently as R-2 CAR T-cells. An issue that may arise from this system is the non-coordinated and sustained activation of the T-cells as the scDb is continually produced by the CAR. The sustained CAR signalling mediated by the scDb may induce T-cell exhaustion through the upregulation of inhibitory receptors and induce apoptosis. This could perhaps be ameliorated by substituting the CD28 costimulatory domain with 4-1BB however, there are conflicting reports as to whether 4-1BB also facilitates tonic signalling[315,316]. Investigating if the scDb CARs show enhanced proliferation, continuous cytokine production or exhaustion markers remains to be undertaken to address this question.

6.2 Future Directions

The comparison of lower avidity scFvs and F-2 CAR T-cells showed that higher avidity does not translate into greater *in vivo* efficacy. In fact, the opposite appears to be the case with some lower avidity CARs prolonging the survival of leukaemia bearing mice. To further investigate the reason behind this observation the on and off-rate of these scFvs should be measured. Evidence supports both K_d and K_{off} as determinants of T-cell function[120,317]. A fast off-rate, which measures how quickly an antibody dissociates from its antigen, may favour serial triggering and killing by the T-cell. Live cell imaging to observe CAR T-cell and target interactions would provide more information on the duration of interactions and the motility of CAR T-cells. It has been hypothesised that there is an "affinity ceiling" which is an upper limit to increased responsiveness of high affinity interactions. Therefore, increasing the affinity of scFvs past this threshold does not improve CAR T-cell function and can lead to attenuation of expansion[318]. Analysis of the high affinity engineered c58c61 TCR and human T-cell activation in response to variation in pMHC affinity showed that there is a bell-shaped curve with reduced cytokine production at high peptide MHC concentrations. The researchers concluded that intermediate affinity interactions produces the greatest response at low pMHC doses[319]. Similarly, results shown here reveal that exceedingly lower avidity significantly limited effector function (Y03 and G01). An experiment to compare Y04, Y05 and G02 cell functionality targeting LO68 cells expressing varying levels of CD19 would give further insight. The expectation is that the lower to intermediate avidity scFvs will produce a larger response to lower levels of CD19. Another parameter that could potentially be measured is downregulation of the CAR, which has been described previously[296]. In T-cells, internalization of the TCR is a characteristic of serial triggering and engagement by

agonist ligand. As such, there may be differences in down-regulation of the CAR on the T-cell surface between different constructs. Exploring the role of affinity in the design of pCARs is another avenue worth studying. To test the importance of relative affinity of CAR versus CCR for a competing epitope, a panel of CD19 specific pCARs can be constructed in which CAR affinity exceeds that of the CCR, or vice versa. Investigating the avidity of pCAR using z-Movi would also be interesting. The expectation is that the FMC63 scFv in the CCR position would increase avidity compared to the CAR second-generation controls but comparing between pCARs there may be range of avidities. However, as all pCARs behaved in a similar fashion, this suggests that the pCAR structure provides flexibility with respect to relative affinity of the CAR and CCR.

To further investigate the persistence of CAR and pCAR T-cells *in vivo* and their memory recall responses, tumour rechallenge after successful leukaemia elimination could be carried out. However, this would require higher doses of CAR and pCAR T-cells as disease clearance was not established with a sub-optimal dose of $0.5x10^6$ CAR T-cells. To understand the mechanisms behind the superior anti-tumour efficacy of pCAR T-cells, *ex vivo* analysis of CAR T-cells following tumour clearance *in vivo* should provide further insight. After three stimulation cycles with NALM-6 leukaemic cells pCAR T-cells have lower expression of exhaustion markers PD-1, LAG-3 and TIM-3 (Fig 4.8). Additionally, pCAR T-cells showed increased proliferation and sustained IFN-γ production, which may be a reflection of AICD and exhaustion. I hypothesize that second-generation CAR T-cells will show an impaired proliferative and cytotoxic response following stimulation *ex vivo*.

The consistently superior performance of CD19 pCAR T-cells highlights a general principle, namely the importance of juxta-membrane positioning of costimulatory signalling.

However, this did not translate when dual targeting CD20 and CD19 as the 1BB/F pCAR did not show a significant advantage in *in vitro* functional assays (Fig 5.5 and Fig 5.6) . A possible explanation for the underwhelming efficacy of 1BBF is that a long spacer is required for CD20-targeted CARs[267]. In comparison with CD19 CARs, in which a short extracellular spacer is more effective, CD20 long-spacer CAR T-cells consistently demonstrated greater target-cell lysis, cytokine production and T-cell proliferation. CD20 is a tetraspanin-like protein with a small extracellular domain therefore a long spacer is needed to target such membrane proximal epitopes[320]. In comparison, short-spacers optimally target epitopes further from the cell membrane such as CD22 and CD19[267,321]. Therefore, re-designing the 1BB/F pCAR with long extracellular spacer within the aCD20 CCR may enhance its function to a similar capacity of other pCARs. Conversely, it would be interesting to engineer the RBB/ pCARs with long spacers within the CCR to see if this abrogates superiority.

6.3 Final conclusion

In summary, here I present the development of novel pCARs that effectively deliver integrated costimulation via CD28 and 41BB with co-stimulatory modules located in their natural membrane-associated position. There is considerable evidence that synchronous arrangement of both CD28 and 41BB costimulation can synergistically enhance T-cell immune responses[322–324]. Whilst these receptors activate overlapping signal pathways, evidences show the strength and kinetics of responses differ decidedly. Faster and larger scale signalling flux is initiated by CD28-containing CARs whereas 41BB favours a less intense but longer lasting response[140]. My hypothesis was that provision of dual tumour antigen-dependent costimulation would enhance durability and efficacy of CAR T-cells. The results

suggest that pCAR signalling fosters less exhaustion of T-cells and enhanced function *in vivo* compared to conventional second-generation CARs. Moreover, pCARs that target CD19 using scFvs that engage their target with differing avidities showed significantly better leukaemic disease control *in vivo.* Dual targeting CD22-CD19 pCARs were reproducibly superior *in vitro* however, further *in vivo* assessment is required to unpick differences in functionality. Additionally, I explored the role of avidity of CAR T-cells and its implications for the development of future CARs. Specifically, that a lower avidity for target may allow for serial triggering and improve function of CAR T-cells and therefore avidity should be scrutinized when designing CARs.

Chapter 7: Supplementary Data

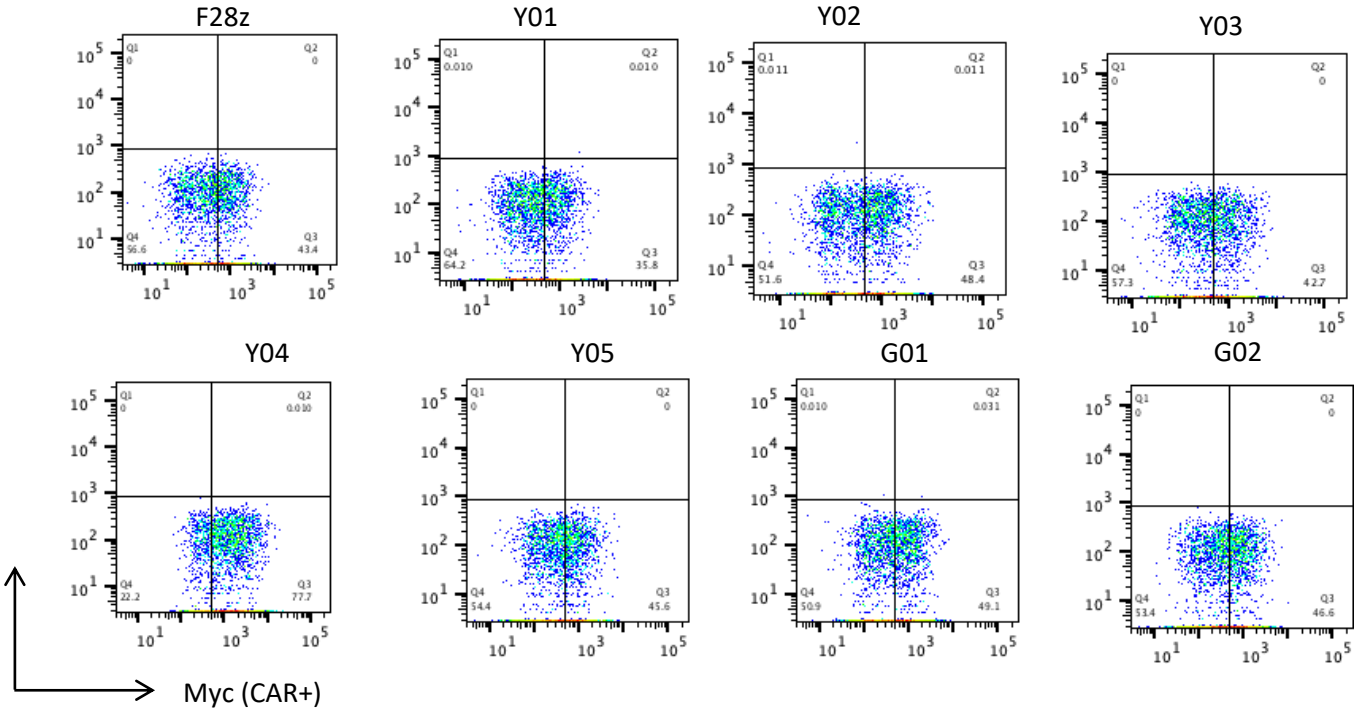

Figure 7.1 Expression of CDR3 mutated and control F-2 CAR in T-cells detected using the myc tag. Primary human T-cells were transduced with the indicated CAR-encoding retroviral vectors and assessed by flow cytometry. The presence of the CARs was detected by flow cytometry after incubation with 9E10 (anti-Myc) antibody followed by goat anti-mouse PE. The level of CAR expression in all cases was compared to untransduced (UT) T-cells probed with the same antibody combinations

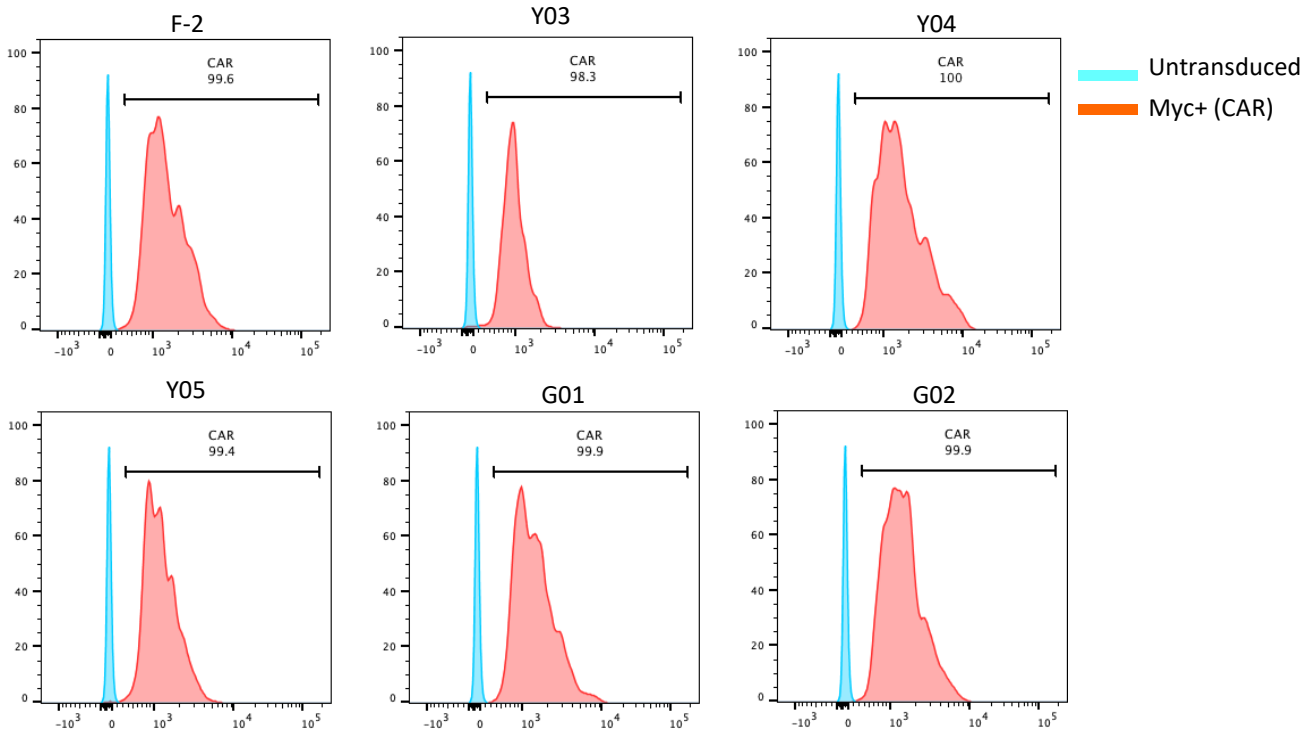

Figure 7.2 Flow cytometry showing CAR expression after FACS sorting. Total transduced CAR$^+$ T-cells were stained with 9e10 (anti-Myc) antibody followed by goat anti-mouse PE. The level of CAR expression in all cases was compared to untransduced (UT) T-cells probed with the same antibody combinations. Plots show population of CAR$^+$ T-cells FACS sorted and used z-Movi experiments.

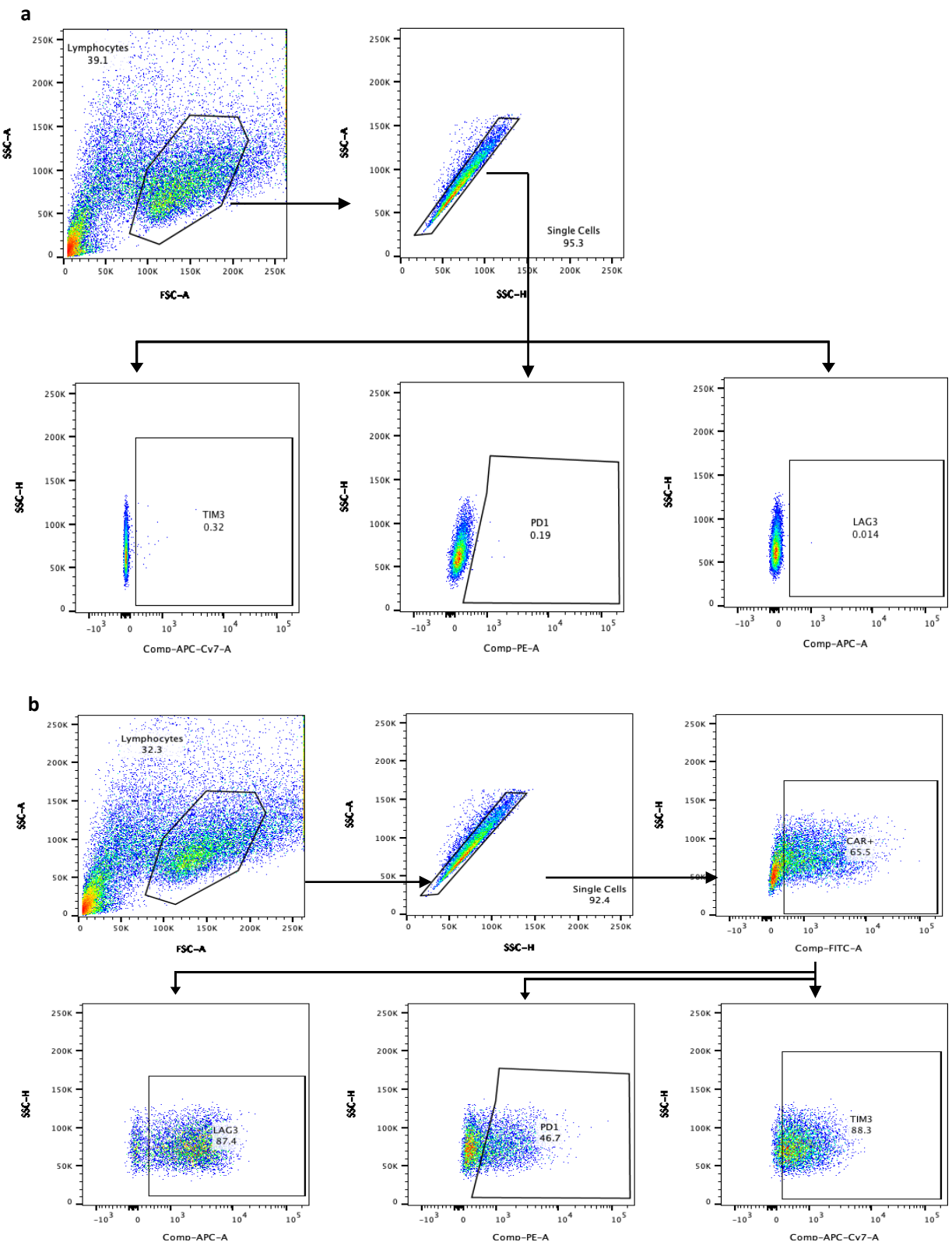

Sample:	LAG3+PD1+TIM3+	LAG3+PD1+TIM3-	LAG3+PD1-TIM3+	LAG3+PD1-TIM3-	LAG3-PD1+TIM3+	LAG3-PD1+TIM3-	LAG3-PD1-TIM3+	LAG3-PD1-TIM3-
F-2.fcs	65.4	23.9	4.28	1.41	1.09	2.03	1.21	0.69
Y04.fcs	65.9	19.2	4.37	2.62	3.06	2.77	1.09	1.02
Y05.fcs	60.9	27.3	4.95	1.94	1.46	1.92	0.85	0.7
G02.fcs	64.3	26.7	3.3	1.34	0.81	1.67	1.03	0.9
FBB/Y04.fcs	52.6	5.39	33.8	2.01	2.4	1.13	1.58	1.03
FBB/Y05.fcs	47.8	3.9	36.6	2.34	4.46	0.95	2.62	1.39
FBB/G02.fcs	36.2	4.19	43.2	3.84	4.58	1.71	4.32	1.97
UT.fcs	6.98	1.16	2.33	1.16	6.98	1.16	52.3	27.9

Figure 7.3 Facs plots showing expression of exhaustion markers LAG3, PD1 and TIM3 and Boolean gating strategy for markers. T-cells were engineered to express the indicated CARs or pCARs. $5x10^5$ of the indicated transduced CAR or pCAR T-cells were co-cultivated with $2.5x10^5$ LO68-CD19 tumour cells. After 72h, T-cells were harvested and expression of LAG3, PD1 and TIM3 analysed by flow cytometry. a) Shows gating strategy set by isotype controls. A representative sample is shown in (b) illustrating the gating for each cell surface marker which was used to create Boolean gates as shown in the table.

Bibliography

1. Jaffe ES, Barr PM, Smith SM. Understanding the New WHO Classification of Lymphoid Malignancies: Why It's Important and How It Will Affect Practice. *Am Soc Clin Oncol Educ B*. Epub ahead of print 2017. DOI: 10.1200/edbk_175437.

2. Swerdlow SH, Campo E, Pileri SA, et al. The 2016 revision of the World Health Organization classification of lymphoid neoplasms. *Blood*. Epub ahead of print 2016. DOI: 10.1182/blood-2016-01-643569.

3. Ward E, DeSantis C, Robbins A, et al. Childhood and adolescent cancer statistics, 2014. *CA Cancer J Clin*. Epub ahead of print 2014. DOI: 10.3322/caac.21219.

4. Hunger SP, Mullighan CG. Acute lymphoblastic leukemia in children. *New England Journal of Medicine*. Epub ahead of print 2015. DOI: 10.1056/NEJMra1400972.

5. Inaba H, Greaves M, Mullighan CG. Acute lymphoblastic leukaemia. *The Lancet*. Epub ahead of print 2013. DOI: 10.1016/S0140-6736(12)62187-4.

6. Mejía-Aranguré JM. *Etiology of acute leukemias in children*. 2016. Epub ahead of print 2016. DOI: 10.1007/978-3-319-05798-9.

7. Sehgal S, Mujtaba S, Gupta D, et al. High incidence of Epstein Barr virus infection in childhood acute lymphocytic lukemia: A preliminary study. *Indian J Pathol Microbiol*. Epub ahead of print 2010. DOI: 10.4103/0377-4929.59186.

8. Gérinière L, Bastion Y, Dumontet C, et al. Heterogeneity of acute lymphoblastic

leukemia in HIV-seropositive patients. *Ann Oncol*. Epub ahead of print 1994. DOI: 10.1093/oxfordjournals.annonc.a058876.

9. Jabbour E, O'Brien S, Konopleva M, et al. New insights into the pathophysiology and therapy of adult acute lymphoblastic leukemia. *Cancer*. Epub ahead of print 2015. DOI: 10.1002/cncr.29383.

10. Pui CH, Robison LL, Look AT. Acute lymphoblastic leukaemia. *The Lancet*. Epub ahead of print 2008. DOI: 10.1016/S0140-6736(08)60457-2.

11. Stanulla M, Schrappe M. Treatment of Childhood Acute Lymphoblastic Leukemia. *Semin Hematol*. Epub ahead of print 2009. DOI: 10.1053/j.seminhematol.2008.09.007.

12. Vijayakrishnan J, Studd J, Broderick P, et al. Genome-wide association study identifies susceptibility loci for B-cell childhood acute lymphoblastic leukemia. *Nat Commun*. Epub ahead of print 2018. DOI: 10.1038/s41467-018-03178-z.

13. Chessells JM, Harrison G, Richards SM, et al. Down's syndrome and acute lymphoblastic leukaemia: Clinical features and response to treatment. *Arch Dis Child*. Epub ahead of print 2001. DOI: 10.1136/adc.85.4.321.

14. Shah A, John BM, Sondhi V. Acute lymphoblastic leukemia with treatment-naïve fanconi anemia. *Indian Pediatr*.

15. German J. Bloom's syndrome. XX. The first 100 cancers. *Cancer Genet Cytogenet*. Epub ahead of print 1997. DOI: 10.1016/S0165-4608(96)00336-6.

16. Kuiper RP, Schoenmakers EFPM, van Reijmersdal S V., et al. High-resolution genomic

profiling of childhood ALL reveals novel recurrent genetic lesions affecting pathways involved in lymphocyte differentiation and cell cycle progression. *Leukemia*. Epub ahead of print 2007. DOI: 10.1038/sj.leu.2404691.

17. Mullighan CG, Goorha S, Radtke I, et al. Genome-wide analysis of genetic alterations in acute lymphoblastic leukaemia. *Nature*. Epub ahead of print 2007. DOI: 10.1038/nature05690.

18. Mullighan CG, Collins-Underwood JR, Phillips LAA, et al. Rearrangement of CRLF2 in B-progenitor-and Down syndrome-associated acute lymphoblastic leukemia. *Nat Genet*. Epub ahead of print 2009. DOI: 10.1038/ng.469.

19. Zhang J, Mullighan CG, Harvey RC, et al. Key pathways are frequently mutated in high-risk childhood acute lymphoblastic leukemia: A report from the Children's Oncology Group. *Blood*. Epub ahead of print 2011. DOI: 10.1182/blood-2011-03-341412.

20. Bennett JM, Catovsky D, Daniel M -T, et al. Proposals for the Classification of the Acute Leukaemias French-American-British (FAB) Co-operative Group. *Br J Haematol*. Epub ahead of print 1976. DOI: 10.1111/j.1365-2141.1976.tb03563.x.

21. Harris NL, Jaffe ES, Diebold J, et al. The World Health Organization Classification of Neoplasms of the Hematopoietic and Lymphoid Tissues: Report of the Clinical Advisory Committee Meeting - Airlie House, Virginia, November, 1997. *Hematol J*. Epub ahead of print 2000. DOI: 10.1038/sj.thj.6200013.

22. Vardiman JW, Thiele J, Arber DA, et al. The 2008 revision of the World Health Organization (WHO) classification of myeloid neoplasms and acute leukemia:

Rationale and important changes. *Blood*. Epub ahead of print 2009. DOI: 10.1182/blood-2009-03-209262.

23. Arber DA, Orazi A, Hasserjian R, et al. The 2016 revision to the World Health Organization classification of myeloid neoplasms and acute leukemia. *Blood*. Epub ahead of print 2016. DOI: 10.1182/blood-2016-03-643544.

24. Shiraz P, Payne KJ, Muffly L. The current genomic and molecular landscape of philadelphia-like acute lymphoblastic leukemia. *Int J Mol Sci* 2020; 21: 1–17.

25. Alvarnas JC, Brown PA, Aoun P, et al. Acute Lymphoblastic Leukemia, Version 2.2015. *J Natl Compr Cancer Netw*. Epub ahead of print 2015. DOI: 10.6004/jnccn.2015.0153.

26. Tobias J, Hochhauser D. *Cancer and its Management: Seventh Edition*. 2014. Epub ahead of print 2014. DOI: 10.1002/9781118468753.

27. Rubnitz JE. Current Management of Childhood Acute Myeloid Leukemia. *Pediatr Drugs*. Epub ahead of print 2017. DOI: 10.1007/s40272-016-0200-6.

28. Balduzzi A, Valsecchi MG, Uderzo C, et al. Chemotherapy versus allogeneic transplantation for very-high-risk childhood acute lymphoblastic leukaemia in first complete remission: Comparison by genetic randomisation in an international prospective study. *Lancet*. Epub ahead of print 2005. DOI: 10.1016/S0140-6736(05)66998-X.

29. Schrappe M, Hunger SP, Pui CH, et al. Outcomes after induction failure in childhood acute lymphoblastic leukemia. *N Engl J Med*. Epub ahead of print 2012. DOI: 10.1056/NEJMoa1110169.

30. Miranda-Filho A, Piñeros M, Znaor A, et al. Global patterns and trends in the incidence of non-Hodgkin lymphoma. *Cancer Causes Control*. Epub ahead of print 2019. DOI: 10.1007/s10552-019-01155-5.

31. Bray F, Ferlay J, Soerjomataram I, et al. Global cancer statistics 2018: GLOBOCAN estimates of incidence and mortality worldwide for 36 cancers in 185 countries. *CA Cancer J Clin*. Epub ahead of print 2018. DOI: 10.3322/caac.21492.

32. Horvat M, Zadnik V, Šetina TJ, et al. Diffuse large B-cell lymphoma: 10 years' real-world clinical experience with rituximab plus cyclophosphamide, doxorubicin, vincristine and prednisolone. *Oncol Lett*. Epub ahead of print 2018. DOI: 10.3892/ol.2018.7774.

33. Gouveia GR, Siqueira SAC, Pereira J. Pathophysiology and molecular aspects of diffuse large B-cell lymphoma. *Rev Bras Hematol Hemoter*. Epub ahead of print 2012. DOI: 10.5581/1516-8484.20120111.

34. Miao Y, Medeiros LJ, Li Y, et al. Genetic alterations and their clinical implications in DLBCL. *Nature Reviews Clinical Oncology*. Epub ahead of print 2019. DOI: 10.1038/s41571-019-0225-1.

35. Lieber MR. Mechanisms of human lymphoid chromosomal translocations. *Nature Reviews Cancer*. Epub ahead of print 2016. DOI: 10.1038/nrc.2016.40.

36. Deutsch AJA, Aigelsreiter A, Staber PB, et al. MALT lymphoma and extranodal diffuse large B-cell lymphoma are targeted by aberrant somatic hypermutation. *Blood*. Epub ahead of print 2007. DOI: 10.1182/blood-2006-06-030494.

37. Gordon MS, Kanegai CM, Doerr JR, et al. Somatic hypermutation of the B cell receptor genes B29 (Igβ, CD79b) and mb1 (Igα, CD79a). *Proc Natl Acad Sci U S A*. Epub ahead of print 2003. DOI: 10.1073/pnas.0735266100.

38. Chapuy B, Stewart C, Dunford AJ, et al. Molecular subtypes of diffuse large B cell lymphoma are associated with distinct pathogenic mechanisms and outcomes. *Nat Med*. Epub ahead of print 2018. DOI: 10.1038/s41591-018-0016-8.

39. Pasqualucci L, Neumeister P, Goossens T, et al. Hypermutation of multiple proto-oncogenes in B-cell diffuse large-cell lymphomas. *Nature*. Epub ahead of print 2001. DOI: 10.1038/35085588.

40. Basso K, Dalla-Favera R. Germinal centres and B cell lymphomagenesis. *Nat Rev Immunol*. Epub ahead of print 2015. DOI: 10.1038/nri3814.

41. Karube K, Campo E. MYC Alterations in Diffuse Large B-Cell Lymphomas. *Seminars in Hematology*. Epub ahead of print 2015. DOI: 10.1053/j.seminhematol.2015.01.009.

42. Coiffier B, Lepage E, Brière J, et al. Chop chemotherapy plus rituximab compared with chop alone in elderly patients with diffuse large-B-cell lymphoma. *N Engl J Med*. Epub ahead of print 2002. DOI: 10.1056/NEJMoa011795.

43. Marcus R, Imrie K, Solal-Celigny P, et al. Phase III study of R-CVP compared with cyclophosphamide, vincristine, and prednisone alone in patients with previously untreated advanced follicular lymphoma. *J Clin Oncol*. Epub ahead of print 2008. DOI: 10.1200/JCO.2007.13.5376.

44. Van Den Neste E, Schmitz N, Mounier N, et al. Outcome of patients with relapsed

diffuse large B-cell lymphoma who fail second-line salvage regimens in the International CORAL study. *Bone Marrow Transplant*. Epub ahead of print 2016. DOI: 10.1038/bmt.2015.213.

45. Crump M, Neelapu SS, Farooq U, et al. Outcomes in refractory diffuse large B-cell lymphoma: Results from the international SCHOLAR-1 study. *Blood*. Epub ahead of print 2017. DOI: 10.1182/blood-2017-03-769620.

46. Yang Y. Cancer immunotherapy: Harnessing the immune system to battle cancer. *Journal of Clinical Investigation*. Epub ahead of print 2015. DOI: 10.1172/JCI83871.

47. Dunn GP, Old LJ, Schreiber RD. The Three Es of Cancer Immunoediting. *Annu Rev Immunol*. Epub ahead of print 2004. DOI: 10.1146/annurev.immunol.22.012703.104803.

48. Schreiber RD, Old LJ, Smyth MJ. Cancer immunoediting: Integrating immunity's roles in cancer suppression and promotion. *Science*. Epub ahead of print 2011. DOI: 10.1126/science.1203486.

49. Hicklin DJ, Wang Z, Arienti F, et al. β2-Microglobulin mutations, HLA class I antigen loss, and tumor progression in melanoma. *J Clin Invest*. Epub ahead of print 1998. DOI: 10.1172/JCI498.

50. Takeda K, Smyth MJ, Cretney E, et al. Critical role for tumor necrosis factor-related apoptosis-inducing ligand in immune surveillance against tumor development. *J Exp Med*. Epub ahead of print 2002. DOI: 10.1084/jem.20011171.

51. Straus SE, Jaffe ES, Puck JM, et al. The development of lymphomas in families with

autoimmune lymphoproliferative syndrome with germline Fas mutations and defective lymphocyte apoptosis. *Blood*. Epub ahead of print 2001. DOI: 10.1182/blood.V98.1.194.

52. Kalbasi A, June CH, Haas N, et al. Radiation and immunotherapy: A synergistic combination. *Journal of Clinical Investigation*. Epub ahead of print 2013. DOI: 10.1172/JCI69219.

53. Coley WB. The treatment of malignant tumors by repeated inoculations of erysipelas: With a report of ten original cases. *Clin Orthop Relat Res*.

54. Rosenberg SA, Lotze MT, Muul LM, et al. Observations on the Systemic Administration of Autologous Lymphokine-Activated Killer Cells and Recombinant Interleukin-2 to Patients with Metastatic Cancer. *N Engl J Med*. Epub ahead of print 1985. DOI: 10.1056/NEJM198512053132327.

55. Atkins MB, Lotze MT, Dutcher JP, et al. High-dose recombinant interleukin 2 therapy for patients with metastatic melanoma: Analysis of 270 patients treated between 1985 and 1993. *J Clin Oncol*. Epub ahead of print 1999. DOI: 10.1200/jco.1999.17.7.2105.

56. Maloney DG, Grillo-López AJ, White CA, et al. IDEC-C2B8 (rituximab) anti-CD20 monoclonal antibody therapy in patients with relapsed low-grade non-Hodgkin's lymphoma. *Blood*. Epub ahead of print 1997. DOI: 10.1182/blood.V90.6.2188.

57. Reff ME, Carner K, Chambers KS, et al. Depletion of B cells in vivo by a chimeric mouse human monoclonal antibody to CD20. *Blood*. Epub ahead of print 1994. DOI:

10.1182/blood.v83.2.435.bloodjournal832435.

58. Schietinger A, Greenberg PD. Tolerance and exhaustion: Defining mechanisms of T cell dysfunction. *Trends in Immunology*. Epub ahead of print 2014. DOI: 10.1016/j.it.2013.10.001.

59. Kvistborg P, Philips D, Kelderman S, et al. Anti-CTLA-4 therapy broadens the melanoma-reactive CD8+ T cell response. *Sci Transl Med*. Epub ahead of print 2014. DOI: 10.1126/scitranslmed.3008918.

60. Ribas A, Shin DS, Zaretsky J, et al. PD-1 blockade expands intratumoral memory T cells. *Cancer Immunol Res*. Epub ahead of print 2016. DOI: 10.1158/2326-6066.CIR-15-0210.

61. Hodi FS, O'Day SJ, McDermott DF, et al. Improved survival with ipilimumab in patients with metastatic melanoma. *N Engl J Med*. Epub ahead of print 2010. DOI: 10.1056/NEJMoa1003466.

62. Chow LQM, Haddad R, Gupta S, et al. Antitumor activity of pembrolizumab in biomarker-unselected patients with recurrent and/or metastatic head and neck squamous cell carcinoma: Results from the phase Ib KEYNOTE-012 expansion cohort. *J Clin Oncol* 2016; 34: 3838–3845.

63. Rizvi NA, Hellmann MD, Snyder A, et al. Mutational landscape determines sensitivity to PD-1 blockade in non-small cell lung cancer. *Science (80-)*. Epub ahead of print 2015. DOI: 10.1126/science.aaa1348.

64. Ansell SM, Lesokhin AM, Borrello I, et al. PD-1 blockade with nivolumab in relapsed or

refractory Hodgkin's lymphoma. *N Engl J Med*. Epub ahead of print 2015. DOI: 10.1056/NEJMoa1411087.

65. Schadendorf D, Hodi FS, Robert C, et al. Pooled analysis of long-term survival data from phase II and phase III trials of ipilimumab in unresectable or metastatic melanoma. *J Clin Oncol*. Epub ahead of print 2015. DOI: 10.1200/JCO.2014.56.2736.

66. Wolchok JD, Weber JS, Maio M, et al. Four-year survival rates for patients with metastatic melanoma who received ipilimumab in phase II clinical trials. *Ann Oncol*. Epub ahead of print 2013. DOI: 10.1093/annonc/mdt161.

67. Topalian SL, Sznol M, McDermott DF, et al. Survival, durable tumor remission, and long-term safety in patients with advanced melanoma receiving nivolumab. *J Clin Oncol*. Epub ahead of print 2014. DOI: 10.1200/JCO.2013.53.0105.

68. Pai-Scherf L, Blumenthal GM, Li H, et al. FDA Approval Summary: Pembrolizumab for Treatment of Metastatic Non-Small Cell Lung Cancer: First-Line Therapy and Beyond. *Oncologist*. Epub ahead of print 2017. DOI: 10.1634/theoncologist.2017-0078.

69. Larkin J, Chiarion-Sileni V, Gonzalez R, et al. Combined nivolumab and ipilimumab or monotherapy in untreated Melanoma. *N Engl J Med*. Epub ahead of print 2015. DOI: 10.1056/NEJMoa1504030.

70. Postow MA, Chesney J, Pavlick AC, et al. Nivolumab and ipilimumab versus ipilimumab in untreated melanoma. *N Engl J Med*. Epub ahead of print 2015. DOI: 10.1056/NEJMoa1414428.

71. Rosenberg SA, Spiess P, Lafreniere R. A new approach to the adoptive

immunotherapy of cancer with tumor-infiltrating lymphocytes. *Science (80-)*. Epub ahead of print 1986. DOI: 10.1126/science.3489291.

72. Rosenberg SA, Packard BS, Aebersold PM, et al. Use of Tumor-Infiltrating Lymphocytes and Interleukin-2 in the Immunotherapy of Patients with Metastatic Melanoma. *N Engl J Med*. Epub ahead of print 1988. DOI: 10.1056/NEJM198812223192527.

73. Verdegaal EME, Visser M, Ramwadhdoebé TH, et al. Successful treatment of metastatic melanoma by adoptive transfer of blood-derived polyclonal tumor-specific CD4+ and CD8+ T cells in combination with low-dose interferon-alpha. *Cancer Immunol Immunother*. Epub ahead of print 2011. DOI: 10.1007/s00262-011-1004-8.

74. Goff SL, Smith FO, Klapper JA, et al. Tumor infiltrating lymphocyte therapy for metastatic melanoma: Analysis of tumors resected for TIL. *J Immunother*. Epub ahead of print 2010. DOI: 10.1097/CJI.0b013e3181f05b91.

75. Joseph RW, Peddareddigari VR, Liu P, et al. Impact of clinical and pathologic features on tumor-infiltrating lymphocyte expansion from surgically excised melanoma metastases for adoptive T-cell therapy. *Clin Cancer Res*. Epub ahead of print 2011. DOI: 10.1158/1078-0432.CCR-10-2769.

76. Geukes Foppen MH, Donia M, Svane IM, et al. Tumor-infiltrating lymphocytes for the treatment of metastatic cancer. *Molecular Oncology*. Epub ahead of print 2015. DOI: 10.1016/j.molonc.2015.10.018.

77. Clay TM, Custer MC, Sachs J, et al. Efficient transfer of a tumor antigen-reactive TCR

to human peripheral blood lymphocytes confers anti-tumor reactivity. *J Immunol*.

78. Cohen CJ, Zheng Z, Bray R, et al. Recognition of fresh human tumor by human peripheral blood lymphocytes transduced with a bicistronic retroviral vector encoding a murine anti-p53 TCR. *J Immunol*. Epub ahead of print 2006. DOI: 10.4049/jimmunol.177.8.5746.

79. Kuball J, Schmitz FW, Voss RH, et al. Cooperation of human tumor-reactive CD4+ and CD8+ T cells after redirection of their specificity by a high-affinity p53A2.1-specific TCR. *Immunity*. Epub ahead of print 2005. DOI: 10.1016/j.immuni.2004.12.005.

80. Schaft N, Willemsen RA, de Vries J, et al. Peptide Fine Specificity of Anti-Glycoprotein 100 CTL Is Preserved Following Transfer of Engineered TCRαβ Genes Into Primary Human T Lymphocytes. *J Immunol*. Epub ahead of print 2003. DOI: 10.4049/jimmunol.170.4.2186.

81. Xue SA, Gao L, Thomas S, et al. Development of a Wilms' tumor antigen-specific T-cell receptor for clinical trials: Engineered patient's T cells can eliminate autologous leukemia blasts in NOD/SCID mice. *Haematologica* 2010; 95: 126–134.

82. Parkhurst MR, Joo J, Riley JP, et al. Characterization of genetically modified T-cell receptors that recognize the CEA:691-699 peptide in the context of HLA-A2.1 on human colorectal cancer cells. *Clin Cancer Res*. Epub ahead of print 2009. DOI: 10.1158/1078-0432.CCR-08-1638.

83. Johnson LA, Morgan RA, Dudley ME, et al. Gene therapy with human and mouse T-cell receptors mediates cancer regression and targets normal tissues expressing

cognate antigen. *Blood*. Epub ahead of print 2009. DOI: 10.1182/blood-2009-03-211714.

84. Rapoport AP, Stadtmauer EA, Binder-Scholl GK, et al. NY-ESO-1-specific TCR-engineered T cells mediate sustained antigen-specific antitumor effects in myeloma. *Nat Med*. Epub ahead of print 2015. DOI: 10.1038/nm.3910.

85. Pollack SM, Ingham M, Spraker MB, et al. Emerging targeted and immune-based therapies in sarcoma. *Journal of Clinical Oncology*. Epub ahead of print 2018. DOI: 10.1200/JCO.2017.75.1610.

86. Bendle GM, Linnemann C, Hooijkaas AI, et al. Lethal graft-versus-host disease in mouse models of T cell receptor gene therapy. *Nat Med*. Epub ahead of print 2010. DOI: 10.1038/nm.2128.

87. Torikai H, Reik A, Liu PQ, et al. A foundation for universal T-cell based immunotherapy: T cells engineered to express a CD19-specific chimeric-antigen-receptor and eliminate expression of endogenous TCR. *Blood*. Epub ahead of print 2012. DOI: 10.1182/blood-2012-01-405365.

88. Bishop D, Gottlieb D, Micklethwaite K. shRNA-mediated TCR knockdown as a foundation for allogeneic CAR19 T-cells generated by single-step genetic modification with the piggyBac transposase. *Cytotherapy*. Epub ahead of print 2018. DOI: 10.1016/j.jcyt.2018.02.013.

89. Kuwana Y, Asakura Y, Utsunomiya N, et al. Expression of chimeric receptor composed of immunoglobulin-derived V resions and T-cell receptor-derived C regions. *Biochem*

Biophys Res Commun. Epub ahead of print 1987. DOI: 10.1016/0006-291X(87)90502-X.

90. Eshhar Z, Waks T, Gross G, et al. Specific activation and targeting of cytotoxic lymphocytes through chimeric single chains consisting of antibody-binding domains and the γ or ζ subunits of the immunoglobulin and T-cell receptors. *Proc Natl Acad Sci U S A*. Epub ahead of print 1993. DOI: 10.1073/pnas.90.2.720.

91. Gross G, Waks T, Eshhar Z. Expression of immunoglobulin-T-cell receptor chimeric molecules as functional receptors with antibody-type specificity. *Proc Natl Acad Sci U S A*. Epub ahead of print 1989. DOI: 10.1073/pnas.86.24.10024.

92. Sadelain M, Brentjens R, Rivière I. The basic principles of chimeric antigen receptor design. *Cancer Discovery*. Epub ahead of print 2013. DOI: 10.1158/2159-8290.CD-12-0548.

93. Hacein-Bey-Abina S, Garrigue A, Wang GP, et al. Insertional oncogenesis in 4 patients after retrovirus-mediated gene therapy of SCID-X1. *J Clin Invest*. Epub ahead of print 2008. DOI: 10.1172/JCI35700.

94. Howe SJ, Mansour MR, Schwarzwaelder K, et al. Insertional mutagenesis combined with acquired somatic mutations causes leukemogenesis following gene therapy of SCID-X1 patients. *J Clin Invest*. Epub ahead of print 2008. DOI: 10.1172/JCI35798.

95. Scholler J, Brady TL, Binder-Scholl G, et al. Decade-long safety and function of retroviral-modified chimeric antigen receptor T cells. *Sci Transl Med*. Epub ahead of print 2012. DOI: 10.1126/scitranslmed.3003761.

96. Eyquem J, Mansilla-Soto J, Giavridis T, et al. Targeting a CAR to the TRAC locus with CRISPR/Cas9 enhances tumour rejection. *Nature* 2017; 543: 113–117.

97. Jinek M, Chylinski K, Fonfara I, et al. A programmable dual-RNA-guided DNA endonuclease in adaptive bacterial immunity. *Science (80-)*. Epub ahead of print 2012. DOI: 10.1126/science.1225829.

98. Rupp LJ, Schumann K, Roybal KT, et al. CRISPR/Cas9-mediated PD-1 disruption enhances anti-Tumor efficacy of human chimeric antigen receptor T cells. *Sci Rep*. Epub ahead of print 2017. DOI: 10.1038/s41598-017-00462-8.

99. Grupp SA, Kalos M, Barrett D, et al. Chimeric antigen receptor-modified T cells for acute lymphoid leukemia. *N Engl J Med*. Epub ahead of print 2013. DOI: 10.1056/NEJMoa1215134.

100. Qasim W, Zhan H, Samarasinghe S, et al. Molecular remission of infant B-ALL after infusion of universal TALEN gene-edited CAR T cells. *Sci Transl Med*. Epub ahead of print 2017. DOI: 10.1126/scitranslmed.aaj2013.

101. Benjamin R, Graham C, Yallop D, Jozwik A, Ciocarlie O, Jain N, Jabbour EJ, Maus MV, Frigault M, Boissel N, Larghero J, Baruchel A, Mohty M, De Moerloose B, Bloor A, Frey NV, Zinaï A, Balandraud S, Philippe A, Fouliard S, Gauthier L, Pauly J, Konto C, Berm QW. Preliminary data on safety, cellular kinetics and anti-leukemic activity of UCART19, an allogeneic anti-CD19 CAR T-cell product, in a pool of adult and pediatric patients with high-risk CD19+ relapsed/refractory B-cell acute lymphoblastic leukemia. *Blood* 2018; 132(Suppl: 896.

102. Van Der Stegen SJC, Hamieh M, Sadelain M. The pharmacology of second-generation chimeric antigen receptors. *Nature Reviews Drug Discovery*. Epub ahead of print 2015. DOI: 10.1038/nrd4597.

103. Till BG, Jensen MC, Wang J, et al. Adoptive immunotherapy for indolent non-hodgkin lymphoma and mantle cell lymphoma using genetically modified autologous CD20-specific T cells. *Blood*. Epub ahead of print 2008. DOI: 10.1182/blood-2007-12-128843.

104. Finney HM, Lawson AD, Bebbington CR, et al. Chimeric receptors providing both primary and costimulatory signaling in T cells from a single gene product. *J Immunol*.

105. Enblad G, Karlsson H, Gammelgård G, et al. A phase I/IIa trial using CD19-targeted third-generation CAR T cells for lymphoma and leukemia. *Clin Cancer Res*. Epub ahead of print 2018. DOI: 10.1158/1078-0432.CCR-18-0426.

106. Morgan RA, Yang JC, Kitano M, et al. Case Report of a Serious Adverse Event Following the Administration of T Cells Transduced With a Chimeric Antigen Receptor Recognizing ERBB2. *Mol Ther* 2010; 18: 843–851.

107. Maus M V., Haas AR, Beatty GL, et al. T cells expressing chimeric antigen receptors can cause anaphylaxis in humans. *Cancer Immunol Res*. Epub ahead of print 2013. DOI: 10.1158/2326-6066.CIR-13-0006.

108. Turtle CJ, Hanafi LA, Berger C, et al. CD19 CAR-T cells of defined CD4+:CD8+ composition in adult B cell ALL patients. *J Clin Invest*. Epub ahead of print 2016. DOI: 10.1172/JCI85309.

109. Hege KM, Bergsland EK, Fisher GA, et al. Safety, tumor trafficking and immunogenicity of chimeric antigen receptor (CAR)-T cells specific for TAG-72 in colorectal cancer. *J Immunother Cancer* 2017; 5: 1–14.

110. Alabanza L, Pegues M, Geldres C, et al. Function of Novel Anti-CD19 Chimeric Antigen Receptors with Human Variable Regions Is Affected by Hinge and Transmembrane Domains. *Molecular Therapy*, 2017. Epub ahead of print 2017. DOI: 10.1016/j.ymthe.2017.07.013.

111. Hombach AA, Schildgen V, Heuser C, et al. T Cell Activation by Antibody-Like Immunoreceptors: The Position of the Binding Epitope within the Target Molecule Determines the Efficiency of Activation of Redirected T Cells. *J Immunol*. Epub ahead of print 2007. DOI: 10.4049/jimmunol.178.7.4650.

112. Haso W, Lee DW, Shah NN, et al. Anti-CD22-chimeric antigen receptors targeting B-cell precursor acute lymphoblastic leukemia. *Blood*. Epub ahead of print 2013. DOI: 10.1182/blood-2012-06-438002.

113. James SE, Greenberg PD, Jensen MC, et al. Antigen Sensitivity of CD22-Specific Chimeric TCR Is Modulated by Target Epitope Distance from the Cell Membrane. *J Immunol*. Epub ahead of print 2008. DOI: 10.4049/jimmunol.180.10.7028.

114. Srivastava S, Riddell SR, Hutchinson F. Engineering CAR-T Cells: Design Concepts. 2015; 36: 494–502.

115. Hudecek M, Kosasih PL, Sommermeyer D, et al. Receptor Af fi nity and Extracellular Domain Modi fi cations Affect Tumor Recognition by ROR1-Speci fi c Chimeric Antigen

Receptor T Cells. 2013; 1: 3153–3165.

116. Hudecek M, Sommermeyer D, Kosasih PL, et al. The nonsignaling extracellular spacer domain of chimeric antigen receptors is decisive for in vivo antitumor activity. *Cancer Immunol Res*. Epub ahead of print 2015. DOI: 10.1158/2326-6066.CIR-14-0127.

117. Wilkie S, Picco G, Foster J, et al. Retargeting of Human T Cells to Tumor-Associated MUC1: The Evolution of a Chimeric Antigen Receptor. *J Immunol* 2008; 180: 4901–4909.

118. Maude SL, Frey N, Shaw P a., et al. Chimeric Antigen Receptor T Cells for Sustained Remissions in Leukemia. *N Engl J Med* 2014; 371: 1507–17.

119. Porter DL, Hwang W-T, Frey N V., et al. Chimeric antigen receptor T cells persist and induce sustained remissions in relapsed refractory chronic lymphocytic leukemia. *Sci Transl Med* 2015; 7: 303ra139-303ra139.

120. Ghorashian S, Kramer AM, Onuoha S, et al. Enhanced CAR T cell expansion and prolonged persistence in pediatric patients with ALL treated with a low-affinity CD19 CAR. *Nat Med*. Epub ahead of print 2019. DOI: 10.1038/s41591-019-0549-5.

121. Morin SO, Giroux V, Favre C, et al. In the absence of its cytosolic domain, the CD28 molecule still contributes to T cell activation. *Cell Mol Life Sci*. Epub ahead of print 2015. DOI: 10.1007/s00018-015-1873-7.

122. Sadelain M, Rivière I, Riddell S. Therapeutic T cell engineering. *Nature*. Epub ahead of print 2017. DOI: 10.1038/nature22395.

123. Schuster SJ, Bishop MR, Tam CS, et al. Tisagenlecleucel in adult relapsed or refractory

diffuse large B-cell lymphoma. *N Engl J Med* 2019; 380: 45–56.

124. Maude SL, Laetsch TW, Buechner J, et al. Tisagenlecleucel in Children and Young Adults with B-Cell Lymphoblastic Leukemia. *N Engl J Med* 2018; 378: 439–448.

125. Locke FL, Ghobadi A, Jacobson CA, et al. Long-term safety and activity of axicabtagene ciloleucel in refractory large B-cell lymphoma (ZUMA-1): a single-arm, multicentre, phase 1–2 trial. *Lancet Oncol*. Epub ahead of print 2019. DOI: 10.1016/S1470-2045(18)30864-7.

126. Otten GR, Germain RN. Split anergy in a CD8+ T cell: Receptor-dependent cytolysis in the absence of interleukin-2 production. *Science (80-)* 1991; 251: 1228–1231.

127. Laplante M, Sabatini DM. Regulation of mTORC1 and its impact on gene expression at a glance. *J Cell Sci* 2013; 126: 1713–1719.

128. Hsieh AC, Costa M, Zollo O, et al. Genetic Dissection of the Oncogenic mTOR Pathway Reveals Druggable Addiction to Translational Control via 4EBP-eIF4E. *Cancer Cell* 2010; 17: 249–261.

129. Boomer JS, Green JM. An enigmatic tail of CD28 signaling. *Cold Spring Harbor perspectives in biology* 2010; 2: a002436.

130. Maurer U, Preiss F, Brauns-Schubert P, et al. GSK-3 -at the crossroads of cell death and survival. *Journal of Cell Science* 2014; 127: 1369–1378.

131. Okkenhaug K, Rottapel R. Grb2 forms an inducible protein complex with CD28 through a Src homology 3 domain-proline interaction. *J Biol Chem* 1998; 273: 21194–21202.

132. Chen L, Flies DB. Molecular mechanisms of T cell co-stimulation and co-inhibition. *Nature Reviews Immunology* 2013; 13: 227–242.

133. Wölfl M, Kuball J, Eyrich M, et al. Use of CD137 to study the full repertoire of CD8+ T cells without the need to know epitope specificities. *Cytometry Part A* 2008; 73: 1043–1049.

134. DeBenedette MA, Shahinian A, Mak TW, et al. Costimulation of CD28- T lymphocytes by 4-1BB ligand. *J Immunol*; 158.

135. Arch RH, Thompson CB. 4-1BB and Ox40 Are Members of a Tumor Necrosis Factor (TNF)-Nerve Growth Factor Receptor Subfamily That Bind TNF Receptor-Associated Factors and Activate Nuclear Factor κB. *Mol Cell Biol* 1998; 18: 558–565.

136. Cannons JL, Choi Y, Watts TH. Role of TNF Receptor-Associated Factor 2 and p38 Mitogen-Activated Protein Kinase Activation During 4-1BB-Dependent Immune Response. *J Immunol* 2000; 165: 6193–6204.

137. Croft M. The role of TNF superfamily members in T-cell function and diseases. *Nature Reviews Immunology* 2009; 9: 271–285.

138. Brentjens RJ, Santos E, Nikhamin Y, et al. Genetically targeted T cells eradicate systemic acute lymphoblastic leukemia xenografts. *Clin Cancer Res* 2007; 13: 5426–5435.

139. Li G, Boucher JC, Kotani H, et al. 4-1BB enhancement of CAR T function requires NF-κB and TRAFs. *JCI insight*; 3. Epub ahead of print 20 September 2018. DOI: 10.1172/jci.insight.121322.

140. Cells CART, Salter AI, Ivey RG, et al. Phosphoproteomic analysis of chimeric antigen receptor signaling reveals kinetic and quantitative differences that affect cell function. 2018; 6753: 1–18.

141. Guedan S, Chen X, Madar A, et al. ICOS-based chimeric antigen receptors program bipolar TH17/ TH1 cells. *Blood* 2014; 124: 1070–1080.

142. Pulè MA, Straathof KC, Dotti G, et al. A chimeric T cell antigen receptor that augments cytokine release and supports clonal expansion of primary human T cells. *Mol Ther* 2005; 12: 933–941.

143. Kagoya Y, Tanaka S, Guo T, et al. A novel chimeric antigen receptor containing a JAK-STAT signaling domain mediates superior antitumor effects. *Nat Med*. Epub ahead of print 2018. DOI: 10.1038/nm.4478.

144. Kane LP, Weiss A. The PI-3 kinase/Akt pathway and T cell activation: Pleiotropic pathways downstream of PIP3. *Immunological Reviews* 2003; 192: 7–20.

145. Mata M, Gerken C, Nguyen P, et al. Inducible activation of myD88 and CD40 in CAR T cells results in controllable and potent antitumor activity in preclinical solid tumor models. *Cancer Discov* 2017; 7: 1306–1319.

146. Geng D, Zheng L, Srivastava R, et al. Amplifying TLR-MyD88 signals within tumor-specific T cells enhances antitumor activity to suboptimal levels of weakly immunogenic tumor antigens. *Cancer Res* 2010; 70: 7442–7454.

147. Geng D, Zheng L, Srivastava R, et al. When Toll-like receptor and T-cell receptor signals collide: A mechanism for enhanced CD8 T-cell effector function. *Blood* 2010;

116: 3494–3504.

148. Munroe ME, Bishop GA. A Costimulatory Function for T Cell CD40. *J Immunol* 2007; 178: 671–682.

149. Rogers NJ, Jackson IM, Jordan WJ, et al. CD40 can cotimulate human memory T cells and favors IL-10 secretion. *Eur J Immunol* 2003; 33: 1094–1104.

150. Brentjens RJ, Davila ML, Riviere I, et al. CD19-Targeted T Cells Rapidly Induce Molecular Remissions in Adults with Chemotherapy-Refractory Acute Lymphoblastic Leukemia. *Sci Transl Med* 2013; 5: 177ra38-177ra38.

151. Van Zelm MC, Reisli I, Van Der Burg M, et al. An antibody-deficiency syndrome due to mutations in the CD19 gene. *N Engl J Med*. Epub ahead of print 2006. DOI: 10.1056/NEJMoa051568.

152. Scheuermann RH, Racila E. CD19 antigen in leukemia and lymphoma diagnosis and immunotherapy. *Leuk Lymphoma*. Epub ahead of print 1995. DOI: 10.3109/10428199509059636.

153. Kochenderfer JN, Wilson WH, Janik JE, et al. Eradication of B-lineage cells and regression of lymphoma in a patient treated with autologous T cells genetically engineered to recognize CD19. *Blood*. Epub ahead of print 2010. DOI: 10.1182/blood-2010-04-281931.

154. Kochenderfer JN, Feldman SA, Zhao Y, et al. Construction and Preclinical Evaluation of an Anti-CD19 Chimeric Antigen Receptor. 2009; 32: 689–702.

155. Brudno JN, Kochenderfer JN. Chimeric antigen receptor T-cell therapies for

lymphoma. *Nat Rev Clin Oncol* 2018; 15: 31–46.

156. Kochenderfer JN, Dudley ME, Kassim SH, et al. Chemotherapy-refractory diffuse large B-cell lymphoma and indolent B-cell malignancies can be effectively treated with autologous T cells expressing an anti-CD19 chimeric antigen receptor. *J Clin Oncol*. Epub ahead of print 2015. DOI: 10.1200/JCO.2014.56.2025.

157. Neelapu SS, Locke FL, Bartlett NL, et al. Axicabtagene Ciloleucel CAR T-Cell Therapy in Refractory Large B-Cell Lymphoma. *N Engl J Med* 2017; NEJMoa1707447.

158. Imai C, Mihara K, Andreansky M, et al. Chimeric receptors with 4-1BB signaling capacity provoke potent cytotoxicity against acute lymphoblastic leukemia. *Leukemia* 2004; 18: 676–684.

159. Imai C, Mihara K, Andreansky M, et al. Chimeric receptors with 4-1BB signaling capacity provoke potent cytotoxicity against acute lymphoblastic leukemia. *Leukemia*. Epub ahead of print 2004. DOI: 10.1038/sj.leu.2403302.

160. Schuster SJ, Svoboda J, Chong EA, et al. Chimeric antigen receptor T Cells in refractory B-Cell lymphomas. *N Engl J Med*. Epub ahead of print 2017. DOI: 10.1056/NEJMoa1708566.

161. Park JH, Rivière I, Gonen M, et al. Long-Term Follow-up of CD19 CAR Therapy in Acute Lymphoblastic Leukemia. *N Engl J Med* 2018; 378: 449–459.

162. Neelapu SS, Tummala S, Kebriaei P, et al. Chimeric antigen receptor T-cell therapy-assessment and management of toxicities. *Nature Reviews Clinical Oncology*. Epub ahead of print 2018. DOI: 10.1038/nrclinonc.2017.148.

163. Lee DW, Gardner R, Porter DL, et al. Current concepts in the diagnosis and management of cytokine release syndrome. *Blood*. Epub ahead of print 2014. DOI: 10.1182/blood-2014-05-552729.

164. Lee DW, Santomasso BD, Locke FL, et al. ASTCT Consensus Grading for Cytokine Release Syndrome and Neurologic Toxicity Associated with Immune Effector Cells. *Biology of Blood and Marrow Transplantation*. Epub ahead of print 2019. DOI: 10.1016/j.bbmt.2018.12.758.

165. Gust J, Hay KA, Hanafi LA, et al. Endothelial activation and blood–brain barrier disruption in neurotoxicity after adoptive immunotherapy with CD19 CAR-T cells. *Cancer Discov*. Epub ahead of print 2017. DOI: 10.1158/2159-8290.CD-17-0698.

166. van der Stegen SJC, Davies DM, Wilkie S, et al. Preclinical In Vivo Modeling of Cytokine Release Syndrome Induced by ErbB-Retargeted Human T Cells: Identifying a Window of Therapeutic Opportunity? *J Immunol*. Epub ahead of print 2013. DOI: 10.4049/jimmunol.1301523.

167. Norelli M, Camisa B, Barbiera G, et al. Monocyte-derived IL-1 and IL-6 are differentially required for cytokine-release syndrome and neurotoxicity due to CAR T cells. *Nat Med* 2018; 24: 739–748.

168. Giavridis T, Van Der Stegen SJC, Eyquem J, et al. CAR T cell-induced cytokine release syndrome is mediated by macrophages and abated by IL-1 blockade letter. *Nat Med* 2018; 24: 731–738.

169. Parker KR, Migliorini D, Perkey E, et al. Single-Cell Analyses Identify Brain Mural Cells

Expressing CD19 as Potential Off-Tumor Targets for CAR-T Immunotherapies. *Cell*. Epub ahead of print 2020. DOI: 10.1016/j.cell.2020.08.022.

170. Ying Z, Huang XF, Xiang X, et al. A safe and potent anti-CD19 CAR T cell therapy. *Nat Med* 2019; 25: 947–953.

171. Ghorashian S, Kramer AM, Onuoha S, et al. Enhanced CAR T cell expansion and prolonged persistence in pediatric patients with ALL treated with a low-affinity CD19 CAR. *Nat Med*. Epub ahead of print 2019. DOI: 10.1038/s41591-019-0549-5.

172. Gardner RA, Finney O, Annesley C, et al. Intent-to-treat leukemia remission by CD19 CAR T cells of defined formulation and dose in children and young adults. *Blood*. Epub ahead of print 2017. DOI: 10.1182/blood-2017-02-769208.

173. Bhojwani D, Sposto R, Shah NN, et al. Inotuzumab ozogamicin in pediatric patients with relapsed/refractory acute lymphoblastic leukemia. *Leukemia* 2019; 33: 884–892.

174. Majzner RG, Mackall CL. Tumor antigen escape from car t-cell therapy. *Cancer Discovery*. Epub ahead of print 2018. DOI: 10.1158/2159-8290.CD-18-0442.

175. Fischer J, Paret C, El Malki K, et al. CD19 isoforms enabling resistance to CART-19 immunotherapy are expressed in B-ALL patients at initial diagnosis. *J Immunother*. Epub ahead of print 2017. DOI: 10.1097/CJI.0000000000000169.

176. Sotillo E, Barrett DM, Black KL, et al. Convergence of acquired mutations and alternative splicing of CD19 enables resistance to CART-19 immunotherapy. *Cancer Discov* 2015; 5: 1282–1295.

177. Braig F, Brandt A, Goebeler M, et al. Resistance to anti-CD19/CD3 BiTE in acute

lymphoblastic leukemia may be mediated by disrupted CD19 membrane trafficking. *Blood* 2017; 129: 100–104.

178. Orlando EJ, Han X, Tribouley C, et al. Genetic mechanisms of target antigen loss in CAR19 therapy of acute lymphoblastic leukemia. *Nat Med*; 24. Epub ahead of print 2018. DOI: 10.1038/s41591-018-0146-z.

179. Majzner RG, Heitzeneder S, Mackall CL. Harnessing the Immunotherapy Revolution for the Treatment of Childhood Cancers. *Cancer Cell*. Epub ahead of print 2017. DOI: 10.1016/j.ccell.2017.03.002.

180. Gardner R, Wu D, Cherian S, et al. Acquisition of a CD19-negative myeloid phenotype allows immune escape of MLL-rearranged B-ALL from CD19 CAR-T-cell therapy. *Blood*. Epub ahead of print 2016. DOI: 10.1182/blood-2015-08-665547.

181. Rayes A, Mcmasters RL, O'Brien MM. Lineage Switch in MLL-Rearranged Infant Leukemia Following CD19-Directed Therapy. *Pediatr Blood Cancer*. Epub ahead of print 2016. DOI: 10.1002/pbc.25953.

182. Jacoby E, Nguyen SM, Fountaine TJ, et al. CD19 CAR immune pressure induces B-precursor acute lymphoblastic leukaemia lineage switch exposing inherent leukaemic plasticity. *Nat Commun*. Epub ahead of print 2016. DOI: 10.1038/ncomms12320.

183. Hamieh M, Dobrin A, Cabriolu A, et al. CAR T cell trogocytosis and cooperative killing regulate tumour antigen escape. *Nature* 2019; 1.

184. Fry TJ, Shah NN, Orentas RJ, et al. CD22-targeted CAR T cells induce remission in B-ALL that is naive or resistant to CD19-targeted CAR immunotherapy. *Nat Med* 2018;

24: 20–28.

185. Ruella M, Xu J, Barrett DM, et al. Induction of resistance to chimeric antigen receptor T cell therapy by transduction of a single leukemic B cell. *Nat Med*. Epub ahead of print 2018. DOI: 10.1038/s41591-018-0201-9.

186. Qin H, Ramakrishna S, Nguyen S, et al. Preclinical Development of Bivalent Chimeric Antigen Receptors Targeting Both CD19 and CD22. *Mol Ther Oncolytics* 2018; 11: 127–137.

187. Schneider D, Xiong Y, Wu D, et al. A tandem CD19 / CD20 CAR lentiviral vector drives on-target and off-target antigen modulation in leukemia cell lines. 2017; 1–17.

188. Hossain N, Sahaf B, Abramian M, Spiegel JY, Kong K, Kim S, Mavroukakis S, Oak J, Natkunam Y, Meyer EH, Frank MJ, Feldman SA, Long SR, Qin H, Fry TJ, Muffly LS, Mackall CL MD. Phase I experience with a bi-specific CAR targeting CD19 and CD22 in adults with B-cell malignancies. *Blood*.

189. Amrolia PJ, Wynn R, Hough R, Vora A, Bonney D, Veys P, Rao K, Chiesa R, Al-Hajj M, Cordoba SP, Onuoha S, Kotsopoulou E, Khokhar NZ, Pule M PV. Simultaneous targeting of CD19 and CD22: phase I study of AUTO3, a bicistronic chimeric antigen receptor (CAR) T-cell therapy, in pediatric patients with relapsed/refractory B-cell acute lymphoblastic leukemia (r/r B-ALL): Amelia Study. *Blood 2018;132(Suppl 1):279*.

190. Autolus Therapeutics Presents Encouraging Additional Data Showcasing Clinical Progress of Programmed T Cell Therapy Pipeline in Blood Cancers, https://www.globenewswire.com/news-release/2020/01/30/1977423/0/en/Autolus-

Therapeutics-Presents-Encouraging-Additional-Data-Showcasing-Clinical-Progress-of-Programmed-T-Cell-Therapy-Pipeline-in-Blood-Cancers.html.

191. Mirzaei HR, Jamali A, Jafarzadeh L, et al. Construction and functional characterization of a fully human anti-CD19 chimeric antigen receptor (huCAR)-expressing primary human T cells. *J Cell Physiol*. Epub ahead of print 2019. DOI: 10.1002/jcp.27599.

192. Brudno JN, Shi V, Stroncek D, et al. T Cells Expressing a Novel Fully-Human Anti-CD19 Chimeric Antigen Receptor Induce Remissions of Advanced Lymphoma in a First-in-Humans Clinical Trial. *Blood*. Epub ahead of print 2016. DOI: 10.1182/blood.v128.22.999.999.

193. Fraietta JA, Lacey SF, Orlando EJ, et al. Determinants of response and resistance to CD19 chimeric antigen receptor (CAR) T cell therapy of chronic lymphocytic leukemia. *Nat Med* 2018; 24: 563–571.

194. Turtle CJ, Hay KA, Hanafi LA, et al. Durable molecular remissions in chronic lymphocytic leukemia treated with CD19-Specific chimeric antigen Receptor-modified T cells after failure of ibrutinib. *J Clin Oncol*. Epub ahead of print 2017. DOI: 10.1200/JCO.2017.72.8519.

195. Busch DH, Fräßle SP, Sommermeyer D, et al. Role of memory T cell subsets for adoptive immunotherapy. *Seminars in Immunology*. Epub ahead of print 2016. DOI: 10.1016/j.smim.2016.02.001.

196. Petersen CT, Hassan M, Morris AB, et al. Improving T-cell expansion and function for adoptive T-cell therapy using ex vivo treatment with PI3Kd inhibitors and VIP

antagonists. *Blood Adv*. Epub ahead of print 2018. DOI: 10.1182/bloodadvances.2017011254.

197. Guedan S, Madar A, Casado-Medrano V, et al. Single residue in CD28-costimulated CAR T cells limits long-term persistence and antitumor durability. *J Clin Invest*. Epub ahead of print 2020. DOI: 10.1172/JCI133215.

198. Boucher JC, Li G, Shrestha B, et al. Mutation of the CD28 costimulatory domain confers increased CAR T cell persistence and decreased exhaustion. *J Immunol*.

199. Cells CART, Gunset G, Plotkin J, et al. Structural Design of Engineered Costimulation Determines Tumor Rejection Kinetics and Article Structural Design of Engineered Costimulation Determines Tumor Rejection Kinetics and Persistence of CAR T Cells. *Cancer Cell* 2015; 28: 415–428.

200. Park JH, Palomba ML, Batlevi CL, et al. A Phase I First-in-Human Clinical Trial of CD19-Targeted 19-28z/4-1BBL 'Armored' CAR T Cells in Patients with Relapsed or Refractory NHL and CLL Including Richter's Transformation. *Blood* 2018; 132: 224.

201. Maher J, Brentjens RJ, Gunset G, et al. Human T-lymphocyte cytotoxicity and proliferation directed by a single chimeric TCRζ/CD28 receptor. *Nat Biotechnol*. Epub ahead of print 2002. DOI: 10.1038/nbt0102-70.

202. Brudno JN, Maric I, Hartman SD, et al. T cells genetically modified to express an anti–B-Cell maturation antigen chimeric antigen receptor cause remissions of poor-prognosis relapsed multiple myeloma. *J Clin Oncol*. Epub ahead of print 2018. DOI: 10.1200/JCO.2018.77.8084.

203. Pulè MA, Straathof KC, Dotti G, et al. A chimeric T cell antigen receptor that augments cytokine release and supports clonal expansion of primary human T cells. *Mol Ther*. Epub ahead of print 2005. DOI: 10.1016/j.ymthe.2005.04.016.

204. Xiong W, Chen Y, Kang X, et al. Immunological Synapse Predicts Effectiveness of Chimeric Antigen Receptor Cells. *Mol Ther*. Epub ahead of print 2018. DOI: 10.1016/j.ymthe.2018.01.020.

205. Karlsson H, Svensson E, Gigg C, et al. Evaluation of intracellular signaling downstream chimeric antigen receptors. *PLoS One*. Epub ahead of print 2015. DOI: 10.1371/journal.pone.0144787.

206. Zhong XS, Matsushita M, Plotkin J, et al. Chimeric antigen receptors combining 4-1BB and CD28 signaling domains augment PI 3 kinase/AKT/Bcl-X L activation and CD8 T cell-mediated tumor eradication. *Mol Ther*. Epub ahead of print 2010. DOI: 10.1038/mt.2009.210.

207. Guedan S, Posey AD, Shaw C, et al. Enhancing CAR T cell persistence through ICOS and 4-1BB costimulation. *JCI insight*. Epub ahead of print 2018. DOI: 10.1172/jci.insight.96976.

208. Wang J, Jensen M, Lin Y, et al. Optimizing adoptive polyclonal T cell immunotherapy of lymphomas, using a chimeric T cell receptor possessing CD28 and CD137 costimulatory domains. *Hum Gene Ther*. Epub ahead of print 2007. DOI: 10.1089/hum.2007.028.

209. Milone MC, Fish JD, Carpenito C, et al. Chimeric receptors containing CD137 signal

transduction domains mediate enhanced survival of T cells and increased antileukemic efficacy in vivo. *Mol Ther*. Epub ahead of print 2009. DOI: 10.1038/mt.2009.83.

210. Tammana S, Huang X, Wong M, et al. 4-1BB and CD28 signaling plays a synergistic role in redirecting umbilical cord blood t cells against b-cell malignancies. *Hum Gene Ther*. Epub ahead of print 2010. DOI: 10.1089/hum.2009.122.

211. Heczey A, Louis CU, Savoldo B, et al. CAR T Cells Administered in Combination with Lymphodepletion and PD-1 Inhibition to Patients with Neuroblastoma. *Mol Ther*. Epub ahead of print 2017. DOI: 10.1016/j.ymthe.2017.05.012.

212. Louis CU, Savoldo B, Dotti G, et al. Antitumor activity and long-term fate of chimeric antigen receptor-positive T cells in patients with neuroblastoma. *Blood*. Epub ahead of print 2011. DOI: 10.1182/blood-2011-05-354449.

213. Pule MA, Savoldo B, Myers GD, et al. Virus-specific T cells engineered to coexpress tumor-specific receptors: Persistence and antitumor activity in individuals with neuroblastoma. *Nat Med*. Epub ahead of print 2008. DOI: 10.1038/nm.1882.

214. Cells C, Ramello MC, Benzaïd I, et al. An immunoproteomic approach to characterize the CAR interactome and signalosome. 2019; 9777: 1–16.

215. Muliaditan T, Halim L, Whilding LM, et al. Optimized delivery of dual co-stimulation and anti-tumor activity using parallel chimeric antigen receptors (pCARs).

216. Nicholson IANC, Lenton KA, Little DJ, et al. CONSTRUCTION AND CHARACTERISATION OF A CD19 SPECIFIC SINGLE CHAIN Fv FRAGMENT FOR IMMUNOTHERAPY OF B

LINEAGE LEUKAEMIA AND LYMPHOMA. 1997; 34: 1157–1165.

217. Mansfield E, Amlot P, Pastan I, et al. Recombinant RFB4 immunotoxins exhibit potent cytotoxic activity for CD22-bearing cells and tumors. *Blood* 1997; 90: 2020–2026.

218. Shan D, Press OW, Tsu TT, et al. Characterization of scFv-Ig constructs generated from the anti-CD20 mAb 1F5 using linker peptides of varying lengths. *J Immunol*.

219. Cooper LJN, Topp MS, Serrano LM, et al. T-cell clones can be rendered specific for CD19: Toward the selective augmentation of the graft-versus-B-lineage leukemia effect. *Blood* 2003; 101: 1637–1644.

220. Whilding LM, Parente-Pereira AC, Zabinski T, et al. Targeting of Aberrant αvβ6 Integrin Expression in Solid Tumors Using Chimeric Antigen Receptor-Engineered T Cells. *Mol Ther* 2017; 25: 259–273.

221. Parente-Pereira AC, Wilkie S, Van der Stegen SJC, et al. Use of retroviral-mediated gene transfer to deliver and test function of chimeric antigen receptors in human T-cells. *J Biol Methods*. Epub ahead of print 2014. DOI: 10.14440/jbm.2014.30.

222. Kochenderfer JN, Dudley ME, Feldman SA, et al. B-cell depletion and remissions of malignancy along with cytokine-associated toxicity in a clinical trial of anti-CD19 chimeric-antigen-receptor-transduced T cells. *Blood*. Epub ahead of print 2012. DOI: 10.1182/blood-2011-10-384388.

223. Cole DK, Pumphrey NJ, Boulter JM, et al. Human TCR-Binding Affinity is Governed by MHC Class Restriction. *J Immunol*. Epub ahead of print 2007. DOI: 10.4049/jimmunol.178.9.5727.

224. van der Merwe PA, Davis SJ. Molecular interactions mediating T cell antigen recognition. *Annu Rev Immunol*.

225. Caruso HG, Hurton L V., Najjar A, et al. Tuning sensitivity of CAR to EGFR density limits recognition of normal tissue while maintaining potent antitumor activity. *Cancer Res*. Epub ahead of print 2015. DOI: 10.1158/0008-5472.CAN-15-0139.

226. Richman SA, Nunez-Cruz S, Moghimi B, et al. High-Affinity GD2-specific CAR T cells induce fatal encephalitis in a preclinical neuroblastoma model. *Cancer Immunol Res*. Epub ahead of print 2018. DOI: 10.1158/2326-6066.CIR-17-0211.

227. Kalergis AH, Boucheron N, Doucey MA, et al. Efficient T cell activation requires an optimal dwell-time of interaction between the TCR and the pMHC complex. *Nat Immunol*. Epub ahead of print 2001. DOI: 10.1038/85286.

228. Thomas S, Xue SA, Bangham CRM, et al. Human T cells expressing affinity-matured TCR display accelerated responses but fail to recognize low density of MHC-peptide antigen. *Blood*. Epub ahead of print 2011. DOI: 10.1182/blood-2010-12-326736.

229. Davenport AJ, Jenkins MR, Cross RS, et al. CAR-T cells inflict sequential killing of multiple tumor target cells. *Cancer Immunol Res*. Epub ahead of print 2015. DOI: 10.1158/2326-6066.CIR-15-0048.

230. Drent E, Themeli M, Poels R, et al. A Rational Strategy for Reducing On-Target Off-Tumor Effects of CD38-Chimeric Antigen Receptors by Affinity Optimization. *Mol Ther*. Epub ahead of print 2017. DOI: 10.1016/j.ymthe.2017.04.024.

231. Chmielewski M, Hombach A, Heuser C, et al. T Cell Activation by Antibody-Like

Immunoreceptors: Increase in Affinity of the Single-Chain Fragment Domain above Threshold Does Not Increase T Cell Activation against Antigen-Positive Target Cells but Decreases Selectivity. *J Immunol*. Epub ahead of print 2004. DOI: 10.4049/jimmunol.173.12.7647.

232. Liu X, Jiang S, Fang C, et al. Affinity-tuned ErbB2 or EGFR chimeric antigen receptor T cells exhibit an increased therapeutic index against tumors in mice. *Cancer Res*. Epub ahead of print 2015. DOI: 10.1158/0008-5472.CAN-15-0159.

233. Park S, Shevlin E, Vedvyas Y, et al. Micromolar affinity CAR T cells to ICAM-1 achieves rapid tumor elimination while avoiding systemic toxicity. *Sci Rep*. Epub ahead of print 2017. DOI: 10.1038/s41598-017-14749-3.

234. Viganò S, Utzschneider DT, Perreau M, et al. Functional avidity: A measure to predict the efficacy of effector T cells? *Clinical and Developmental Immunology*. Epub ahead of print 2012. DOI: 10.1155/2012/153863.

235. Oren R, Hod-Marco M, Haus-Cohen M, et al. Functional Comparison of Engineered T Cells Carrying a Native TCR versus TCR-like Antibody–Based Chimeric Antigen Receptors Indicates Affinity/Avidity Thresholds. *J Immunol* 2014; 193: 5733–5743.

236. Sibener L V., Fernandes RA, Kolawole EM, et al. Isolation of a Structural Mechanism for Uncoupling T Cell Receptor Signaling from Peptide-MHC Binding. *Cell*. Epub ahead of print 2018. DOI: 10.1016/j.cell.2018.06.017.

237. Kamsma D, Bochet P, Oswald F, et al. Single-Cell Acoustic Force Spectroscopy: Resolving Kinetics and Strength of T Cell Adhesion to Fibronectin. *Cell Rep* 2018; 24:

3008–3016.

238. Chakraborty AK, Weiss A. Insights into the initiation of TCR signaling. *Nature Immunology*. Epub ahead of print 2014. DOI: 10.1038/ni.2940.

239. Zhong S, Malecek K, Johnson LA, et al. T-cell receptor affinity and avidity defines antitumor response and autoimmunity in T-cell immunotherapy. *Proc Natl Acad Sci U S A*. Epub ahead of print 2013. DOI: 10.1073/pnas.1221609110.

240. Turatti F, Figini M, Balladore E, et al. Redirected activity of human antitumor chimeric immune receptors is governed by antigen and receptor expression levels and affinity of interaction. *J Immunother*. Epub ahead of print 2007. DOI: 10.1097/CJI.0b013e3180de5d90.

241. Bortoletto N, Scotet E, Yoichi M, et al. Optimizing anti-CD3 affinity for effective T cell targeting against tumor cells. *European Journal of Immunology*. Epub ahead of print 2002. DOI: 10.1002/1521-4141(200211)32:11<3102::AID-IMMU3102>3.0.CO;2-C.

242. Wang E, Wang LC, Tsai CY, et al. Generation of potent T-cell immunotherapy for Cancer using DAP12-based, multichain, chimeric immunoreceptors. *Cancer Immunol Res*. Epub ahead of print 2015. DOI: 10.1158/2326-6066.CIR-15-0054.

243. Riese MJ, Wang LCS, Moon EK, et al. Enhanced effector responses in activated CD8+ T cells deficient in diacylglycerol kinases. *Cancer Res*. Epub ahead of print 2013. DOI: 10.1158/0008-5472.CAN-12-3874.

244. Whilding LM, Halim L, Draper B, et al. CAR T-cells targeting the integrin αvβ6 and co-expressing the chemokine receptor CXCR2 demonstrate enhanced homing and

efficacy against several solid malignancies. *Cancers (Basel)* 2019; 11: 1–17.

245. Gargett T, Brown MP. The inducible caspase-9 suicide gene system as a 'safety switch' to limit on-target, off-tumor toxicities of chimeric antigen receptor T-cells. *Front Pharmacol*. Epub ahead of print 2014. DOI: 10.3389/fphar.2014.00235.

246. Lin H, Lee E, Hestir K, et al. Discovery of a cytokine and its receptor by functional screening of the extracellular proteome. *Science (80-)*. Epub ahead of print 2008. DOI: 10.1126/science.1154370.

247. Singer M, Wang C, Cong L, et al. A Distinct Gene Module for Dysfunction Uncoupled from Activation in Tumor-Infiltrating T Cells. *Cell*. Epub ahead of print 2016. DOI: 10.1016/j.cell.2016.08.052.

248. Brentjens RJ, Santos E, Nikhamin Y, et al. Genetically targeted T cells eradicate systemic acute lymphoblastic leukemia xenografts. *Clin Cancer Res*. Epub ahead of print 2007. DOI: 10.1158/1078-0432.CCR-07-0674.

249. Locke FL, Westin JR, Miklos DB, et al. Phase 1 Results from ZUMA-6: Axicabtagene Ciloleucel (axi-cel; KTE-C19) in Combination with Atezolizumab for the Treatment of Patients with Refractory Diffuse Large B Cell Lymphoma (DLBCL). *Blood*.

250. Ngiow SF, Von Scheidt B, Akiba H, et al. Anti-TIM3 antibody promotes T cell IFN-γ-mediated antitumor immunity and suppresses established tumors. *Cancer Res*. Epub ahead of print 2011. DOI: 10.1158/0008-5472.CAN-11-0096.

251. Vardhana SA, Hwee MA, Berisa M, et al. Impaired mitochondrial oxidative phosphorylation limits the self-renewal of T cells exposed to persistent antigen. *Nat*

Immunol. Epub ahead of print 2020. DOI: 10.1038/s41590-020-0725-2.

252. Shah NN, Fry TJ. Mechanisms of resistance to CAR T cell therapy. *Nature Reviews Clinical Oncology*. Epub ahead of print 2019. DOI: 10.1038/s41571-019-0184-6.

253. Locke FL, Ghobadi A, Jacobson CA, et al. Articles Long-term safety and activity of axicabtagene ciloleucel in refractory large B-cell lymphoma (ZUMA-1): a single-arm , multicentre , phase 1 – 2 trial. *Lancet Oncol* 2019; 20: 31–42.

254. Ruella M, June CH. Chimeric Antigen Receptor T cells for B Cell Neoplasms: Choose the Right CAR for You. *Current Hematologic Malignancy Reports*. Epub ahead of print 2016. DOI: 10.1007/s11899-016-0336-z.

255. Hegde M, Corder A, Chow KK, et al. Combinational Targeting offsets antigen escape and enhances effector functions of adoptively transferred T cells in glioblastoma. *Mol Ther*. Epub ahead of print 2013. DOI: 10.1038/mt.2013.185.

256. Ruella M, Barrett DM, Kenderian SS, et al. Dual CD19 and CD123 targeting prevents antigen-loss relapses after CD19-directed immunotherapies. *J Clin Invest*. Epub ahead of print 2016. DOI: 10.1172/JCI87366.

257. Hegde M, Mukherjee M, Grada Z, et al. Tandem CAR T cells targeting HER2 and IL13Rα2 mitigate tumor antigen escape. *J Clin Invest*. Epub ahead of print 2016. DOI: 10.1172/JCI83416.

258. Bielamowicz K, Fousek K, Byrd TT, et al. Trivalent CAR T cells overcome interpatient antigenic variability in glioblastoma. *Neuro Oncol*. Epub ahead of print 2018. DOI: 10.1093/neuonc/nox182.

259. Lee DW, Kochenderfer JN, Stetler-Stevenson M, et al. T cells expressing CD19 chimeric antigen receptors for acute lymphoblastic leukaemia in children and young adults: A phase 1 dose-escalation trial. *Lancet* 2015; 385: 517–528.

260. Raponi S, Stefania De Propris M, Intoppa S, et al. Flow cytometric study of potential target antigens (CD19, CD20, CD22, CD33) for antibody-based immunotherapy in acute lymphoblastic leukemia: Analysis of 552 cases. *Leuk Lymphoma*. Epub ahead of print 2011. DOI: 10.3109/10428194.2011.559668.

261. Davies DM, Maher J. Gated chimeric antigen receptor T-cells: The next logical step in reducing toxicity? *Translational Cancer Research*. Epub ahead of print 2016. DOI: 10.21037/tcr.2016.06.04.

262. Brandt LJB, Barnkob MB, Michaels YS, et al. Emerging Approaches for Regulation and Control of CAR T Cells: A Mini Review. *Frontiers in Immunology*. Epub ahead of print 2020. DOI: 10.3389/fimmu.2020.00326.

263. Fedorov VD, Themeli M, Sadelain M. PD-1- and CTLA-4-based inhibitory chimeric antigen receptors (iCARs) divert off-target immunotherapy responses. *Sci Transl Med*. Epub ahead of print 2013. DOI: 10.1126/scitranslmed.3006597.

264. Kloss CC, Condomines M, Cartellieri M, et al. Combinatorial antigen recognition with balanced signaling promotes selective tumor eradication by engineered T cells. *Nat Biotechnol* 2013; 31: 71–75.

265. Wilkie S, Van Schalkwyk MCI, Hobbs S, et al. Dual targeting of ErbB2 and MUC1 in breast cancer using chimeric antigen receptors engineered to provide complementary

signaling. *J Clin Immunol* 2012; 32: 1059–1070.

266. Grada Z, Hegde M, Byrd T, et al. TanCAR: A novel bispecific chimeric antigen receptor for cancer immunotherapy. *Mol Ther - Nucleic Acids*. Epub ahead of print 2013. DOI: 10.1038/mtna.2013.32.

267. Zah E, Lin MY, Anne SB, et al. T cells expressing CD19/CD20 bispecific chimeric antigen receptors prevent antigen escape by malignant B cells. *Cancer Immunol Res* 2016; 4: 498–508.

268. Shah NN, Zhu F, Taylor C, et al. A Phase 1 Study with Point-of-Care Manufacturing of Dual Targeted, Tandem Anti-CD19, Anti-CD20 Chimeric Antigen Receptor Modified T (CAR-T) Cells for Relapsed, Refractory, Non-Hodgkin Lymphoma. *Blood*. Epub ahead of print 2018. DOI: 10.1182/blood-2018-99-110194.

269. Rivière I, Brose K, Mulligan RC. Effects of retroviral vector design on expression of human adenosine deaminase in murine bone marrow transplant recipients engrafted with genetically modified cells. *Proc Natl Acad Sci U S A*. Epub ahead of print 1995. DOI: 10.1073/pnas.92.15.6733.

270. Olsson C, Michaëlsson E, Parra E, et al. Biased dependency of CD80 versus CD86 in the induction of transcription factors regulating the human IL-2 promoter. *Int Immunol*. Epub ahead of print 1998. DOI: 10.1093/intimm/10.4.499.

271. Engel P, Gribben JG, Freeman GJ, et al. The B7-2 (B70) costimulatory molecule expressed by monocytes and activated B lymphocytes is the CD86 differentiation antigen. *Blood*. Epub ahead of print 1994. DOI:

10.1182/blood.v84.5.1402.bloodjournal8451402.

272. Haso W, Lee DW, Shah NN, et al. Anti-CD22-chimeric antigen receptors targeting B-cell precursor acute lymphoblastic leukemia. *Blood* 2013; 121: 1165–1171.

273. James SE, Greenberg PD, Jensen MC, et al. Antigen Sensitivity of CD22-Specific Chimeric TCR Is Modulated by Target Epitope Distance from the Cell Membrane. *J Immunol* 2008; 180: 7028–7038.

274. Shalabi H, Kraft IL, Wang HW, et al. Sequential loss of tumor surface antigens following chimeric antigen receptor T-cell therapies in diffuse large B-cell lymphoma. *Haematologica*. Epub ahead of print 2018. DOI: 10.3324/haematol.2017.183459.

275. Wherry EJ. T cell exhaustion. *Nature Immunology*. Epub ahead of print 2011. DOI: 10.1038/ni.2035.

276. Hombach AA, Rappl G, Abken H. Arming Cytokine-induced Killer cells with chimeric antigen receptors: CD28 outperforms combined CD28-OX40 'super-stimulation'. *Mol Ther*. Epub ahead of print 2013. DOI: 10.1038/mt.2013.192.

277. Velasquez MP, Szoor A, Vaidya A, et al. CD28 and 41BB costimulation enhances the effector function of CD19-specific engager T cells. *Cancer Immunol Res* 2017; 5: 860–870.

278. Ribas A, Wolchok JD. Cancer immunotherapy using checkpoint blockade. *Science*. Epub ahead of print 2018. DOI: 10.1126/science.aar4060.

279. Baumeister SH, Freeman GJ, Dranoff G, et al. Coinhibitory Pathways in Immunotherapy for Cancer. *Annu Rev Immunol*. Epub ahead of print 2016. DOI:

10.1146/annurev-immunol-032414-112049.

280. Köksal H, Dillard P, Josefsson SE, et al. Preclinical development of CD37CAR T-cell therapy for treatment of B-cell lymphoma. *Blood Adv*. Epub ahead of print 2019. DOI: 10.1182/bloodadvances.2018029678.

281. Polson AG, Williams M, Gray AM, et al. Anti-CD22-MCC-DM1: An antibody-drug conjugate with a stable linker for the treatment of non-Hodgkin's lymphoma. *Leukemia*. Epub ahead of print 2010. DOI: 10.1038/leu.2010.141.

282. Piccaluga PP, Arpinati M, Candoni A, et al. Surface antigens analysis reveals significant expression of candidate targets for immunotherapy in adult acute lymphoid leukemia. *Leukemia and Lymphoma*. Epub ahead of print 2011. DOI: 10.3109/10428194.2010.529206.

283. Raetz EA, Cairo MS, Borowitz MJ, et al. Chemoimmunotherapy reinduction with epratuzumab in children with acute lymphoblastic leukemia in marrow relapse: A children's oncology group pilot study. *J Clin Oncol*. Epub ahead of print 2008. DOI: 10.1200/JCO.2007.15.3528.

284. Hiraga J, Tomita A, Sugimoto T, et al. Down-regulation of CD20 expression in B-cell lymphoma cells after treatment with rituximab-containing combination chemotherapies: Its prevalence and clinical significance. *Blood* 2009; 113: 4885–4893.

285. Foran JM, Norton AJ, Micallef INM, et al. Loss of CD20 expression following treatment with rituximab (chimaeric monoclonal anti-CD20): A retrospective cohort analysis. *Br J Haematol*. Epub ahead of print 2001. DOI: 10.1046/j.1365-2141.2001.03019.x.

286. Hinrichs CS, Spolski R, Paulos CM, et al. IL-2 and IL-21 confer opposing differentiation programs to CD8+ T cells for adoptive immunotherapy. *Blood*. Epub ahead of print 2008. DOI: 10.1182/blood-2007-09-113050.

287. Janas ML, Groves P, Kienzle N, et al. IL-2 Regulates Perforin and Granzyme Gene Expression in CD8 + T Cells Independently of Its Effects on Survival and Proliferation . *J Immunol*. Epub ahead of print 2005. DOI: 10.4049/jimmunol.175.12.8003.

288. Pipkin ME, Sacks JA, Cruz-Guilloty F, et al. Interleukin-2 and Inflammation Induce Distinct Transcriptional Programs that Promote the Differentiation of Effector Cytolytic T Cells. *Immunity*. Epub ahead of print 2010. DOI: 10.1016/j.immuni.2009.11.012.

289. Dotti G, Gottschalk S, Savoldo B, et al. Design and development of therapies using chimeric antigen receptor-expressing T cells. *Immunol Rev*. Epub ahead of print 2014. DOI: 10.1111/imr.12131.

290. Kunert A, Straetemans T, Govers C, et al. TCR-engineered T cells meet new challenges to treat solid tumors: Choice of antigen, T cell fitness, and sensitization of tumor milieu. *Frontiers in Immunology*. Epub ahead of print 2013. DOI: 10.3389/fimmu.2013.00363.

291. Tan MP, Gerry AB, Brewer JE, et al. T cell receptor binding affinity governs the functional profile of cancer-specific CD8+ T cells. *Clin Exp Immunol*. Epub ahead of print 2015. DOI: 10.1111/cei.12570.

292. Irving M, Zoete V, Hebeisen M, et al. Interplay between T cell receptor binding

kinetics and the level of cognate peptide presented by major histocompatibility complexes governs CD8+ T cell responsiveness. *J Biol Chem*. Epub ahead of print 2012. DOI: 10.1074/jbc.M112.357673.

293. Kersh GJ, Kersh EN, Fremont DH, et al. High- and low-potency ligands with similar affinities for the TCR: The importance of kinetic in TCR signaling. *Immunity*. Epub ahead of print 1998. DOI: 10.1016/S1074-7613(00)80647-0.

294. Rosette C, Werlen G, Daniels MA, et al. The Impact of duration versus extent of TCR occupancy on T cell activation: A revision of the kinetic proofreading model. *Immunity*. Epub ahead of print 2001. DOI: 10.1016/S1074-7613(01)00173-X.

295. Jenkins MR, Tsun A, Stinchcombe JC, et al. The Strength of T Cell Receptor Signal Controls the Polarization of Cytotoxic Machinery to the Immunological Synapse. *Immunity*. Epub ahead of print 2009. DOI: 10.1016/j.immuni.2009.08.024.

296. Lehner M, Götz G, Proff J, et al. Redirecting T cells to ewing's sarcoma family of tumors by a chimeric NKG2D receptor expressed by lentiviral transduction or mRNA transfection. *PLoS One*. Epub ahead of print 2012. DOI: 10.1371/journal.pone.0031210.

297. Maus M V., Plotkin J, Jakka G, et al. An MHC-restricted antibody-based chimeric antigen receptor requires TCR-like affinity to maintain antigen specificity. *Mol Ther - Oncolytics*. Epub ahead of print 2016. DOI: 10.1038/mto.2016.23.

298. Makita S, Ph KI, Kurosawa S, et al. Chimeric antigen receptor T-cell therapy for B-cell non-Hodgkin lymphoma : opportunities and challenges Structure of anti-CD19 CAR.

2019; 1–14.

299. Kawalekar OU, O'Connor RS, Fraietta JA, et al. Distinct Signaling of Coreceptors Regulates Specific Metabolism Pathways and Impacts Memory Development in CAR T Cells. *Immunity*. Epub ahead of print 2016. DOI: 10.1016/j.immuni.2016.01.021.

300. Fraser JD, Irving BA, Crabtree GR, et al. Regulation of interleukin-2 gene enhancer activity by the T cell accessory molecule CD28. *Science (80-)*. Epub ahead of print 1991. DOI: 10.1126/science.1846244.

301. Esensten JH, Helou YA, Chopra G, et al. CD28 Costimulation: From Mechanism to Therapy. *Immunity*. Epub ahead of print 2016. DOI: 10.1016/j.immuni.2016.04.020.

302. Zapata JM, Perez-Chacon G, Carr-Baena P, et al. CD137 (4-1BB) signalosome: Complexity is a matter of TRAFs. *Frontiers in Immunology*. Epub ahead of print 2018. DOI: 10.3389/fimmu.2018.02618.

303. Philipson BI, O'Connor RS, May MJ, et al. 4-1BB costimulation promotes CAR T cell survival through noncanonical NF-κB signaling. *Sci Signal* 2020; 13: 1–14.

304. Sadelain M, Rivière I, Riddell S. Therapeutic T cell engineering. *Nature* 2017; 545: 423–431.

305. Lo ASY, Taylor JR, Farzaneh F, et al. Harnessing the tumour-derived cytokine, CSF-1, to co-stimulate T-cell growth and activation. *Mol Immunol* 2008; 45: 1276–1287.

306. Gargett T, Yu W, Dotti G, et al. GD2-specific CAR T Cells Undergo Potent Activation and Deletion Following Antigen Encounter but can be Protected from Activation-induced Cell Death by PD-1 Blockade. *Mol Ther*. Epub ahead of print 2016. DOI:

10.1038/mt.2016.63.

307. Corse E, Gottschalk RA, Krogsgaard M, et al. Attenuated T cell responses to a high-potency ligand in vivo. *PLoS Biol*. Epub ahead of print 2010. DOI: 10.1371/journal.pbio.1000481.

308. Engels B, Chervin AS, Sant AJ, et al. Long-term persistence of CD4+ but rapid disappearance of CD8+ T cells expressing an MHC class I-restricted TCR of nanomolar affinity. *Mol Ther*. Epub ahead of print 2012. DOI: 10.1038/mt.2011.286.

309. Chervin AS, Stone JD, Soto CM, et al. Design of T-cell receptor libraries with diverse binding properties to examine adoptive T-cell responses. *Gene Ther*. Epub ahead of print 2013. DOI: 10.1038/gt.2012.80.

310. Janicki CN, Jenkinson SR, Williams NA, et al. Loss of CTL function among high-avidity tumor-specific CD8+ T cells following tumor infiltration. *Cancer Res*. Epub ahead of print 2008. DOI: 10.1158/0008-5472.CAN-07-5008.

311. Abramson JS, Gordon LI, Palomba ML, et al. Updated safety and long term clinical outcomes in TRANSCEND NHL 001, pivotal trial of lisocabtagene maraleucel (JCAR017) in R/R aggressive NHL. *J Clin Oncol* 2018; 36: 7505–7505.

312. Teachey DT, Rheingold SR, Maude SL, et al. Cytokine release syndrome after blinatumomab treatment related to abnormal macrophage activation and ameliorated with cytokine-directed therapy. *Blood*. Epub ahead of print 2013. DOI: 10.1182/blood-2013-02-485623.

313. Turtle CJ, Hanafi LA, Berger C, et al. Immunotherapy of non-Hodgkin's lymphoma with

a defined ratio of CD8+ and CD4+ CD19-specific chimeric antigen receptor-modified T cells. *Sci Transl Med*. Epub ahead of print 2016. DOI: 10.1126/scitranslmed.aaf8621.

314. Moeller M, Kershaw MH, Cameron R, et al. Sustained antigen-specific antitumor recall response mediated by gene-modified CD4+ T helper-1 and CD8+ T cells. *Cancer Res*. Epub ahead of print 2007. DOI: 10.1158/0008-5472.CAN-07-1141.

315. Long AH, Haso WM, Shern JF, et al. 4-1BB costimulation ameliorates T cell exhaustion induced by tonic signaling of chimeric antigen receptors. *Nat Med*. Epub ahead of print 2015. DOI: 10.1038/nm.3838.

316. Gomes-Silva D, Mukherjee M, Srinivasan M, et al. Tonic 4-1BB Costimulation in Chimeric Antigen Receptors Impedes T Cell Survival and Is Vector-Dependent. *Cell Rep*. Epub ahead of print 2017. DOI: 10.1016/j.celrep.2017.09.015.

317. Nauerth M, Weißbrich B, Knall R, et al. TCR-ligand koff rate correlates with the protective capacity of antigen-specific CD8+ T cells for adoptive transfer. *Sci Transl Med*. Epub ahead of print 2013. DOI: 10.1126/scitranslmed.3005958.

318. Corse E, Gottschalk RA, Allison JP. Strength of TCR–Peptide/MHC Interactions and In Vivo T Cell Responses. *J Immunol*. Epub ahead of print 2011. DOI: 10.4049/jimmunol.1003650.

319. Lever M, Lim HS, Kruger P, et al. Architecture of a minimal signaling pathway explains the T-cell response to a 1 million-fold variation in antigen affinity and dose. *Proc Natl Acad Sci U S A*. Epub ahead of print 2016. DOI: 10.1073/pnas.1608820113.

320. Engel P, Wagner N, Miller AS, et al. Identification of the ligand-binding domains of

CD22, a member of the immunoglobulin superfamily that uniquely binds a sialic acid-dependent ligand. *J Exp Med*. Epub ahead of print 1995. DOI: 10.1084/jem.181.4.1581.

321. James SE, Greenberg PD, Jensen MC, et al. Antigen sensitivity of CD22-specific chimeric T cell receptors is modulated by target epitope distance from the cell membrane. *J Immunol* 2008; 180: 7028–7038.

322. Melero I, Bach N, Hellström KE, et al. Amplification of tumor immunity by gene transfer of the co-stimulatory 4-1BB ligand: Synergy with the CD28 co-stimulatory pathway. *Eur J Immunol*. Epub ahead of print 1998. DOI: 10.1002/(SICI)1521-4141(199803)28:03<1116::AID-IMMU1116>3.0.CO;2-A.

323. Wen T, Bukczynski J, Watts TH. 4-1BB Ligand-Mediated Costimulation of Human T Cells Induces CD4 and CD8 T Cell Expansion, Cytokine Production, and the Development of Cytolytic Effector Function. *J Immunol*. Epub ahead of print 2002. DOI: 10.4049/jimmunol.168.10.4897.

324. Maus M V., Thomas AK, Leonard DGB, et al. Ex vivo expansion of polyclonal and antigen-specific cytotoxic T lymphocytes by artificial APCs expressing ligands for the T-cell receptor, CD28 and 4-1BB. *Nat Biotechnol*. Epub ahead of print 2002. DOI: 10.1038/nbt0202-143.

Appendix

Common antibodies used:

Name	Company (clone)	Dilution	Application
Mouse 9E10 hybridoma supernatant		20 µL/test	FC
Biotin anti-c-myc Epitope Tag	Biolegend (9E10)	5 µg/test	FC
Alexa Fluor® 647 anti-human CD223 (LAG-3)	Biolegend (11C3C65)	5 µL/test	FC
PE anti-human CD279 (PD-1)	Biolegend (EH12.2H7)	5 µL/test	FC
APC/Cy7 anti-human CD366 (Tim-3)	Biolegend (F38-2E2)	5 µL/test	FC
Alexa Fluor® 488 Streptavidin	Biolegend	5 µL/test	FC
FITC anti-human CD19	Biolegend (HIB19)	5 µL/test	FC
APC anti-human CD22	Biolegend (HIB22)	5 µL/test	FC
Recombinant human CD19 Protein, With C-Fc Tag	ACRO Biosystems	0.5-1.0 µg/test	FC
Recombinant Human CD19 Fc Chimera Protein	R&D Systems	0.5-1.0 µg/test	FC
Human MS4A1 / CD20 Protein, Fc Tag	ACRO Biosystems	0.5-1.0 µg/test	FC
Goat anti-mouse (GAM) PE	Dako	1:100	FC
Goat antihuman/mouse Alexa Fluor 647	Jackson Laboratories	0.25 µL/test	FC
PE anti-human CD45RA	Biolegend (HI100)	5 µL/test	FC
APC anti-human CD197 (CCR7)	Biolegend (G043H7)	5 µL/test	FC
Zombie NIR™ Fixable Viability	Biolegend	1:1000	FC
APC anti-DYKDDDDK Tag	Biolegend (L5)	5 µL/test	FC

Primers

FMC63

Fwd: 5’ ACTACAAGGACGACGATGACAAGGGAGACGCGTCTGACATCCAGATGACCCAGACCAC 3’

Rev: 3’ CAGGTCCTCTTCAGAGATCAGTTTCTGTTCCACCTCAATTGCGGCCGCGCTG 5’